Microbial electrochemical snorkel for nitrate reduction in constructed wetlands

Joanna Rogińska

▶ **To cite this version:**

Joanna Rogińska. Microbial electrochemical snorkel for nitrate reduction in constructed wetlands. Chemical Sciences. Université de Lorraine, 2021. English. NNT : 2021LORR0314 . tel-03708886

HAL Id: tel-03708886
https://hal.univ-lorraine.fr/tel-03708886

Submitted on 29 Jun 2022

HAL is a multi-disciplinary open access archive for the deposit and dissemination of scientific research documents, whether they are published or not. The documents may come from teaching and research institutions in France or abroad, or from public or private research centers.

L'archive ouverte pluridisciplinaire **HAL**, est destinée au dépôt et à la diffusion de documents scientifiques de niveau recherche, publiés ou non, émanant des établissements d'enseignement et de recherche français ou étrangers, des laboratoires publics ou privés.

AVERTISSEMENT

Ce document est le fruit d'un long travail approuvé par le jury de soutenance et mis à disposition de l'ensemble de la communauté universitaire élargie.

Il est soumis à la propriété intellectuelle de l'auteur. Ceci implique une obligation de citation et de référencement lors de l'utilisation de ce document.

D'autre part, toute contrefaçon, plagiat, reproduction illicite encourt une poursuite pénale.

Contact : ddoc-theses-contact@univ-lorraine.fr

LIENS

Code de la Propriété Intellectuelle. articles L 122. 4
Code de la Propriété Intellectuelle. articles L 335.2- L 335.10
http://www.cfcopies.com/V2/leg/leg_droi.php
http://www.culture.gouv.fr/culture/infos-pratiques/droits/protection.htm

Ecole Doctorale C2MP (Chimie - Mécanique - Matériaux - Physique)

Thèse

Présentée et soutenue publiquement pour l'obtention du titre de

DOCTEUR DE l'UNIVERSITE DE LORRAINE

Mention : Chimie

par **Joanna ROGINSKA**

Sous la direction de Mathieu ETIENNE et Frédéric JORAND

Microbial electrochemical snorkel for nitrate reduction in constructed wetlands

Soutenue publiquement le 14 décembre 2021

Membres du jury :

Rapporteurs :	Dr. Nicolas BERNET	Directeur de recherche, INRAE, Narbonne
	Dr. Sebastià PUIG	Professeur agrégé, Université de Girona, Girona
Examinateurs :	Dr. Alain BERGEL	Directeur de recherche - INP Toulouse – Université Toulouse 3, Toulouse
	Dr. Manon GUILLE-COLLIGNON	Maître de conférence, Sorbonne Université, Paris
	Dr. Marie-Noëlle PONS	Directeur de recherche, Université de Lorraine, Nancy
Directeur de thèse :	Dr. Mathieu ETIENNE	Directeur de Recherche - CNRS, Nancy
Invité :	Dr. Frédéric JORAND	Professeur - Université de Lorraine, Nancy

Abstract

The exceeded nitrate concentration in waters is caused by the use of nitrogen fertilizers in agriculture and may result in negative environmental consequences. One of the solutions are constructed wetlands – wastewater treating engineered systems. However, this approach might not be fast enough, especially in periods when nitrate concentration is high and in not sufficiently big wetlands. This thesis is exploring strategies for accelerating nitrate reduction. The denitrification requires an electron donor, such as organic carbon. These compounds appear more in the sediment, while nitrate is present in water, hence we hypothesized that increasing the sediment/water interface will facilitate the access to electron donors and accelerate denitrification, and we evaluated this in the first part of this work. Other strategy to increase this interface was to implement a bioelectrochemical system (BES) with nitrate-reducing biocathode. The BES we studied is a Microbial Electrochemical Snorkel (MES), which consists of one piece of electrode immersed in two different media, here in sediment and water. On the part in sediment an anodic biofilm is developed, which is oxidizing the organic matter. The electrons are then transported to the part of electrode in water, where the cathodic biofilm grows and the reduction of oxygen or nitrate process occurs.

This work aims to create the conditions for developing MES with nitrate-reducing biocathodic part and to characterize its electrochemical properties, microbial community and nitrate reduction efficiency. A literature review about the nitrate-reduction biocathodes is provided in Chapter 1. Chapter 2 describes the materials and methods used in this work. Chapter 3 explores the effect of increasing the water/sediment interface on nitrate reduction. To increase this interface, sediment was arranged vertically in the tubes made of water-permeable tissue. This experiment was first performed in stationary state and by increasing the interface area 10 times, the nitrate reduction was increased up to 6.5 times. The volume of the sediment, its origin and composition, did not have a significant influence on nitrate reduction. This experiment was later repeated in flow, which resulted in 3.5 times faster nitrate reduction, stable for 53 days. The scenario of applying this method in the constructed wetland is considered.

Chapter 4 covers the preliminary studies of MES: the choice of electrode materials and the ratio between part in water and sediment. The development of MES is confirmed by electrochemical analysis and study of microbial community. The addition of nitrate caused the increase of cathodic current and shift of potential. The laboratory results were compared with the results on the field.

Next, MES of increased size and optimized distribution between sediment and water was built (Chapter 5), which confirmed the improvement in nitrate reduction. An increase of cathodic current was observed after addition of nitrate, and it decreased after nitrate was reduced. This current was linked to electron transfer reaction occurring at relatively high potentials when compared to the literature. Microbial analysis showed the significant differences between the community on biocathodes and in sediment and water.

The final chapter is exploring potential role of electrodes in sediments for accelerating nitrate removal. It was implemented by integrating electrode in vertical sediment tubes that were studied in Chapter 3. Stainless steel and carbon felt electrodes were tested, and the latter caused indeed fast nitrate reduction. However, additional experiments showed that the mechanism is not nitrate reduction on the electrode. Carbon felt in sediment caused the release of species and the rapid nitrate reduction occurring in water. Changing the water eliminated the advantage in nitrate reduction. But, clear electrochemical reaction could still be observed at the electrode in sediment after nitrate addition.

Résumé

La concentration excessive de nitrates dans les eaux est due à l'utilisation d'engrais azotés dans l'agriculture et peut avoir des conséquences environnementales négatives, telles que l'eutrophisation des eaux de surface, l'augmentation des émissions de N_2O (un gaz à effet de serre) ou des effets toxiques directs pour la faune aquatique [1]. L'une des solutions proposées pour réduire la quantité de nitrates dans l'eau est la construction de zones humides - des systèmes d'ingénierie qui utilisent les processus naturels tels que la végétation, les sédiments et les bactéries des zones humides pour aider à traiter les eaux usées [2]. Cependant, cette approche peut ne pas être assez rapide, surtout dans les périodes où la concentration de nitrates est élevée et dans les zones humides de taille insuffisante. Cette thèse explore alors des stratégies complémentaires pour accélérer la réduction des nitrates. La réaction de dénitrification nécessite un donneur d'électrons, qui dans le cas général est représenté par des composés organiques. Ces composés se retrouvent davantage dans les sédiments, alors que le nitrate est en solution dans toute la colonne d'eau. Nous avons donc émis l'hypothèse que l'augmentation de l'interface sédiment/eau faciliterait l'accès aux donneurs d'électrons et accélérerait la dénitrification, ce que nous avons évalué dans la première partie de ce travail. Une manière de relier les sources d'électrons dans les sédiments aux ions nitrates était de mettre en œuvre un système bioélectrochimique. Le système exploré dans cette thèse est un tuba électrochimique microbien, qui consiste en une seule pièce d'électrode, immergée dans deux milieux différents, ici les sédiments et l'eau. Dans le sédiment, un biofilm anodique peut être développé sur l'électrode, qui oxyde la matière organique. Les électrons sont transportés vers la partie se trouvant dans l'eau, où un biofilm cathodique se développe et le processus de réduction se produit. Les accepteurs d'électrons peuvent être ici l'oxygène ou le nitrate.

L'un des objectifs de ce travail est de créer les conditions dans lesquelles le tuba électrochimique avec partie biocathodique réduisant les nitrates est développé et de caractériser ses propriétés bioélectrochimiques, la communauté microbienne de son biofilm et l'efficacité de la réduction des nitrates.

Le Chapitre 1 présente une revue de la littérature sur les biocathodes pour réduction des nitrates. Le Chapitre 2 décrit les matériaux et méthodes utilisés dans ce travail. Le Chapitre 3 décrit la zone humide artificielle et étudie l'effet de l'augmentation de l'interface eau/sédiment sur la réduction des nitrates et explore à partir d'un modèle les conséquences de l'amélioration des performances en dénitrification dans la zone humide de Rampillon.

Le Chapitre 4 couvre les études préliminaires du tuba électrochimique : le choix des matériaux de l'électrode et la proportion entre la partie dans l'eau et dans les sédiments. De plus, le développement du système est confirmé par des analyses électrochimiques ainsi que par l'étude de la communauté microbienne. L'ajout de nitrate provoque alors l'augmentation du courant cathodique et le déplacement du potentiel. Les résultats obtenus en laboratoire ont été comparés aux résultats obtenus sur le terrain.

Cette expérience a été suivie par la construction d'un autre tuba électrochimique avec une taille d'électrodes plus importante et une configuration optimisée (Chapitre 5). Cette expérience conduit à une nette augmentation de la vitesse de réduction des nitrates en lien avec les réponses électrochimiques. L'étude des communautés microbiennes de ces biocathodes a alors été menée pour tenter d'identifier les microorganismes en lien avec ces performances.

Enfin, le dernier chapitre de ce travail est consacré à l'exploration du rôle d'électrodes dans les sédiments sur la réduction des nitrates.

Acknowledgements

First of all, I would like to acknowledge my supervisors. Mathieu Etienne, thank you so much for accepting me to participate in “LowNitrate” project, as well as for your guidance, knowledge, countless pieces of useful advises and patience for my doubts and mistakes. Frédéric Jorand, thank you for all your help during this time, especially for advices in microbiological experiments performed during these studies.

I would like to thank to Alain Walcarius for accepting me in his group and for his suggestions and critical opinions over the years that helped me bring this work to completion. Special thanks for the members of the team: Christelle Despas, Marc Hebrant, Grégoire Herzong, Liang Liu, Michel Perdicakis and Neus Vila, who not only helped me many times with their expertise and experience, but also created nice and supportive work atmosphere. I would like to also acknowledge Claire Genois for support in everyday laboratory life as well as Jean-Paul Moulin and Gérard Paquot for their incredible engineering skills. I am also grateful to the secretaries of our laboratory: Christelle Charbaut, Marie Tercier, Sandrine Lemoine, Alzira Soares-Vinot and Jacqueline Druon, who helped me a lot with dealing with complicated French paperwork. I also would like to thank the PhD students and post-docs in LCPME - indispensable companion during all coffee breaks, lunches and after-work parties and trips: Magda Kaliszczak, Taisiia Sikolenko, Himanshu Maheshwari, Qiao Liu, Ranine El Hage, Vincent Feynerol, Julius Gajdar, Mariela Brites Helu, Martha Collins, Guofeng Lu, Jose Vivo Vilches, Cheryl Karman, Wahid Ullah, Tauquir Nasir, Ning Dang, Jianren Wang, Deomila Basing, Stéphane Pinck, Wassim El Housseini, Delphine Truong, Laura Figel and Samuel Ahoulou. In particular, I would like to thank Maciek Mierzwa, because he was the one who first informed me about the internship in Nancy, back in 2017, when he was a PhD student in LCPME. I would like to also thank the students who helped with this project during their internship: Caroline Hazemann, Lise Pignon, Pierre Flaux and Louis Robbe.

I would like to sincerely thank the members of jury for the thesis defense, Nicolas Bernet, Sebastià Puig, Marie-Noelle Pons, Alain Bergel and Manon Guille-Collignon, for dedicating their time to evaluate my research. Certainly, their remarks and suggestion will help to improve the quality of this work. Additionally, I would like to thank Marie-Noelle Pons and Sylvie Dousset for their giving me helpful suggestions as members of my monitoring committee.

With other members of the project “LowNitrate”, which were: Julien Tournebize, Cédric Chaumont and Théodore Bouchez from INRAE, Frédéric Barriere and Timothe Philippon from Université de Rennes and Alain Bergel and his co-workers from Université de Toulouse, we were meeting regularly during these years and we spent hours on valuable discussions and exchanging ideas. I am truly grateful for the opportunity to work with you.

I would like to thank Ulo Mander and members of his group: Mikk Espenberg, Martin Maddison, Kuno Kasak, Rauno Lust and others, for warmly welcoming me in Tartu, Estonia where I spent 10 weeks on a research internship.

I am really grateful for numerous friendships which I made during my stay in Nancy. Dasha, Dorota, Houda, Toni, Waldez, Lesha, Valeriia, Shantanu, Satish, Anna, Erika, Matteo, Ziad, Kamil, Miguel, Ricardo, Audrey and all the others, we had a lot of amazing moments together and you made this time unforgettable.

Finally, I would like to thank my family and friends in Poland, who were constantly supporting me from the distance and during my visits. My mom and dad encouraged me to take this opportunity, even though it meant that I would not be close. They also took care of our beloved black cat and they were regularly sending me his pictures which were cheering me up. With my closest friends in Poland: Alicja, Karolina, Agnieszka, Robert, Kasia and Monika I chatted almost every day, therefore when I was visiting Warsaw, it felt like I never left.

Last but not least, I would like to acknowledge The French National Research Agency for funding LowNitrate project and therefore my PhD (ANR-17-CE04-0004), and International mobility support for PhD students–DrEAM (Université de Lorraine) for funding my internship in Estonia.

Table of contents

List of abbreviations

Ag/AgCl - Silver chloride electrode

BES - Bioelectrochemical System

BOD - Biological Oxygen Demand

COD - Chemical Oxygen Demand

CV - Cyclic Voltammetry

CW - Constructed Wetlands

DO - Dissolved Oxygen

MES - Microbial Electrochemical Snorkel

MEC - Microbial Electrolysis Cell

MFC - Microbial Fuel Cell

NCC - Net Cathodic Compartment

NRB - Nitrate-reducing Biocathode

NRR - Nitrate Reduction Rate

OCP - Open-circuit Potential

SCE - Standard Calomel Electrode

SHE - Standard Hydrogen Electrode

SMFC - Sediment Microbial Fuel Cell

TCC - Total Cathodic Compartment

TEA - Terminal Electron Acceptor

1. Introduction

1.1. Nitrate in the environment

Due to the growing population and development of humans, the emission of different pollutants, such as carbon and nitrogen species is increasing and contributing to climate changes and other negative environmental effects. Among these pollutants there is nitrate, which can contaminate surface and ground waters, leaking from agricultural fields fed with nitrogen fertilizers. In order to decrease its quantity in water, many approaches were already investigated, such as separation-based, chemical and biological methods. One of the latter is denitrification - the microbial nitrate reduction to nitrogen. The first part of this chapter will therefore introduce the nitrogen cycle, current challenges connected with increasing nitrate concentration and the common methods of nitrate removal.

Bioelectrochemical Systems (BES), which employ microbes as catalysts to convert chemical energy into electrical energy (or conversely), have emerged in recent years for water purification and energy recovery. Currently, the research using bioelectrochemical nitrate reduction on biocathodes is gaining more and more attention. The nitrate-reducing biocathodes (NRB) are proved to efficiently treat nitrate-polluted wastewater. However, they require specific conditions and they were not yet applied in bigger scale. In this chapter, the current knowledge about the NRBs will be summed up. The fundamentals of biocathodes will be discussed, as well as the progress made in applying them for nitrate reduction. NRBs will be compared with other nitrate-removal techniques and the challenges and opportunities of this approach will be identified.

1.1.1. Nitrogen cycle

In the natural N cycle, the fixation of gaseous dinitrogen (N_2) requires energy in order to break N⁝ N triple bond. This energy can be physical (lighting), creating the nitric (NO) or nitrous oxides (N_2O), or chemical, catalyzed by nitrogen fixing bacteria, producing ammonia (NH_3). The latter can be also produced in the process of ammonification - bacterial transformation of nitrogen organic compounds to ammonia. Then, it can be used by the nitrifying bacteria in nitrification, which is an aerobic process of biological oxidation of ammonia to nitrogen oxides. Usually, nitrification occurs in two sequential oxidative steps, performed by different bacterial genera: ammonia oxidation to nitrite (NO_2^-) by bacteria which use ammonia as electron donor and nitrite oxidation to nitrate (NO_3^-) by bacteria which use nitrate in this purpose (Fig. 1.1). In both cases, molecular oxygen is the electron acceptor and

carbon dioxide is the carbon source [1]. Then, nitrous oxides can be assimilated by plants or reduced in denitrification: a microbial process of dissimilatory reduction of nitrate or nitrite to gaseous oxides: nitric oxide or nitrous oxide, which can be further reduced to dinitrogen (N_2) [2]. Another metabolic group of bacteria was evidenced relatively recently in anoxic environments: the anammox bacteria (anaerobic ammonium oxidation) [3]. These bacteria carry out a denitrification decoupled from the oxidation of organic carbon in anoxia, i.e. they directly couple the oxidation of ammonium to the reduction of nitrate. Finally, the anaerobic respiration of chemoorganotrophic microbes, in the organic matter rich environment, can result in dissimilatory nitrate reduction to ammonium (DNRA) (Figure 1.1.). Generally, reactive nitrogen can exist in the form of ammonium, nitrate, nitrite, nitrous and nitric oxides, nitrous and nitric acids, peroxyacyl nitrates, as well as nitrogen organic compounds such as amino acids and other compounds, which circulate between atmosphere, terrestrial and marine ecosystems [4,5].

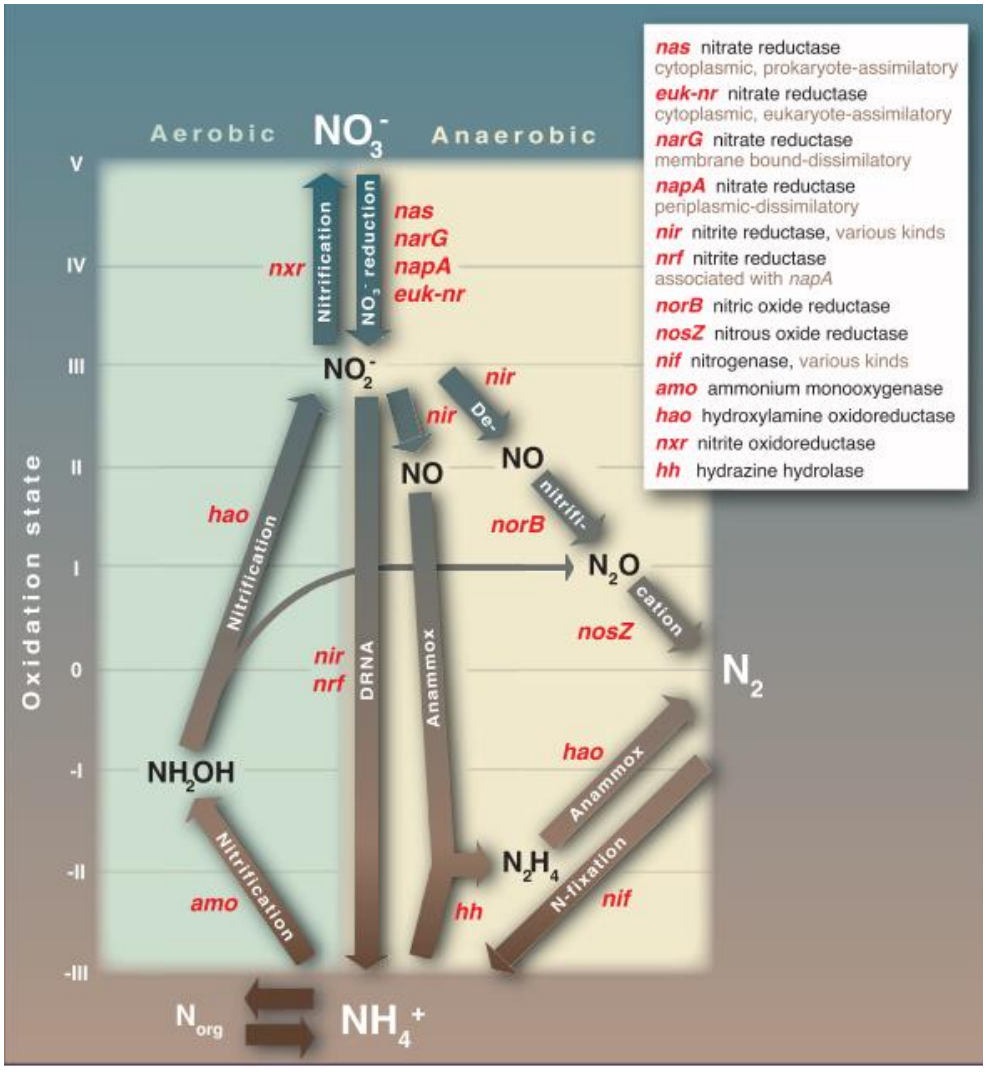

Figure 1.1 *Major transformations in the nitrogen cycle* [5]

Nowadays, half of the global nitrogen fixation is anthropogenic [6], formed mainly in the Haber-Bosch process, but also by substantial legume crops and fossil fuel combustion (Fig. 1.2) [7]. Currently the production of alimentation for around 48% of the world population depends on nitrogen fertilizer input synthetized in Haber-Bosch process; this fertilizer is also used for biofuel and bioenergy production [8]. However, such disturbance of the natural cycle raises a question about the effect on the environment. Burning fossil fuels releases carbon from the ground to the atmosphere in form of CO_2, which disturbs the natural global carbon cycle and is the main cause of climate change. The possible scenarios are now the matter of global discussions which had a consequence in enacting the Paris Agreement. Within a framework of it, about 190 countries agreed to aim for climate neutrality in order to limit the global temperature increase to 1.5 $^{\circ}$C. Yet, less attention is put on the consequence of also significant disturbance of nitrogen cycle on the climate and environment [9]. Fig. 1.2 compares the natural (purple) and anthropogenic (brown) rates of nitrogen flux in the modern nitrogen cycle. The anthropogenic operations provide around 45% of total fixed nitrogen produced annually. From 1960 to 2000, the use of nitrogen fertilizer increased by 800%. The excess of nitrogen in soil increases productivity and CO_2 uptake of ecosystem, but decreases the biodiversity. Moreover, in regions where soils are poor in N, its addition will first increase fecundity and C storage, but it will ultimately lead to increased losses of N and cations from soils. The most nitrogen species in these fertilizers is NH_4^+, which is easily transformed to NO_3^-, which later leaks to surface and ground waters. Fluxes of human-fixed N reaching various bodies of water result in eutrophication, blooms of nuisance and even toxic algae, and creating the environment harmful for aquatic fauna. Part of these nitrogen species will be incompletely denitrified, creating nitrous oxide, which also contributes to the climate changes (N_2O is a greenhouse gas of global warming potential of 265-300 times relative to CO_2, mole to mole) and substantial contribution to acid raining and photochemical smog [5,7,10]. Moreover, the presence of nitrate in drinking water can be toxic for humans, which is mainly attributed to its reduction to nitrite. Nitrite causes oxidation of hemoglobin (Hb) to metHb, which is unable to transport oxygen to tissues. The condition when the metHb is above 10% of hemoglobin is called methaemoglobinaemia and is particularly dangerous for infants. High intake of nitrate and/or nitrite could be also carcinogenic [11]. European Union allows up to 11.3 mg $N\text{-}NO_3^- L^{-1}$ (50 mg $NO_3^- L^{-1}$) and 0.14 mg $N\text{-}NO_2^- L^{-1}$ (0.5 mg $NO_2^- L^{-1}$) in drinking water, with a condition that $[NO_3^-]/50 + [NO_2^-]/3 \leq 1$ [12], while in the United States the limit is 10 mg $N\text{-}NO_3^- L^{-1}$ and 1 mg $N\text{-}NO_2^- L^{-1}$ [13].

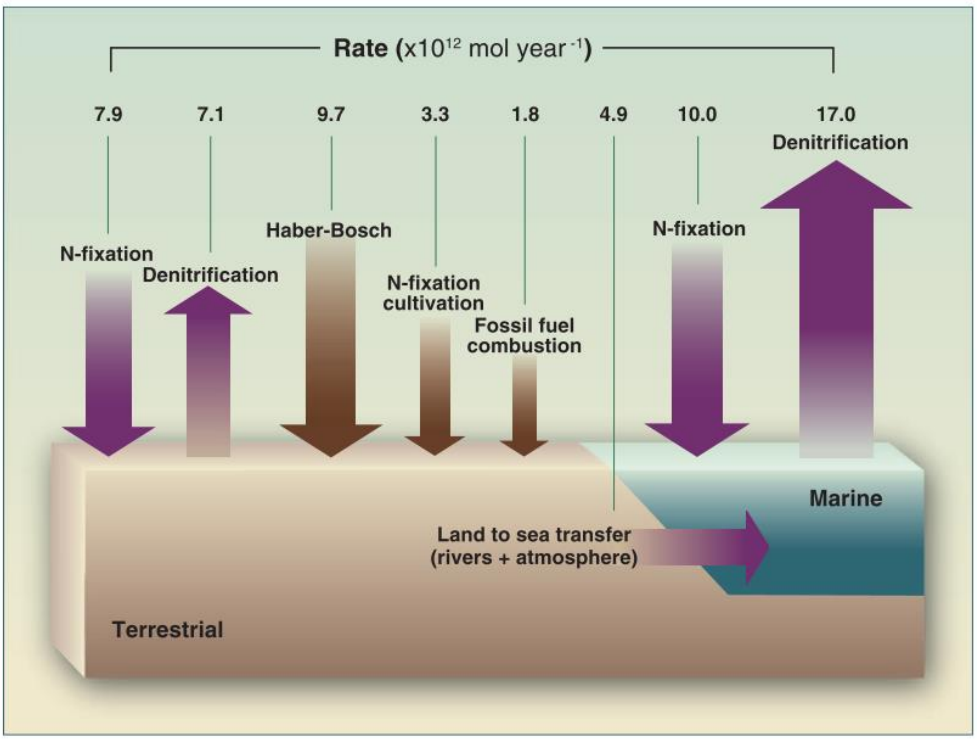

Figure 1.2 *Rates of nitrogen flux in the modern nitrogen cycle. The purple arrows are showing natural processes and the brown arrows show anthropogenic ones* [5].

European Union recognized the hazard and in 1991, it adopted the "Nitrate Directive" concerning the protection of waters against pollution caused by nitrates from agricultural sources. It aimed to maintain the good water quality in Europe by preventing the nitrate leaking from agricultural sources and by promoting the use of good agricultural practices. The member countries were obliged to limit the use of nitrogen fertilizers, use the safe manure storage methods in order to prevent the leaking, to determine the buffer zones between the surface water and the area of use of fertilizers and to monitor the level of nitrate in surface and ground waters and to identify the "Nitrate Vulnerable Zones" [14]. In 2020, the University of Hertfordshire (UK) published the final report of European Commission's project ""Providing support in relation to the identification of approaches and measures in action programs under Directive 91/676/EC" which created an inventory of the nitrate action programs implied in member countries and regions, as well as the web application collecting these programs [15].

1.2. Nitrate removal methods

There are several methods of nitrate removal which can be divided into physical, chemical, electrochemical [16], as well as biological and bioelectrochemical. This part will

introduce the principle of each of them, with a special focus on bioelectrochemical methods, in particular on Microbial Electrochemical Snorkel.

1.2.1. Physical methods

Physical methods of nitrate removal are separation-based and include reverse osmosis, ion exchange and adsorption. Reverse osmosis is a process using a partially permeable membrane, in which the applied pressure overcomes the osmotic pressure which allows the separation of unwanted ions or other molecules [17–19]. Activated carbon can be used to adsorb the nitrate from water, however its activation requires the high temperature or chemical treatment. There are currently studies focusing on increasing the nitrate uptake by activated carbon [20–22]. Clay and clay-minerals can also be used for nitrate adsorption from water [23]. Ion exchange is a method in which nitrate-loaded water is passing through anion exchange resin bed, where nitrate ions are exchanged for chloride. Once the resin's exchange capacity is exhausted, it can be regenerated using the concentrated chloride solution [24,25]. All in all, most of the separation-based methods are effective but expensive, they are not always selective for nitrate, and require reprocessing of the generated waste brine [26]. This nitrate brine could be purified with electrochemical methods, however the challenge of this approach is to combine the reduction of nitrate with oxidation of released ammonium as well as to avoid formation of undesired by-products of this reaction [27,28].

1.2.2. Chemical and photochemical methods

Chemical methods involve nitrate reduction by metals, for example zero valent iron [29] or magnesium [30]. The big scale application of these methods is limited by the difficulty of preventing the formation of ammonia or other undesired products and by the limitation of reaction rate by diffusion in large particles. However, using powdered metals raises another challenge of latter separation [26]. Another approach is to use photocatalytic reduction of nitrate over semiconductor materials, such as titanium dioxide. This technique could be used in treating brine containing nitrate from separation-based methods, however, it required also additional electron donor, for example formic acid [31].

1.2.3. Electrochemical methods

Electrochemical methods include electrocoagulation and electrodialysis. Electrocoagulation is a process of water treatment which consists of several steps: first, a sacrificial anode is oxidized which results in formation of oxides, hydroxides or oxyhydroxides.

These ions are a cause of destabilization of contaminants which results in coagulation and formation of floc, which can be more easily separate from clean water [32]. In electrodialysis, the applied electric potential difference influences the transport of ions through ion-exchange membrane. The electrodialysis cell consist of two compartments: diluted feed and concentrated brine; which are formed by anion-and cation exchange membranes placed between two electrodes. The pollutant ions are migrating to a given electrode through the membrane. Usually, the electrodialysis cell is composed of many unites of membranes and electrodes [33–36].

1.2.4. Biological methods

The main biological method of nitrate removal is denitrification, which was already briefly defined in Part 1.1. The complete denitrification consists of four reduction steps from nitrate towards dinitrogen, with the use of 5 moles of electrons per mole of nitrogen [37]:

$NO_3^- + 2\ e^- + H_2O \rightarrow NO_2^- + 2OH^-$ Eq.1.1

$NO_2^- + e^- + H_2O \rightarrow NO + 2OH^-$ Eq.1.2

$NO + e^- + ½\ H_2O \rightarrow ½\ N_2O + OH^-$ Eq.1.3

$½\ N_2O + e^- + H_2O \rightarrow ½\ N_2 + 2OH^-$ Eq.1.4

Denitrifying bacteria are mostly facultative anaerobes, yet denitrification occurs in the absence of oxygen and nitrogen oxides are terminal electron acceptors in the respiratory process. In heterotrophic denitrification, organic carbon source such as carbohydrates, organic alcohols, amino acids and fatty acids is also required to act as electron donor and for cell growth. In addition, some denitrifying bacteria can however utilize inorganic compounds, such as dihydrogen or reduced sulfur compounds as electron donors in autotrophic denitrification [1,38]. Abundance of accessible electron donors and low oxygen concentration are the two most important factors for the denitrification to occur [39–41]. Other parameters, such as nitrate concentration, hydraulic conditions, pH, temperature, water composition (salinity, inhibitory substances) or microbial communities have secondary effects [42,43]. For efficient nitrate reduction to dinitrogen, a proper C/N ratio should be kept. For easily accessible compounds the chemical oxygen demand (COD, $mgO_2\ L^{-1}$)/N-NO_3^- w/w ratio might be from 3.0 to 6.0, depending on the nature of carbon compound and on the bacterial species. Consequently, the C/N ratio is a factor influencing the final product of heterotrophic denitrification [44]. In the process of electron transportation from its donor to acceptor, the organism gains energy which can be used for the synthesis or for maintaining existing cell mass [1]. For some bacteria, the main product of nitrogen oxides reduction can be ammonia (NH_4^+), however, such process is

no longer considered a denitrification. Denitrification can occur in terrestrial, freshwater and marine systems, where nitrate and nitrite are present in the environment [45]. The large scale application of biological denitrification brings several challenges, such as the risk of gaseous nitrous oxide production, the need to dose precise amount of carbon compounds, big enough to ensure complete denitrification and low enough to prevent excessive growth of biomass and redundancy of organic compounds in effluent, and necessity to keep low oxygen concentration [46].

Hydrogenotrophic denitrification (autotrophic denitrification with the use of H_2 as electron donor) is an interesting process because of the high selectivity for nitrate removal and lack of harmful by-product; the only products are dinitrogen and water so there is no need for post-treatment. However, main limitation is the fact that use of dihydrogen can create an explosive atmosphere in treatment plants [47].

Many different strategies can be employed to improve the heterotrophic biological denitrification in water, such as sludge systems or denitrifying bioreactors. In general, the activated sludge process is using biological floc composed of bacteria and protozoa to treat wastewaters [48]. Denitrification can occur in a process of anaerobic digestion with the use of anaerobic methanogenic sludge [49]. Denitrifying bioreactors include denitrification beds, denitrification walls, denitrification layers or woodchips bioreactors. They have solid carbon substrates in the flow path of water contaminated with nitrate. These substrates, usually fragmented wood products, prevent the shortage of electron donors so the reactor can last up to 15 years [50]. More simple concept, constructed wetlands (CW) in free surface flow configuration are ecological engineering systems which take advantage of the processes which occur in the natural wetlands, such as wetland vegetation, sediments and microbial communities of wetlands to assist in treating waters in controlled environment [51].

The combinations of different methods are also studied, for example nitrate removal by ion exchange, where brine is later treated by biological denitrification [52].

Table 1.1 *Advantages and disadvantages of the main treatment processes of nitrate reduction* [53]

Method	**Advantages**	**Disadvantages**
Reverse osmosis	• Very efficient, produces high-quality water • Multiple contaminant removal • Can be automatized • Easy to use	• High energy cost • Need for pre- and post-treatment of water • Generates waste brine

Electrodialysis	• Lower pressure than reverse osmosis • Long lifespan of the membrane • Can be adapted to any size system	• May require a pre-treatment • Need for constant pH regulation • May produce waste from washing the membranes • Expensive
Ion exchange	• Very efficient • Can be automatized • Stable operation	• Generates waste brine • Expensive
Biological denitrification	• Lower cost than separation-based methods • Good efficiency • No need for chemical substances	• Longer time of operation than other technics • Efficiency may depend on inlet water parameters • Need for additional processes in order to eliminate products of bacterial activity • Need for maintenance and monitoring of biomass and its composition • Highly dependent of the organic electron donor (the limiting factor)

1.2.5. Bioelectrochemical systems for denitrification

Bioelectrochemical methods are employing electrode materials to link electrochemistry with biological denitrification. They include microbial fuel cells (MFC), microbial electrochemical snorkel (MES), microbial electrolysis cells (MEC) and their modifications.

Bioelectrodes

The BES have at least one bioelectrode, i.e. an electrode covered by an electroactive biofilm that is using this electrode support as electron donor or electron acceptor for bacterial metabolism. In general, most of microorganisms oxidize the organic matter and the electrons released in this process are used in the cellular respiration. Respiratory enzymes catalyze the transfer of these electrons from organic compounds to terminal electron acceptors (TEA), such as oxygen, nitrate, sulfate etc. which are then reduced. These TEA can diffuse inside of the bacterial cell to accept the electron. However, some bacteria, called *exoelectrogens*, can transfer the electron outside of the cell and use solid conductive material, such as metal oxide, as TEA in the process of *exoelectrogenesis*. These bacteria can form bioanodes on the solid electrodes.

Another possibility is to, instead of organic compounds, use the electrode as electron donor, and bacteria which have this ability can form biocathodes.

The extracellular electron transfer can occur by two main pathways: direct electron transfer or indirect electron transfer via mediator or by extracellular polymeric substances of biofilms (Fig. 1.3) [54]. The direct electron transfer requires a physical contact between electrode surface and bacterial cell membrane or nanowires. This membrane should contain redox macromolecules such as cytochromes which exchange the electron. If the microorganisms are not capable of such direct electrons exchange, the mediators or by-products can be used to carry the electron between cell and electrode by indirect - mediated electron transfer. Some bacteria can excrete redox compounds which can be used for electron transfer. Manganese or iron can be also used as soluble exogenous oxygen mediators [55,56]. The extracellular polymeric substances of biofilm can contribute to both direct or indirect electron transfer. It helps attaching cells to the solid electrode, therefor shortens the gap between cell membrane and electrode's surface for direct transfer. In case of indirect transfer, the polymeric substances are beneficial because it accumulates electron shuttles between bacteria and elector donors or acceptors [57].

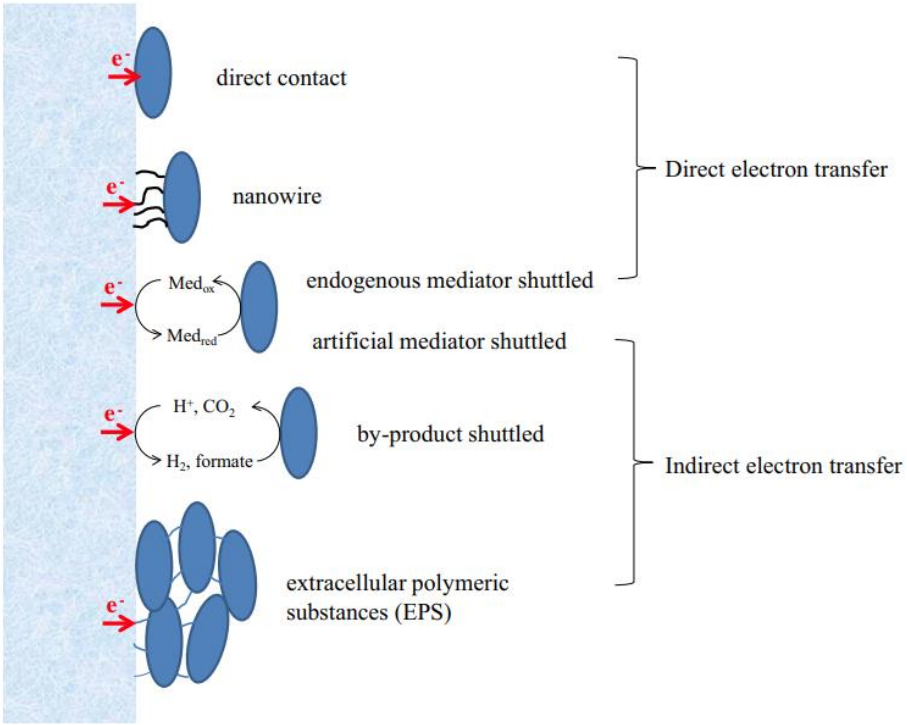

Figure 1.3 *Different pathways of cathodic electron transfer* [54]

Microbial Fuel Cells (MFC)

MFC is a bioelectrochemical system capable of energy production from biomass with utilization of bacteria [58]. The standard MFC is shown on Fig. 1.4. It consists of two compartments separated by an ion-exchange membrane. In one compartment, the oxidation of electron donors (usually some organic compounds, for example acetate) occurs on the biofilm covering the electrode – the electrode here plays the role of electron acceptor. The generated current is then transported to the electrode in the second compartment, where reduction of electron acceptor occurs. Generally, in MFC at least one electrode should be a bioelectrode – bioanode or biocathode. Usually, when the MFC is designed to produce power, the oxygen is used as the electron acceptor. Many modifications were proposed to increase the cathodic efficiency, including the air-cathode MFC, in which the uptake of oxygen from the air eliminates the necessity of energy consuming air bubbling of the water [59]. In terms of denitrification, the nitrate reduction occurs at biocathode in anaerobic environment, with the electrode as the only electron donor [60].

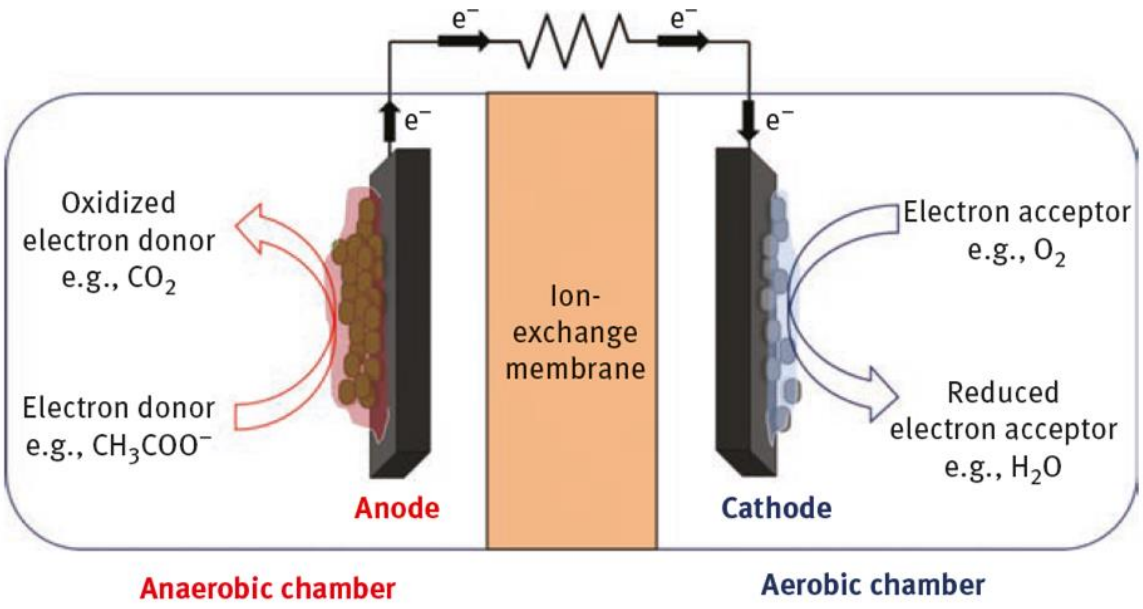

Figure 1.4 *A schematic diagram of two-chamber MFC* [56]

Except power production, the main focus of the studies of MFC equipped with NRB is efficiency in nitrate treatment. Nitrate reduction rate (NRR) achieved with NRB should be competitive with other methods for nitrate removal, such as mentioned before CWs or denitrifying bioreactors. For CWs, the highest reported values of NRR are in a range of about 3.7 to 4.5 g $N\text{-}NO_3^-$ m^{-3} day^{-1} [61,62]. Denitrification walls have the NRR of up to 5.5 g $N\text{-}NO_3^-$ m^{-3} day^{-1} [50,63,64] and for denitrification beds, it could be up to 22-23 g $N\text{-}NO_3^-$ m^{-3}

day^{-1} [50,65]. The articles exploring NRB are giving a wide range of values of NRR which are listed in Tables 1 and 2 in Appendix 1. Some of the most efficient nitrate reducing BES will be cited in the next section.

For example, in one of the early works describing MFC with NRB, Virdis et al. reached NRR of 410 g $N\text{-}NO_3^-$ m^{-3} day^{-1}. This setup was created to treat one stream of wastewater containing acetate and ammonium, which was turned to anaerobic anodic chamber in order to remove organic compounds, then it was passing through external aerobic nitrification stage and finally the denitrification occurred in cathodic chamber. The acetate was removed completely in this study and only very small concentrations of nitrate were present in the effluent of cathodic chamber, however, some nitrate was reduced to ammonium in the cathodic chamber. The COD/N ratio was 4.48 g COD g^{-1} $N\text{-}NO_3^-$ and the best denitrification values were achieved for the resistance of 5-10 Ω [66]. Clauwaert et al. were operating their BES in MFC mode (BES producing electrical energy) and MEC mode (electrical energy is applied to BES to drive the electrochemical reactions). The NRR was up to 500 g $N\text{-}NO_3^-$ m^{-3} day^{-1} when the pH in cathodic compartment was kept at a constant value of 7.2, comparing to 220 g $N\text{-}NO_3^-$ m^{-3} day^{-1} without the pH control [67]. Zhang et al. prepared a denitrifying BES consisting of two chambers, in which the cathode's potential was kept at 0.0415 V vs SHE (-0.2 V vs SCE). They were following nitrate reduction starting from different initial concentrations and they described the results of reduction rate by Monod equation, which allowed to estimate that the maximum NRR in this experiment can be up to 1330 g $N\text{-}NO_3^-$ m^{-3} day^{-1} [68]. Clauwaert et al. in the first work describing MFC with NRB obtained 146 g $N\text{-}NO_3^-$ m^{-3} day^{-1} [37]. Al-Mamun et al. combined MFC with anaerobic sequencing batch reactor which allowed to treat insoluble, polymeric and complex organic compounds together with nitrate, coupling it with recovering energy. They reached the rate up to 125.7 g $N\text{-}NO_3^-$ m^{-3} day^{-1} [69]. One of the highest reported NRR values so far was the one by Vijay et al., who used soil and cow manure and combined heterotrophic and autotrophic denitrification to remove 6500 g $N\text{-}NO_3^-$ m^{-3} day^{-1}. The electrode surface was relatively low and there was cow manure and soil in the cathodic chamber (sources of bacteria but also electron donors), therefore probably the significant part of nitrate was removed by biological denitrification. Nevertheless, closed circuit MFC increased the rate by two up to three times comparing to the open circuit one which means that bioelectrochemical denitrification also played a role [70].

These examples are showing that employing bioelectrochemical nitrate reduction can be beneficial to treat nitrate-polluted waters in bigger scale. The NRR can be much higher than those which were obtained with CW or denitrifying bioreactors. However, the research of NRB

is still in its early stage. NRB are usually prepared in smaller scale and the NRR per 1 m^3 is calculated on the basis of laboratory results. Increasing the scale could decrease the efficiency. Choosing the most optimal system for application could also be difficult because of very different materials and conditions in different studies. For example, due to the popular choice of electrode materials for which the active surface area is difficult to define, such as graphite granules or felt, comparison of efficiencies vs electrode area is problematic. The prize of its application is an additional question. Nevertheless, the MFC employing NRB have a great potential to be used for treating polluted wastewaters.

Microbial Electrolysis Cells (MEC)

MEC are devices similar to MFC, also consisting of two electrodes in two compartments, separated by a membrane (Fig. 5). The electrodes are connected to the electrode power sources, so the difference is that in MEC the power is required in order to produce the hydrogen and/or other chemical compounds. For nitrate removal application, this hydrogen can be used as the electron donor to reduce nitrate in the process of autotrophic denitrification [71]. In order to eliminate the need of external power supply, MEC is sometimes paired with MFC, which produces electric energy needed for hydrogen production [72]. Recently, applying three air cathode MFCs connected in series with MEC, resulted in increasing denitrification rate from 56.5% to 80.6% (control experiment was autotrophic denitrification MFC, starting concentrations were 20-50 mg N-NO_3^- L^{-1}) [73].

Microbial Electrochemical Snorkel (MES)

A specific type of MFC is a MES. It is composed of two electrodes in shortcut, which could be even simplified to one piece of electrode immersed in two different environments: sediment and water (Fig. 1.5). In sediment, the anodic biofilm formed on the electrode oxidizes the available electron donors. Since the sediment is anaerobic and also poor in nitrates, the access of electron acceptors is limited so the solid electrode can be used in this role. Therefore, the electrons released in the oxidation are then transported via the electrode to the cathodic biofilm formed on the part in water, where they are used to reduce the electron acceptor: oxygen, nitrate or other compound. Since the two bioelectrodes are in shortcut, no power can be produced in such configuration but it allows reaching the maximum current. First MES was described in 2011 [74]. Two different concepts were described in this manuscript, called by authors “short-circuit MFC” and “MES”. Short-circuit MFC here consisted of 0.5 mg Pt cm^{-2} carbon felt as air-cathode and another piece of pre-colonized carbon felt as anode, connected in short-circuit. MES was a titanium rod connecting colonized graphite felt in the sediment and

platinum-covered part in water. The systems aimed for COD removal and they reached around 55% of removal - to compare, the traditional MFC with 1000Ω resistance reached 35% of COD removal. MES was also studied for treating the oil-contaminated sediment. In the study from 2015, the contaminated sediment was covered with sand and with graphite granules serving as oxygen reduction catalyst; also, the oxygenated seawater was used and the graphite rod MES was inserted vertically. The MES accelerated the oxidative reactions in the sediment, the oxygen uptake and CO_2 evolution in microcosms [75]. The same group continued to study this type of MES and confirmed its effect on the bulk sediment. They noticed the increased reduction of sulfate driven by organic contaminant oxidation [76].

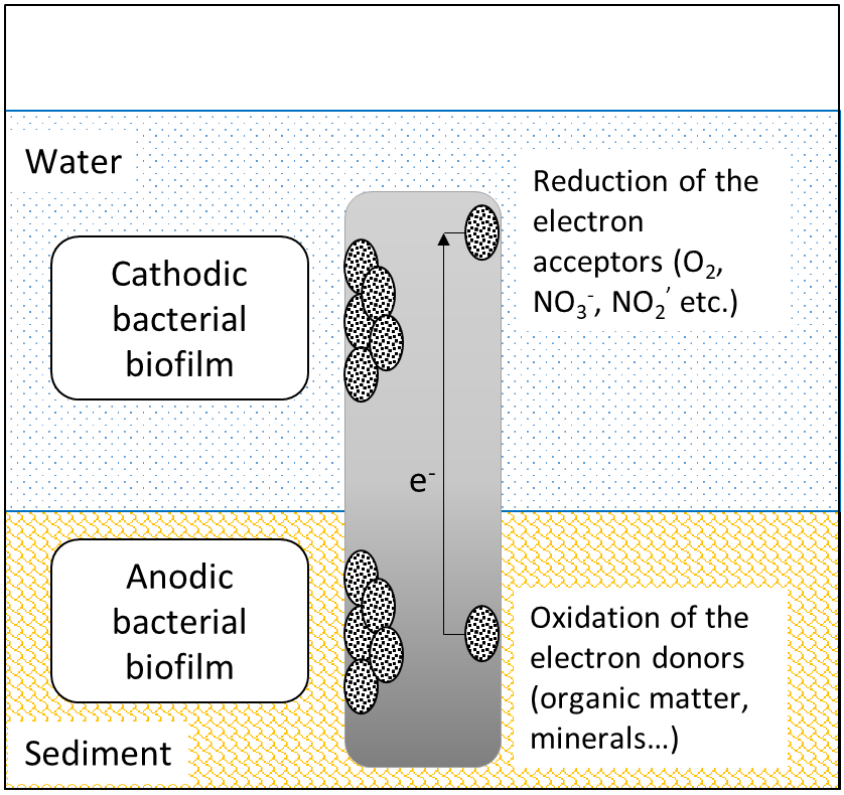

Figure 1.5 *Schematic diagram of Microbial Electrochemical Snorkel*

In order to move towards an application in constructed wetlands, a new concept was tested: Electroactive Biofilm-Based Constructed Wetlands. The MES was consisting of calcined petroleum coke placed in the columns through which the contaminated influent was passing [77]. The presence of the electrode increased the COD and phosphate removal efficiency. The increase of ammonium removal was also noticed but associated with plants present in the system. Also, the positive electric potentials were measured in the system containing electrodes, which is interpreted as confirmation of presence of electroactive biofilms; current density was then calculated basing on these potential values. In the

corresponding control experiments with sand, potential was always zero and so was the corresponding current density.

MES could be also applied for metal recovery and recently first tests were performed with copper [78]. The setup consisted of graphite anode in the sediment and copper foil cathode in $CuSO_4$ solution over it. The electrodes were in shortcut, with or without a proton exchange membrane (PEM) between them. The total copper removal occurred in 2 days in MES without PEM and it took 10 days in MES with PEM or with control MFC (R = 510Ω). Therefore, applicability of MES for this purpose was first demonstrated and there is a field for further exploration.

Another article was more focused on the microbial mechanism of MES [79]. Here, the snorkel was graphite rod, which was partially in the serum bottle with *Shewanella decolorationis*, partially in air (not colonized). It confirmed that *S. decolorationis* can use the MES as an alternative electron transfer pathway for oxygen reduction.

Little research was so far dedicated to study the nitrate removal using MES. In 2015, Yang et al. reported MES consisting of a piece of carbon felt in the sediment and iron rod connecting sediment and water environment [80]. The authors achieved the very good results of 98% of nitrate removal in MES system in 16 days comparing to 29% in 24 days for control experiment with sediment but without MES. However, the initial nitrate concentration was around 2 mg $N\text{-}NO_3^-$ L^{-1} (8.8 mg NO_3^- L^{-1}), while the World Health Organization described surface water concentrations up to 18 mg NO_3^- L^{-1} as low [11]. European Union defines the nitrate-contaminated water as water with nitrate concentration over 50 mg NO_3^- L^{-1} [14], therefore such low concentrations are usually not considered as a pollution. Moreover, a green rust-like coating was found on a cathodic part of MES. Green-rust is a generic name for a mix of Fe^{II}-Fe^{III} double hydroxysalt minerals, which is a corrosion crust on iron and steel surfaces. It can lead to a conclusion that the nitrate reduction did not occur by biocathodic reduction, but by chemical reaction with iron and/or by reaction with contribution of nitrate-reducing bacteria [81–83].

Another publication does not focus exactly on MES but it is worth mentioning because it studies the influence of different applied resistance on efficiency of MES in nitrate treatment [84]. Sediment MFC (SMFC) was used, in which both anode and cathode were carbon felt, acclimated in a lake for two months, and the resistance was varying from 1000 to 1Ω. It was found that with decreasing resistance, the current density and nitrate removal efficiency are increasing, which confirms a concept of MES. The SMFC with 1Ω resistance achieved 60%

nitrate removal in 115h, with also low starting nitrate concentration of 2.5 mg $N\text{-}NO_3^-$ L^{-1} (11 mg NO_3^- L^{-1}), which was the concentration of nitrate in the lake.

1.3. Nitrate-reducing biocathodes

As it was explained in the previous section, BES coupled with NRB can give promising results in terms of denitrification. However, growing a NRB requires specific environment. This chapter will describe the concept of biocathodes and define the conditions necessary for development of NRB, such as anaerobic environment, the optimal pH, the optimal polarization or external resistance, the best electrode materials, and the influence of water conductivity. The results will also be analyzed, including comparison of the cyclic voltammetries and discussion about bacterial communities. Finally, the products of nitrate reduction will be discussed, as well as the possibility of changing the role of bioelectrode: switch between bioanodic and biocathodic conditions.

1.3.1. Biocathodes

Historically, the current generated by bacteria was first observed by Potter in 1911 [85]. In the early stage studies, electron shuttles or mediators were added in order to ensure the electron transfer from inside the cell to the electrode yet in 1999 it was discovered that certain bacteria are capable of producing power in absence of these exogenous mediators [86,87]. Since then, the number of studies on MFCs is increasing and various modifications of architecture, electrodes, electrolytes, microbiota and membranes are described in order to increase the efficiency of the device. One of the bottlenecks is cathodic performance. Very often, the cathode is made of, doped or covered with platinum which serves as a catalyst, because it has a low overpotential for oxygen reduction [88]. However, it has limited availability, high cost and possible negative environmental effects. Non precious metal-based catalysts, such as lead, cobalt or iron based material were also studied and showed promising improvements in power output, but the general concerns are risk of metal leaching from the cathode and sensibility for conditions occurring in MFC, for example decrease of catalytic activity in sulfate or chloride-rich, or high pH environment. Another solution is to use a mediator in the cathodic chamber, which transfer electrons from the electrode to terminal electron acceptor. They also reduce overpotential and usually are reversible redox species. The most commonly used mediator is ferricyanide, which reacts in a following way:

$$[Fe(CN)_6]^{3-} + e^- \rightarrow [Fe(CN)_6]^{4-} \qquad (E'^0 = 0.358\ V) \qquad \text{Eq. 1.5}$$

$$O_2 + [Fe(CN)_6]^{4-} + 4H^+ \rightarrow [Fe(CN)_6]^{3-} + 2H_2O \qquad \text{Eq. 1.6}$$

Ferricyanide has fast reduction kinetics, relatively high redox potential, and it is well soluble in water. However, it is not a sustainable choice for application for electricity generation, because it is sensitive to light, due to the low rate of regeneration by oxygen it should be regularly replenished, and in long-term operation it can diffuse through the membrane [89].

The idea of using microbial catalyst on a cathode came after the first proof that the electrode can serve directly as the electron donor for bacteria, which was described in 2004 [90]. In this study, the electrode poised at -500 mV vs Ag/AgCl was the only possible electron donor in nitrate-rich anaerobic environment. The source of bacteria was sediment inoculum. In such setup, nitrate was reduced to nitrite, which was not observed in control experiment without polarization or with dead bacteria; moreover, the negative current was observed when nitrate was added to the cathodic chamber. Microbial analysis and further tests showed that the bacteria species responsible for this reduction was *Geobacter* sp. Soon after, another study was published, in which the current (200 mA) was applied to the biocathode and with the sludge from sewage treatment plant used as bacteria source. In this study, for the first time the complete denitrification on biocathode (nitrate to dinitrogen) was observed. Moreover, the decrease of nitrate concentration in the experimental environment resulted in potential decrease from -80 to -260 mV vs Ag/AgCl [91].

In 2007, the first MFC in which microorganisms performed the complete denitrification in cathodic chamber, at a rate up to 0.146 kg NO_3^--N m^{-3} net cathodic compartment (NCC) d^{-1} or 0.080 kg NO_3^--N m^{-3} total cathodic compartment (TCC) d^{-1}, using only electrons supplied by microorganisms from the anodic chamber, oxidizing organic material [37]. No H_2 was detected in the gas product. The authors tested different external resistance or applied voltages between anode and cathode. They found that with fixed external resistance, the produced current was proportional to the denitrification rate; moreover, the higher voltage between electrodes was mainly realized by higher cathodic potential and it limits the energy per mole gain since the external resistance was consuming some energy. Besides, no further denitrification and current production was observed when the cathodic potential was higher than 0 V vs SHE. The maximum power production in this setup was 8 W m^{-3} NCC when the external resistance was 25Ω. Generally, power production when nitrate is electron acceptor is not competitive to MFC with oxygen-reducing biocathode, for example in the same MFC operating either with oxygen or with nitrate, the produced power was 10.27 and 1.92 W m^{-2}, respectively [92]. However, the ability of water treatment from nitrate makes it interesting for further studying.

1.3.2. Conditions for best performance of NRB

While analyzing the different publications about the NRBs, one can notice a number of conditions applied in order to successfully grow an efficient biocathode. Usually the NRB is grown in anaerobic environment, neutral pH, on a carbon or metal electrode with a specific potential applied, and with a mixed bacterial community. Each of these conditions was carefully verified by at least few groups. This section will focus on summarizing the results of these studies.

Anaerobic environment

The nitrate-reducing biocathodes are usually kept in the anaerobic environment, in order to prevent the competitive reaction with oxygen. The low dissolved oxygen (DO) concentration, together with electron donor availability, are considered two most important factors for the effective work of denitrifying bacteria in groundwater [41,42]. The oxidation of the organic matter is preferably performed with the electron acceptor which can supply the most energy to the microorganism, which is dioxygen. In water with low oxygen concentration, the facultative anaerobic bacteria (which can use oxygen or other compounds as electron acceptor) will use nitrate for their metabolism instead. In case of low oxygen and nitrate concentration, the next preferable electron acceptors will be manganese oxides, iron oxides, sulfates and carbon dioxide. Tables 1&2 in Appendix 1 are summing up the atmospheres used in different studies.

There are several studies which were investigating the exact influence of oxygen on nitrate reduction on biocathode. Guo et al. tested three different concentrations of oxygen in the catholyte of MFC: 1.5, 3.4 and 4.4 mg O_2 L^{-1}, while the concentration of nitrate and ammonium was 473 and 104 mg of NO_3^- and NH_4^+ L^{-1}, respectively [93] (Table 1.2). The higher concentrations of oxygen were decreasing the conversion of nitrate and ammonium as well as produced power. The microbial community was also affected: in more oxygen-rich environment, there was more aerobic nitrifying and less anaerobic denitrifying bacteria. Sima et al. tested five concentrations of DO in water of a SMFC for nitrogen removal (nitrification and denitrification), which were 0, 1, 3, 5 and 8 mg L^{-1} [94] (Table 1.2). The low oxygen concentration initially had a negative influence on nitrification due to the intensive competition between nitrifying and oxygen consuming bacteria, however in longer time the ammonium concentration was gradually decreasing. There was no nitrate accumulation in sediment and water in these anoxic conditions, while the concentrations above 5 mg L^{-1} favored such accumulations. All in all, the authors concluded that the concentration of 3 mg L^{-1} is an optimal

compromise between nitrification, which requires oxygen and denitrification, in which there is a competition with oxygen, and allows to achieve the best TN removal.

Zhang and Angelidaki were studying the effect of DO on the nitrate and nitrite reduction and power production in SMFC [95] (Table 1.2). As expected, the nitrate and nitrite removal was less and less effective with increasing levels of DO, however for the power the effect was different. The high power density was observed initially with low DO concentration (close to 0 mg L^{-1}), it decreased when the DO was 3.2 mg L^{-1}, and then increased again with DO of 8 mg L^{-1}. The authors explain it by initial effect of inhibition of denitrification process on the electrode, and with increasing DO concentration, the oxygen took the role of the electron acceptor. Based on these examples, one can conclude that DO concentration around 3 mg L^{-1} can be considered as a limit above which the denitrification process is inhibited.

However, in case of simultaneous nitrification/denitrification processes, some manuscripts report denitrification above this value of 3 mg L^{-1}. Virdis et al. observed successful denitrification up to 4.4 mg L^{-1} of DO, above which it was inhibited [96] (Table 1.2). Furthermore, one year later the same group increased this limit and reported a BES for again simultaneous nitrification and denitrification, which achieved the maximum nitrogen removal efficiency at 5.7 mg O_2 L^{-1} [97] (Table 1.2). Zhu et al. were also performing nitrification and denitrification in cathodic chamber and they found that the concentration of 5 mg L^{-1} was optimal for nitrogen removal, but higher concentrations were inhibiting denitrification [98] (Table 1.2). There are a few explanations of this efficiency of nitrate reduction in the presence of oxygen. Its excess could be consumed during the nitrification process which can occur in bulk water, but in the deeper layers of the biofilm the conditions can be anoxic and the development of denitrifying microorganism is possible [66,99]. Zhu et al. showed this phenomenon by measuring DO in the depths of biofilm. The conditions were anoxic up to 0.35 mm of the biofilm and DO was gradually increasing up to 1.3 mm, where the value was as in the bulk solution (5 mg L^{-1}) [98]. Another explanation is the aerobic denitrification - a process in which bacteria can simultaneously use dioxygen and nitrate in as terminal electron acceptors in its respiration [100,101]. For example, *Pseudomonas aeruginosa* was found to use both these electron acceptors in concentrations of DO up to 2.2 mg L^{-1} [102]. Recently, a few studies were describing aerobic denitrification in MFCs [103–105], yet they are mostly focused on coupling this process with nitrification or other reactions like phenol removal. Furthermore, Sun et al. studied the algal-bacterial biocathode which was operating in two stages alternately: during the "day", with light and oxygen as electron acceptor and at "night", in a dark with nitrate as electron acceptor [106]. The power produced by this BES was higher during the day (110 mW

m^{-2}) than night (40 mW m^{-2}), however, the complete ammonium and high nitrate removal of 86% in 192h was achieved (high starting concentrations of 314 and 330 mg $N\text{-}NH_4^+$ and $N\text{-}NO_3^-$ L^{-1} were used). Therefore, there could be situations when denitrification can occur in oxygen concentrations higher than 3 mg L^{-1}.

Table 1.2 *Summary of chosen studies of influence of oxygen concentration on nitrate reduction*

Type of BES	Dissolved oxygen mg L^{-1}	Starting nitrogen concentration	Nitrate reduction rate	Energy production	Reference
MFC	1.5	0.722 g L^{-1} KNO_3	1.565 mg $(L \cdot h)^{-1}$	1776 mW m^{-3}	[93]
	3.4		1.382 mg $(L \cdot h)^{-1}$	1764 mW m^{-3}	
	4.4		1.174 mg $(L \cdot h)^{-1}$	1021 mW m^{-3}	
SMFC	0	14.16 and 864.43 mg of TN in water and sediment, respectively	42.11% of TN (after 49 days)	7.24 mW m^{-2}	[94]
	1		55.22% of TN (after 49 days)	9.69 mW m^{-2}	
	3		60.55% of TN (after 49 days)	34.77 mW m^{-2}	
	5		56% of TN (after 49 days)	34.96 mW m^{-2}	
	8		38.35% of TN (after 49 days)	67.21 mW m^{-2}	
SMFC	0	10 mg-N/l	~62%	41.3 mW m^{-2}	[95]
	1.1		~55%	~37 mW m^{-2}	
	3.2		~27%	24.8 mW m^{-2}	

	7.8		7.8%	55.5 mW m^{-2}	
MFC Flow: 0.7 Ld^{-1}, HRT 6.86h	1.97	53 mg N – NH_3 L^{-1}	66.9% of TN	0.19 mW	[96]
	4.35		94.1% of TN	0.89 mW	
	5.02		80.3% of TN	1.79 mW	
	7.24		29.0% of TN	2.74 mW	
BES for nitrification and denitrification	3.2	13 mg N L^{-1} (NH_4^+)	3.12 mg TN L^{-1} h^{-1}		[97]
	4.7		3.18 mg TN L^{-1} h^{-1}		
	5.7		3.39 mg TN L^{-1} h^{-1}		
	7		2.95 mg TN L^{-1} h^{-1}		
MFC	4.2	~77 mg N L^{-1}	0.029 kg TN m^{-3} d^{-1}		[98]
	5		0.064 kg TN m^{-3} d^{-1}		
	6		Inhibition of denitrification process		

Influence of pH

Protons are necessary in each step of denitrification (Eq. 1.1 to 1.4), therefore it is important to have the proper pH in a cathodic chamber. In most of the definitions of the MFC, the protons are said to be released on bioanode, cross the proton-exchange membrane and be used on biocathode. In reality, this transport is not sufficient enough and there is local acidification in anodic compartment and local alkalization in cathodic one, which may cause electrode deactivation [107]. Indeed, lower pH of anodic effluent and higher pH of cathodic

effluent, in function of electrodes' potential, was measured by Pous et al. [108]. Keeping the correct pH in the region of biocathode is important for achieving the best performance. This is why in many publications the authors use phosphate buffer as catholyte [70,106,109–124]. Rezaee et al. made a composite carbon felt/multiwall carbon nanotube biocathode and they were testing it in different conditions, including pH values variating from 6 to 9 [125] (Table 1.3). They found that nitrate reduction was more efficient in pH 7 and 8 (over 80 %) than in 6 (less than 60%) and 9 (less than 50%). Vijay et al. studied the influence of cathodic pH on the nitrate reduction efficiency and they tested very wide range of pH: 2, 4, 6, 7 and 9 [70] (Table 1.3). They had a similar conclusion that pH was the most optimal for this kind of experiment. Clauwaert et al. increased the nitrate removal from 0.22 to 0.5 kg NO_3^--Nm^{-3} NCC d^{-1} by keeping the constant pH value of 7.2 (in the control experiment without pH control, the pH of catholyte was increasing due to cathodic reactions) [67]. Cheng et al. proposed a solution of changing the role of bioelectrode by switching the potential and providing either electron donors or acceptors [126]. In this way, the biofilm that once acted like cathode and alkalized the environment, can later profit from this higher pH in the role of bioanode. All in all, pH in a range 7-8 should be the optimal for NRB performance.

Table 1.3. *Summary of chosen studies of influence of pH on nitrate reduction*

Type of BES	pH	Starting nitrogen concentration	Nitrate reduction rate	Reference
BES	6	50 mg NO_3^-–N L^{-1} 6h	55.3%	[125]
	7		85.5%	
	8		84.2%	
	9		43.4%	
MFC	2	345 mg NO_3^-–N L^{-1}	50%	[70]
	4		55%	
	6		76%	
	7		97%	
	9		91%	

Biocathode polarization

In many of the studies of biocathodes for nitrate reduction, the potential is applied on electrode, and it was found crucial to ensure good performance. This potential should be generally low enough to drive the growth of bacteria and high enough to prevent the electrolysis of water [127]. Above 0 V vs SHE the efficiency of cathodic denitrifying bacteria is severely limited [60]. In most of the articles, one can find that the applied potential was from around -0.3 V [92,117,118,128–130] or -0.25 [120,127,131], up to around -0.1 V vs SHE [121,128,132] (See Table 1&2, Appendix 1). In some studies, applying the potentials of -0.7 V or lower were found to increase NRR but the mechanism included electrolysis of water and hydrogenotrophic denitrification with the use of created hydrogen [122,133].

Several studies were focused on applying different potentials in order to find the optimal value. Virdis et al. were studying the influence of four tested potential values (100, 0, -100 and -200 mV vs SHE) applied on biocathode on current and nitrate removal [134] (Table 1.4). They found that the highest current and nitrate removal was for -100 mV vs SHE. At lower potential values (-200 mV), higher residual current as well as higher N_2O reduction rates were observed. In the same study, also different currents were applied to cathode, and the highest nitrate reduction, however together with highest N_2O accumulation, was observed for the highest current (15 mA). Pous et al. applied the wide range of potentials from +0.597 to -0.703 v vs SHE while using acetate or water as electron donor [135]. In this study, the optimal nitrate removal rate and the lowest accumulation of undesired intermediates was achieved with applied potential of -0.123 V vs SHE and with water used as electron donor. Yu et al. were using *Thiobacillus denitrificans* to grow biocathodes on following potentials: -0.5, -0.3, -0.1 and +0.25 V vs SHE, and they found that the NRR is the higher, the lower potential [136] (Table 1.4). Gregoire et al. developed a biocathode by applying the relatively high potential of -0.055 V vs SHE (-0.250 V vs Ag/AgCl) and they observed maximum current density of -905 mA/m^2 [123] (Table 1.4). Potential was then shifted to more negative value of -0.153 V vs SHE (-0.350 V vs Ag/AgCl) and the big increase of current up to -3200 mA/m^2 was observed. Yet, when the higher potential of +0.197 V vs SHE was applied to grow another biocathode (0 V vs Ag/AgCl), no current was flowing between the bioelectrodes, which is an indication that the biocathode was not operating at this potential. Nguyen et al. wanted to develop the nitrate-reducing biocathodes operating on high potentials by applying potentials from +0.97 to +1.197 V vs SHE (-0.1 to +1 V vs Ag/AgCl) [137]. They did not observe any significant difference in nitrate removal while changing these potentials and it was lower than the control without applied

potentials. To sum up, the potential in the range from -0.3 to -0.1 V vs SHE should be the most suitable.

Table 1.4. *Summary of chosen studies of influence of applied potential on nitrate reduction or measured current*

Type of BES	Applied potential	Starting nitrogen concentration	Nitrate reduction rate	Current	Reference
MFC	100 mV vs SHE	0.652 g $NaNO_3 \cdot L^{-1}$ 200 $mL \cdot min^{-1}$	-0.327 mM-N h^{-1}	7.8 mA	[134]
	0 mV vs SHE		-0.432 mM-N h^{-1}	10.4 mA	
	-100 mV vs SHE		-0.484 mM-N h^{-1}	12.4 mA	
	-200 mV vs SHE		-0.424 mM-N h^{-1}	11.3 mA	
BES	-500 mV vs SHE	2 mM of nitrate	75.6% after 15 days	160.8 µA	[136]
	-300 mV vs SHE		58.5% after 15 days	76.5 µA	
	-100 mV vs SHE		48.4% after 15 days	29.5 µA	
	250 mV vs SHE		26.8% after 15 days	11.4 µA	
MFC	197 mV vs SHE	0.606 g KNO_3 L^{-1}		No catalytic current	[123]
	-53 mV vs SHE			−905 mA m^{-2}	

External resistance

Cathodic potential can be applied, but the potential difference between anode and cathode can also be established with a proper resistor. According to Ohm's Law (I = U/R), the current is increasing with decreasing resistance, and the nitrate removal increases with increased current. However, when the resistance decreases and the current increases, the voltage must also decrease, and this will cause the decrease of power (P = I*U). This simple reasoning gave the basics for the idea of described earlier MES, but it was also proven in several articles about MFCs. Jia et al. studied nitrate removal in MFC and they observed total denitrification in 25h and average I = 0.41 mA when R = 10Ω was applied. In the same time, with R = 1000Ω, only 38% of nitrate was consumed and I = 0.12 mA [138]. Similarly, in study of Virdis et al., for reactor with R = 5Ω the nominal current production was 24.3 mA and the nitrate concentration dropped almost completely (from 55 to 1.6 mg $N\text{-}NO_3^-$ L^{-1}); for R = 100Ω the current was 4.8 mA and nitrate removal was very limited (from 66.7 to 54 mg $N\text{-}NO_3^-$ L^{-1}). However, the optimal power for this study was achieved for R = 20Ω [66]. Pous et al. noticed that with the lower external resistance, more nitrate can be introduced with achieving always complete denitrification (three times more nitrate with 5Ω comparing to 50Ω) and the maximum power was produced for R = 25Ω. In the study of Wang et al., the nitrate reduction was 60% with R = 1Ω and only 12% with R = 510Ω [84], but the power density was decreasing with decreasing external resistance. More information about applied resistances can be found in Table 1&2 in Appendix 1. In summary, one has to choose between the optimal power and optimal nitrate reduction.

Electrode material

The base-materials for electrodes should be conductive, chemically stable, have good mechanical strength and low cost. For the bioelectrodes, the additional requirements are high surface roughness, good biocompatibility and ability to transfer electrons between bacteria and electrode surface [139]. Various carbon and metal materials are used as the electrode material in the MFCs with NRB, and they are listed in Tables 1&2 in Appendix 1. Zhang et al. were comparing the current and power density while using graphite felt, carbon paper or stainless steel as electrode material for oxygen-reducing biocathode [140]. They found the best performance for graphite felt (350 mA m^{-2} and 109.5 mW m^{-2}) and very poor results for stainless steel ((18 mA m^{-2} and 3.1 mW m^{-2}) (Fig. 1.6).

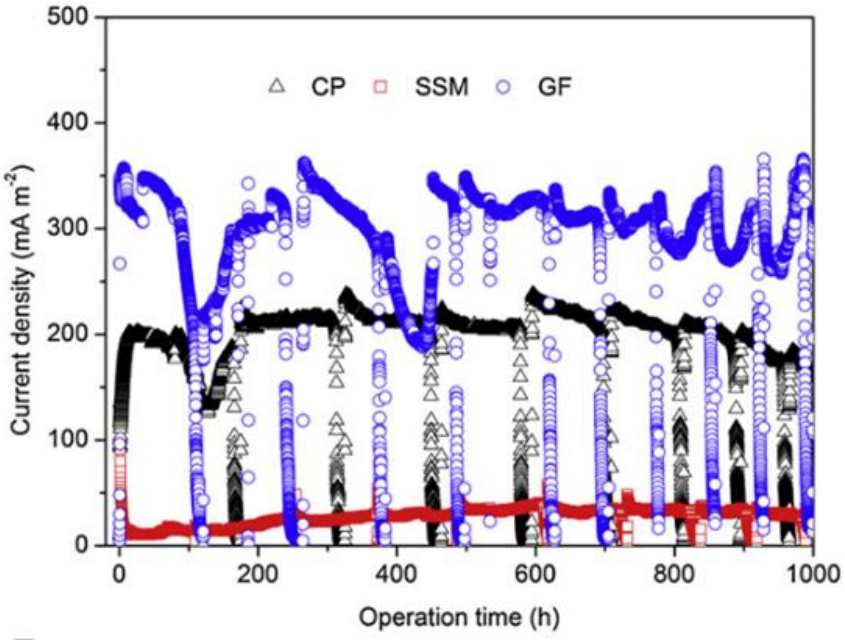

Figure 1.6 *Current density for different materials used in MFCs. CP - carbon paper, SSM - stainless steel mesh, GF - graphite felt* [140]

Indeed, in the great majority of studies about NRB, different carbon materials are used as the electrode, for example carbon paper [95,109,124,130], carbon cloth [136,141], graphite felt [110,112,113,116,122,137,142–144], carbon felt [68,111,145–149], graphite rods and bars [70,117,123,128,150,151], graphite or carbon brushes [69,120,152,153] and graphite granules [37,66,67,92,115,118,119,131,132,134,154–156]. Some studies also use composites in order to increase the performance, for example carbon felt/multiwall carbon nanotube composite [125]. Different carbon materials can favor development of different microbial communities [157]. However, another publication was comparing granular graphite and stainless steel mesh as the NRB material in MFC for swine manure treatment [158]. They found the similar results for nitrate reduction for both of these materials and they concluded that in longer perspective, stainless steel mesh is more promising because of the clogging effect in graphite granules compartment. Erable et al. immersed graphite and stainless steel electrodes into the marine sediments and they found that in the same medium, these two electrodes were colonized by different microbial community which lead to development of anodic and cathodic properties for graphite and steel respectively [159]. Yet except of that, the number of studies involving stainless steel as cathodic material is still very limited. Metals as iron and nickel were also tested as cathode materials. The MES with iron gave good results for treating water of low nitrate concentrations [80], however some rust-like coating were observed on the cathodic part of iron rod, therefore the mechanism could involve the chemical reactions with iron rather than

bioelectrochemical process [81]. Nickel foam was used to create an algal-bacterial biocathode which could use oxygen and nitrate as electron acceptor during day and night mode respectively [106]. Such biocathode resulted in good nitrate removal efficiency of 86% in 192h, starting from the concentration of 330 mg $N\text{-}NO_3^-$ L^{-1}. To conclude, carbon-based materials are the most popular choice for NRB, however there are also studies with metal electrodes.

Medium conductivity

Puig et al. studied relationship between influent ionic strength and nitrate removal [155]. For lower ionic strength (lower than 1600 µS cm^{-1}), the reduced nitrate removal efficiency as well as the accumulation of nitrite and nitrous oxide was observed, which is caused by limitation of proton and electron transport by higher resistance of the medium. Moreover, the energy production was also limited with lower ionic strength influents, and the factors responsible for energy loss were identified: cathodic overpotential was the cause of 83-90% of total loss, anodic overpotential for 1% and ionic transport for 8-12% of loss. The energy losses in cathodic compartment are caused by the mass and charge transfers overpotentials in enzymatic reactions in denitrification process.

1.3.3. Cyclic votlammograms of NRB

Cyclic voltammetry is widely used for studying the NRB and several groups were trying to identify the potential values of nitrate reduction peak. To our best knowledge, the highest reduction peak for nitrate was observed so far by Cheng et al., with photoelectrotrophic denitrification system, where denitrification biocathode was coupled with TiO_2 photoanode [160]. In biocathode with nitrate, they found the onset potential and peak potential of nitrate reduction of 0.15 and 0 V vs SHE, respectively, while no or little signals were present for abiotic cathode with nitrate or biocathode without nitrate (Fig. 1.7 A). A little bit more negative onset potential was found in the study of Yi et al. who prepared a bioelectrochemical system aiming for detection of biological oxygen demand (BOD) and nitrate [161]. The NRB developed in this experiment had the onset potential of below -0.1 V vs Ag/AgCl which should correspond to around 0.09 V vs SHE (Fig. 1.7 B). Gregoire et al. in their study focused on enrichment of NRB (for example by keeping anaerobic conditions, additional carbon source) in order to achieve a higher current; they also developed biocathode by applying two different potentials on the electrode [123]. When the potential applied on biocathode was lower (- 0.25 V vs Ag.AgCl), on the CV there was more clear reduction peak with an onset potential of -0.125 V vs Ag/AgCl (0.07 V vs SHE) (Fig. 1.7 C). The reduction signal on CV was less clear in case of the NRB developed at more positive applied potential of 0 V vs Ag/AgCl.

A number of publications show reduction wave starting around 0 V vs SHE (-0.2 V vs Ag/AgCl). Pous et al. performed several CVs of the microcosms sampled from denitrifying biocathodes in different media, such as NO_3^-, NO_3^- + NO_2^-, NO_2^- or buffer. Fig. 1.7 D demonstrates the example of CV from this study. They found that the peak with the onset potential of -0.25 V vs Ag/AgCl (-0.055 V vs SHE), with the inflection point at -0.3 V vs Ag/AgCl (-0.105 V vs SHE), which was visible in media with NO_3^- or NO_3^- + NO_2^-, was representing the reduction of nitrate to nitrite. Another signal around -0.7 V vs Ag/AgCl (-0.505 V vs SHE), visible in media with NO_3^- + NO_2^- or only NO_2^-, was further nitrite reduction. No clear signals were observed for blank electrode [128]. The same group created one more bioelectrochemical system, which was aiming to reduce nitrate and arsenite [132]. While performing the CV, they found the derived formal potential of nitrate reduction to be -0.02 V vs SHE (Fig. 1.7 E). In other study, they developed a bioelectrode which, depending on conditions, was oxidizing acetate or reducing nitrate. For this bioelectrode, the reduction wave was starting at around -0.05 V vs SHE and the formal potential of nitrate reducing signal was -0.175 V vs SHE (Fig. 1.7 F) [117]. Kondaveeti and Min were comparing biocathode with abiotic carbon and platinum cathodes [124]. For the biocathode, the observed reduction peak was at -0.2 V vs Ag/AgCl (around 0 V vs SHE).

More negative potentials were also attributed to nitrate reduction in some of the publications. Huang et al. were testing the denitrifying properties of modified carbon felt cathodes [145]. They observed different peaks of nitrate reduction: -0.45 V vs SCE for bare electrode and -0.332 V vs SCE for ce-doped birnessite modified one ((Fig. 1.7 G). Yu et al. were studying nitrate removal with biocathode colonized by *Thiobacillus denitrificans* [136]. They observed the peak of nitrate reduction at -0.31 V vs SHE (Fig. 1.7 H). Furthermore, Vijay at al. prepared an MFC which aimed for simultaneous removal of nitrate and uranium. In this study, the peak attributed to nitrate reduction was at the low potential of -0.552 V vs Ag/AgCl (-0.335 V vs SHE).

In general, in most of the studies nitrate potential peak was starting in a range 0 - 0.1 V vs SHE, but lower potential values were also attributed to nitrate reduction. In order to clearly identify the peak of nitrate reduction, it is necessary to compare it with adequate control experiment without nitrate. Differences in CVs can be the consequence of different microbial community present on the biocathode.

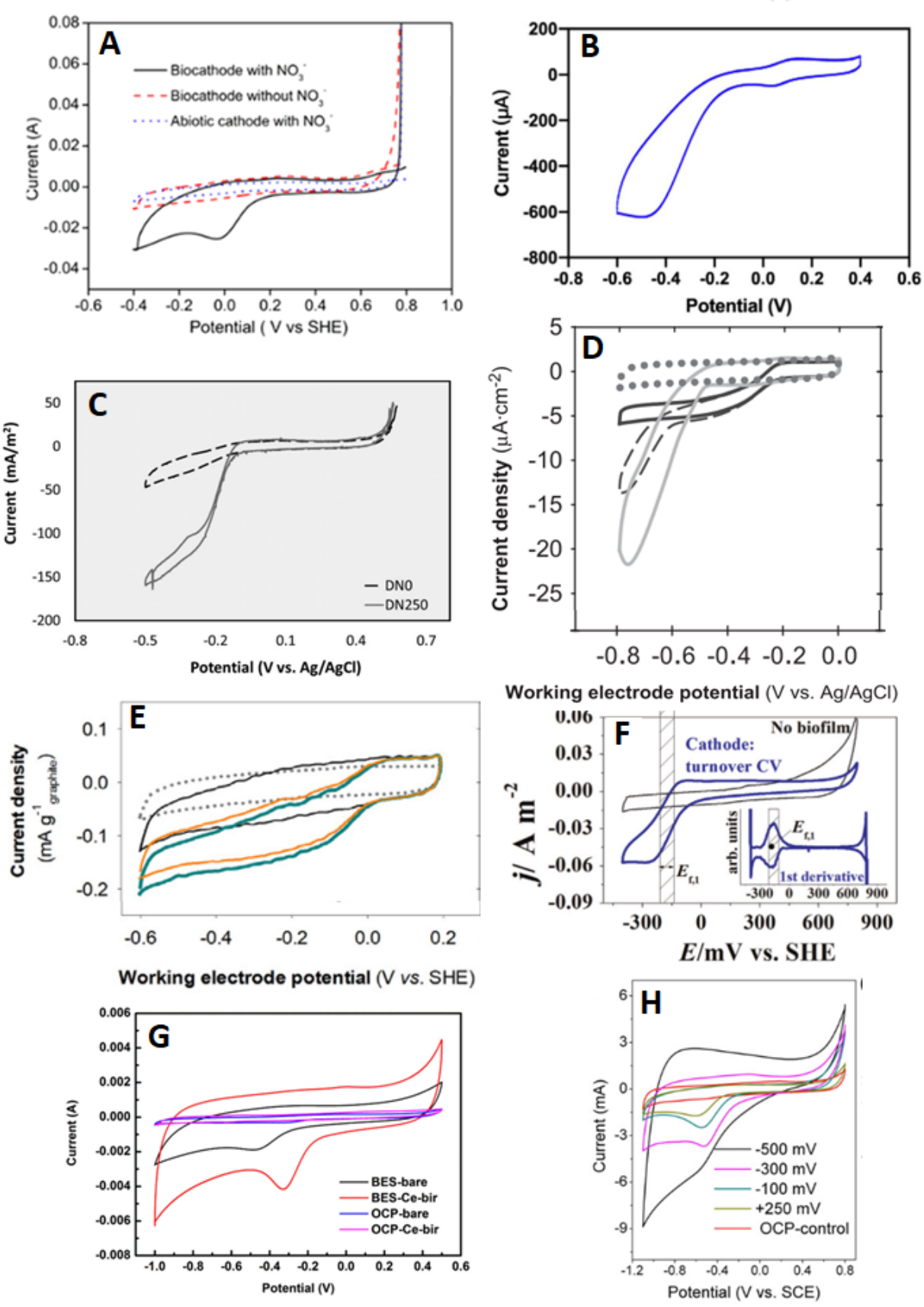

Figure 1.7 *Examples of cyclic voltammograms of NRB A. NRB (black line) compared with control experiments of biocathode without nitrate (red dashed line) or abiotic cathode with*

nitrate (blue dotted line), scan rate 0.5 mV s^{-1} [160] *B. NRB in presence of nitrate, scan rate 10 mV s^{-1}* [161] *C. CVs of NRBs developed on applied potentials of 0 (dashed line) and -250 (plain line) mV vs Ag/AgCl, scan rate: 0.2 mV s^{-1}* [123] *D. NRB in presence of only nitrate (dark gray plain line), nitrate and nitrite (dashed line), only nitrite (light gray plain line) and blank electrode (dotted line). Scan rate: 0.5 mV s^{-1}* [128] *E. NRB in presence of nitrate (green line) and nitrate plus arsenite (orange line), compared with controls: abiotic (dotted line) and CV of biocathode in buffer (black line). Scan rate: 1 mV s^{-1}* [132] *F. CV of electroactive biofilm in cathodic conditions (poised potential: -303 mV vs SHE, lack of electron donor, nitrate in the environment). Blue line represents cathodic scan and black line - the control without biofilm. Scan rate: 1 mV s^{-1}* [117] *G. NRB developed with applied potential of -500 mV vs SHE on bare (black line) or modified (red line) carbon felt electrodes, compared with OCP systems without applied potential (blue and violet lines)* [145] *H. CVs of NRB developed at different applied potentials: -500 mV (black), -300 mV (violet), -100 mV (turquoise), +250 mV (olive) and OCP (red). Scan rate: 10 mV s^{-1}* [136]

1.3.4. Bacteria

Fundamental understanding of microbial community present on NRB is demanded to have a complete overview of the studied BES and to maximize its efficiency. Many studies do not use the specific bacterial species, but mixed communities from previous BES, wastewater treatment park, sediment etc., as it is listed in Table 1&2, in Appendix 1. Therefore, in many articles the important part is characterization of the bacteria present on NRB. Both electrochemically and non-electrochemically active microorganisms can influence the overall performance because of their syntrophic cooperation. Several methods of analysis are employed, which can be divided into techniques for studying electroactive microbes, microbial community and extracellular electron transfer [162]. One of the most common methods is using 16S rRNA-gene sequencing to identify the bacterial communities.

Proteobacteria is the phylum the most known for the electroactive properties and it is found on both anodes and cathodes of MFCs. Gregory et al., who first observed the nitrate reduction with electrode being the only electron donor, also studied the differences between the microbial community on the electrode poised at -0.5 V vs Ag/AgCl and the control electrode without current flow [90]. They found the increase of *Geobacteraceae* family (*δ-Proteobacteria)* on polarized electrodes, most of the sequences strongly related to *Geobacter grbiciae*. There was also more *γ-Proteobacteria* on the poised electrodes, and more *β-Proteobacteria* on the controls.

Generally, all classes of *Proteobacteria* can be found on biocathodes. One of the most common are *β-Proteobacteria* and among them, the most cited genus is *Thiobacillus*, especially *Thiobacillus denitrificans*. *Thiobacillus* spp. were confirmed to be able to reduce nitrate to nitrite with the use of electrode as a sole electron donor [121,136]. It was observed when an electrode was poised between -0.12 V vs SHE [121] up to -0.5 V vs SHE [136]. *Thauera* sp., which is known to be an aerobic nitrate-reducing bacterium, was also found on several NRB [120,146,148,163]. Similarly *Azoarcus* sp. is reported to be present at NRB active for nitrate reduction [131,164,165].

Cong et al. observed the domination of *β-Proteobacteria* on the carbon biocathode with applied current and of *α-Proteobacteria* when the current was not applied [165]. Chen et al. found the biggest relative abundance of *Proteobacteria* (in total 66.2%), in particular *β-Proteobacteria* (50%) in the cathodic chamber after 80 days of operating of MFC. Another present *phyla* were *Bacteroidetes* (21.6%), *Chlorobi* (8.1) and *Actinobacteria* (4.1) [166]. The authors continued the experiment and analyzed the bacterial community after 350 days of operation of MFC. In this longer perspective, the total percentage of *Proteobacteria* was relatively stable, but the number of *γ-Proteobacteria* increased significantly and replaced *β-Proteobacteria* which became scarcely presented. The amount of *Bacteroidetes* and *Actinobacteria* were also rather unchanged, however *Chlorobi* disappeared and *Planctomycetes* and *Firmicutes* become present [92].

Jiang et al. compared the biocathode exposed to nitrate as sole electron acceptor with the initial sludge, which was used to colonize it [148]. The percentage of *Proteobacteria*, mainly *β-Proteobacteria* and *α-Proteobacteria*, increased on biocathode. Percentage of *Bacteroidetes* remained roughly the same, but there was no more *Chloroflexi* and *Acidobacteria* on the bioelectrode (which was present in the sludge), however, bacteria from new *phylum* - *Thermi* appeared. Gue et al. were comparing the bacterial community on biocathodes of open- and closed-circuit MFC with the raw sludge [93]. On both electrodes, *Proteobacteria* became the dominant *phylum* (which was *Bacteroidetes* in case of the sludge), and its percentage was higher with the closed circuit. Also, *Chloroflexi* and *Acidobacteria* increased its presence on the electrodes, which is opposite effect to the one described by Jiang et al.

Philippon et al. were studying bacterial communities on polarized biocathodes placed in different regions of laboratory constructed wetland - in water, in sediment and on the interface. In this study, the experiment was performed in triplicate, however the increase of current after nitrate addition was observed on just two out of three electrodes. The authors noticed that the response to nitrate correlates with presence of certain *genera* in the biofilm:

Azoarcus (*β-Proteobacteria*) and *Pontibacter* (*Bacteroidetes*). They conclude that these genera could potentially be the key species involved in bioelectrochemical denitrification [131].

The specific conditions of biocathode can influence not only the different bacteria species, but also their number. Specific cathode conditions and voltage can cause the low abundance of bacteria on closed circuit cathode in comparison to open circuit one in the work of Guo et al [93].

1.3.5. Reaction products

The complete denitrification results dinitrogen, however, side products such as nitrite or nitrous oxide can be accumulated. This is highly undesirable because these compounds are pollutants more harmful than nitrate itself. Nitrite is toxic for aquatic fauna and flora as well as for humans (especially infant) by oral exposure [167,168] and nitrous oxide is significantly contributing to the greenhouse gas footprint [169]. Therefore, the researchers studying NRB in many articles are giving information about the products of the process.

Pous et al. built an MFC which was operating for three months [154]. They saw accumulation of different products during different operation periods: between days 31 and 45, around 43% of accumulated nitrate was in the form of nitrite. Later, nitrite was almost completely removed, but during the days 84-97 authors estimated that 60% of nitrate was in the form of nitrous oxide (based on coulombic efficiency, electron transfer and Tafel plot). It can be concluded that the biofilm is maturing and growth of bacteria catalyzing different reactions is promoted depending on availability of the compounds. In a different study, these researchers again observed that between 34.4 and 54.1% of reduced nitrate accumulated in the form of nitrite indicating that nitrite reduction rate is lower than nitrate reduction rate. By analyzing the biocathode with CV, they also found that nitrite reduction happens on more negative potential than nitrate [128].

Doan et al. saw that increased current applied on biocathode increases the nitrate removal, but also the accumulation of nitrous oxide [170]. Up to 70% of reduced nitrate was accumulated as nitrous oxide when applied current was 20A m^{-2}.

Virdis et al. observed that the nitrous oxide production was changing with different potentials applied on biocathode. 0.209 mM-N h^{-1} was produced when 0 V vs SHE was applied and when the potential decreased to -0.25 V vs SHE, the nitrous oxide emission dropped to 0.072 mM-N h^{-1}. However, N_2O could be also reduced on the biocathode, but with much slower rate [134]. Rather different effects were observed by Yu et al., who tested biocathodes with applied potentials from -0.5 to +0.25 V vs SHE. They saw that more nitrite was accumulated

with lower potential applied, for example for +0.25 V there was 0.19 mM and for -0.5 V there was 1.39 mM of nitrite. However, no clear influence of potential on the nitrous oxide accumulation was observed in this study [136].

Srinivasan et al. tried to determine the specific factor influencing the nitrite concentration by changing electron donor concentrations, DO or pH. However, none of these factors influenced the nitrite accumulation (about 66% of the initial nitrogen-nitrate) in this study [171]. Therefore, it seems that the cathodic potential could have a major influence on the nitrite and nitrous oxide accumulations but the exact nature of this influence is still to be studied.

1.3.6. Changing purpose of bioelectrode

A biofilm on the bioelectrode does not have to necessarily keep the same role: in some studies, the functions of biofilms were modified by changing polarization and providing different substrates. Such role switching has an important advantage of preventing exceeded acidification or alkalization around the electrode. Usually, oxidation reactions on anode lead to decrease of pH and reduction reactions require protons. However, the proton-exchange membrane does not provide a very efficient exchange of H^+ ions in the conditions used [107]. Changing the role of bioelectrode solves the problem because protons released in oxidation phase would be consumed during reduction. This operation was applied for oxygen [172] and nitrate reduction [126]. In case of nitrate, the first study was described by Cheng et al. in 2012, who created the ano-cathodophilic biofilm and proved the concept by providing the proper pH. They observed the inhibition of anodic reaction due to the acidification - when this effect was neutralized by adding sodium hydroxide, anodic current production resumed. The same biofilm was also used as biocathode when sodium acetate was replaced by sodium nitrate, which resulted in reversal of current (Fig 1.8 A). Such change of behavior was repeated several times, with 85 and 87% of anodic oxidation and cathodic reduction efficiency, respectively [126]. Pous et al. also developed a "switchable" biofilm which operated like bioanode in the presence of acetate and with applied potential of +0.397 V vs SHE, yet could be switched to cathodic conditions by applying -0.303 V vs SHE and nitrate (Fig. 1.8 B). The "switch" was also causing the current inversion and it could be done several times. They obtained the nitrate removal rate of 0.532 g $N\text{-}NO_3^-$ m^{-2} d^{-1}. They found that both acetate oxidation and nitrate reduction were taking place at the same formal potential of -0.175 V vs SHE, which could suggest that a similar electron transfer mechanism is used in both processes [117].

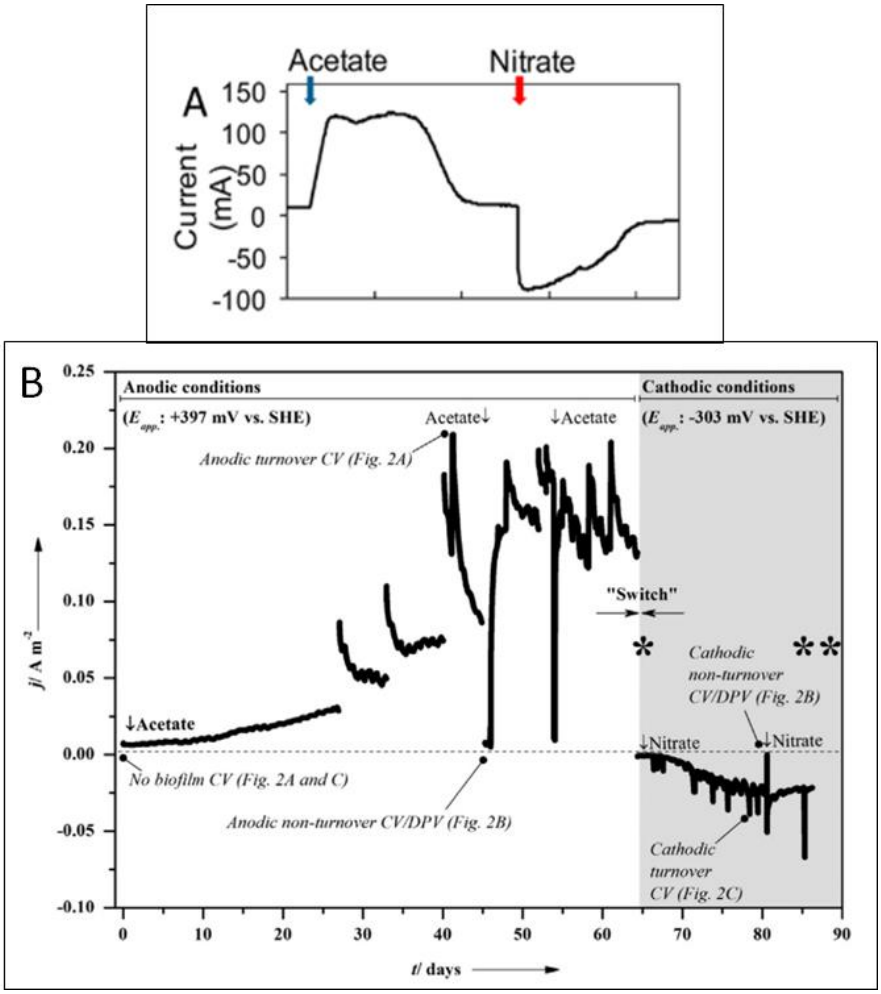

Figure 1.8 *Examples of changes in current after "switching" electrode conditions from bioanodic to biocathodic. A. The electrode potential was -0.203 V vs SHE (-0.4 V vs Ag/AgCl). The pH was controlled on values 6.8−7.5. The electrode was fed either with acetate or with nitrate* [126] *B. In bioanodic state, the electrode potential was 0.397 V vs SHE and acetate was available in electrolyte. In biocathodic state, the potential was -0.303 V vs SHE and nitrate was added* [117]

Yun et al. developed a biocathode from bioanode by changing potential form +0.15 to -0.4 V vs SHE; this biocathode was tested to treat the water polluted not only by nitrate, but also by two others model pollutants: nitrobenzene (nitroaromatic) and Acid Orange 7 (azo-dye) [173]. Similarly, Liang et al. changed the potential from +0.44 to -0.26 V vs SHE to change biofilm from anodic to cathodic which allowed to reach up to 98% efficiency of nitrate reduction. However, in this case the anodic bacteria disappeared from the electrode and it was impossible to recreate bioanodic behavior [120]. Lin et al., with the use of this method, obtained a very high reduction rate of 2.74 g $N\text{-}NO_3^-$ m^{-2} d^{-1} [174]. Yi et al. tested another application -

they used the bidirectional extracellular electron transfer of *Shewanella loihica* for detection of BOD and nitrate [161].

1.4. NRB coupled with other applications

Very often, the studies about NRB are coupled with other applications. Articles about MFC are usually also describing the power production of the device. Other research is linking nitrate reduction with removal of other pollutants, such as ammonium, perchlorate, sulphur compounds etc. This chapter will describe the BES used in these purposes and results from different approaches.

1.4.1. Power production

BES equipped with NRB are very often coupling water treatment with recovering energy. The maximum power of MFC can be found by analyzing its bell-shaped power-current curve (Fig. 1.9, situation (a)). However, the maximal efficiency for water treatment is achieved with the maximal current, and therefore the low or none voltage (Fig.1.9, situation (b)) [81]. According to Ohm's low ($P = U \cdot I$), there is no power produced with $U \approx 0$. Therefore, the highest power production is not necessarily equal to the highest efficiency in denitrification. Clauwaert et al. found that the highest denitrification rate was achieved for current equal to 58 A m^{-3} NCC and voltage equal to 0.075 V. Yet, the highest power of 8 W m^{-3} NCC was for I = 35 A m^{-3} NCC and U = 0.214 V [37]. Virdis et al. observed the biggest NRR of 410 g N-NO_3^- m^{-3} day^{-1} when the resistance was 5Ω. The current for this resistance was 133 A m^{-3} NCC and the power was 13 W m^{-3} NCC. When the resistance was 20Ω, the reduction rate decreased to 345 g N-NO_3^- m^{-3} day^{-1} and the current was 99 A m^{-3} NCC but the power increased to the maximum which was 34 W m^{-3} NCC [66].

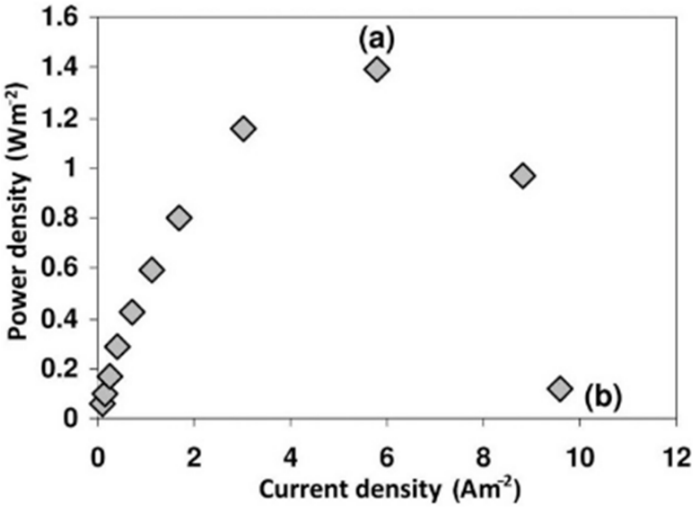

Figure 1.9 *Power-current curve of MFC* [81]

Several attempts were realized in order to increase either current or power density of NRB. Gregoire et al. by changing the potential of biocathode from -0.055 to -0.155 V vs SHE (-0.25 to -0.35 V vs Ag/AgCl) increased the current from -905 to -3200 mA m^{-2} [123]. Samrat et al. were comparing phosphate and carbonate buffered solutions (PBS and BBS, respectively) as catholyte in MFC with seawater bacteria. They found the increase of power and current from 0.6 W m^{-3} and 7.5 A m^{-3} to 2.1 W m^{-3} and 26.6 A m^{-3} after PBS was replaced by BBS. It could be explained by the fact that when the P content decreased, the bacteria went to resource acquisition mode and increased the nitrate reduction and therefore energy production [149]. Al-Mamun et al. were studying the influence of initial nitrate loading on (among others) current and power. By increasing the influent nitrate concentration from 41 to 140 g $N\text{-}NO_3^-$ m^{-3} day^{-1} (extreme concentrations in the article), the specific current production increased from 16.2 to 27.4 A m^{-3} NCC and specific power production increased from 1.77 to 5.2 W m^{-3} NCC [115]. In a different study, the same group was again changing the initial nitrate concentrations from 25 to 200 g $N\text{-}NO_3^-$ m^{-3} day^{-1} and estimated 150 g $N\text{-}NO_3^-$ m^{-3} day^{-1} to be the most optimal in terms of current and power production, which for this experiment were 45.88 A m^{-3} NCC and 7.1 W m^{-3} NCC [69]. Chen et al. observed a very big difference of current peak depending on the modification of carbon-based electrodes in the beginning phase of the study (after adding medium containing nitrate). However, after this initial phase, all electrodes were going towards similar values of current [156].

Oxygen-reducing biocathode is generally more efficient in energy production. For example, Xie et al. built a three chamber MFC with one anodic and two cathodic compartments. One of the cathodic compartments was aerobic and dedicated to nitrification coupled with

oxygen reduction and the other, anaerobic one, was reducing nitrate. The power produced in aerobic and anaerobic chamber was respectively 14 and 7.2 W m^{-3} NCC [175]. Zhang et al. proposed a similar MFC but in shape of tube in which the outer chamber was aerobic cathodic compartment, the middle was anodic and the inner one was anaerobic cathodic, devoted for nitrate reduction. They found that anaerobic chamber was producing 0.001 kWh m^{-3} NCC and aerobic one, even after subtracting the energy required for its operation (pump), produced 0.031 kWh m^{-3} NCC [176]. Sun et al. prepared a photo-bioelectrochemical system equipped with algal-bacterial biocathode, which was reducing oxygen during the day and nitrate during the night. The maximum power was 110 mW m^{-2} and 40 mW m^{-2} in day and night mode, respectively [106]. This is why perhaps the main focus for NRB should be efficiency in nitrate reduction. However, the studies of NRB are still young and the great increase of power production efficiency could be still achieved. More results of power production reached up to date in BES with NRB can be found in Table 1&2, Appendix 1.

1.4.2. Nitrification-denitrification MFC

Bioelectrochemical systems are often used to combine several processes of water treatment. Denitrification can be coupled with nitrification. Nitrification is a process of ammonium oxidation to nitrate which can be later reduced to dinitrogen in denitrification. Simultaneous nitrification and denitrification (SND) require careful choice of conditions in order to keep both reactions on similar rate to avoid nitrate or nitrite accumulation. Several ideas were already studied, which also included removing other pollutants, for example excess of organic carbon. These approaches will be discussed in this part.

Biological nitrification (in the solution) and bioelectrochemical denitrification (on the biocathode) can be integrated into one, cathodic compartment (Fig. 1.10) [96–98]. One of the challenges of this solution is to find the optimal DO concentration in the catholyte, as oxygen is required in nitrification, but it is inhibiting denitrification. However, as discussed in part 1.3.2, discussion about anaerobic environment, several articled proved that oxygen concentrations between 4 and 5 mg L^{-1} should not inhibit denitrification, because in the deeper layers of biofilm conditions should still be anoxic [98]. Therefore, these DO concentrations are a compromise which allows reaching the optimal nitrogen removal rate. Virdis et al. found that the optimal DO concentration in their experiment was 4.35 mg L^{-1} which allowed to achieve 94% efficiency of TN removal (starting ammonium concentration was 0.111 kg N m^{-3} d^{-1}) [66]. Moreover, the protons released during nitrification are helping to balance the optimal pH in the catholyte which can be alkalized due to cathodic reactions. Another challenge is necessity of

providing carbon and electron source for the nitrification step. These carbon compounds can serve as electron donors competitive to electrode for denitrifiers [98].

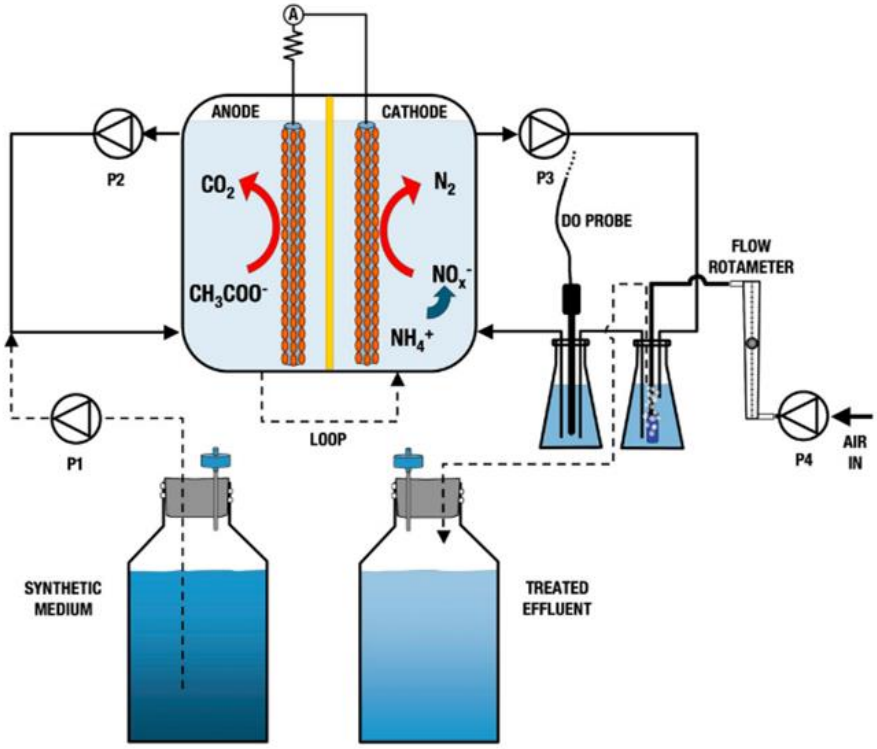

Figure 1.10 *An example of nitrification-denitrification BES, proposed by Virdis et al.* [66]

SMFC and similar constructed wetlands-MFCs (CW-MFC) were also used for simultaneous nitrification and denitrification. CW-MFC are MFCs integrated into constructed wetlands. By applying CW-MFC with three biocathodes, Xu et al. increased both nitrification and denitrification rates 1.8 times comparing to the control experiment [177]. Qiu et al. coupled SMFC with oxygen-producing submerged plants. The presence of these plants increased nitrification rate in both BES and control experiments, however, nitrate was present in the effluents. On the other hand, the setups without plants were less efficient in terms of nitrification, and less nitrate was found in the effluent. One can conclude that in this experiment the submerged plants and aerobic environment had bigger impact than presence of BES [178].

Another approach is to perform nitrification and denitrification in separated chambers. San-Martín et al. prepared a stack BES with 5 pairs of anodes and cathodes, with separated nitrification chamber (Fig. 1.11 A). The wastewater polluted with COD and nitrogen was first referred to anodic chamber in order to oxidize organic compounds. Later, it was passing the external nitrification chamber where ammonium was oxidized and produced nitrate was finally removed in the cathodic chamber. This study was an interesting step towards application in urban wastewater treatment plant, however improvement on the stage of nitrification is still

necessary. For the moment, the TN removal was 70% [179]. Liang et al. created two-stage MFC system with oxic biocathodic compartment where oxygen was reduced and nitrification occurred, and anoxic biocathodic compartment for denitrification (Fig. 1.11 B). Owing to the oxic part and to increased scale (50 l), the MFC was producing power and removing COD and ammonium from water (95 and 97% respectively, with starting concentrations of 70 mg $N\text{-}NH_4$ L^{-1}). However, even with the longest HRT (18h), in the effluent there was still around 11 mg $N\text{-}NO_3^-$ L^{-1} which results in 84% of efficiency of TN removal [180]. Similar setup with two cathodic chambers: one aerobic and one anaerobic was studied in the work of Li et al. In aerobic chamber, simultaneous reduction of oxygen and short-cut nitrification occurred - the later one is the process of oxidizing ammonium to nitrite (instead of nitrate) (Fig. 1.11 C). Nitrite was then reduced in the second, anaerobic cathodic chamber. This setup was also producing power and removing nitrogen with the efficiency of 99.9% (with starting concentration of 50 mg $N\text{-}NH_4$ L^{-1}, in 4 days) [181].

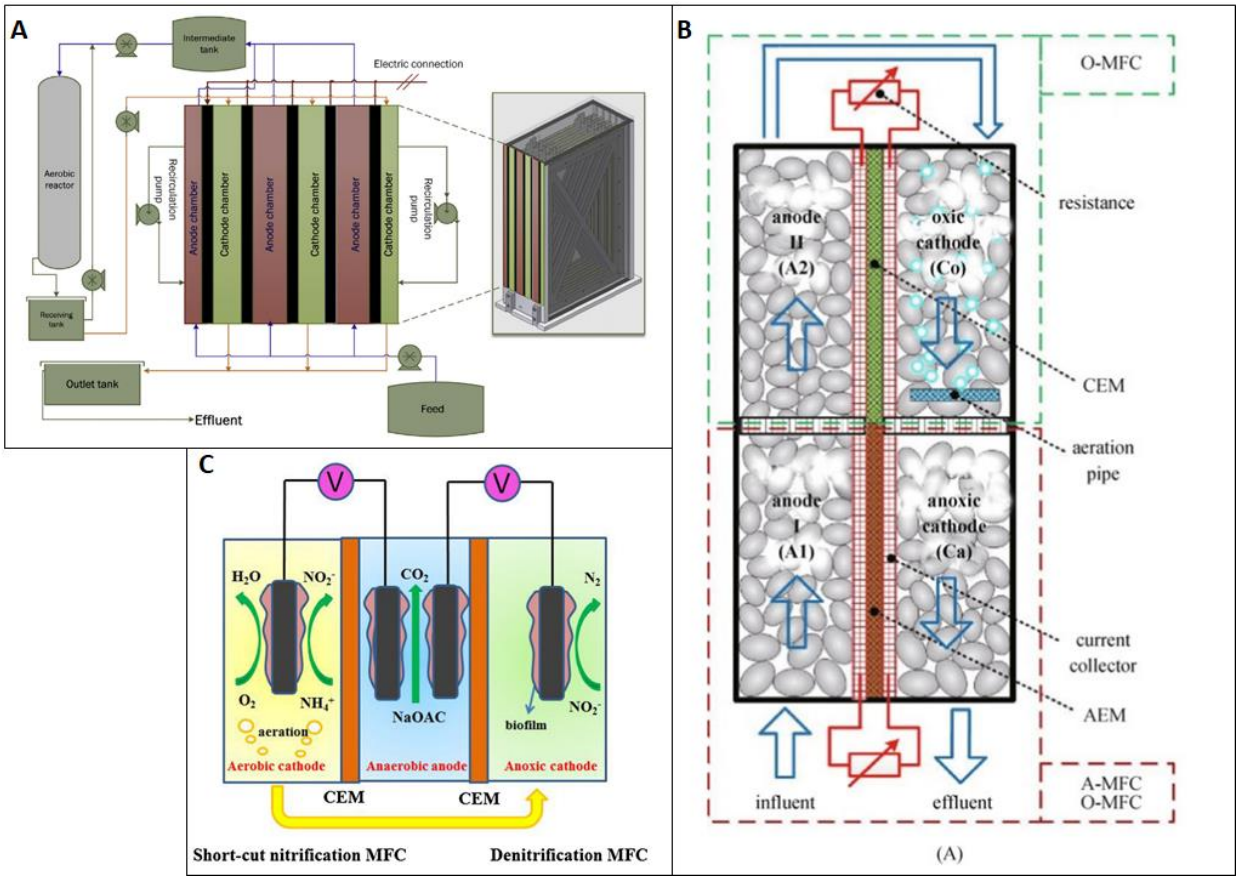

Figure 1.11 *Examples of the nitrification-denitrification MFC A.* [179] *B.* [180] *C.* [181]

1.4.3. NRB coupled with anammox

Another strategy to remove nitrogen from water is coupling denitrification with anaerobic ammonium oxidation (anammox) - a process of anaerobic ammonium oxidation coupled with nitrite reduction, like in the following reaction [182]:

$$NH_4^+ + NO_2^- \rightarrow N_2 + 2\ H_2O$$

One of the bottlenecks of anammox process is by-product nitrate accumulation. In order to overcome it, denitrification was proposed to be coupled with this process. Biological denitrification requires supplying of organic compounds as electron and carbon source for bacteria. However, these compounds can restrain the anammox bacteria. By using the electrode as electron source, bioelectrochemical denitrification solves this problem therefore its coupling with anammox is an interesting idea to be studied. Li et al. proposed to introduce ammonium and nitrite to the cathodic chamber of MFC, inoculated with anammox biomass. They observed an improvement in TN removal in closed circuit system in comparison to open circuit [183]. Similar experiment was performed by Qiao et al., who were choosing the optimal conditions for coupling anammox and autotrophic denitrification via electrochemical technology. They found that with voltage of 1.5 V and the NO_2^--N/NH_4^--N ratio of 1.28, the efficiency of TN removal was 99% (1.38 kg $N \cdot m^{-3} \cdot d^{-1}$) [184].

1.4.4. NRB coupled with perchlorate removal

Salts of perchlorate (ClO_4^-) are often used as oxidizers in rocket fuels, fireworks, missiles etc. It can be also present in fertilizers and therefore later contaminate soil and water [185]. Perchlorate is toxic for human health even in small doses and in European Union, its concentration in food should not exceed 10 $\mu g \cdot kg^{-1}$ [186]. Perchlorate can be reduced in MFCs. NRB can be adapted to reduce perchlorate by gradually changing the influent concentrations of both electron acceptors [187]. They can be also reduced simultaneously, however Xie et al. noticed that increasing nitrate concentrations can gradually decrease the efficiency of perchlorate reduction [188], this effect was also confirmed in other studies [189]. Nevertheless, Jiang et al. obtained the efficiency of the simultaneous perchlorate and nitrate removal (in proportion 1:1) of 40.97% and 86.03%, respectively, while the efficiency for sole perchlorate was 53.14% and for sole nitrate 87.05% [148]. Wang et al. observed that the decrease of the concentration of perchlorate was very much accelerated after nitrate was reduced: therefore, both salts could have been completely removed in 120h. They also found that optimal biocathodic potential for this reaction was -0.2 V vs SHE [190].

1.4.5. NRB coupled with removal of sulfur compounds

Sulfide can be emitted to wastewater from petrochemical plants or some manufactures; it can be also generated by biological breakdown of sulfates in anaerobic environment [191]. Sulfide can be used in autotrophic denitrification, and the two main products can be obtained [192]:

$$5\ S^{2-} + 2\ NO_3^- + 12\ H^+ \rightarrow 5\ S^0 + N_2 + 6\ H_2O$$

$$1.25\ S^{2-} + 2\ NO_3^- + 2\ H^+ \rightarrow 1.25\ SO_4^{2-} + N_2 + H_2O$$

Usually, recovered S^0 is a main purpose of studies. In MFC, sulfide, instead of or together with organic matter, can be used as an electron donor in anodic chamber [193]. Its oxidation can be coupled with nitrate reduction in cathodic chamber [194]. Zhong et al. obtained a stable removal of sulfide and nitrate in MFC, combined with the power recovery [195]. Cai et al. built an efficient MFC for simultaneous sulfide and nitrate treatment, obtaining 99.4% and 96.5% of removal respectively, regardless the initial concentration of sulfide (between 60 and 540 mg L^{-1}) and ratio between pollutants [196].

1.4.6. NRB coupled with removal of other pollutants

The compounds such as sulfate, phosphate and uranium were also coupled with nitrate reduction in bioelectrochemical systems. Tetteth et al. created a macrophyte cathode SMFC, which was removing COD, nitrate and sulfate, reaching up to 99% for the two last pollutants (with starting concentrations of 125.6 mg $N\text{-}NO_3^-$ L^{-1} and 75 $S\text{-}SO_4^{2-}$ L^{-1}) [152]. Ge et al. constructed pyrite-based CW-MFC which was simultaneously removing COD, nitrate and total phosphorus [197]. Vijay et al. were searching the solution for treatment of nuclear wastewater, which contains nitrate and uranium. They added glycerol-3-phosphate, which by employing the phosphatase enzyme, released phosphate which with uranium creates insoluble uranyl phosphate. In the same time, nitrate reduction and power production were also achieved in this study [143]. All in all, nitrate reduction has a potential to be coupled with numerous other processes.

1.5. Conclusions

This chapter summarized the current research about NRB. Based on the literature review, in order to grow a NRB, one should apply potential in a range from -0.3 to -0.1 V vs SHE on electrode made of carbon or metal like stainless steel, keep the DO level below 3 mg

L^{-1} and pH in the range 7-8. Chosen single-strain cultures as well as mixed communities from wastewater treatment plants or sediments can be used as a source of bacteria. Using these parameters should allow to achieve the optimal denitrification rate, energy production and to eliminate the undesired side products. The efforts are also made towards coupling nitrate reduction with other reactions. However, the specific conditions which are easily applicable in laboratory scale, such as anaerobic atmosphere, optimal pH and C/N ratio, could be difficult to reach in bigger scale application, for example in wastewater treatment park or in constructed wetland. We find this the biggest challenge of further research on NRB.

Nevertheless, taking into consideration that this relatively recent subject is attiring more and more attention of researchers which corresponds to growing number of studies in this domain, one can predict that the optimal, low-price and efficient nitrate reducing system employing NRB could be designed and applied in the near future. One solution could come from the bioelectrochemical system in snorkel configuration.

1.6. Context and aim of the thesis

This thesis is a part of the ANR project "Low Nitrate", which is a project involving several partners from France: Le Laboratoire de Chimie Physique et Microbiologie pour les Matériaux et l'Environnement (UMR CNRS/Université de Lorraine), Laboratoire de Génie Chimique, (CNRS/Université de Toulouse 3/INPT), Institut des Sciences Chimiques de Rennes (UMR CNRS/Université de Rennes 1) and two research units: HYCAR and PROSE from INRAE (previously IRSTEA), Antony. The goal of the project is to design a passive microbial electrochemical technology applicable to artificial wetlands or other similar ecosystems for the removal of nitrogen (nitrate). Denitrification is a microbial process of nitrate reduction to dinitrogen, and the denitrifying microbes require electron donor and carbon source for their metabolism, in which they can use nitrate as electron acceptor. One of the limitations is the fact that the electron donors such as organic carbon compounds appear in the sediment, while nitrate is present in water. Therefore, the denitrification is likely to occur on the water/sediment interface. The goal of this thesis is to make the electron donors in the sediments more accessible for denitrification.

Firstly, the influence of water/sediment interface on nitrate reduction rate is evaluated. The goal is to confirm that this inaccessibility of electron donors in water is a limiting factor for denitrification. This strategy will be tested in stationary state and in flow, and will be considered to be applied in constructed wetland.

In the next part, we will explore the same idea but with electrochemical approach, by studying Microbial Electrochemical Snorkel for nitrate reduction. This BES was not yet effectively applied for nitrate reduction, however, its simplicity can be a great advantage in terms of field application. MES is a piece of electrode which conducts electrons released during organic matter oxidation by anodic biofilm in sediment. They can be used in water by cathodic biofilm to induce efficient and low cost denitrification. Firstly, we will focus on studying the fundamental properties of the MES and choosing the optimal design. We will confirm development of snorkel and shows the differences in its anodic and cathodic parts in terms of electrochemical response and microbial community. Then conclusions from this first series of experiments will be used to optimize MES, in order to clearly see the accelerated denitrification, and to deeper study the electrochemical response for nitrate in the environment, the ability of MES to accelerate nitrate reduction, as well as microbial community of biocathodes.

Finally, the last part will explore the possibility of increasing the rate of nitrate reduction with electrodes located only in the sediment layer. This could be a way to maintain low oxygen concentrations at proximity of bioelectrodes when the surface water of the wetland is oversaturated with oxygen. Unlike oxygen, nitrate can diffuse into the sediment up to a couple centimeters. Therefore, we will explore if the electrode in the sediment, in bigger water/sediment interface configuration (which is also bigger surface for nitrate diffusion), will have an impact on acceleration of nitrate reduction. In the end, we will discuss the current challenges and opportunities regarding the application of MES for nitrate reduction in constructed wetland.

2. Materials and methods

2.1. Materials

The sediment has been taken from a constructed wetland of Rampillon (77, Seine-et-Marne, France [198,199]) and from a wetland in Ville-sur-Illon (88, Vosges, France [200]); both wetlands were built to intercept surface water and mitigate non-point source pollution from agricultural field (annual average nitrate concentration above 60 mg NO_3^- L^{-1}). All sediments were kept in a cool dark space (the composition of the sediments are provided in Table 2.1 and 2.2). No significant differences in denitrification rates were observed between these two sediments so both were used; the origin of the sediment is indicated in the corresponding Table or Figure caption. Results obtained from Rampillon's sediment are presented in the manuscript and results obtained from Ville sur Illon's sediment are presented in Supplementary material.

Table 2.1 *Sediment analysis. Organic sulfur and carbon*

Sample	S total (%)	C_{org} (%)
Rampillon A 1 (March)	0.09	1.44
Rampillon A 2	0.09	1.50
Rampillon A 3	0.09	1.49
Rampillon B 1 (September)	0.14	1.55
Rampillon B 2	0.11	1.34
Rampillon B 3	0.10	1.61
Ville Sur Illon B 1	0.16	4.44
Ville-sur-Illon B 2	0.16	4.94
Ville-sur-Illon B 3	0.15	5.35

Table 2.2 *Sediment analysis. Inorganic matter*

Sample	Sc	SiO_2	Al_2O_3	Fe_2O_3	MnO	MgO	CaO
	µg/g	%	%	%	%	%	%
Rampillon A 1	7.85	59.55	7.85	2.97	0.059	0.60	9.90
Rampillon A 2	7.89	59.08	7.98	3.03	0.060	0.61	10.02
Rampillon A 3	8.08	59.19	7.92	3.00	0.058	0.60	9.93
Rampillon B 1	6.49	64.73	6.73	2.44	0.045	0.48	8.64
Rampillon B 2	6.62	63.92	6.78	2.47	0.045	0.49	8.71
Rampillon B 3	6.67	64.70	6.69	2.43	0.046	0.49	8.85
Ville-sur-Illon B 1	5.77	34.46	6.37	2.16	0.040	4.08	18.15
Ville-sur-Illon B 2	5.71	34.33	6.27	2.11	0.039	4.18	18.20
Ville-sur-Illon B 3	5.61	34.22	6.30	2.12	0.039	4.07	17.91

Sample	Sc	Na_2O	K_2O	TiO_2	P_2O_5	PF	Total
	µg/g	%	%	%	%	%	%
Rampillon A 1	7.85	0.61	1.48	0.71	0.16	15.48	99.38
Rampillon A 2	7.89	0.61	1.50	0.71	0.16	15.80	99.57
Rampillon A 3	8.08	0.61	1.49	0.72	0.16	15.80	99.48
Rampillon B 1	6.49	0.64	1.40	0.69	0.12	14.13	100.04
Rampillon B 2	6.62	0.63	1.40	0.68	0.12	14.53	99.76
Rampillon B 3	6.67	0.62	1.39	0.68	0.12	13.03	99.03
Ville-sur-Illon B 1	5.77	0.23	2.23	0.36	0.15	31.51	99.72
Ville-sur-Illon B 2	5.71	0.23	2.21	0.35	0.14	31.74	99.79
Ville-sur-Illon B 3	5.61	0.23	2.21	0.35	0.14	31.62	99.19

The synthetic water medium had following composition: 0.6 mM $CaSO_4$, 0.15 mM Na_2SO_4, 0.5 mM $NaHCO_3$, 0.2 mM NaCl, 0.2 mM KCl, 0.3 mM $MgCl_2$, which is based on the composition of the contracted wetland of Rampillon. In order to keep the natural conditions, no additional buffers, vitamins or any other compounds were added to the reactor, except from addition of nitrate in order to follow denitrification. All experiments have been performed in cylindrical reactors (d = 20 cm, height = 50 cm, S=0.031m²) made of PMMA (Plexiglas), in which there was 5 cm of sediment and 25 cm of water unless otherwise stated. Graphite felt

GFD6EA was provided by SGL, Germany. 316L stainless steel wire was provided by SAF-FRO (∅ 1.2 mm diameter). Stainless steel mesh 316L was provided by Gantois industries (St Die des Vosges, France) (∅ 0.56 mm, nominal aperture 1000 µm and 41% transparency). Iron bare (∅ 1 cm) and wire (∅ 1 mm) were taken from the laboratory stock. Stainless steel wires that we insulated with a heat-shrinking polymer tubing have been used for all electrical connections with elements of the devices.

2.2. Electrochemical studies

Electrochemical measurements were performed in the laboratory with potentiostat SP-150 Biologic in a two or in a three electrodes system. All potentials were measured versus SCE and reported hereafter versus SHE after proper correction ($E_{SCE/KClsat}$ = 0.248 V). The simultaneous potential and current measurement were obtained by connecting all electrodes in water as working electrode and all electrodes in sediment as counter electrode. Cyclic voltammetry (CV) was run at a scan rate of 1 mV s^{-1}. CV in the field were done with similar parameters, but with using a portable PalmSens4 potentiostat.

In order to measure simultaneously short circuit current and mixed potential, Zero-Resistance Amperometry (ZRA) was employed, which in Biologic settings is called Electrochemical Noise (ECN) (Electrochemical Applications → Corrosion). ECN is usually used in the corrosion studies in order to measure low fluctuations in corrosion current and potential on the metal-solution interface that originate from pitting on corroding metal at E_{OCP}. It is combining measurement of electrochemical potential noise and electrochemical current noise. Technically, in case of MES no noise is measured, but this technique allows to apply zero volts between anodic and cathodic parts, which imitates classical MES yet allows for deeper electrochemical analysis. In order to use it, MES should be divided into two parts, each of them immersed in different medium (rich in electron donors or rich in electron acceptors). By using ECN, the current between these two parts and the direction of electron flows can be measured, which confirms directly the principle of MES. As the MES is in short circuit, the mixed potential can be also measured versus a reference electrode.

2.3. Ion chromatography

Ion chromatography was used to monitor the nitrate reduction rate. It was carried out using a Metrohm 882 Compact IC plus instrument controlled by MagIC NetTM 3.1 software and equipped with chemical (Metrohm suppressor MSM II for chemical) and sequential

(Metrohm CO_2 suppressor MCS) suppression modules and a conductivity detector. Separations were performed on a Metrosep A Supp 4-250/4.0 column packed with polyvinyl alcohol with quarternary ammonium groups (9 µm particle size) and associated with a guard column (Metrosep A supp 4/5 guard). The mobile phase consisted of a mixture of 1.8 mmol L^{-1} Na_2CO_3 and 1.7 mmol L^{-1} $NaHCO_3$ in ultrapure water (18.2 MV. cm at 293 K). The flow rate was 1 mL min^{-1} and the sample loop volume was 20mL. Standard solutions were prepared from a commercial multi-element standard solution of 1000 mg mL^{-1} of NO_3^-, Cl^-, SO_4^{2-} and NO_2^- (SCP Science).

2.4. Microbial studies

The biofilm was detached from the electrode by placing the electrodes in sterile water and subjected to ultrasounds (two treatments at 25 W for 1 min) from a probe positioned one centimeter above the coupon surface (VibraCell, 250 W, 20 kHz, probe of 10 mm in diameter, BioBlock Scientific).

The V4-V5 region of the 16S rRNA genes was amplified and sequence with the 515 F (5'-GTGYCAGCMGCCGCGGTA-3') and 928R (5'-CCCCGYCAATTCMTTTRAGT-3') primers and the Ion Torrent PGM platform. All reads were imported into Galaxy to be proceeded with FROGS pipeline [201]. For the preprocessing, reads with length between 400bp and 430bp were kept. The clustering and chimera removal tools followed the guidelines of FROGS. OTUs with low abundance were trimmed by keeping only those appearing more than 0.005% in the whole dataset. Taxonomic assignment of OTUs was performed using Silva 132 SSU as reference database.

2.5. Reactor and tubes in Chapter 3

All experiments have been performed in cylindrical reactors (d = 20 cm, height = 50 cm, S=0.031m²) made of PMMA (Plexiglas). The synthetic water medium had following composition: 0.6 mM $CaSO_4$, 0.15 mM Na_2SO_4, 0.5 mM $NaHCO_3$, 0.2 mM NaCl, 0.2 mM KCl, 0.3 mM $MgCl_2$. Unless specified otherwise, the water initially contained 2.4 mmol $NaNO_3$ (150 mg NO_3^- L^{-1}, 33.9 mg N-NO_3^- L^{-1}). The experiments were kept in the dark, in 20-22°C. 10 ml samples were retrieved regularly from the bottom of reactors.

The tubes were prepared with polypropylene, non-woven and calendered from virgin fiber (surface mass: 100 g m^{-2}; filtration opening: 90 µm). In the experiments showed on Schematic 2.1B, the tube had a diameter of 8.5 cm and height of 25 cm. It was filled with sediment so that the water/sediment interface was now mainly vertical and not horizontal as in

control experiments. To increase interface even more, 6 tubes were placed in the reactor (Schematic 2.1 C) and filled also with Sediment1. Their diameter was smaller than in previous one (∅= 6 cm, h = 25cm). The dimensions are presented in Table 2.3.

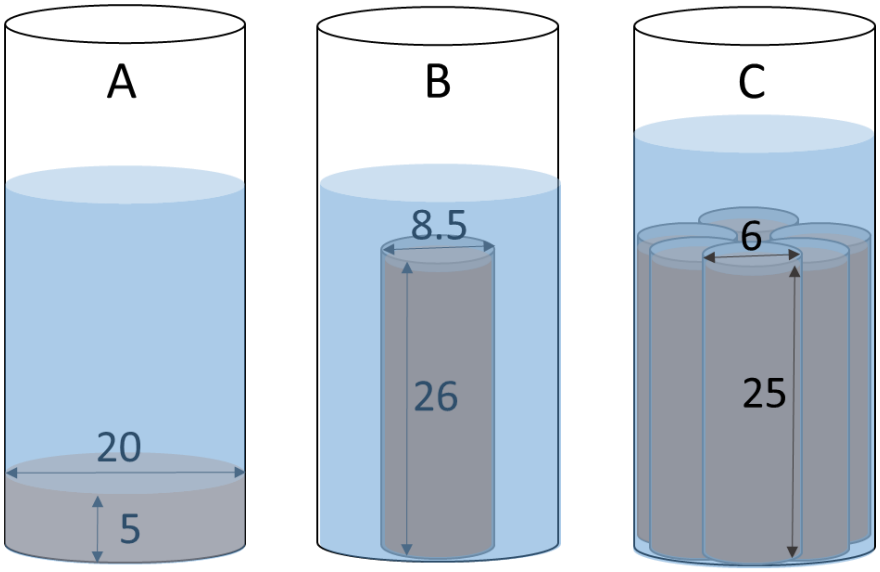

Schematic. 2.1. *Scheme of experiments: A. Control experiment consisting of the sediment in the bottom of reactor B. Water/sediment interface increased 2.5 times C. Water/sediment interface increased 10 times.*

Table 2.3. *The details of three experiments: sediment/water interface areas, sediment and water volumes and height of water column*

Experiment	Sediment/water interface	Sediment volume	Water volume	Height of water column
A: Control	314 cm^2	1.57 l	7.69 l	29.4 cm
B: 1 tube	806 cm^2	1.42 l	7.95 l	29.8 cm
C: 6 tubes	3140 cm^2	4.24 l	8.73 l	41.3 cm

2.6. Preliminary experiments in Chapter 4

In the initial experiment, eight different snorkels have been compared for their potential application for biocathode is snorkel configuration. 4 stainless steel wires and 4 iron wires have been placed in two reactors, one for stainless steel and one for iron. All wires had the same

length but different parts have been exposed to water or sediment and isolated with plastic cover. The wire was accessible from outside of reactor for the potential measurement. Four configurations have been tested with varying water:sediment ratios: 0:1; 1:1, 5:1, 1:0 (Schematic 2.2). The potential of the wires in this environment has been measured daily with a Methrom 605 potential-meter.

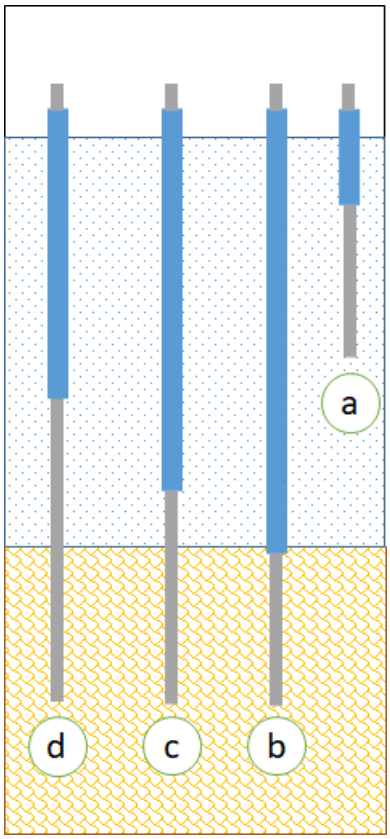

Schematic 2.2. *Scheme of the electrodes placed in different zones of a laboratory wetland in order to measure their potentials: (a) only in water, (b) only in sediment, (c) in water and sediment in proportion 1:5, and (d) in water and sediment in proportion 1:1.*

To choose the correct ratio between part in water and part in sediment, a similar experiment has been tested but using stainless steel grid as electrodes in both sediment and water. Two ratios between water and sediment electrode were tested: they were either of the same size (8 × 4 cm) or the electrode in sediment was 4 times bigger than electrode in water (anode: 2 connected pieces 8 × 4 cm, one above another; cathode: 4 × 4 cm) (Schematic 2.3). All connections were done with isolated stainless steel wires.

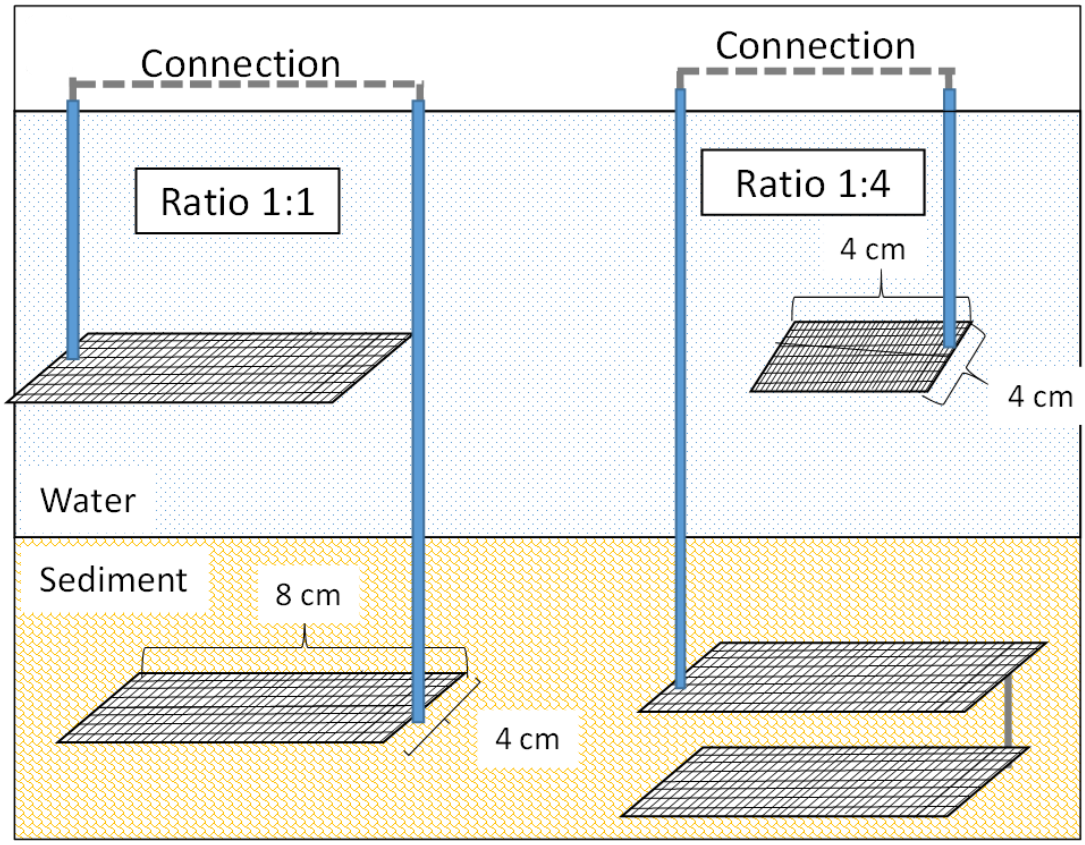

Schematic 2.3. *Scheme of stainless steel grid positions and sizes to evaluate microbial electrochemical snorkels with different anode to cathode ratios. Sediments from Rampillon was used to build this setup.*

Finally, in order to verify the influence of the material of electrode in water on the resulting mixed potential, graphite felt electrode in sediment (8 × 4 cm) and in water (3.5 × 1 cm) were connected with stainless steel wire (Schematic 2.4). A part of stainless steel wire was isolated from water and was accessible from outside of the reactor for monitoring of redox potentials. Two analogous experiments have been also prepared with iron wire instead of stainless steel to confirm corrosion phenomena.

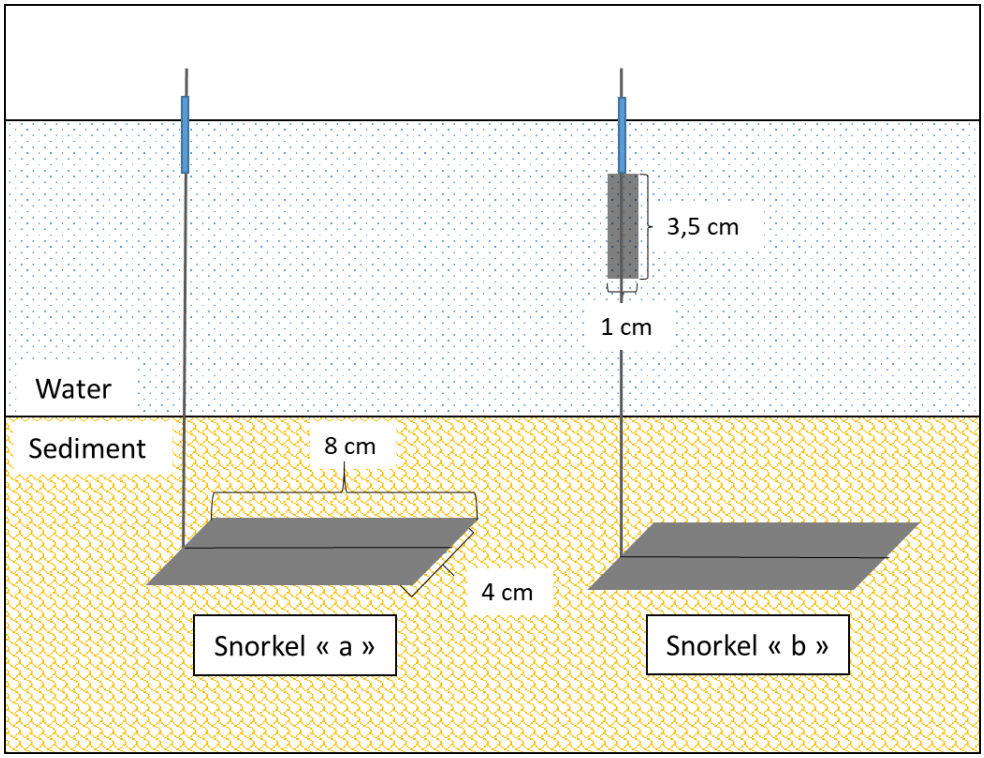

Schematic 2.4*. Scheme of the two snorkels with carbon felt. Snorkel "a" consists of graphite felt in the sediment and a stainless steel or iron wire in water. Snorkel "b" is the same setup, but with additional piece of the carbon felt in water. Sediments from Rampillon was used to build this setup.*

2.7. Model snorkel in laboratory wetland and in field constructed wetland in Chapter 4

Schematic 2.5. reports the electrochemical snorkel that was designed and evaluated both in laboratory wetlands and *on-field* in the constructed wetland of Rampillon (France). Numbering of the electrode starts in the bottom (Electrode1), up to the electrode positioned at the top (Electrode10). 8 pieces of stainless steel grid, of size 10 × 10 cm, have been placed one above another in a distance of 0.5 cm. 2 additional pieces, Electrodes9 and 10 have been placed above them, so the Electrode9 was 1.5 cm above the Electrode8, and Electrode10 was 1 cm above 9. In order to keep this distance and avoid short cut between them, plastic separators have been placed on the sides. Each electrode had a stainless steel wire attached, which has been exposed to water only in the place of connection. These wires have been connected above the level of water, so for most of the time the electrodes were connected all together in short-circuit and they were disconnected only for electrochemical measurements.

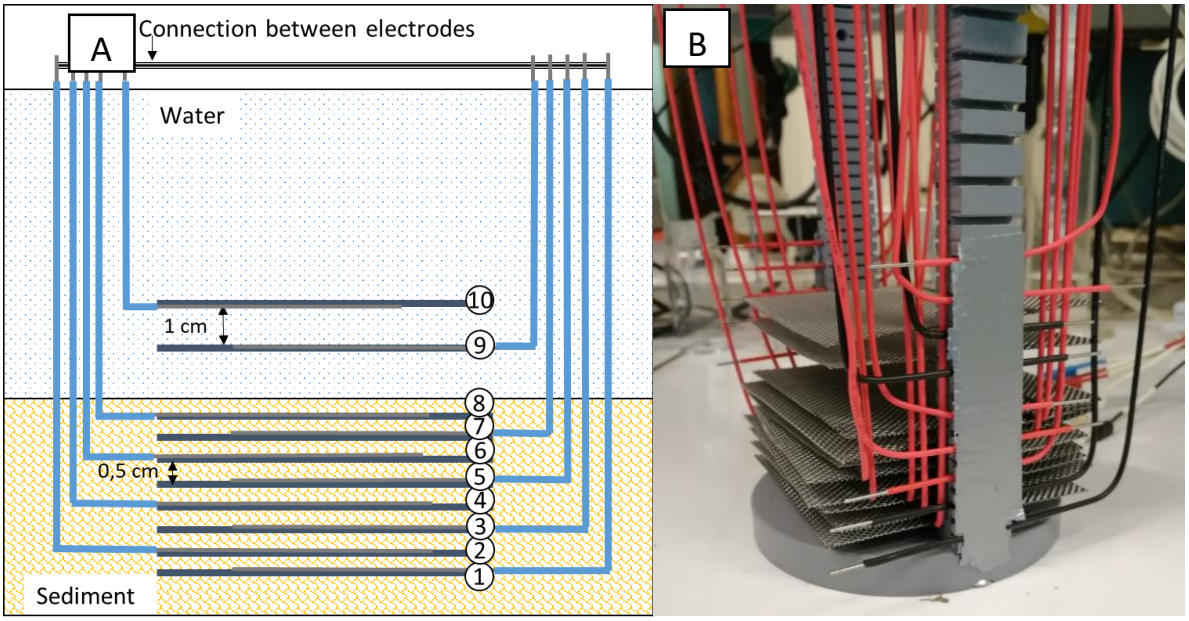

Schematic 2.5. *A. Scheme of the Microbial Electrochemical Snorkel that was evaluated both in laboratory and on-field. The electrodes are numbered from the bottom (lowest Electrode1, in sediment) to the top (highest Electrode10, in water). The electrodes are made of stainless steel grid. B. A photo of the Snorkel (Photo by Author).*

A first system was placed in the plexiglas laboratory reactor. The same system has been placed simultaneously in Rampillon on the 10.04.2019 in a small section of field water-sediment column delimited by a PVC tube of similar dimensions as the laboratory reactor, with openings that allowed the water to flow through. The acclimation lasted for over 1 month. The potential as well as concentration of nitrate were measured in the flowing water on the 10th of April, 20th of April and 15th of May 2019. Control experiments were also prepared in the laboratory, which consisted of stainless steel grid electrodes of the same size positioned either in the sediment or in water. Electrical connections were done as reported before.

2.8. MES design in Chapter 5

In the same reactors as described previously, 12 stainless steel grid anodes of the diameter of 20 cm were placed in the sediment from Ville-sur-Illon, in order to achieve the anode/cathode ratio 6:1. The electrodes were separated by 3D printed plastic separators which were preventing the shortcut between them by ensuring the distance of 0.5 cm (3D printing was done with the use of PruscaSlicer printer with PolyLactic Acid (PLA)) (Schematic 2.6). 2 cm above the top layer of sediment, two other electrodes were placed, also separated by 0.5 cm. The reactor was finally filled with synthetic wastewater and the Ag/AgCl reference electrode

was placed in its upper part. As in the previous experiment in Chapter 4, each electrode had a connection allowing to study it individually. The preliminary experiment was performed and then repeated in triplicate.

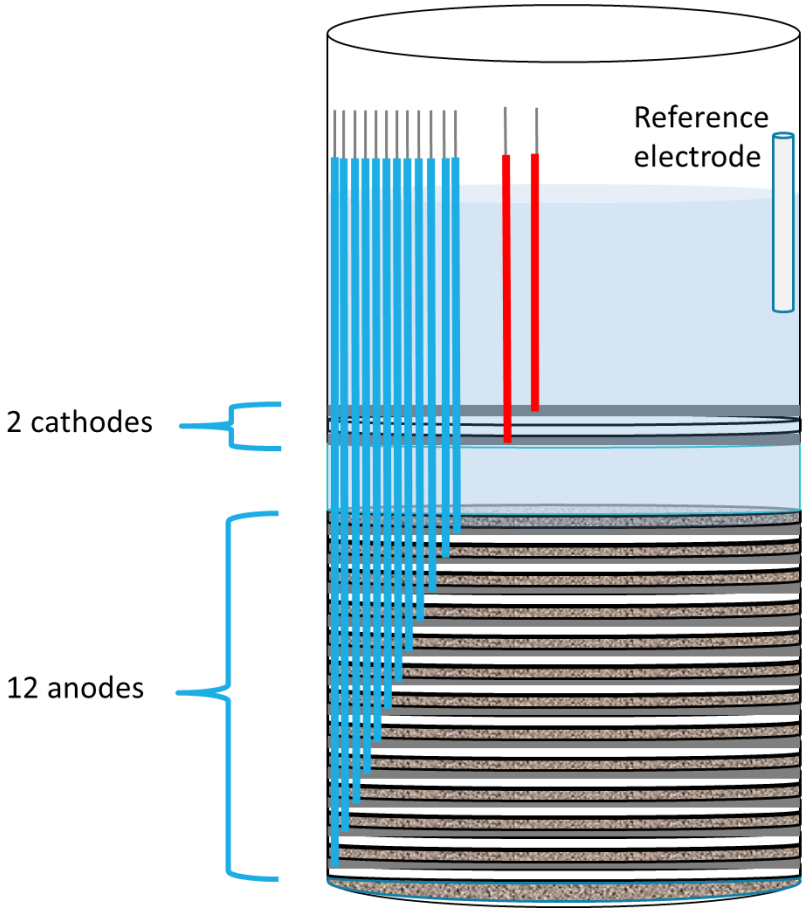

Schematic 2.6. *Scheme of the MES in increased scale. Fourteen stainless steel grid electrodes of diameter of 20 cm were used: 12 in the sediment and 2 in water. Reference electrode was above the electrodes in water.*

2.9. MES in Chapter 6

The tubes filled with sediment were inserted in the reactors of 11 cm diameter and 50 cm height. The synthetic water medium was reaching the level of 30 cm. The tubes had a height of 25 cm and diameter of 6 cm. The tubes with or without electrodes were tested in this chapter. The control (tubes without electrodes) experiments were prepared as in the previous chapter. The MES were prepared in a similar way. Stainless steel grid or activated graphite felt were used as tested electrodes materials. All MES had an electrode inside of the tube, consisting of two pieces of material (6 x 25 cm) (Schematic 2.7, Material B). Additionally, a part of the experiments had another piece of electrode around the tube (Schematic 2.7, Material A). The

summary of the experiments is given in Table 2.4. Except from preliminary studies, all experiments were performed in triplicate.

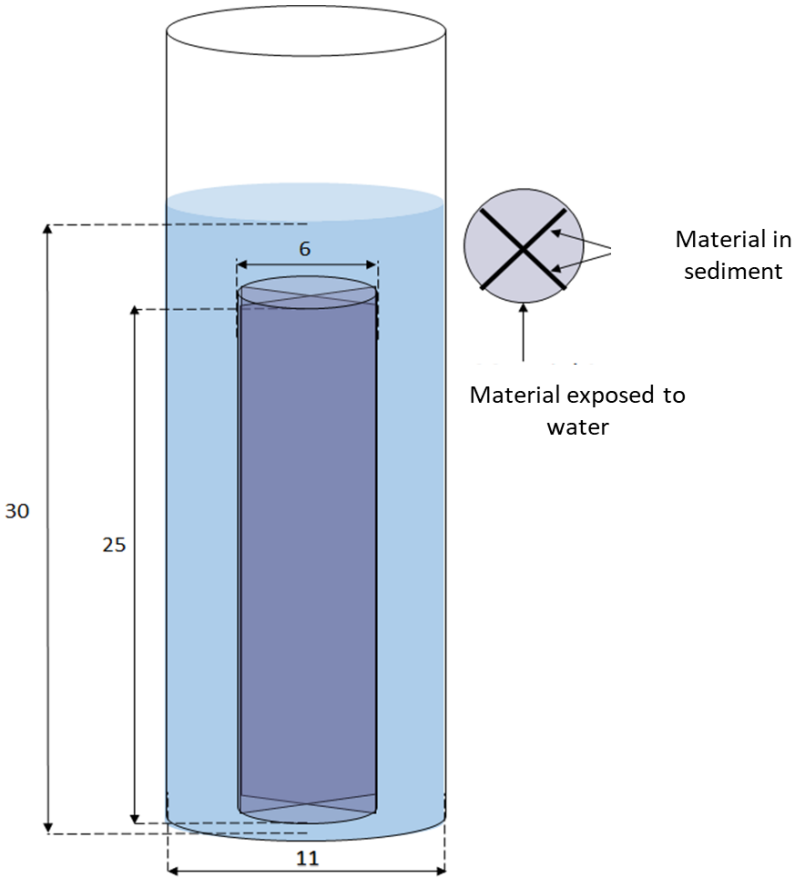

Schematic 2.7 *The experiment with tube and electrode*

Table 2.4. *Summary of the experiments*

	Experiment	Material exposed to water	Material in sediment
Preliminary studies	Graphite0	Graphite felt	Graphite felt
	Steel0	Stainless steel	Stainless steel
	Control0	Polypropylene tissue	----
Experiments with stainless steel	Steel1	Stainless steel	Stainless steel
	Steel2	Polypropylene tissue	Stainless steel
	Control1	Polypropylene tissue	----
Experiments with graphite felt	Graphite1	Stainless steel	Graphite felt
	Graphite2	Polypropylene tissue	Graphite felt
	Control2	Polypropylene tissue	----

3. The influence of sediment/water interface on nitrate removal in constructed wetlands

3.1. Introduction

Denitrification is a microbial process involving reduction of nitrogen oxides (nitrate NO_3^- and nitrite NO_2^-) to gaseous nitrogen (nitric oxide NO, nitrous oxide N_2O or N_2) [2]. It can occur in terrestrial, freshwater and marine systems, where nitrate and nitrite are present in the environment [45]. The most important factors for the denitrification to occur are anoxic conditions and availability of electron donors, for example accessible organic compounds or H_2 [39,40]. The organic compounds should be provided by keeping optimal C/N ratio [39]. There is also a number of other parameters, such as nitrate concentration, hydraulic conditions, temperature, pH, weather, other compounds (salinity, inhibitory substances) or microbial communities [42,43].

Considerable number of approaches was proposed to reduce the N concentrations in aquatic zones. Biological denitrification is based on introducing the nitrate-containing sewage to mixed culture of bacteria in anaerobic conditions [202,203]. It can be coupled with other processes, such as nitrification or phosphorus removal in different sludge systems [204–206]. The other methods are denitrifying bioreactors, such as denitrification beds, denitrification walls, denitrification layers or woodchips bioreactors, have solid carbon substrates in the flow path of contaminated water. These substrates, usually fragmented wood products, prevent the shortage of electron donors so the reactor can last up to 15 years [50]. More simple concept, constructed wetlands (CW) in free surface flow configuration are ecological engineering systems which take advantage of the processes which occur in the natural wetlands, such as wetland vegetation, sediments and microbial communities of wetlands to assist in treating waters in controlled environment [51,207]. Constructed or artificial wetlands are adapted particularly to intercept drain flow [5]. The size of wetland and the area of agricultural fields which drain to it, hydraulic retention time, inflow nitrate concentration, the weather and temperature, wetland hydrology, the macrophytic vegetation and microbiology are all influencing the nitrate removal efficiency in the wetlands [208]. Wetland should be sufficiently large to treat the water draining from the corresponding area, however, the costs of its construction increase with larger wetlands [208]. The water to catchment ratio should not be lower than 1% [209], also because extensive agricultural drainage could modify the soil properties and hydrological regimes [210]. Tanner and Kadlec found that doubling the wetland

area from 1 to 2% of catchment ratio increased the nitrate removal by 75% but further increase from 2 to 4% brought only 43% of additional improvement [211]. Koskiaho and Puustinen compared an older wetland with 5% of catchment ratio and a newer one with 1.3%, and found the average efficiency of 54% and 9% of total nitrogen removal, respectively [212]. Alternative solutions in context of reduced land availability are requested to decrease constructed wetland surface.

Two most commonly studied CWs are free water surface (FWS) and horizontal subsurface flow (HSSF), another basic type is vertical flow (VF). In general, FWS are found to be more efficient, because they better moderate to high level of biological oxygen demand (BOD), total suspended solids, ammonia, total nitrogen and total phosphorus. However, HSSF are more efficient for tertiary BOD levels, pathogens and nitrate [213]. For example, in a constructed wetland in Taiwan, two flows were compared and the nitrate removal rate in HSSF was 1.27 times higher than in FWS [214]. However, the HSSF was filled with gravel, which increases the cost and reduces the efficient volume.

In this chapter, the influence of water-sediment interface area on the rate of nitrate removal on a given surface of constructed wetland is studied. A vertical structure was designed in order to increase this interfacial area and promotes the access of denitrifying bacteria to nitrate. A linear correlation between the nitrate removal rate and the water/sediment interface area was found. Experiments were also performed with water flow mimicking the conditions in constructed wetlands over several months. The evolution of nitrate, nitrite and ammonium concentration in stationary and flow conditions were monitored. A simple model was used to predict the surface of constructed wetland needed to reach the threshold for potable water from a highly polluted draining water. The calculated data are compared to experimental data. Finally, the potential benefit of such 3D design in the CW of Rampillon (France) is discussed.

3.2. Different sediments have similar nitrate removal rate

Sediments from two different constructed wetlands were used in this work: Sediment1 from Rampillon, Ile-de-France (Paris area) and Sediment2 from Ville-sur-Illon, Lorraine. Sediments in Parisian Basin are loamy and in Lorraine Plateau, they are clayed. The chemical composition of the studied sediments was analyzed, including two forms of Sediment1: wet collected in February 2018 (Sediment1A) and dry collected in September 2018 (Sediment1B). In the second constructed wetland there is no period of drying: the water is always present, therefore wet Sediment2: was collected in January 2019. Before studying the denitrification, the compositions of used sediment was analyzed. The results of this analysis are shown in

Tables 2.1 and 2.2. Table 2.1 presents the total amount of sulfur and organic carbon. There is a small concentration of sulfur in all sediments which does not exceed 0.15%. There is a difference in the amount of organic carbon which is 1.49±0.09% for Sediment1A and Sediment1B and 4.91±0.46% for Sediment2. Table 2.2 shows the concentrations of inorganic oxides (SiO_2, Al_2O_3, Fe_2O_3, MnO, MgO, CaO, Na_2O, K_2O, TiO_2, P_2O_5) in both sediments. The amount of some of the salts are also different (MgO, CaO, Na_2O, K_2O, TiO_2) therefore the first question is whether these differences have an influence on the nitrate removal rate.

In order to verify that, several experiments of laboratory wetland were performed at 20°C at controlled temperature room. They contain a 5 cm layer of sediment in the bottom of a tubular reactor (Schematic. 2.1 A, exact information in Table 2.3). Starting nitrate concentration in every experiment in this chapter was 34±2 mg $N\text{-}NO_3^-$ L^{-1}. The results of nitrate removal are shown on Fig. 3.1A. Three experiments containing only Sediment1 collected in different periods were performed and the first-order nitrate removal rate constant k had following vales: 0.052 ± 0.0012 day^{-1} (curve a), 0.040 ± 0.0033 day^{-1} (curve b) and 0.050 ± 0.0057 day^{-1} (curve c) [215]. The average of these values is 0.047 ± 0.0064 day^{-1}. Sediment1 and Sediment2 were also compared in the same experiment. For Sediment2, the k was equal 0.065 ± 0.0044 day^{-1} (curve d). This is a value 1.38 time bigger than the average value for Sediment1. We interpret that this is the consequence of a bigger amount of organic carbon in Sediment2 and/or by the different periods of collecting the sediment. It was noticed that nitrite and ammonium concentrations increased more in experiments made with Sediment1 than in the experiments with Sediment 2, but after 25 days all of these compounds were no longer detected in all experiments (Fig. 3.2).

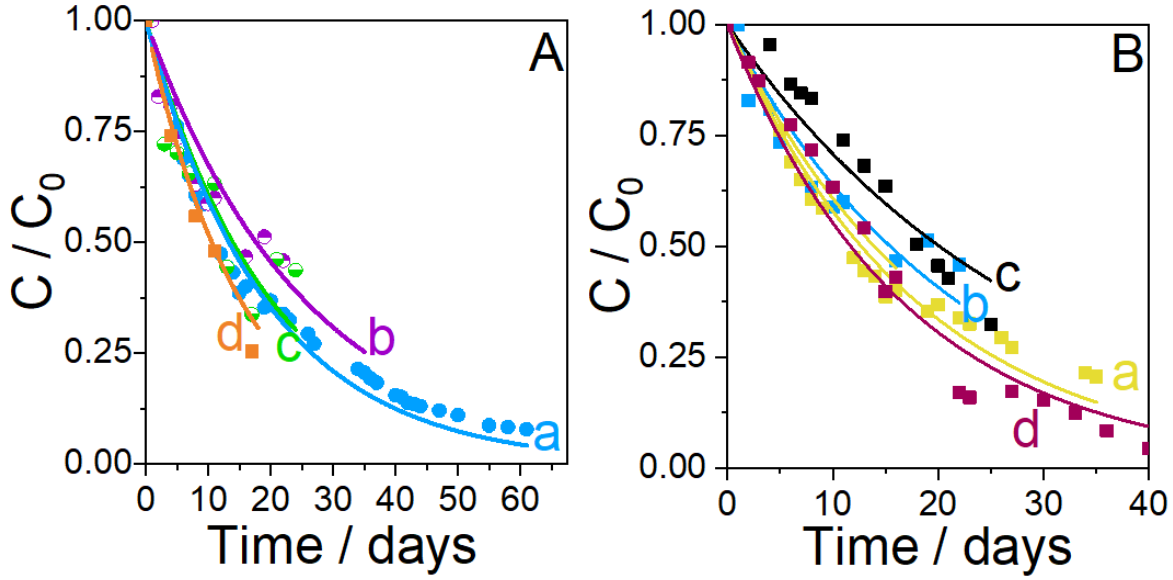

Fig. 3.1. *A. Influence of A. source of the sediment and B. volume of the sediment on nitrate removal. On Fig. 3.1 A: a, b, c - Sediment1; d - Sediment 2. On Fig. 3.2. B: a' - initial volume (V, Sediment1); b' - half of V (Sediment1), c' - 2.5 of V (Sediment2); d' - four times V (Sediment2). First order reaction was considered to adjust the model to experimental data (C =* C_0e^{-kt}*) in all presented experiments* [215].

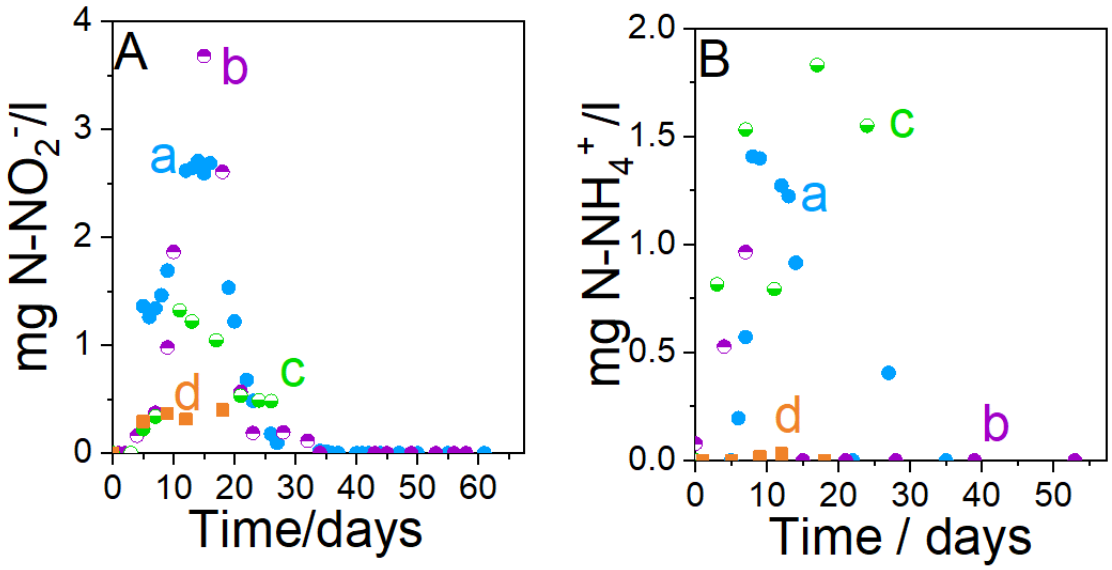

Figure 3.2. *A - Nitrite and B - ammonium concentration in initial experiments comparing different sources of sediment. a, b, c - Sediment1; d - Sediment2.*

Several experiments with varying volume of the sediment at the bottom of the reactor were performed: first of them was half of initial volume of sediment (2.5 cm layer), second with more than two and half times higher volume (12 cm layer) and third with 4 times higher volume (20 cm layer). The results are presented on Fig. 3.1B. The constant k was equal to 0.052 ± 0.0012 day^{-1} (a', sediment1), 0.045±0.003 day^{-1} (b', sediment1), 0.034±0.002 day^{-1} (c', sediment2) and 0.050±0.002 day^{-1} (d', sediment2), for 1, 0.5, 2.5 and 4 times of initial volume, respectively. We therefore conclude that there is no correlation between the volume of the sediment and nitrate removal efficiency. Denitrification performing bacteria require nitrate as electron acceptor and, electron donors, which are here organic compounds in sediment. Although the quantity of electron donors in the reactor increased by increasing the volume of the sediment, these organic compounds remain deep in the sediment and the area where bacteria have access to both electron donors and nitrate in the same time remains limited. However, nitrite production was bigger in experiments during the first month with increased volume of sediment by comparison with other experiments (Fig. 3.3).

The conclusion from these experiments is that neither source of sediment nor its volume is clearly influencing the nitrate reduction rate. The average denitrification rate for all these control experiments is 0.048 ± 0.01 day^{-1} (N = 7), a value that will be used for comparison with further experiments.

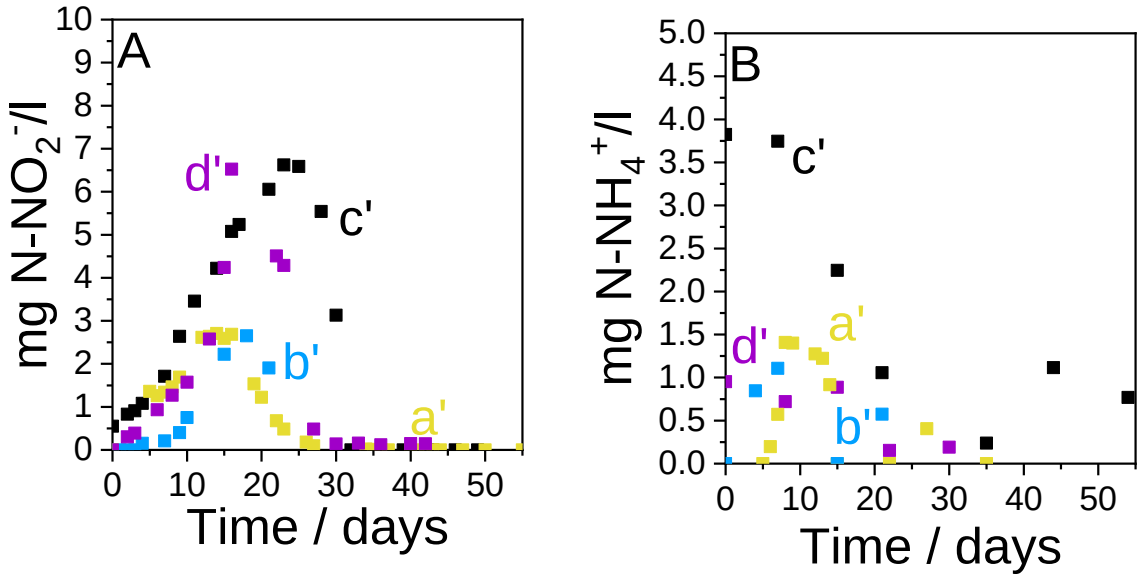

Figure 3.3. *A - Nitrite and B - ammonium concentration in initial experiments comparing different volumes of sediment. a' - original V, b' - half of original V, c' - 2.5 times of original V, d' - 4 times of original V.*

3.3. Increase of the interface between sediment and water increases the nitrate removal rate

In a next step, an experiment was designed to study the influence of the interfacial area between sediment and water on the nitrate removal efficiency. In order to do that, a polypropylene tissue was used - it was permeable for water (and ions in water) but not for the sediment - to build a tube increasing a sediment/water contact area (Schematic 2.1 B). In total, the interfacial area in the control experiments was 314 cm^2 and in this vertical arrangement, it was 806 cm^2 so 2.5 times bigger. The volumes of sediment and of water were comparable for the two experiments. The constant k was 0.12±0.001 day^{-1} for the experiment with vertical arrangement which is 2.5 times higher than the control experiments with sediment in the bottom of the reactor (Fig. 3.4 A).

To increase interface even more, 6 tubes were placed in the reactor (Schematic 2.1 C, Table 2.3) and filled also with Sediment1. The sediment/water interface area was 3140 cm^2, which is 10 times more than in the control experiment. With such architecture, the nitrate removal constant was equal to 0.314±0.021 day^{-1} (Fig. 3.4 B). This value is 6.5 times bigger than for the control experiment. Looking at the 3 values of k for 3 different interface areas, one can conclude that the nitrate reduction rate increases with increasing water/sediment contact surface area (Fig. 3.4 C).

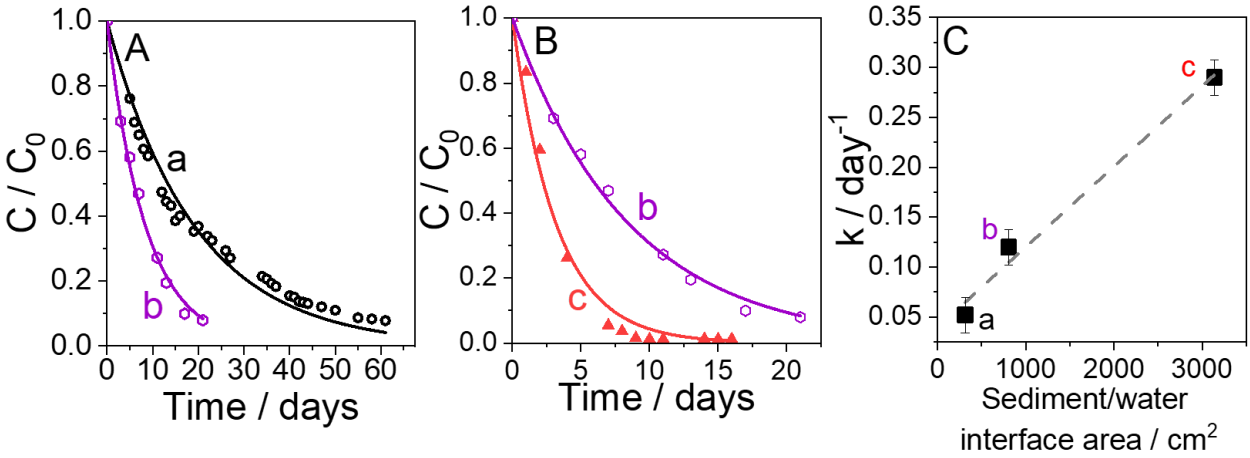

Figure 3.4. *Results of the stationary experiments (Sediment1). a - example experiment with sediment on the bottom of the reactor, b - experiment with one tube - water/sediment interface increased 2.5 times, c - experiment with six tubes - water/sediment interface increased 10 times. A. Comparison of nitrate removal between a and b. B. Comparison of nitrate removal between b and c. C. Linear correlation between water/sediment interface and constant of nitrate removal (R^2 = 0.986).*

In order to evaluate the stability of the nitrate removal properties of the system, nitrate was introduced to the reactor several times, on days 1, 18, 32, 45, 59, 74, 89 and 129 of the experiment. The second nitrate addition was more rapidly treated than the first one (k_2 = 0.392±0.043 day^{-1}), but after that the rate constant was gradually decreasing (Fig. 3.5., k_4 = 0.276±0.009 day^{-1}; k_5 = 0.234±0.001 day^{-1}; k_8 = 0.189±0.007 day^{-1}). We hypothesize that this first increase of the efficiency was caused by of acclimation of the living microorganism, and potentially to the bigger amount of nitrate-reducing bacteria which grew in nitrate-rich environment. However, the later decrease may come from consumption of the organic carbon which serves as the electron donor for these bacteria, or more probably to some limitations imposed by the stagnant water.

This experiment was initially performed with Sediment1 and then repeated with Sediment2. Nitrate was introduced on days 1, 36, 49, 76, 95, 105 and 122. The k from initial nitrate removal was lower than in the previous experiment (k_1 = 0.232±0.001 day^{-1}), however, over the whole experiment the nitrate removal efficiency was very close to the first experiment (Fig. 3.5., k_2 = 0.365±0.014 day^{-1}; k_4 = 0.344±0.017 day^{-1}; k_6 = 0.228±0.001 day^{-1}; k_7 = 0.226±0.01 day^{-1}). We therefore conclude that in the longer perspective, this experiment is repeatable and using very different sediments gives similar results. Moreover, in both experiments the values of nitrite remained low, for most of the time no nitrite was produced, except from occasional peaks which did not exceed 1.2 mg $N\text{-}NO_2^-$ L^{-1} (Fig. 3.6). For the ammonium production, it reached the high value of almost 6 mg $N\text{-}NH_4^+$ in the initial time of the experiment with Sediment1, but after 26 days it decreased and stayed close to 0 for the whole duration (over 160 days). When it comes to Sediment2, an ammonium peak was observed between days 75 and 130 up to over 4 mg $N\text{-}NH_4^+$ L^{-1} (Fig. 3.6). These variations are probably linked to sporadic modifications of the ecological equilibrium in the sediment tube, but rapidly the denitrification was re-established.

Denitrification in wetland does not occur in stagnant conditions, and it was necessary to investigate how the system was behaving in a flow experiment. The results are presented and discussed in the next section.

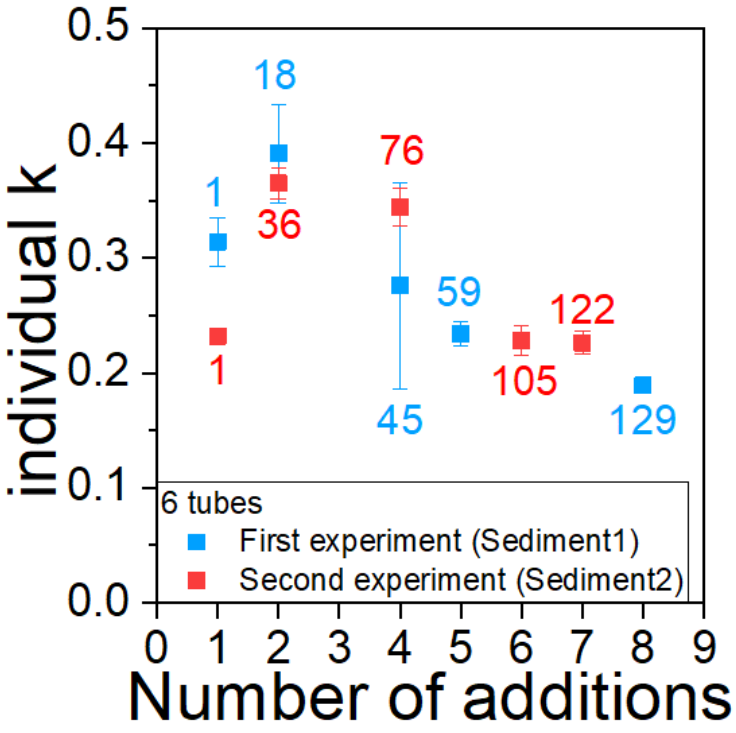

Figure 3.5. *Study of the nitrate removal in longer time, with several introductions of new nitrate. The graph shows the values of nitrate removal rate constant for each addition of nitrate. Sediment 1 was used in First experiment and Sediment 2 was used in Second experiment. The numbers are indicating the days of addition of nitrate during experiment.*

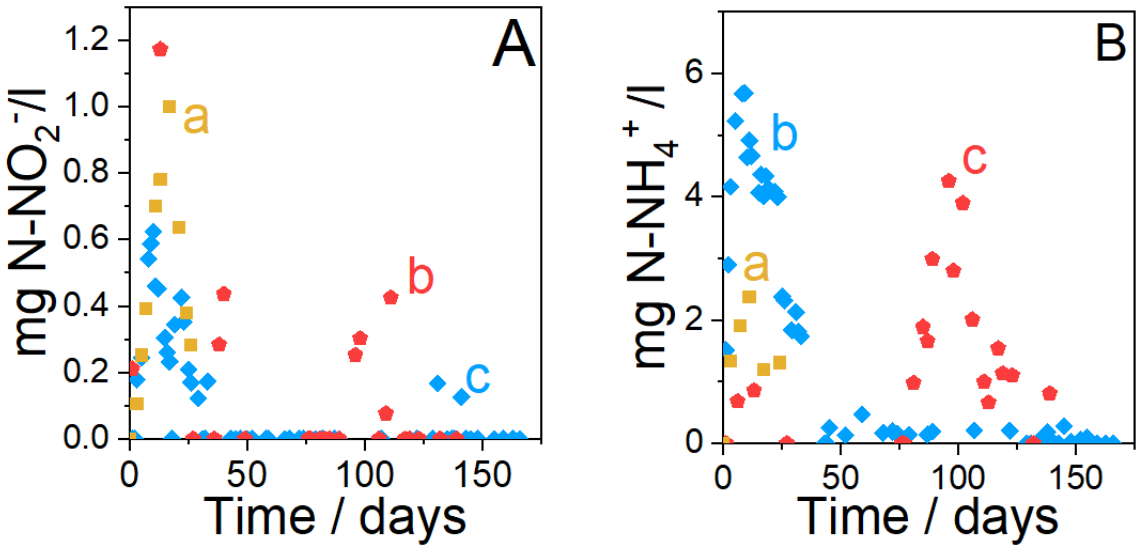

Figure 3.6*. A - Nitrite and B - ammonium concentration in experiments comparing different sediment/water interface. a - interface increase 1.5 times, b - interface increased 10 times (Sediment1), c - interface increased 10 times (Sediment2).*

3.4. Flow experiment

Two reactors were set for the flow experiment. One reactor contained again the 6 tubes with Sediment2 ("Tubes"; Schematic 2.1 C) and the other reactor contained the equivalent volume of sediment but simply on the bottom of the reactor ("Control", similar to Schematic 2.1 A, but sediment height was 13.5 cm and sediment volume was 4.24 l). The synthetic water medium was coming from the same tank for both experiment, the constant flow of 3.4 ml min^{-1} and hydraulic residential time (HRT) of 33h was reached with the use of peristaltic pomp. The inflow was positioned on the bottom of the reactor and the outflow was on its top. The samples were collected from the outlets of the two reactors.

In total, two experiments were done using this flow configuration. In the first one, nitrate of the concentration of 33.9±0.8 mg $N\text{-}NO_3^-$ L^{-1} was constantly introduced into the two reactors for 53 days. The concentration of the outlets was giving stable average values of 22.3±0.7 and 30.1±1.1 mg $N\text{-}NO_3^-$ L^{-1} for Tubes and Control, respectively (Fig. 3.7). The rate constant was calculated with the formula used before, with using HRT as time and it was on average 0.304±0.02 and 0.086±0.004 day^{-1} for Tubes and Control, respectively; the 3D design increased the nitrate removal 3.55 times in this phase. The nitrate removal rate is 89.2 and 270 mg $N\text{-}NO_3^-$ m^{-2} day^{-1} for Control and Tubes, respectively. One can suspect that the mechanism of this faster removal is the release of organic and inorganic carbon which could later react with nitrate in water. However, the concentration of total organic carbon in solutions was almost identical for two experiments: 0.75±0.1 mg L^{-1} and 0.72±0.1 mg L^{-1} for Control and Tubes, respectively (average from three samples), therefore significantly too low to participate in denitrification. The concentration of total inorganic carbon was 16.15±1.2 and 20.11±1.1 mg L^{-1} for Control and Tubes, respectively (average from three samples). The difference in case of inorganic carbon is more clear than for organic one, however it is still not significant enough to explain the 3.5 times increase. Therefore, we interpret this result as the direct consequence of increase the water/sediment interface. Moreover, the nitrite production was significantly lower in the Tubes reactor: the maximum was 0.7 mg $N\text{-}NO_2^-$ L^{-1} and nitrite was no longer detected after day 40. In Control, it was up to 2 mg $N\text{-}NO_2^-$ L^{-1} and nitrite was present during the whole experiment (Fig. 3.8).

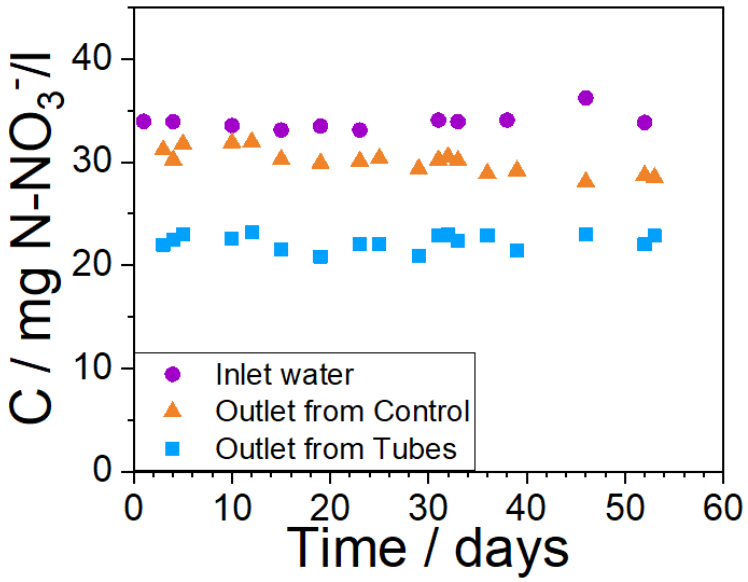

Figure 3.7. *Results of the experiment in flow (Sediment2). Dots (a) represent the inlet concentration, triangles (b) are the outlet concentration of control experiment and squares are the outlet concentrations of the experiment with tubes*

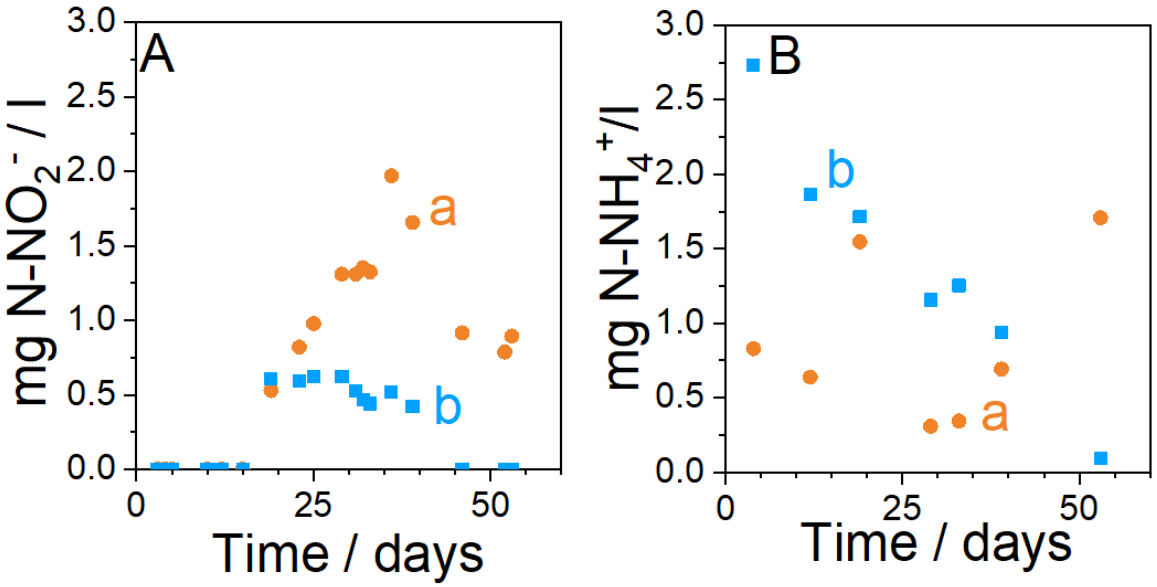

Figure 3.8. *A - Nitrite and B - ammonium concentration in flow experiments in time: a - Control experiment, b - tubes experiment.*

This experiment allowed to significant decrease of the nitrogen nitrate concentration to 22.3 mg $N\text{-}NO_3^-$ L^{-1}, but it was still too elevate to meet safety regulations, which for drinking water are 11.3 mg $N\text{-}NO_3^-$ L^{-1} - in European Union [14] and 10 mg $N\text{-}NO_3^-$ L^{-1} in the USA [216].

Therefore, a theoretical calculation was made in order to predict the wetland surface necessary to meet these standards. First order kinetics was used ($C = C_0 \cdot e^{-kt}$) with the values of k = 0.27 day^{-1} and k = 0.06 day^{-1}, for experiments with Tubes and Control respectively, which is the average of k from five preceding measurements. By calculating C from this formula, with C_0 = 33.9 mg $N\text{-}NO_3^- L^{-1}$, the obtained result is 23.4 which corresponds well to the experimental result. If we imagine a second identical reactor with Tubes connected in series with the first one, it would collect the outlet water from the first one - with nitrate concentration 22.3 mg $N\text{-}NO_3^- L^{-1}$. Concerning this value as C_0, the outlet C for this second reactor also can be calculated with first order kinetics and the result is 16.1 mg $N\text{-}NO_3^- L^{-1}$. Following the same idea, if the third reactor is added, its outlet C would be 11.1 mg $N\text{-}NO_3^- L^{-1,}$ for the forth one it is 7.7 mg $N\text{-}NO_3^- L^{-1}$. From this calculation the conclusion is that reactor four times bigger would be necessary to meet the limits of UE and USA for drinking water, which would have a surface of 0.125 m^2 (Fig. 3.9). The same considerations about the Control experiment (k = 0.06 day^{-1}) would lead to presumption that fourteen reactors in series would be necessary to meet safety limits in treated water, corresponding to surface of 0.44 m^2 - 3.5 times bigger surface. Therefore, the reduction rate increase is the same as in the previous experiment in flow.

These theoretical results for the Tubes experiment were verified experimentally. The outlet concentration was measured and used as inlet concentration for a next experiment. The concentration of nitrate was thus decreasing stepwise. As a result, four steps were necessary to decrease the concentration below desired value. Outlet values for each of 4 steps were respectively: 22.3, 17.2, 12.4 and 7.8 mg $N\text{-}NO_3^- L^{-1}$, which is very close to the calculated value (Fig. 3.9).

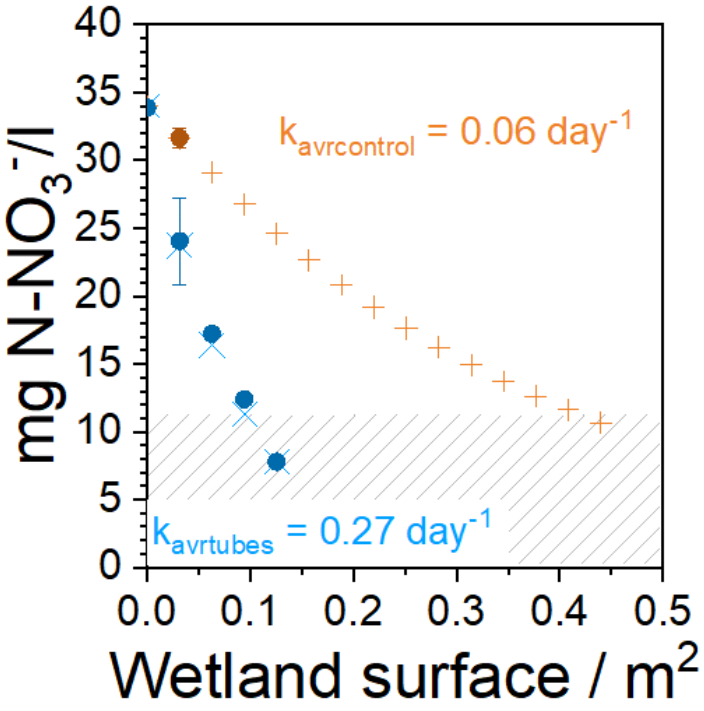

Figure 3.9. *The experimental and calculated wetland surface necessary to reach the low nitrate concentration. Dots - experimental values for tubes (blue) and control (orange) experiments. X - calculated value for tubes experiment. + - calculated value for control experiment.*

3.5. Scenario of application in constructed wetland in Rampillon

As discussed in the previous sections of this manuscript, increasing the interface between sediment and water in an artificial wetland can lead to a significant increase in the denitrification rate, e.g. 3.5 times in the flow experiment. While this preliminary experiments performed at the laboratory level are not necessarily easy to translate in a large wetland like the one in Rampillon, we would like to consider in this section what could be the impact of such kinetic increase on the denitrification performances.

The constructed wetland in Rampillon (Photo 3.1) was created in 2010 in order to collect water draining from Rampillon's watershed. It has a surface of 5300 m^2 and consist of three basins which aims to increase the retention time and mitigation processes. The watershed of Rampillon is 355 ha therefore the wetland's surface is 0.15% of this area [217]. In principle, the water to catchment ratio should not be lower than 1%. In practice a wetland of such size (4 ha in case of Rampillon, 7.5 bigger than the current surface) could be difficult to build, and any robust approach that will allow increasing denitrification should be beneficial.

Photo 3.1. *The constructed wetland in Rampillon (Seine et Marne, FR) (Photo by Author).*

For the discussion, we have considered the inlet and outlet concentrations from the period between autumn 2014 and summer 2015 that are shown on Fig. 3.10. In 36.8% of this calendar period, the measured nitrate concentrations were higher than 11.3 mg $N\text{-}NO_3^-$ L^{-1} (50 mg NO_3^- L^{-1}). The figure shows also a modeled nitrate outlet concentration, calculated by using Tank-In-Series (TIS) model that allows a good description of the experimental data (Fig. 3.10, curve c) [218].

As discussed before, by engineering the water/sediment interface, one can increase the kinetic of the whole wetland in order to globally reach better performances. On Fig. 3.10 B, curve d is a TIS model of outlet nitrate concentration in a situation when the apparent rate coefficient was increased by 3.55 times (the data extracted from the flow experiment in section 3). This change would allow the outlet concentration to stay 11.3 mg $N\text{-}NO_3^-$ L^{-1} in 94% of the calendar period, to be compared with 63% with the actual kinetic, therefore the change would be significant. In order to decrease the number of situations when the concentration is over this limit to below 1%, the apparent rate coefficient should be increased 6.5 times, a value that was reported in section 2 with static experiments (Fig. 3.10 B, curve e).

Of course, the exact method to reach such an increase of the sediment/water surface area needs further optimization and evaluation before to be implemented on a larger scale, but the promising results reported here open a new door for intensification of artificial wetland that can promote their development in agriculture area under high land pressure. For example, one specific area of the wetland could be dedicated for denitrification. This area could be deeper,

filled with tubes in high density. The sediment or soil dug during construction of the wetland would be reused to build tubes. This research showed that the source and composition of sediment does not have a big impact on the denitrification rate. Letting macrophytes such as juncus grow in the tubes [219] could be a strategy for additional increase of denitrification. In previous sections we showed that the production of nitrite and ammonium in experiments with Rampillon's sediment was not significant. Moreover, it was proven that the N_2O emissions in this wetland are less than 0.01% of denitrified nitrate [217]. Therefore, this strategy could be a sustainable way to reduce nitrate in sensitive area with high anthropic pressure.

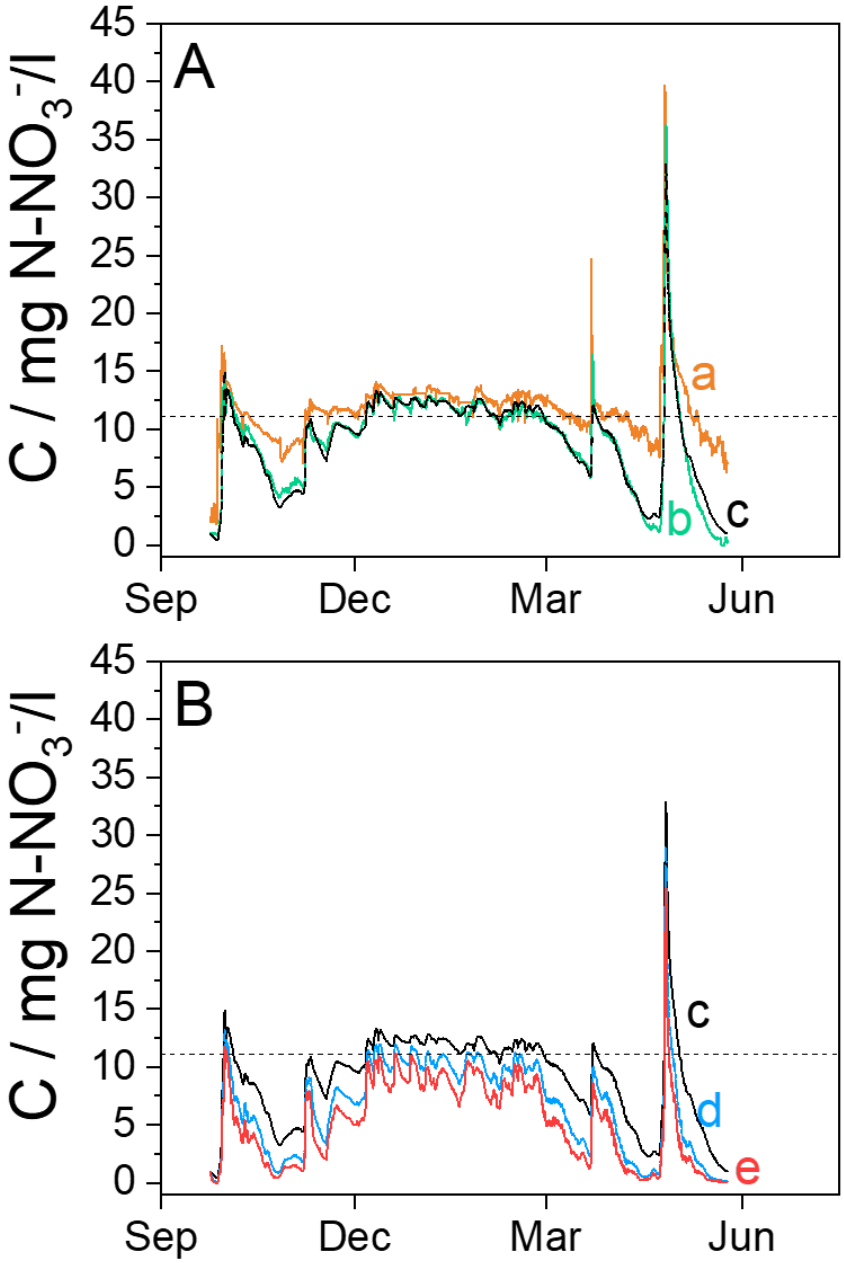

Figure 3.10. *A. The inlet (a) and outlet (b) nitrate concentrations in constructed wetland of Rampillon, between autumn 2014 and summer 2015. Curve c is a Tanks-in-Series model of outlet nitrate concentration of the wetland B. Comparison of a model outlet nitrate concentration (curve c) with a hypothetical outlet nitrate concentration which could be achieved by increasing the water/sediment interface. Curve d: apparent rate coefficient increased 3.55 times, curve e: increased 6.5 times.*

3.6. Conclusions

In this study, we quantitatively measured the influence of the water/sediment interface on nitrate removal rate on the same surface of wetland. We found the linear correlation between the water/sediment interface area and the nitrate removal constant, regardless the origin and composition of the sediment. The experiment performed in flow showed that by increasing the water/sediment interface by 10 times, the nitrate removal rate increased 3.55 times and this effect can last for at least 53 days without losing any efficiency. We showed that this increase of reduction rate corresponds to the wetland surface necessary to reach low nitrate concentration, regardless the sediment's origin and therefore its composition. In the constructed wetland in Rampillon, increasing nitrate removal rate 3.55 times should allow reaching the outlet concentration below 11.3 mg $N\text{-}NO_3^- L^{-1}$ 94% of the calendar period, while currently it is 63%. In order to reach low concentration during 99% of the year, the nitrate removal rate should be increased 6.5 times. In this study, the increase of nitrate removal efficiency was caused by increase water/sediment interface which facilitated access to organic carbon. The question that comes next is whether it is also possible to increase this reactive interface not with the 3D structure but electrochemically, with electrode in snorkel configuration.

4. Electrochemical analysis of a microbial electrochemical snorkel in laboratory and constructed wetlands

4.1. Introduction

This chapter focuses of characterizing and understanding the microbial electrochemical snorkel MES. As discussed before, MES is a short-circuited MFC in which the electrons produced in oxidation reaction on bioanode in sediment can freely flow towards the biocathode in water where they can be used in reduction. The potential of the electrode is therefore a mixed potential [220] and no power can be produced in this configuration, but high current can be achieved. As a result, the water decontamination could be more efficient [81]. Few first reports were already trying to apply MES for nitrate reduction but no deeper electrochemical analysis were yet performed. Although Wang et al. did not use directly the snorkel, they noticed a decrease of power and an increase of current and nitrate removal efficiency with decrease of the applied resistance between some graphite felt electrodes of a sediment MFC, which was acclimated in a lake and later studied in conditions imitating natural [221]. With the resistance of 1Ω they observed a 60% decrease of nitrate in 100h, with initial concentration of 2.5 mg N-NO_3^-/l. This removal corresponds to (on average) 0.1225 mg N-NO_3^-/day. Denitrification of water by MES was also described by Yang et al. [80] who used snorkel composed of graphite felt and iron rod. In their study, with initial concentration of 2 mg N-NO_3^-/l, 98% of nitrate was removed in 16 days, which corresponds to 0.36 mg N-NO_3^-/day. Both of these publications have shown promising results, however, in both reports, the initial nitrate concentration was relatively low so it is not considered as "waters affected by pollution", e.g. by Nitrate Directive (91/676/EEC), which have more than 50 mg NO_3^-/l (i.e., 11.3 mg N-NO_3^-/l).

Here, the electrode material (iron, stainless steel and porous graphite) and configuration in order to obtain the appropriate mixed potential for nitrate removal, without the external polarization are examined. Especially, the potential in the range from -300 to -100 mV vs. SHE is targeted because it should be the most proper for developing the nitrate-reducing biocathode, as discussed in the introduction. A model MES is built, in which cathodic and anodic sides could be studied in their environments individually. The chosen configuration was prepared and installed in a laboratory and in a full size experimental constructed wetland and exposed to nitrate at a concentration relevant for such application. Electrochemistry and microbiology of both systems were then studied and compared, and the challenges of application of MES for denitrification are discussed.

4.2. Preliminary evaluation of materials

In the initial experiments, either stainless steel or iron were used to measure the redox potentials of these two electrode materials in different zones of a laboratory wetland. The goal was to evaluate if these potentials could be suitable to grow the nitrate-reducing biocathode, according to the data reported in the literature (i.e., in the range from -300 to -100 mV vs. SHE). For that, we used metallic wires placed in the reactor in the four different configurations shown on Schematic 2.2. One wire was placed only in water (a) and another one only in sediment (b). Then, two samples were placed both in sediment and in water with different length ratios, i.e. with a longer section in sediment (c) and a similar length in sediment and in water (d). We examined first the behavior of stainless steel electrodes. When placed only in water (Table 4.1; Fig. 4.1, curve a), the potential of the electrode reached values comprised between +450 and +650 mV vs SHE. Such potential values in natural (non-sterile) waters are often interpreted as oxygen reduction potential of biocathode developed on stainless steel [222,223]. Note that no corrosion was observed during the three months of this experiment.

When fully buried in the sediment (Table 4.1; Fig. 4.1, curve b), the potential reached values of around -250 mV vs SHE. This is a typical value found as open circuit potential (OCP) of the bioanode in the literature [224]. Stainless steel wires which were then placed in the interface between sediment and water reached intermediate potential values that stabilize after about two months in a range that would be suitable for the growth of the desired biocathode, i.e. from -140 to -150 mV (Table 4.1; Fig. 4.1, curves c&d).

Iron electrodes show a very different behavior. Regardless of the position, in water, in sediment or at the interface, all iron wires reached immediately very negative potential which was ranging from -400 to -500 mV vs SHE (Table 4.1; Fig. 4.1, curves a’; b’, c’&d’). It has been also observed soon after introducing the wires in the laboratory wetland that the wires became first orange before a thin layer of black residue deposited on the surface of sediment. Clearly, the potential values observed on iron are due to the corrosion of the metal in water and in sediment and not to oxidation of sediment electron donors that are expected at potentials higher than -300 mV vs SHE [225,226].

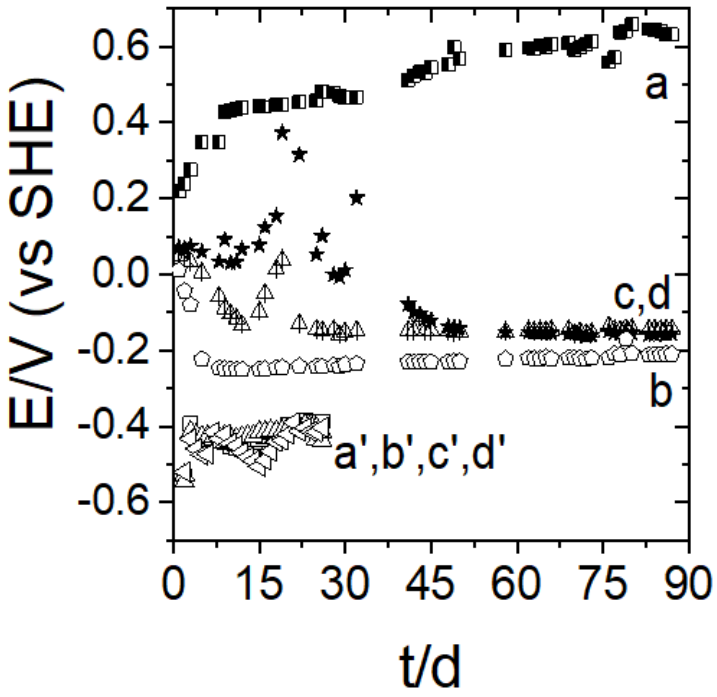

Figure 4.1. *Results of daily potential measurements of different materials in different zones of laboratory wetland: (a, b, c, d) are stainless steel electrodes and (a', b', c', d') are iron electrodes. Sediments from Rampillon.*

Table 4.1. *Summary of redox potential studies of metallic wires connecting sediment and water in different ratios. The long-term potential after stabilization is given in the table; the day-by-day values are reported in Fig. S1 along with a scheme of the experiment. Sediments from Rampillon.*

Material	Water : sediment ratio	E/mV (vs SHE)
Stainless steel	1:0 (only water)	Between +450 and +650
Stainless steel	0:1 (only sediment)	-250
Stainless steel	1:1 (sediment and water)	Between -140 and -150
Stainless steel	1:5 (sediment and water)	Between -140 and -150
Iron	1:0 (only water)	Below -400
Iron	0:1 (only sediment)	Below -400
Iron	1:1 (sediment and water)	Below -400
Iron	1:5 (sediment and water)	Below -400

From this first series of experiments, we conclude that stainless steel electrodes positioned at the water sediment interface can reach the redox potential required to develop the biocathode without external polarization. Moreover, we suspect that iron would not be suitable

because its potential was very negative, in relation with corrosion that was observed in the reactor.

In the next experiment we evaluated 316L stainless steel mesh basic material for the design of this microbial electrochemical snorkel (Schematic 2.3). Similarly as with wires, we implemented two different ratios between the surface of electrode buried in the sediment and the one positioned in water, i.e. 1:1 and 1:4 (four times bigger surface in sediment). In principle, the use of meshes allows to reach a much higher surface area to promote more efficiently electrochemical denitrification.

Fig. 4.2A reports the evolution of potential with time. With ratio 1:4 (curve b), the potential reach rapidly -160 mV vs SHE, 65 mV more negative than with 1:1 ratio (curve a). Thus, we confirm here that stainless steel meshes can be used for the design of an electrochemical snorkel. A more negative mixed potential value is reached when higher surface is introduced in sediment than in water. As shown in Fig. 4.2B, when the contact between the two electrodes was open, the potential of both electrodes rapidly shifted within few hours from the mixed potential towards more negative values for the electrodes that are in sediment, and toward more positive values for the electrodes located in water. Therefore, the mixed potential reached by the snorkel is indeed a function of the individual electrode potentials and their relative surfaces.

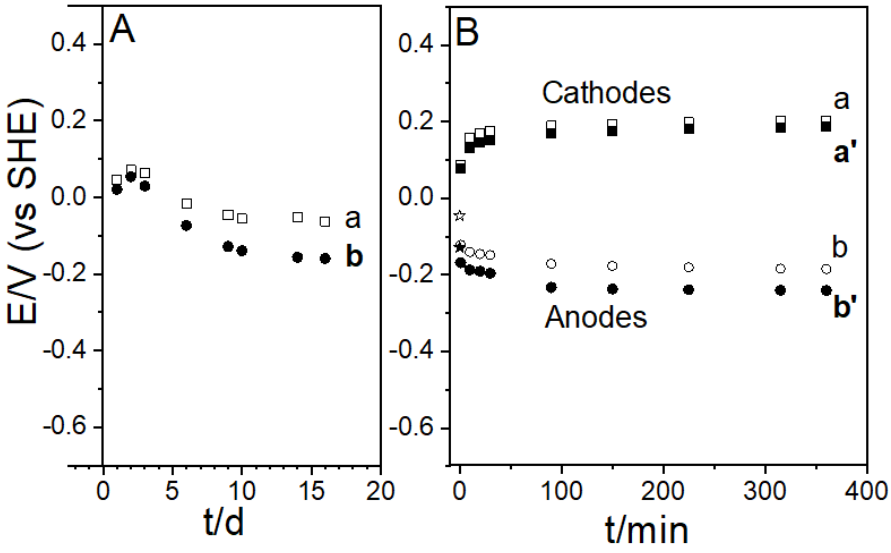

Figure 4.2. *Study of the influence of the electrode size in water and sediment on the potential of connected system. (A) Daily measurements of potentials of connected MES with different ratios: a - ratio 1:1; b - ratio 1:4. (B) Potential variation after disconnecting the two electrodes*

that are located one in sediment and the other in water. Points a (white squares show the values for disconnected cathode for Ratio 1:1, a' (black squares) - for Ratio 1:4. Points b (white circles) show the values for disconnected anode for Ratio 1:1, b' (black circles) - for ratio 1:4.

Before going further, we have also performed few experiments with graphite felt electrode that are widely used in electromicrobiology to support electroactive biofilms because of its very high surface areas. An additional motivation was to evaluate experimentally a previous research reported few years ago that involved a microbial electrochemical snorkel composed of iron in water and graphite felt in the sediment [80]. Here, we first investigated the influence on the potential of the microbial electrochemical snorkel of graphite felt with either iron or stainless steel wires. The graphite felt was placed in sediment and connected with significantly smaller stainless steel or iron wires in water (Schematic 2.4).

The daily potential measurements for the experiment with stainless steel and graphite felt confirmed the expected role of graphite felt in sediment on the mixed potential of the whole system and the electrode reached a more negative potential (-240 mV vs SHE, Fig. 4.3, curve a) than with the stainless steel grid snorkel reported before (-160 mV vs SHE, Fig. 4.1B). Replacing the stainless steel wire with iron led to much lower potential (-467 mV vs SHE, Fig. 4.3, curve a'), a potential linked to the corrosion of iron metal that we discussed already. Although it was already described [80] the combination of graphite felt with iron appears not to be suitable for the construction of a microbial electrochemical snorkel, while the abiotic reactivity of metallic iron with nitrate should still be suitable for removal of nitrate [82,227]. Finally, based on this last experiment, we went further, by adding a piece of graphite felt on the metal wire located in water (Schematic 4.2, snorkel "b"). The motivation was to evaluate a microbial electrochemical snorkel composed only with highly porous graphite felt electrodes connected together with metal wires. The porous electrode in water was much smaller than the one in sediment, with a ratio about 1:9. Despite this favorable design (large anode and small cathode), we observed that the potential of this graphite felt snorkel led to very high potential values, +400 mV vs SHE after two months in the laboratory wetland (Fig. 4.3, curve b). We did not observe so positive potentials when the stainless steel was tested, even when the ratio between anode and cathode was 1:1. This high value should not be suitable for nitrate reduction, and this design was not considered for next steps of this research. When stainless steel wire was replaced with iron, the situation was different but not more favorable. The potential of the snorkel was again very low, -450 mV vs SHE (Fig. 4.3, curve b'). In addition, a large amount of corrosion product was observed.

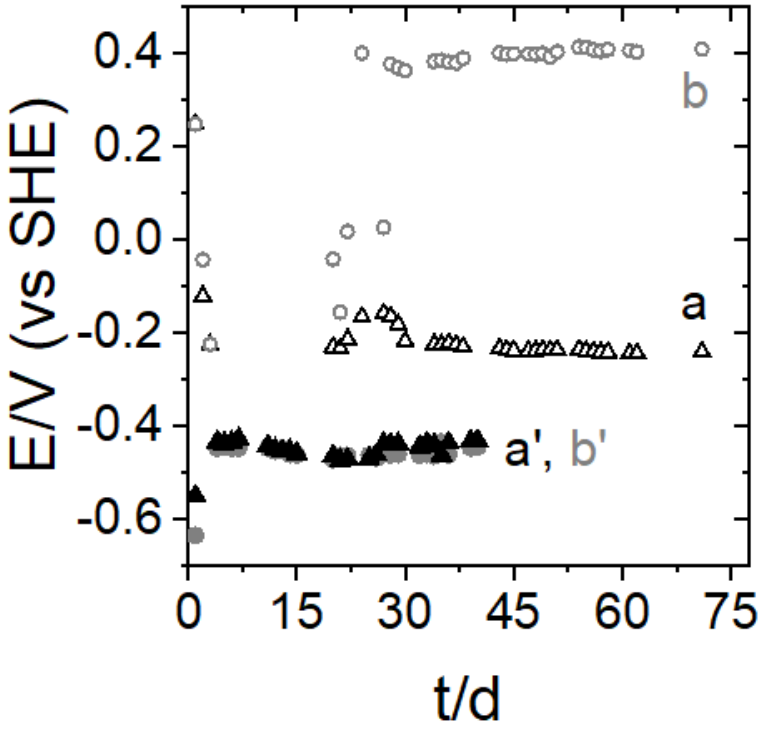

Figure 4.3. *Daily potential measurement with a MESs made of (a) graphite felt in sediment and metallic wire in water and (b) graphite felt in both sediment and water, connected together with a metallic wire. (a&b) were prepared with a stainless steel wire and (a'&b') with an iron wire. Sediments from Rampillon.*

As a conclusion, a snorkel prepared with 316L stainless steel was found the most suitable to reach potentials below -100 mV vs SHE at the interface between sediment and water, without evidence of degradation of the system by corrosion. This material was used in the next step of this study as electrodes in both sediment and water in order to better study the influence on the electrochemical behavior of the environment surrounding the electrodes.

4.3. Design of the stainless steel snorkel and characterization

Laboratory wetland

Schematic 2.5 reports the electrochemical snorkel that was designed and evaluated both in laboratory wetlands and on-field in the constructed wetland of Rampillon (77, France). The setup is composed of 10 stainless steel grid electrodes positioned parallel to each other from 0.5 cm in sediment and 1 cm in water. Numbering of the electrodes starts in the bottom (Electrode1), up to the electrode positioned at the top (Electrode10). All electrodes can be

connected together at the top of the device and, once disconnected, can be analyzed individually.

Fig. 4.4A (points a) shows the redox potential of individual electrodes within this device, measured 4 days after the experiment started. From Electrode1 to Electrode8, all electrodes in the sediment have potential in the range between -120 and -280 mV vs SHE while Electrode9 and Electrode10 have a distinctive high potential of about +200 and +270 mV vs SHE. Because of this clear difference in the measured potentials, we made the hypothesis that all electrodes buried in the sediment would behave as anodes and the two electrodes in synthetic wastewater (Electrode9 & Electrode10) would behave as cathodes.

All anodes grouped together and all cathodes grouped together were connected to a potentiostat for measuring simultaneously their mixed potential and the current flowing between anodic and cathodic sides of this electrochemical snorkel (Fig. 4.4B). A relatively low current of -0.05mA was observed at the beginning of the experiment and the potential value was close to 0. After about two days, the current reached a value in the range of -0.2 mA (curve I) and the potential of the snorkel decreased below -200 mV vs SHE (curve E). The values were kept in that range also after 6 days of starting the experiment, which proves that a snorkel was effectively created and the potential was in the range that is targeted in this study.

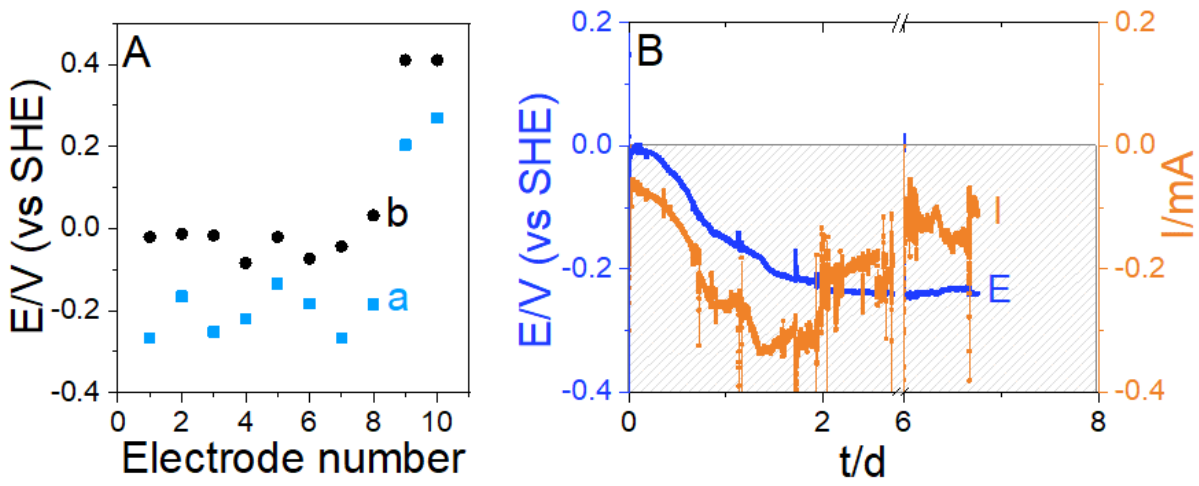

Figure 4.4. *(A) Open circuit potential of each electrode individually in absence of nitrate (a, blue squares) and presence of nitrate (b, black dotes). The potential was measured 1h after disconnecting electrodes from the whole snorkel. (B) Mixed potential of all electrodes connected in short-circuit (blue line) and current flowing between Electrodes 1-8 (anodes - in sediment) and Electrodes 9&10 (cathodes – in water) (orange line). Sediments from Rampillon.*

Cyclic voltammetric characterization was then performed on the different electrodes of this device, initially in the absence of nitrate. Fig. 4.5A&B shows an example of two voltammograms recorded with electrodes buried in sediment (A for Electrode1 and B for Electrode8). These curves are similar to each other, with voltammetric peak for both oxidation and reduction of the redox species present in the sediment. The more interesting signal should be located at the mixed potential of the snorkel and indeed, small oxidation peaks are found close to -100 mV. This oxidation current at anodes is responsible of the current flowing through the snorkel.

Electrode9 and Electrode10 that are considered as cathodic sides behave very differently (Fig. 4.5C&D). A very well defined cathodic wave is observed at +200 mV vs SHE that can be ascribed to the reduction of oxygen. This redox potential (+200 mV vs SHE) is in-between the typical potentials reported for oxygen biocathode [228]. The concentration of oxygen was ~4 mg L^{-1} (0.125 mmol L^{-1}), which was twice lower than in fresh tap water (~8 mg L^{-1}). The decease of oxygen concentration in the reactor compared to tap water could be associated with its consumption in the experiment.

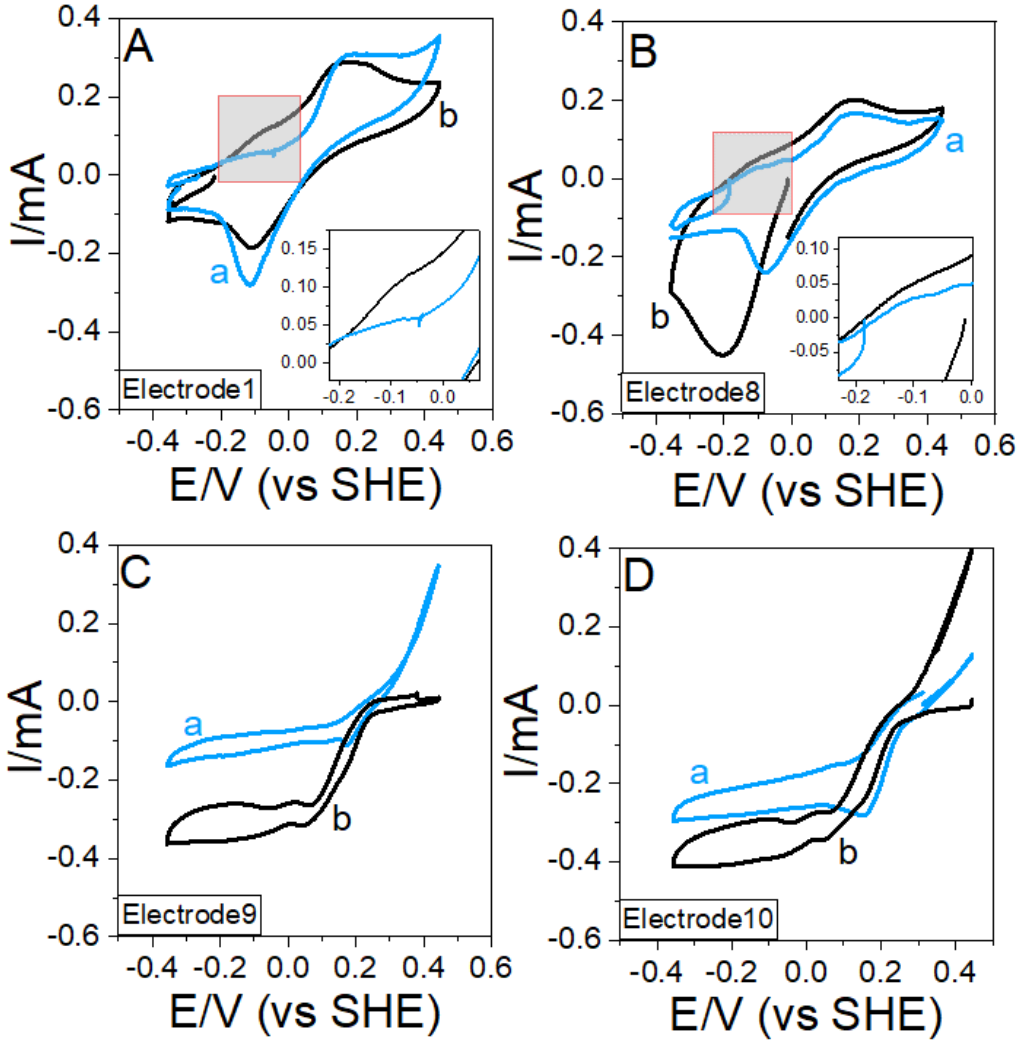

Figure 4.5. *Cyclic voltammetry of different electrodes in presence and absence of nitrate: (A) Electrode1 (lowest in sediment), (B) Electrode8 (highest in sediment), (C) Electrode9 (lower in water) and (D) Electrode10 (higher in water). a (blue line) - without nitrate, b (black line) - with nitrate. Insets: zoom in the low potential region. Sediments from Rampillon.*

At this moment, the bacterial diversity of the biofilms detached from the electrodes, sediment and water was analyzed with 16S rRNA gene analysis. All samples consisted of mixed communities of *Proteobacteria, Bacteroidetes, Cyanobacteria, Firmicutes, Plantomycetes, Chloroflexi* and others, shown on Figure 4.6. The bacteria in the sediment used for the inoculation was composed of major phyla: *Proteobacteria* 33%, *Bacteroidetes* 20%, *Firmicutes* 18%, *Cyanobacteria* 7%, *Acidobacteria* 6% and other *phyla* in less than 5% each. The biofilms on electrodes favored some *phyla* comparing to the community on sediment and water. Generally, on all electrodes the majority was *Proteobacteria* and *Bacteroidetes*, but the

percentage of *Chloroflexi* was also more significant in biofilm electrodes than in sediment and water.

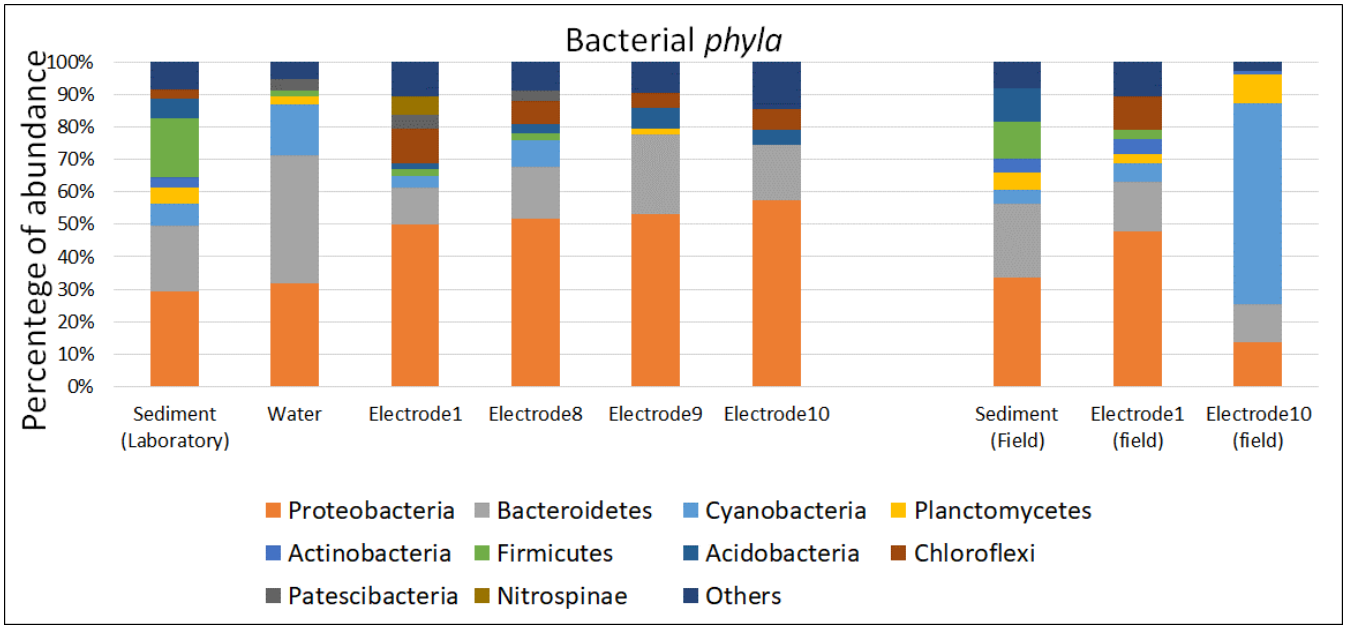

Figure 4.6. *Frequency distribution of bacterial community in sediment and water and on electrodes from 16S rRNA gene analysis.*

The dominating class of *Proteobacteria* was different for electrodes kept in sediment and those which were in water (see Table 4.2). The microbial community on both lowest (1) and highest (8) electrodes in sediment showed that on stainless steel grid the main class was *δ-Proteobacteria*. *Geobacteriaceae* account for 33% of total community in Electrode1 and 18% in Electrode8 (see supplementary data). *Geobacteraceae* is a family which belongs to *δ - Proteobacteria* and it can transfer electrons to electrodes and they are found on the anodes of microbial fuel cell [90]. Its ability to oxidize organic matter by coupling to solid electron acceptor, such as ferric oxide or anodes, has been observed in several papers [229,230]. We conclude from the shape of CV and this 16S analysis that electrodes in sediment have clearly bioanodic behavior that was expected.

Table 4.2 *The detailed data for classes of Proteobacteria.*

Sample	*Proteobacteria* (%)			
	α-	β-	γ-	δ-
Sediment	5	0	15	9
Water	5	0	27	0.5
Electrode 1	1	0	5	44
Electrode 8	1	0	18	32

Electrode 9	6	0	45	1
Electrode 10	5	0	50	1
Sediment (field)	5	0	24	5
Electrode1 (field)	3	0	7	37
Electrode10 (field)	8	0	5	0.6

The community of electrodes in water was dominated by *γ-Proteobacteria* and *Bacteroidetes* (45.9 and 24.5% on Electrode9 and 50.1 and 17% on Electrode10, respectively). Debuy et al. also found that the oxygen-reducing stainless steel biocathode which they developed was also dominated by *γ-Proteobacteria* [231]. Similarly, Rothballer et al. obtained a monophyletic group of unclassified *γ-Proteobacteria* on their high-performing graphite plates biocathodes [232]. Sun et al. tested different biocathode carbon materials and found that *Bacteroidetes* and *Proteobacteria* were the dominant *phyla* on each of them [157]. It has been also shown that O_2-reducing biocathodes dominated by mix of *Proteobacteria* and *Bacteroidetes* achieve significantly bigger current densities than biocathodes with pure culture [233]. It confirms the hypothesis that electrodes 9 and 10 behave like O_2-reducing biocathodes of dissolved oxygen in water column.

As a conclusion, we observed on each side of microbial electrochemical snorkel that there was specialized electroactive biofilms, which communities differed from the community in sediment or water.

The mean concentration of nitrate in the Rampillon's constructed wetland in spring is between 13 and 16 mg $N\text{-}NO_3^-$ L^{-1} but after fertilizer application it can reach around 40 mg $N\text{-}NO_3^-$ L^{-1} [234] and therefore we decided to imitate this most extreme condition for which the device would be needed. After one month a large concentration of nitrate was thus introduced in solution (44 mg $N\text{-}NO_3^-$ L^{-1}, 367 mg $NaNO_3$, 3.14 mmol NO_3^- L^{-1}).

The cyclic voltammetry performed 3 days after nitrate addition confirms that there was a big increase of cathodic current after nitrate addition (Fig. 4.5C&D). We observe a clear cathodic signal starting from at +250 mV followed by a cathodic wave starting around +50 mV on both Electrode9 (Fig. 4.5C) and Electrode10 (Fig. 4.5D). Cheng et al. built a photoelectrotrophic denitrification system in which they observed a nitrate reduction peak with half-wave potential close to 50 mV vs SHE [160]. Gregoire et al. observed similar shapes of the CVs of nitrate-reducing biocathode grown at potential of -250 mV vs Ag/AgCl (-55 mV vs SHE), leading in the presence of nitrate to a cathodic signal with half-wave potential at -200 mV vs Ag/AgCl (~0 mV vs SHE) [123]. Pous et al. found a nitrate reduction wave at -300 mV

vs Ag/AgCl (~-100 mV vs SHE) [128] or around -150 mV vs SHE [117]. Yue et al. for the nitrate-reducing biocathode identified the wave beginning around -300 mV vs Ag/AgCl [161]. Therefore, the cathodic wave we observed in this manuscript in the presence of nitrate, in the region around 100 mV vs SHE is relatively more positive than in most of other studies. Moreover, it also cannot be associated with typical values for oxygen reduction, either more positive (~ 400 mV vs SHE) or closer to 0 V vs SHE [228].

Meanwhile, we observed some significant change in some CV responses recorded with the electrodes in sediment (Fig. 4.5B). After addition of nitrate, a very large reduction signal was observed with a peak at -200 mV vs SHE for Electrode8. Moreover, we measured the OCP of every electrode individually again and we saw that the OCP of all anodes increased to reach a value close to 0 mV vs SHE; the OCP of cathodes increased also to the value around 400 mV (Fig. 4.4A). The mixed potential of the whole snorkel also shifted from negative values to +0.09 V and current increased to -0.55 mA.

Nitrate concentration was monitored simultaneously and compared with the control experiment which consisted of the same amount of the same sediment but without electrodes (See Figure 4.7). The experimental data was fitted to a simple model considering an apparent first order kinetic with $C = C_0 e^{-kt}$. Based on the values from day 0 to 8, we observed the reaction constant $k_{MES} = 0.03 \pm 0.002$ day^{-1} which is 25% higher than $k_{Control} = 0.022 \pm 0.002$ day^{-1}. The experiment was replicated with the sediment from Ville-sur-Illon and a similar behavior was observed (See figures A2.1-A2.4 in the Appendix 2).

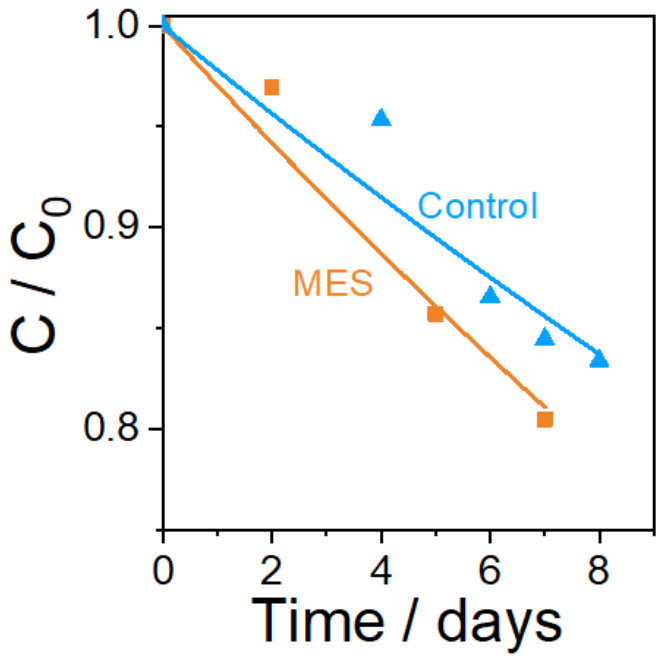

Figure 4.7. *Nitrate removal in laboratory wetland, compared with a control without MES, both prepared with sediment from Rampillon. Results normalized to the same starting concentration C_0 in order to extract the kinetics. The best fit to adjust the model to experimental data was obtained by considering an apparent first order reaction with $C = C_0 e^{-kt}$.*

The most intriguing result comes from the relatively high potential observed in the presence of nitrate and the large cathodic signal that could be observed on some anodes (Figure 4.5B and Figures S2.2A&B and S2.3A&B in the Appendix 2) and we first considered that this change could come from nitrate that diffused into the sediment, interfering with bioanodic processes. It has been shown in several papers that oxygen diffuses into sediment only on very limited depth of about 2-3 mm [235,236], however nitrate diffusion and reduction in sediment is possible and was observed even on 20 cm of sediment depth [237,238]. A control experiment allowed to discard this hypothesis. Two individual electrodes of the same size were placed in the sediment and in water. As expected, these electrodes developed stable potentials after around 7 days from starting which was in the range of OCP of disconnected snorkel electrodes (225 mV vs SHE for electrode in water and -250 mV vs SHE for electrode in sediment). However, addition of nitrate to this control experiment did not change the OCP and the CV responses of these two individual electrodes (Fig. 4.8).

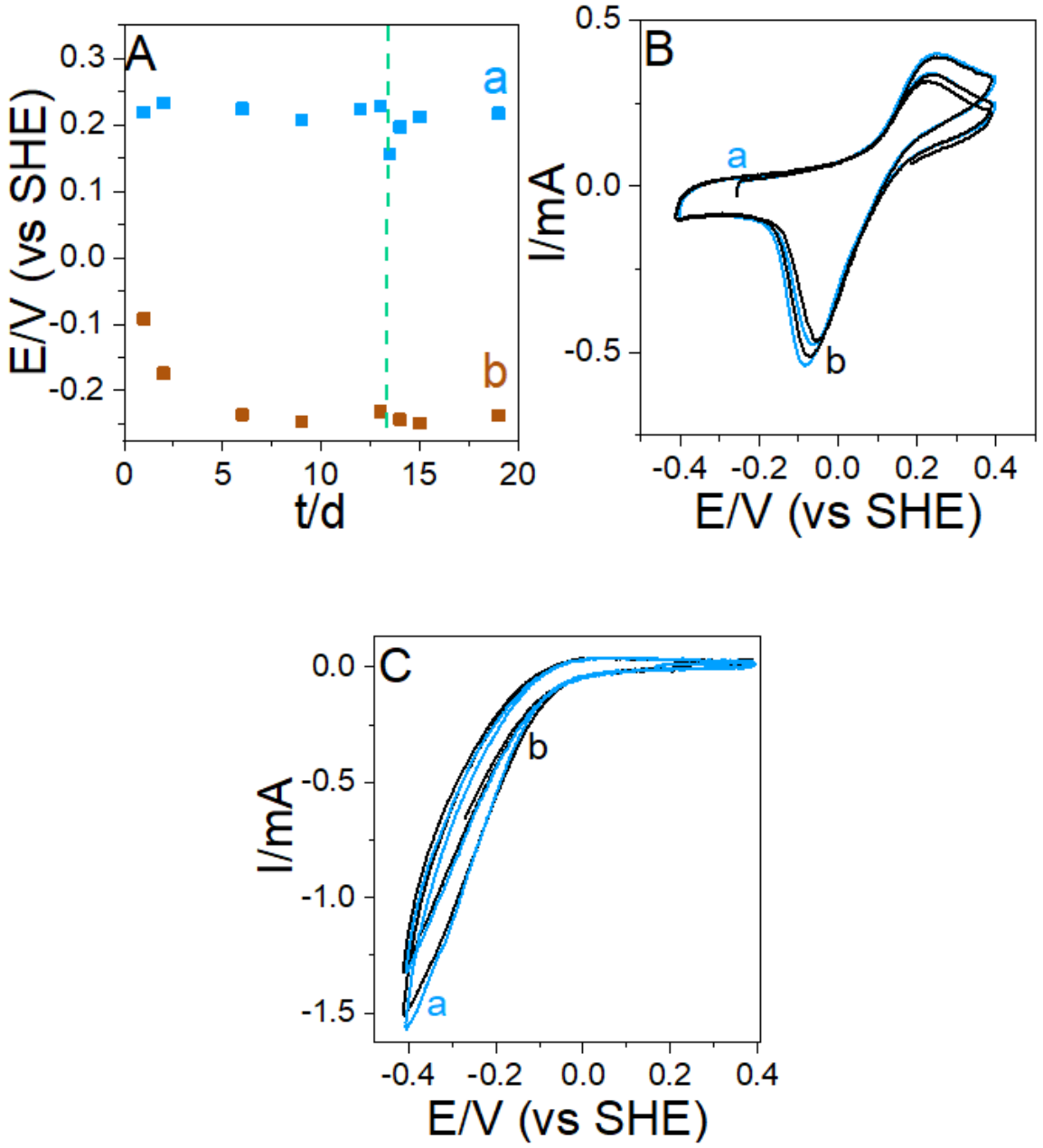

Figure 4.8 *Results for the control experiments which consisted of one electrode in sediment and one in water, not connected. A. Daily potential measurement, a - electrode in water, b - electrode in sediment. Green line indicated the nitrate addition. B. CV of the electrode in sediment without (a, blue) and with (b, black) nitrate C. CV of the electrode in water without (a, blue) and with (b, black) nitrate. Sediments from Ville-sur-Illon.*

Another explanation comes from the increase of current monitored at the cathodic side of the snorkel. Fig. 4.9 reports schematically two situations of the snorkel based on recorded electrochemical responses, depending on the activity of the biocathodic side, delivering low cathodic current (plain line) or high cathodic current (dashed line). The anodic side is

considered more stable with time and only one typical current profile with potential is shown (current unit is here arbitrary). For small cathodic current, the potential of the electrochemical snorkel reaches the low potential region (-200 mV vs SHE for this scenario), with electron coming from a first anodic wave initiated around -300 mV vs SHE (see the insets in Fig. 4.5 A&B). When higher current has to be delivered to the cathode, because of the higher activity of the electroactive biofilm or the higher concentration of oxygen over a sunny day, the high current potential has to be reached (+135 mV vs SHE for this second scenario).

The activity at higher potential could be associated to the accumulation at the surface of the anode of redox species that were detected electrochemically by cyclic voltammetry (for example, see curve b of Fig. 4.5 B). The presence of nitrate in water and in sediment seems to promote the biocathodic activity of the microbial electrochemical snorkel, leading to a rapid transition from a low current biocathode to a high current biocathode. The higher activity of the biocathode requires then the higher current delivered by anode, so the anodic potential also must increase.

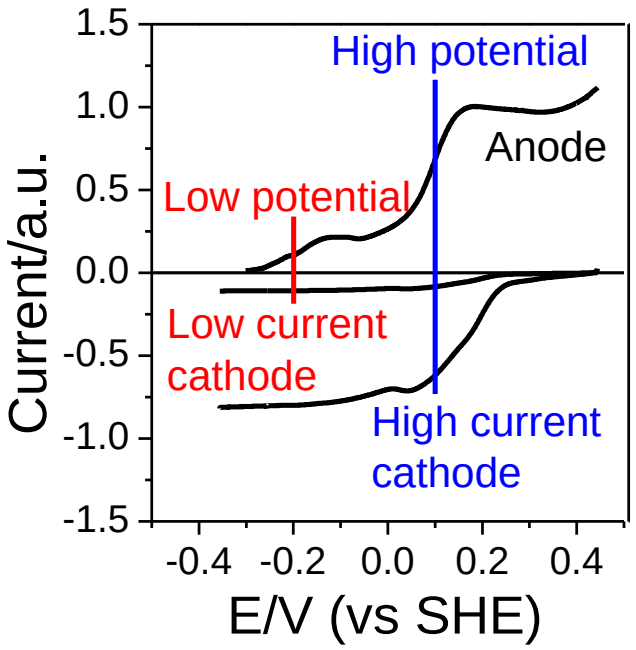

Figure 4.9. *Illustrative scenario leading to either low or high potential microbial electrochemical snorkel.*

4.4. Acclimation in the constructed wetland of Rampillon

The next step of this study has been the introduction of the electrochemical snorkel in the constructed wetland of Rampillon (Seine-et-Marne, France), to evaluate further the

phenomenon observed in the laboratory. A PVC tube, inserted in sediment-water column, allowed to define in the field a volume similar to the laboratory wetland. The snorkel was the same as the one studied previously in laboratory (showed on Schematic 2.5) and it was introduced in the wetland in spring. The natural conditions are very challenging, more light and more oxygen are present in the wetland. Moreover, less controlled composition of water, variations of the temperature are expected. During the period of evaluation, the potential of all connected electrodes was measured and water samples were taken to check the level of nitrate.

Photo 4.1. *Experiments in Rampillon (77, FR) (Photos by Author).*

On the 1st day, not more than one hour after the introduction, the potential value was +48 mV vs SHE and the concentration of nitrate was 30 mg NO_3^- L^{-1}. After 10 days those values were -189 mV and nitrate concentration was 10.8 mg NO_3^- L^{-1}. After 31st day the potential was +398 mV and nitrate concentration was 85.6 mg NO_3^- L. These data confirm that nitrate concentration is influencing the mixed potential value of a snorkel that is more positive when nitrate is in water. Clauwaert *et al.* have seen such correlation and assumed that the potential of the cathode increases with higher current production, which is caused by higher nitrate loading rate [37]. However, it is also very likely that this high potential is caused by the increased concentration of oxygen. The day 31 of the experiment was very sunny therefore the oxygen amount in water was increased due to the activity of algae and cyanobacteria.

On the 31th day of the acclimation, the OCPs of all electrodes as well as CVs of Electrode1 and Electrode10 have been performed in situ, in the wetland (Fig. 4.10 A). As in the experiment in the laboratory, there is a difference in OCP of electrodes in contact with water and with sediment. The electrodes in sediment have the OCP in the same range as we showed before in the presence of nitrate. However, the electrodes in water had higher OCP values than it was in the laboratory, which were +500 mV vs SHE. This is the potential of biocathodic oxygen reduction [228]. The shape of cathodic CV (Fig. 4.10 C) is different from the scans in

laboratory, however a small cathodic wave is observed, starting from potential around +500 mV vs. SHE, about 200 mV more positive than in the laboratory wetland. The CV of Electrode1 located in the sediment has a very similar shape to CVs observed before in the laboratory in presence of nitrate (Fig. 4.10 B).

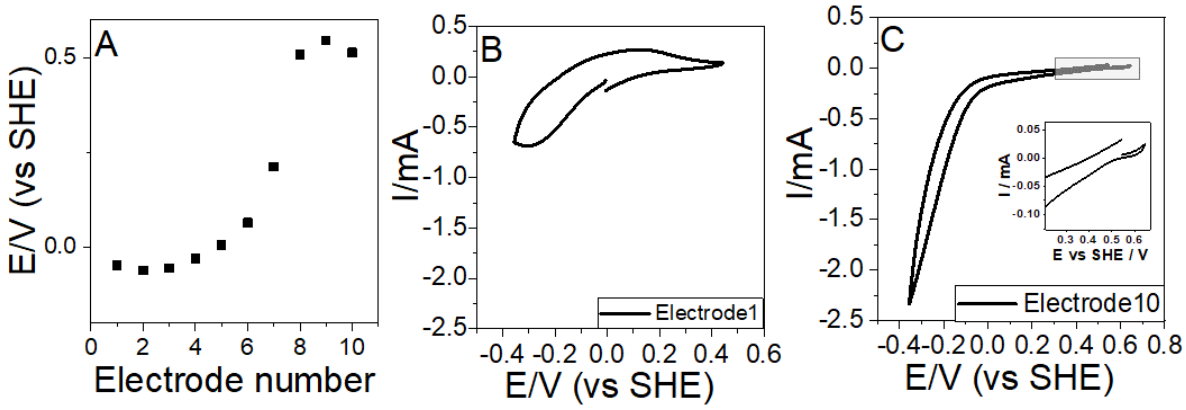

Figure 4.10. *Experiments performed in the wetland: A. OCP of all electrodes B. Cyclic voltammetry of Electrode1 C. Cyclic voltammetry of Electrode10 (the gray fragment is enlarged).*

Bacteria diversity analysis was performed also for two electrodes and sediment from the field (see Figure 4.6). It shows again that the bacterial community is more diverse in the sediment than in the biofilm on electrodes, which consists mostly of bacteria from phyla *Proteobacteria* and *Bacteroidetes*. The microbial community is very similar in the sediment from the field and taken directly from the experiment started in the laboratory.

The community on anodic Electrode1 (field) contains 37% of *δ-Proteobacteria*; 24% of whole community is from *Geobacteraceae* family (see supplementary data). Taking into consideration the shape of the CV and the community, we can say that it is very similar to the electrodes grown in the laboratory and therefore confirm that anodic biofilms were selected during *on-field* operation of the microbial electrochemical snorkel.

However, the specific conditions of the field influenced the biofilm on cathodic Electrode10 (field) which was very different from the Electrode10 grown from the beginning in the laboratory. The community was dominated by *Cyanobacteria*, oxygenic phototroph bacteria (*algae*), favored because of the presence of light and oxygen during spring period. The consequence was a more effective oxygen biocathode and a mixed potential with high value, not a priori suitable for nitrate reduction.

4.5. Conclusion

The potential of the snorkel system depends on its material and on the proportion between electrode in water and in sediment. The best material for electrodes is stainless steel due to its proper mechanical and electrochemical properties, which allows reaching the proper potential. Using a four times bigger electrode in sediment than in water allows in laboratory to compensate the impact of oxygen reduction reaction and to achieve the potential value in range which is often used in the literature for developing nitrate reducing biocathode without applying it externally. This system allowed to develop a bioanode in a sediment and biocathode in water, between which there was a stable current flow. The shapes of CVs as well as microbial community studies confirm the anodic and cathodic roles of electrodes in sediment and water respectively. Addition of nitrate disturbed these conditions and caused the increase of potential, which was caused by the increasing biocathodic activity linked to a 20-25 % increase in the rate of nitrate removal. We observed a significant increase in current CV which could be linked with electrochemical nitrate reduction, at 100 mV vs SHE, which is relatively more positive value than for nitrate-reducing biocathodes described in the literature. The mixed potential of the device reached especially high value in the field, where the presence of sun causes the induced growth of *Cyanobacteria* which increase the oxygen concentration. In order to operate biocathode for nitrate reduction in such sunny environment oversaturated with oxygen and to confirm and enlarge its denitrification activity, it will be necessary to further optimize the architecture of the microbial electrochemical snorkel and by providing a ratio between anode and cathode, to induce a mixed potential suitable for promoting nitrate reduction and denitrification *on-field*.

5. Denitrification on Microbial Electrochemical Snorkel

5.1. Introduction

In the previous chapter it was shown that the potential of MES depends on the ratio between anodic and cathodic parts. One can target specific potential values by building the MES with the proper ratio. The anode/cathode ratio used in the previous experiment, which was 4:1, allowed to reach low potential values which was in the range of potentials in principle necessary to grow a NRB. However, this potential increased after nitrate was added to the reactor, therefore we were interested in finding system which would assure potential values more stable with time and conditions. Moreover, the MES described in Chapter 3 gave a limited improvement in nitrate reduction rate and one of the possible reasons, except for the instable potential, could be insufficient size of the electrodes for the relatively large volume of water. Thus, in this chapter a MES of bigger size, with electrodes covering the whole reactor surface was built, and the anode/cathode ratio was 6:1 (Schematic 2.6). The ambition here was to confirm that MES can increase the denitrification rate in laboratory wetland, that nitrate-reducing biocathode can be grown repeatedly, and to provide more information about ecology of the biocathode.

5.2. Results

5.2.1. Results of a preliminary experiment

In a preliminary experiment, current and potential were constantly measured with the use of zero-resistance amperometry (ZRA). The two cathodes were connected together as working electrode and all anodes as counter electrode. Fig. 5.1. shows the results of the current and potential measurement. In the initial phase, the current values were unstable, but always negative, confirming the electron flow from anodic to cathodic side of MES. After day 11, the current stabilized at the value of about -0.5 mA and the potential stabilized at the value of around -0.23 V vs SHE. Cyclic voltammetry was performed on the two cathodes two weeks after starting the experiment (Fig. 5.2 A and B, curves a). Similarly to the initial cathodic CV in the previous chapter, a cathodic peak followed by cathodic wave was observed. The first signal had a peak potential of around 0.1 V vs SHE and the wave was beginning around -0.05 V vs SHE. Since no nitrate was yet introduced in reactor, these signals could correspond to the reduction of dissolved oxygen. Another possibility is that nitrate or other species were released from the sediment and observed during the CV experiment.

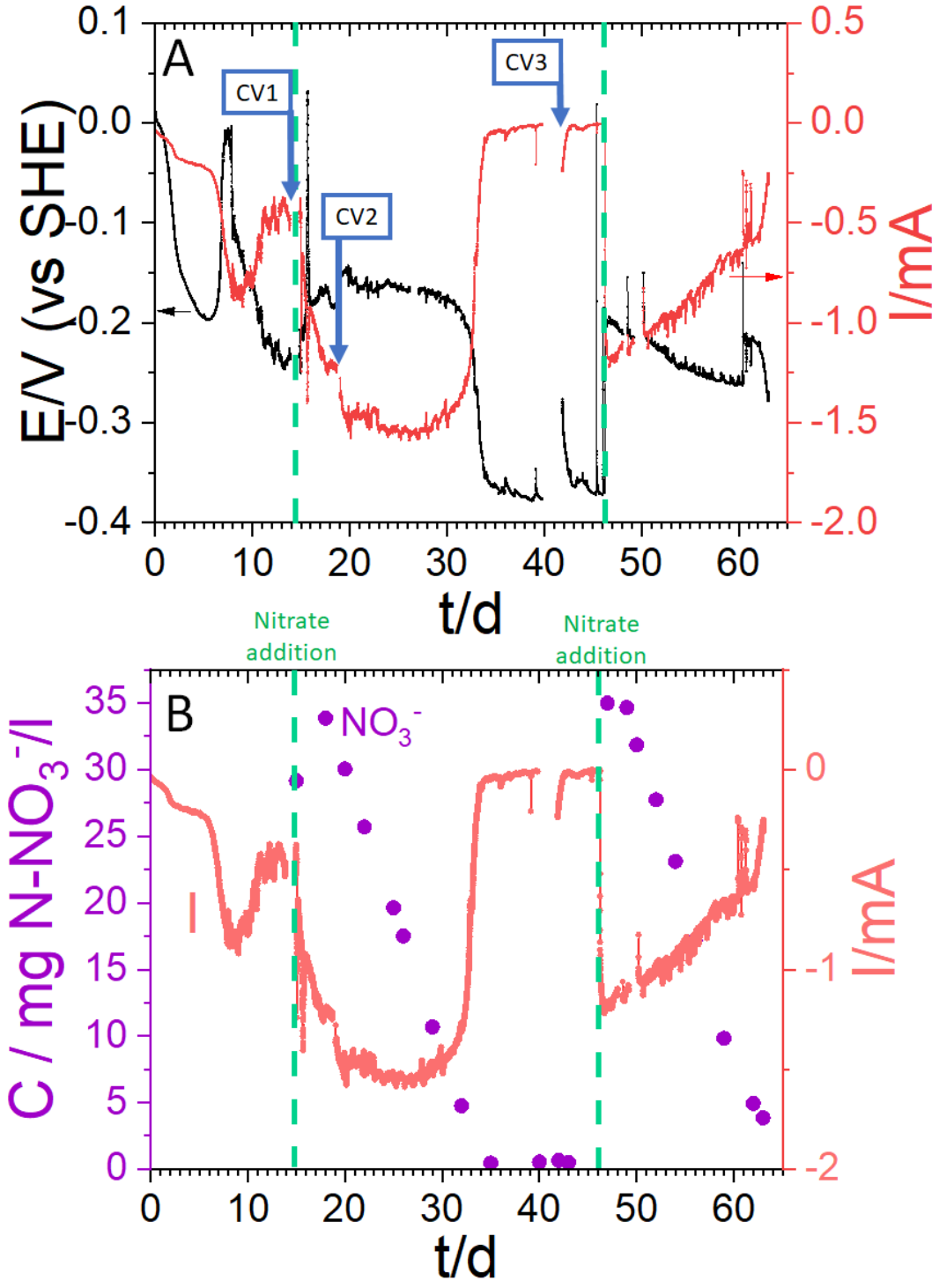

Figure 5.1 *A. Zero-resistance amperometry. The black line represents potential and red one current variations. The moments of CV experiments are indicated. B. The variations of current (red line) during the experiment, coupled with the nitrate concentrations (violet points).*

On day 14, nitrate was added to the experiment and the rapid increase of negative current up to -1.5 mA was observed. The potential also increased but was below -0.15 V vs SHE. Cyclic

voltammetry was performed two days after nitrate addition (Fig. 5.2 A&B, curves b). A large increase of cathodic signals was observed, especially for Cathode1, which is indicating nitrate reduction. This large negative current was relatively stable for around 10 days, after which it decreased almost up to 0 mA, which was coupled with potential decrease up to -0.38 V vs SHE. CV was performed in this period again, and it showed no reduction signals anymore, once again proving that these signals are associated with nitrate reduction (Fig. 5.2 A&B, curves c). Nitrate was added again on the day 45, which caused immediate current and potential increase and this time, both were gradually decreasing while nitrate was reduced.

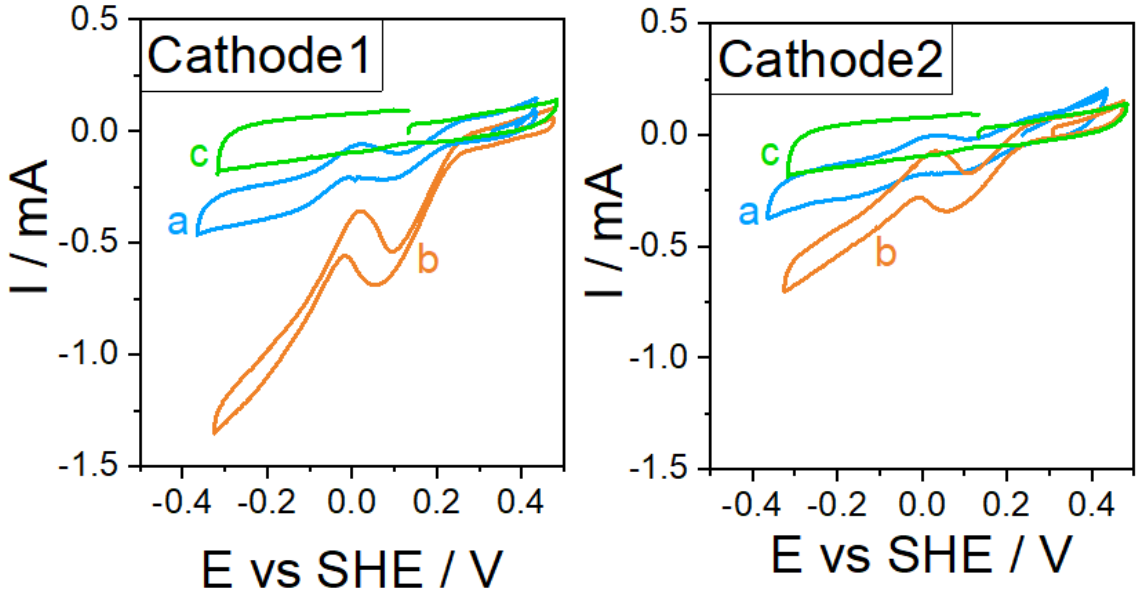

Figure 5.2 *Cyclic voltammetry of Cathode 1 and Cathode 2. a. before nitrate addition b. two days after nitrate addition c. after complete nitrate reduction*

Nitrate concentration was monitored during the experiment. As it is shown on Fig. 5.1 B, changes in nitrate concentration were well corresponding to changes in cathodic current. After nitrate was added, current increased. It decreased again after nitrate was removed from the reactor. Nitrate reduction rate was compared with a control experiment, which had the same volume of sediment and water but no electrodes. As it is shown on Fig. 5.3 A, nitrate reduction was clearly faster in the wetland with MES than in the control. The best fit to adjust the model to experimental data was obtained by considering a zero order reaction with $C = -kt + C_0$. We found k to be 0.037 and 0.053 mg L^{-1} day^{-1} for Control and MES experiments, respectively, which means that the presence of MES increased nitrate reduction rate by 43%. The nitrate reduction after the second addition was very similar to the first one (Fig. 5.3 B). The concentration of nitrite and ammonium was also monitored during the experiment and is

presented of Fig. 5.3 C. Significant concentration of nitrite was observed, with a peak around 17 days after nitrate addition, which is showing the first and second step of denitrification (Section 1.2.3.). After day 17, the nitrite was progressively reduced and it disappeared around 12 days after nitrate was completely reduced. A second increase of concentration of nitrite was observed after second nitrate addition. Small concentrations of ammonium up to 3.5 mg N-NH_4^- L^{-1} were also observed.

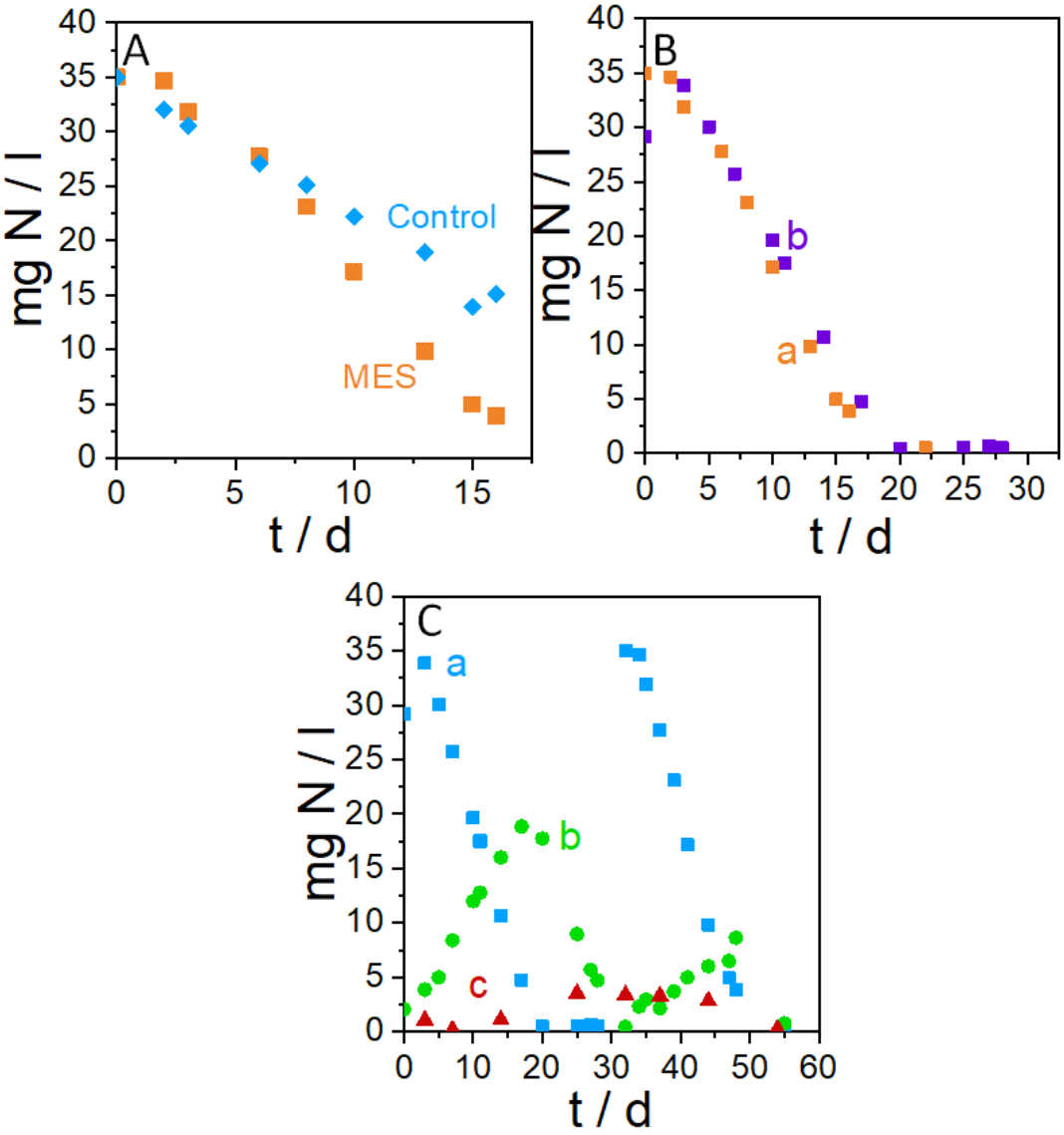

Figure 5.3 *The results of nitrate reduction A. Comparison of nitrate reduction in MES and Control experiment without electrodes. B. Comparison of two nitrate additions: a. first addition b. second addition. C. Changes in concentration of nitrogen species a. nitrate b. nitrite c. ammonium. The day "0" is the day of first nitrate addition.*

On the day 65, when nitrate was removed from the reaction environment, all the electrodes were disconnected. The aim was to confirm that the improved nitrate reduction comes from the electron transfer from anodes to cathodes, and not simply from the presence of electrodes in the environment. Nitrate concentration was measured during this time and is showed on Fig. 5.4 A (curve b). The constant k was found to be 0.043 mg L^{-1} day^{-1}, therefore it was slower than in case of MES (0.053 mg L^{-1} day^{-1}) and a little bit faster than for the control experiment (0.037 mg L^{-1} day^{-1}).

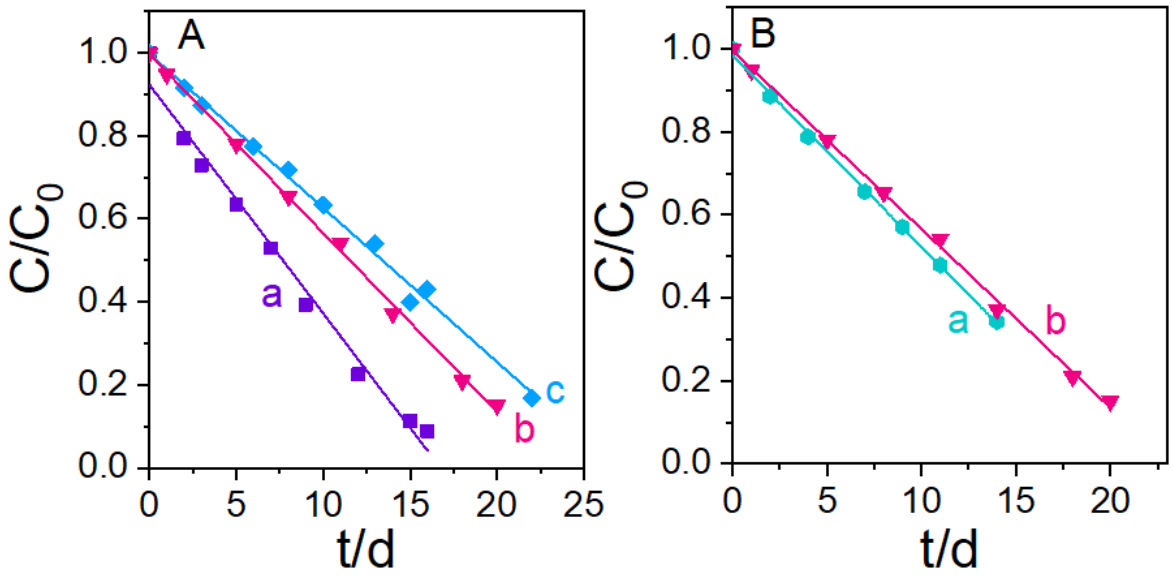

Figure 5.4. *A. Results of nitrate reduction in a. MES with connected electrodes, second addition of nitrate b. The same experiment after disconnecting all the electrodes, c. The control experiment, without any electrodes). B. a. MES after reconnecting the electrodes b. Experiment with disconnected electrodes (the same as before, for comparison).*

After one month of disconnection, all the electrodes were connected again in order to restart the MES. It was monitored with the use of ZRA. As it is shown on Fig. 5.5., a negative current was observed after restarting the experiment, although it was lower than initially. The potential was higher than after starting the experiment. The fluctuating values were probably linked to changes in light and temperature during day and night. However, addition of nitrate did not bring any changes in current and potential.

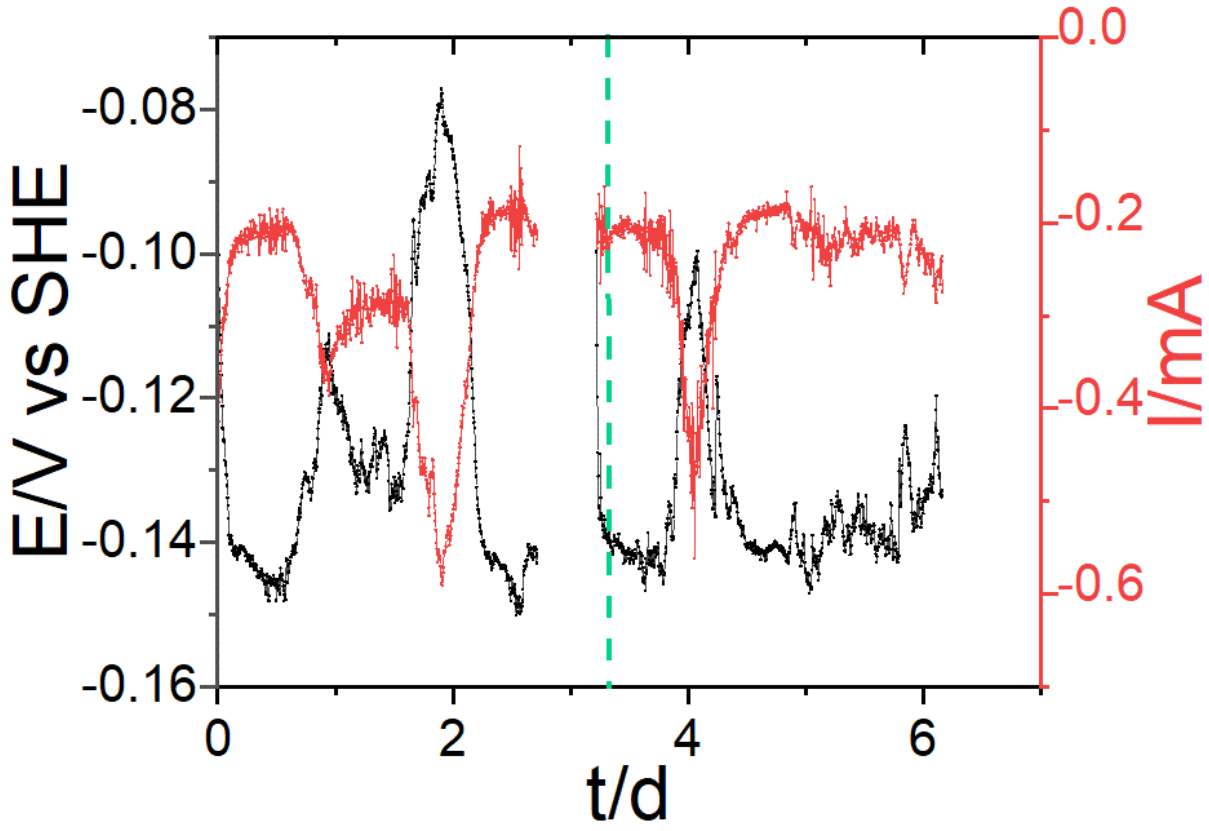

Figure 5.5. *ZRA after reconnecting the electrodes of MES*

Cyclic voltammetry was performed before and after nitrate addition (Fig. 5.6). The presence of nitrate in the reaction environment did not change the shape of the CVs. A small cathodic signal was observed with and without nitrate for Cathode1, with a peak of around -0.2 V vs SHE. Moreover, the nitrate reduction rate was monitored and it is shown on Fig. 5.4B (curve a). The reconnection of electrodes brought a minor effect on nitrate reduction rate (the constant after reconnection was 0.046 mg L^{-1} day^{-1}, and 0.043 mg L^{-1} day^{-1} when electrodes were disconnected).

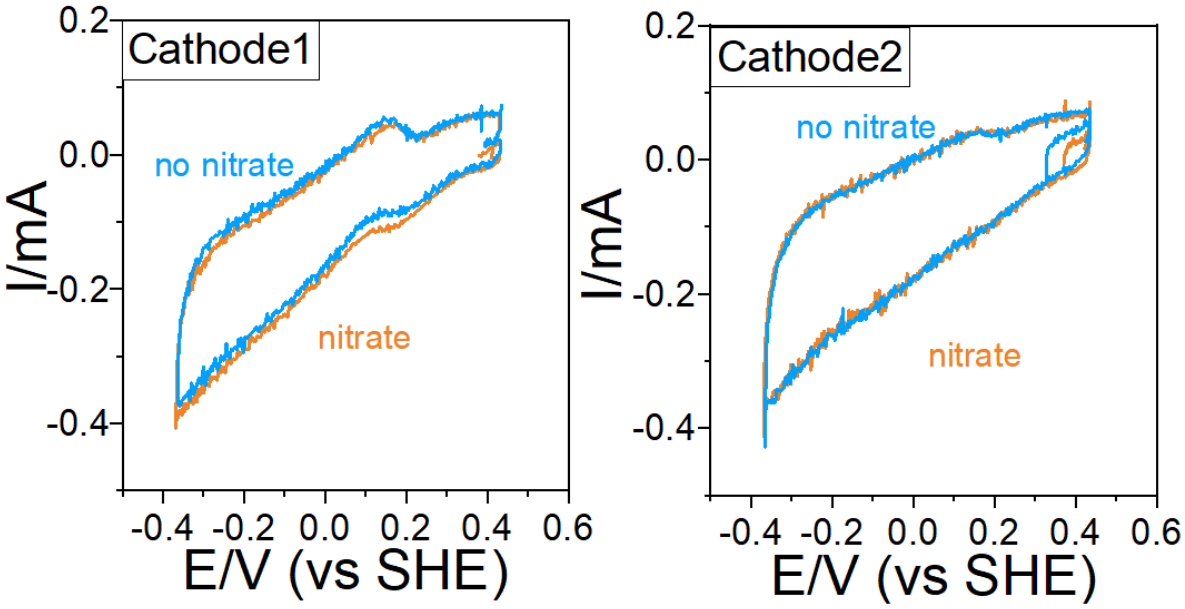

Figure 5.6. *CV after reconnecting the electrodes o MES in absence (blue) and presence (orange) of nitrate*

During the period of disconnection, there were no electrons delivered to biocathode from bioanode. After the system was again in MES mode, the electrochemical response changed. The addition of nitrate did not affect the current and potential measured by ZRA, neither the shape of CVs. The nitrate reduction rate was lower than previously. Therefore, we conclude that due to the lack of electrons, the biofilm was no longer electroactive. Physiology of the bacterial cells could have changed or electroactive cells were replaced by other.

To sum up, this preliminary experiment showed that by changing the ratio between anodic and cathodic sides of the MES, and by increasing the size of these electrodes, it is possible to clearly increase the nitrate removal rate. The presence of nitrate is visible in the increase of current on both ZRA and CV, however the period of disconnection of the electrodes caused the loss of these electrochemical properties. The next step was repetition of this experiment in order to confirm it, and prepare samples for microbial ecology analysis.

5.2.2. Results of the experiments in triplicate

The experiment was repeated in exactly the same setup, with the use of sediment from Ville-sur-Illon, in triplicate. The three experiments will be referred as MES A, MES B and MES C.

Zero-resistance Amperometry (ZRA)

As it is shown on Fig. 5.6 A, B & C, on the beginning of the experiment, in each of three MES monitored by ZRA there was a negative current, confirming the electron flow from anodic to cathodic sides. This is consistent with the previous result. The initial higher currents can be linked to the consumption of oxygen from water in the reactor; after day 12, the concentration of oxygen, which was measured every few days, never exceeded 2 mg L^{-1} in each experiment. Moreover, in each case the potential of the MES was going towards more and more negative values, up to -0.3 V vs SHE, as expected for this ratio between anodes and cathodes.

Nitrate was added on day 20. In MES A, the consequence was a sharp increase of potential up to circa -0.1 V vs SHE. This is however still in the range of potentials sufficiently low for growing NRB. The current was gradually increasing up to the value of -0.6 mA. In MES C, the increase of current was higher, up to -1.2 mA. The reaction of potential was not as rapid as in the MES A, however it was gradually increasing, also up to -0.1 V vs SHE. In case of MES B however, the change in current was very limited (up to around -0.3 mA). Moreover, there was no clear reaction of potential. While nitrate was being consumed, the values of negative currents in MES A and C were decreasing again towards the initial values.

Nitrate was added again on the day 50. This time, the sharp current increase was observed for MES A and C on ZRA - for MES C the increase was bigger (Fig. 5.4 A and C). In case of MES A, the current before addition was about -0.1 mA and after it increased sharply to -0.6 mA, from which it further increased up to -1.3 mA. The potential increased from -0.35 to -0.2 V vs SHE, therefore it was still sufficiently low and suitable for the NRB. In case of MES C, the addition of nitrate caused the shift from -0.2 to -1.2. mA and was also further increasing up to -1.6 mA. Here, the observed potential values were higher and it shifted from -0.2 to -0.05 V vs SHE after nitrate addition. A sharp increase of current was not however observed for MES B. In fact, the current value without nitrate for this experiment was around -0.4 and did not change significantly directly after its addition, but later a slow increase up to -0.8 mA was observed (Fig. 5.4 B). A potential change from -0.2 to -0.05 V vs SHE was observed, however in this experiment it was not so fast and sharp as in case of MES A and C.

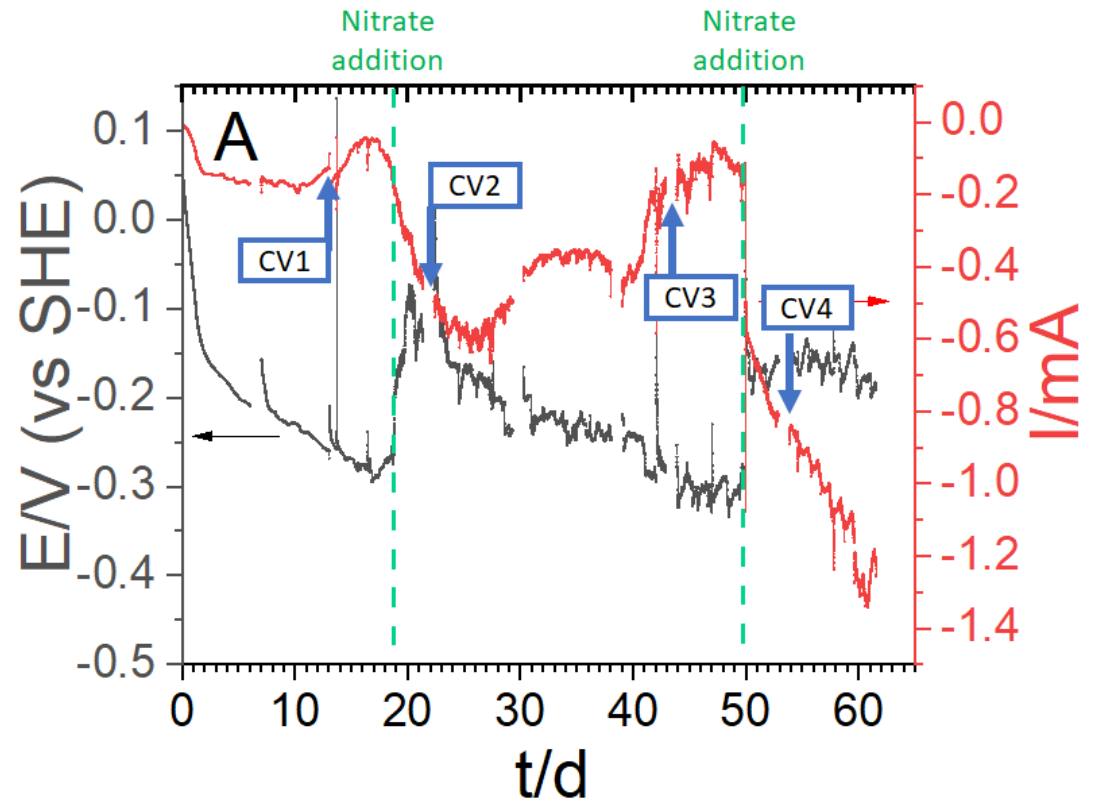
Nitrate addition
Nitrate addition
A
CV1
CV2
CV3
CV4
E/V (vs SHE)
I/mA
t/d

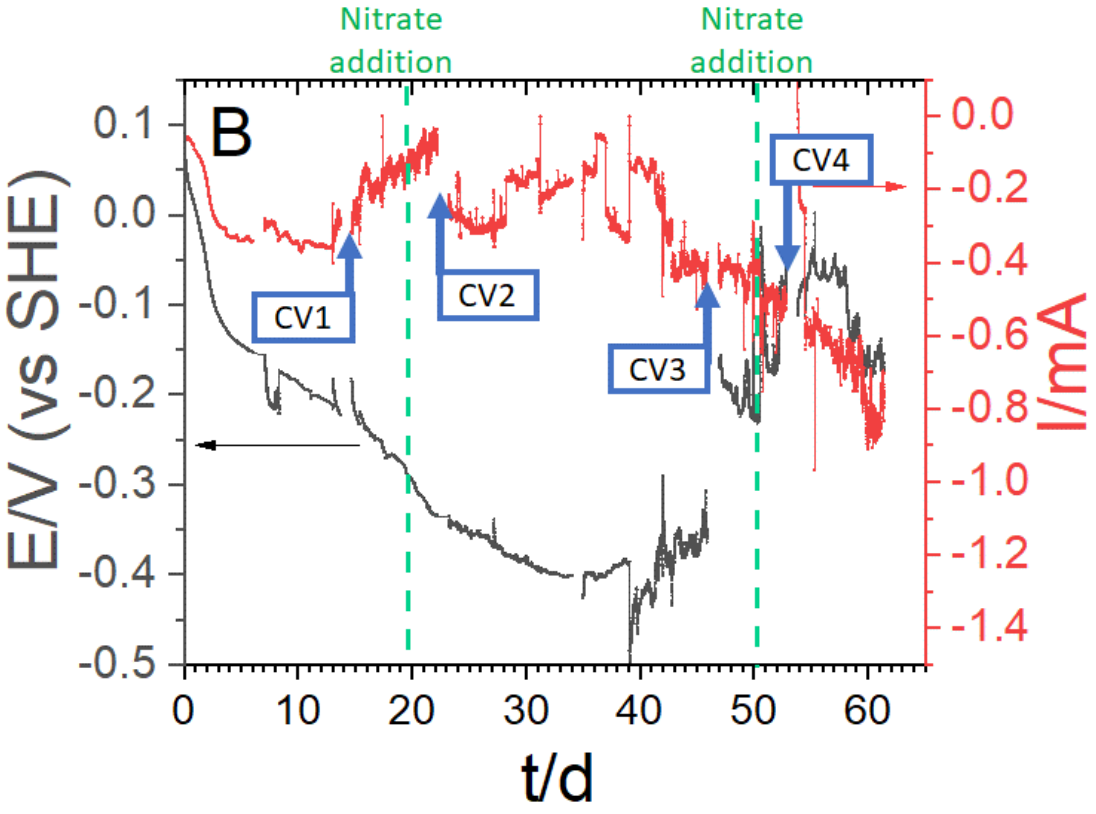
Nitrate addition
Nitrate addition
B
CV1
CV2
CV3
CV4
E/V (vs SHE)
I/mA
t/d

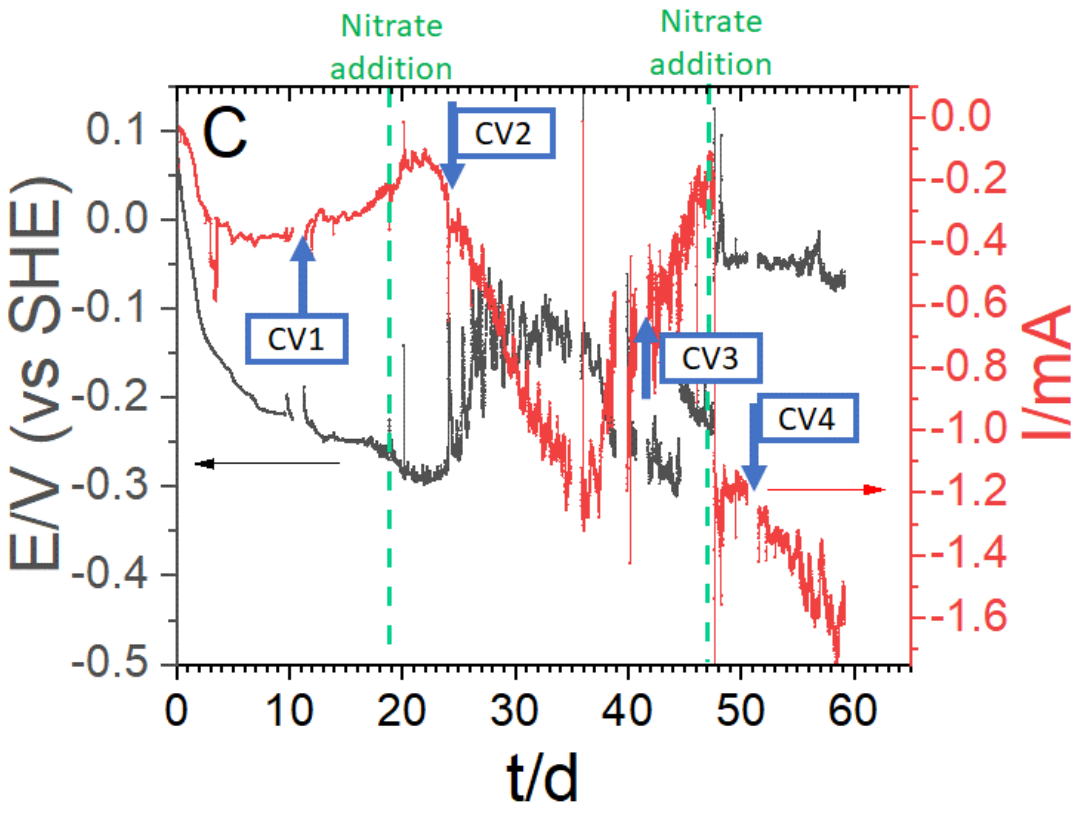

Figure 5.6. *Results of ZRA analysis of respectively MES A, B and C. Black and red lines show the results of variations of respectively potential and current. The moments of performing the CVs are indicated*

Cyclic voltammetry (CV)

Cyclic voltammetry was performed four times during the time of the experiment: on day 13 - CV1, day 25 - CV2, day 44 - CV3 and day 55 - CV4. CV1 and CV3 were performed in absence of nitrate, and CV2 and CV4 with nitrate. The Table 5.1. summarizes the cyclic voltammetries made in this experiment.

Table 5.1. *Summary of cyclic voltammetries performed in the MES experiment in triplicate*

Number of CV	Day	Presence of nitrate	Fig.
CV1	13	Without nitrate	5.7., blue
CV2	25	With nitrate	5.7., violet
CV3	44	Without nitrate	5.8., blue
CV4	55	With nitrate	5.8., violet

CV1 (without nitrate) was performed 13 days after the experiment was started (Fig. 5.7, curves A, blue). Contrarily to the first CV from preliminary experiment, no reduction peak was observed around 0.05 V vs SHE, however in both cathodes in MES A and C, as well as Cathode2 in MES B there was a cathodic wave in more negative region, starting around -0.15 - -0.2 V vs SHE. That could be the reduction of oxygen on stainless steel. The shape of CV was however different in case of Cathode1 of MES B - it showed very big currents. The analysis was repeated, but the results were still similar, therefore we concluded that this cathode behaves differently than the others.

CV2 was performed 4 days after nitrate addition, the results are shown on Fig. 5.7 (all curves B, violet). A cathodic peak appeared for MES A and MES C, starting around +0.2 V vs SHE. It is followed by the cathodic wave, which is starting around 0 V vs SHE. Moreover, MES C shows very much higher currents (up to -1 mA in case of the first cathodic signal and around -1.5 to -1.7 mA for the second one) than MES A (up to -0.3 and -0.6 mA for first and second cathodic signal, respectively). In case of MES B, small cathodic signals were also observed in the same potential regions, with current values of up to -0.15 mA for first signal and -0.4 mA for second signal.

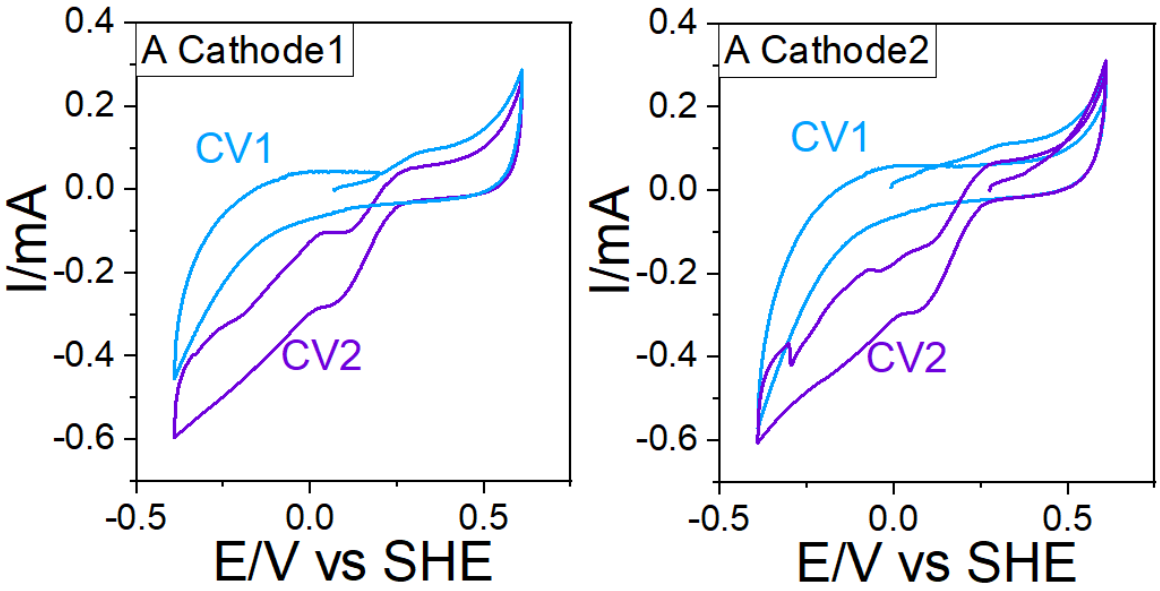

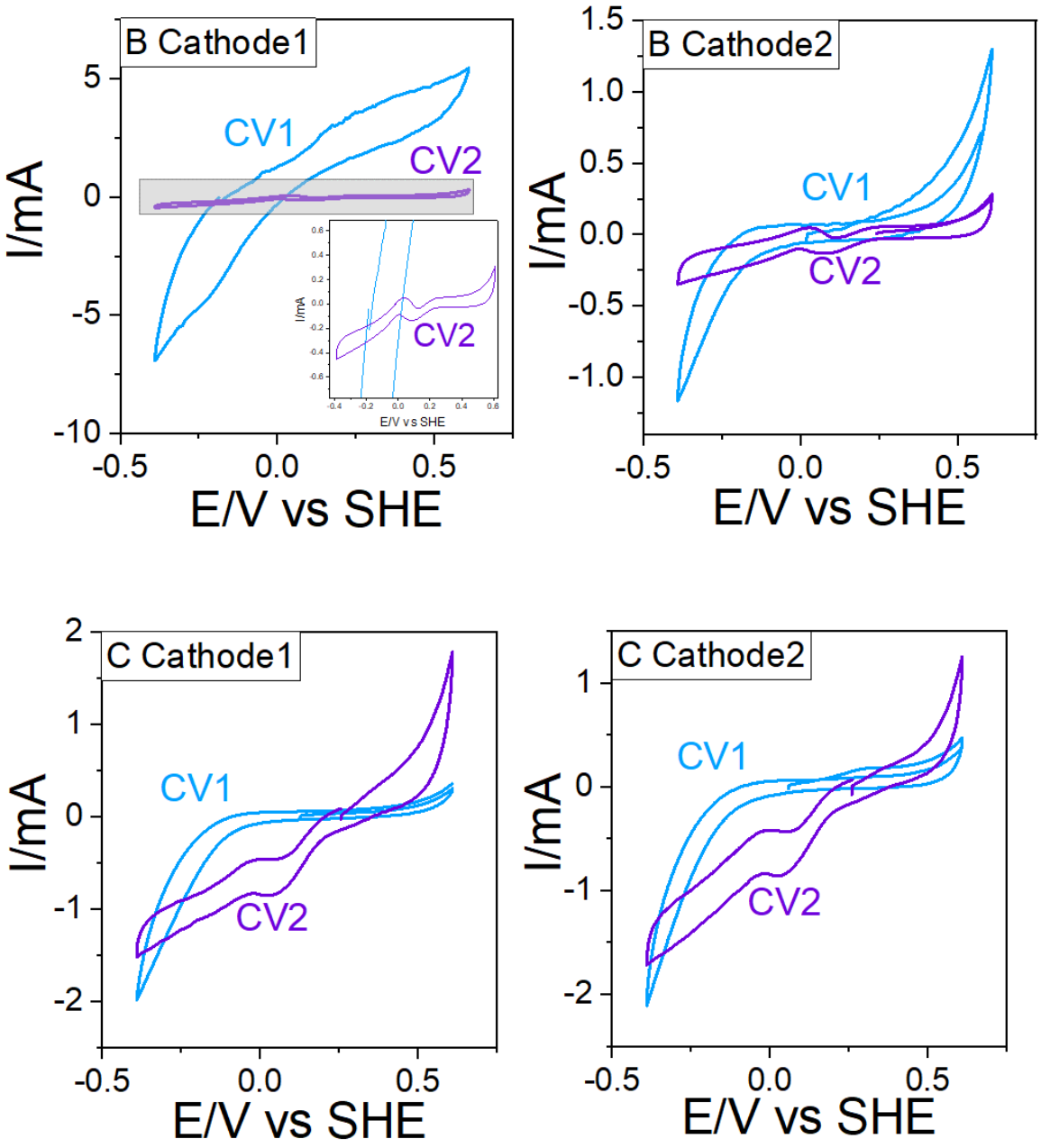

Figure 5.7. *Cyclic voltammetries of cathodes before (CV1, blue line) and after (CV2, purple line) first nitrate addition.*

CV3 was performed again 24 days after the nitrate addition (day 44 of the experiment), when nitrate was reduced from the reaction environment. For Cathode1 of MES A, the shape of CV is very similar to the initial scan without nitrate (Fig. 5.8, A Cathode1, to be compared with Fig. 5.7 A Cathode1). For the CV scan of Cathode2 of MES A, some reduction peaks are still visible, however they are weaker then directly after nitrate reduction and one can predict that they should also disappear in a couple of days. Some reduction signals were however observed for MES C (Fig. 5.8, C Cathode1&2). Some cathodic currents were also observed in

MES B, however, in case of Cathode1 of this MES, the unusually quite current values and different shape were observed again (Fig. 5.8, B Cathode1&2).

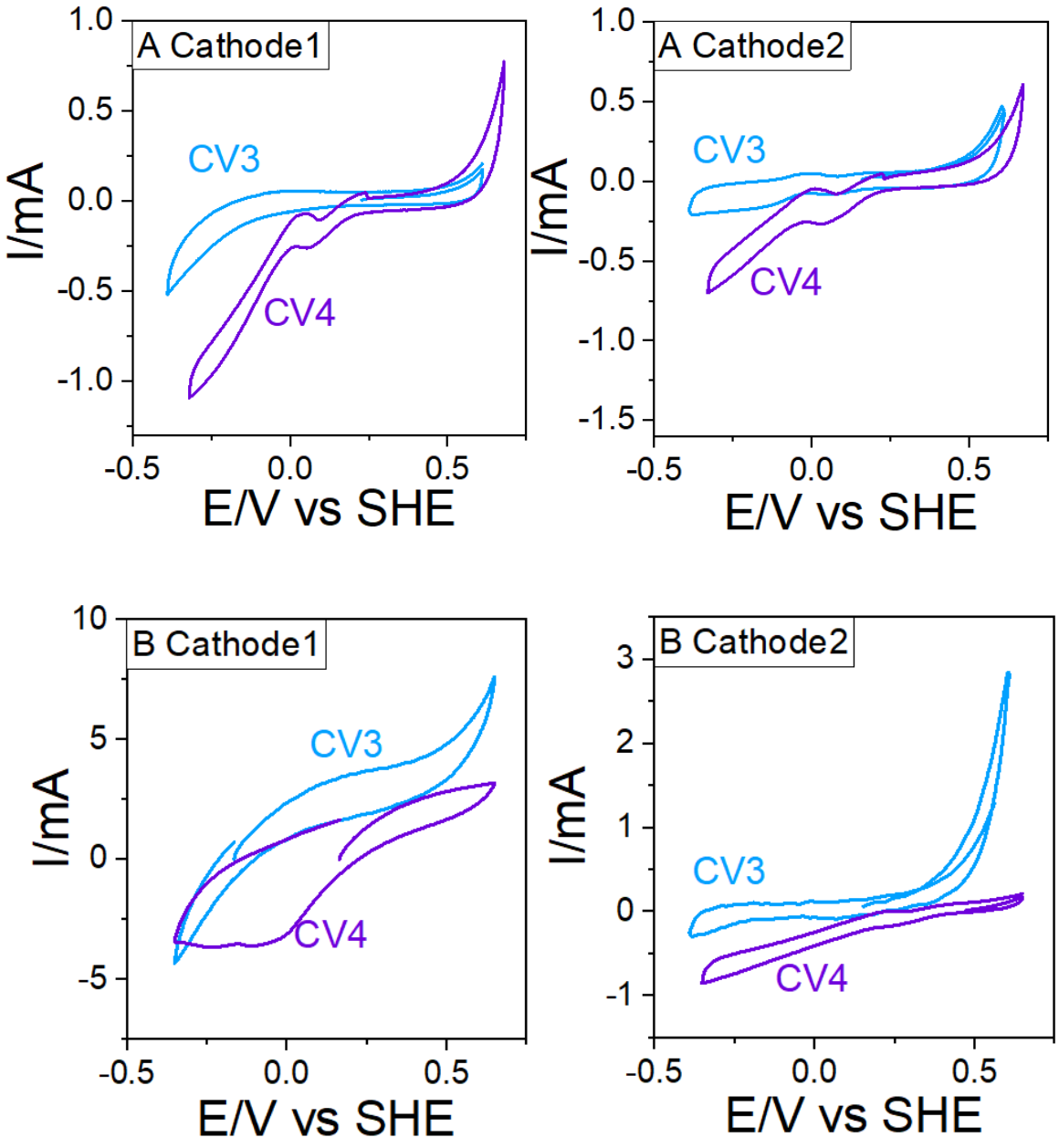

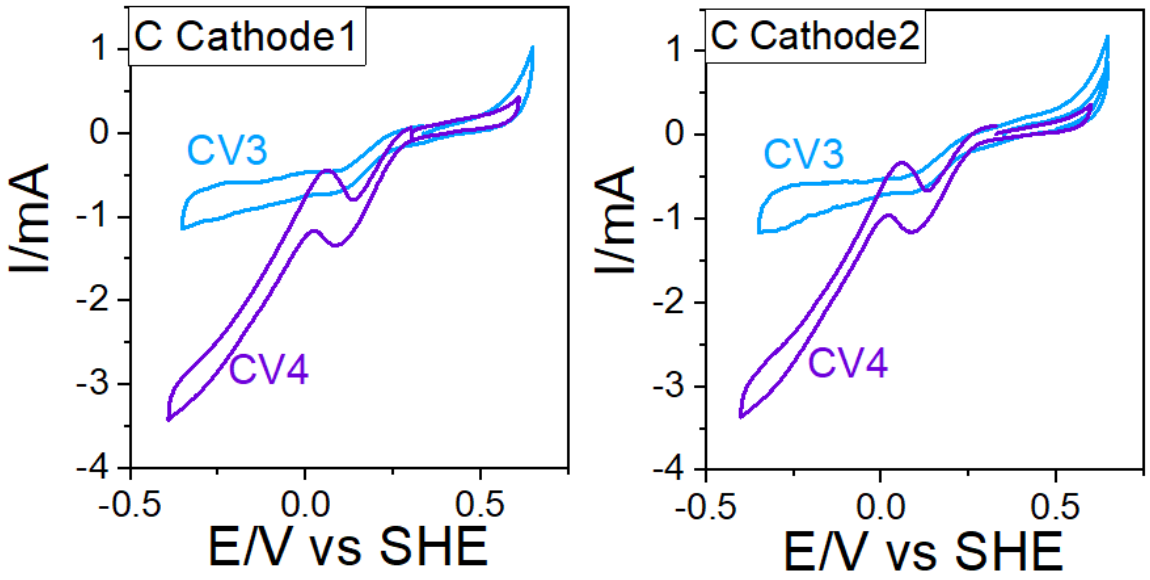

Figure 5.8. *Cyclic voltammetries of cathodes before (CV3, blue line) and after (CV4, purple line) second nitrate addition.*

3 days after second nitrate addition, the experiments were monitored with the CV4 (Fig. 5.8). Again, the clear appearance or current increase of cathodic peaks was observed for MES A&C. The cyclic voltammograms for both cathodes of MES A have very similar shape as in the previous additions, with a similar current value for the first signal, but higher than previously current for the reduction wave. The current values are here higher for Cathode1 than for Cathode2, similarly as in the preliminary experiment describe in this chapter. It could be explained by the fact that because Cathode2 is higher, it is more exposed to oxygen which could be an interfering agent. The other possibility is that Cathode1, being closer to the sediment, could be richer in bacteria.

Voltammograms recorded for MES C showed the highest current values, which is again consistent with results from ZRA. The first cathodic peaks, starting as before at +0.25 V vs SHE, have the current up to -1.5 mA and are followed by cathodic waves, starting around 0 V vs SHE, which achieve currents up to -3.5 mA vs SHE. The CV for Cathode1 MES B again showed untypical high current values and shapes, but one can observe a cathodic peak which is also beginning at +0.25 V vs SHE. The cathodic signals were also observed for Cathode2.

Nitrate reduction

The nitrate reduction rate after the first addition was compared to the control which was the same volume of sediment and water but without electrodes (Fig. 5.9.). Due to the small

differences in measured initial nitrate concentration (which was 150±10 mg NO_3^- L^{-1}), the results of nitrate concentration in time were normalized to C/C_0. Zero-order reaction was considered to obtain the best fit to adjust the model to normalized experimental data. We found that the constant k was equal to 0.046, 0.037 and 0.042 mg L^{-1} day^{-1} for MES A, B and C, respectively. For the control experiment it was 0.041 mg L^{-1} day^{-1}. This control experiment showed faster nitrate reduction then the one showed in the previous part, which might come from the fact that the previous experiment was performed in winter, and this one in sunnier and warmer spring. Initially, the presence of MES did not bring any visible improvement in nitrate reduction rate. The current was gradually decreasing in MES A and C, but for MES B the values were fluctuant and unstable.

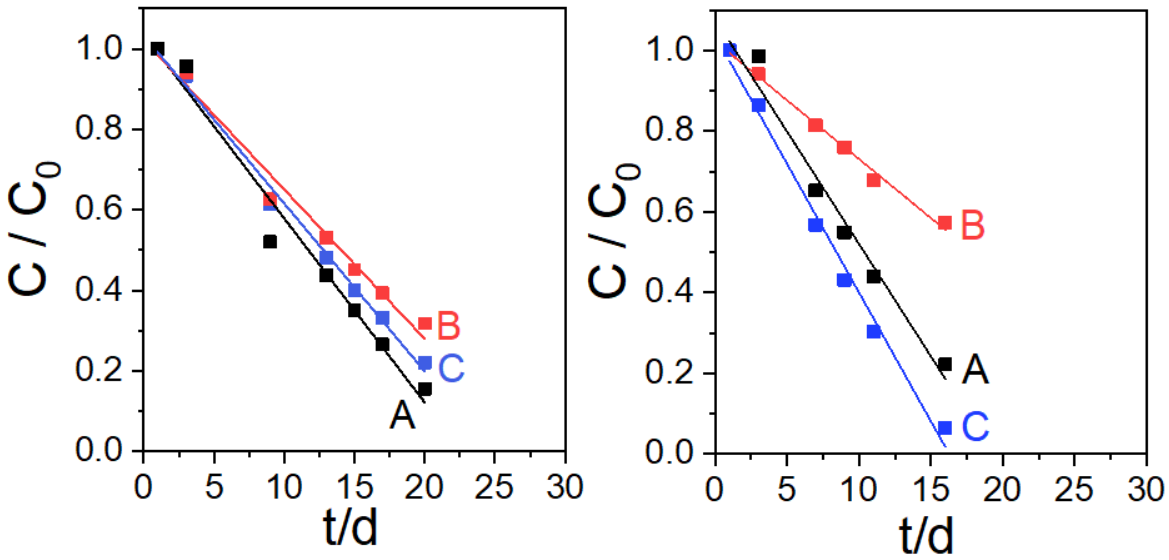

Figure 5.9. *Results of nitrate removal A. first addition of nitrate B. second addition of nitrate. The black, red and blue lines represent results for MES A, B and C, respectively.*

Fig. 5.9 B shows the results of nitrate reduction after second addition. The fastest removal was obtained for MES C, for which k calculated was 0.063 mg L^{-1} day^{-1}. For MES A, k had a little lower value of 0.055 mg L^{-1} day^{-1}, which is still faster than for the previous addition. In MES B, k was 0.03 mg L^{-1} day^{-1}, which is around two times slower than for other two experiments. The values of constants are useful for comparing experiments between them, but because they were calculated with normalized results (C/C_0), they do not represent the actual nitrate reduction rate. In order to estimate it, the linear fit was used for data for MES C. This calculation gave the result of 10.5 mg NO_3^- L^{-1} day^{-1}, or 10.5 g NO_3^- m^{-3} day^{-1}. Fig. 5.10. shows the changes of concentration of nitrogen species: nitrate, nitrite and ammonium during

the experiment (day 0 is here the day of addition of nitrate). The production of nitrite is lower here than in the preliminary experiment, but still relatively high due to the nitrite's toxicity. The highest concentrations were observed for MEC C, which is again linked to its highest activity. There is no peak of nitrite after second addition of nitrate to reactor with MES B. The concentrations of ammonium are again rather low for each of the experiments.

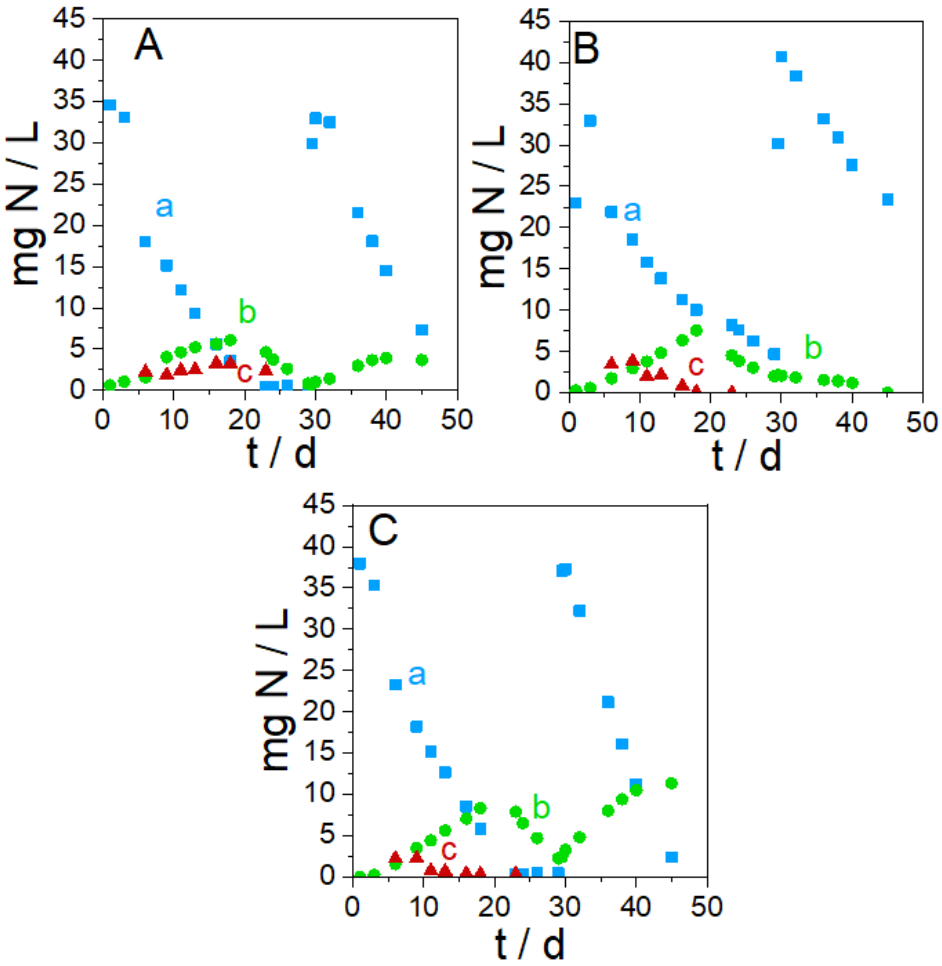

Figure 5.10. *Changes in concentration of nitrogen species a. nitrate b. nitrite c. ammonium. The day "0" is the day of first nitrate addition.*

Discussion

In this study, three snorkels were constantly monitored and a correlation between electrochemical response and nitrate reduction rate was observed. The results of ZRA show that after nitrate was added, the current between anodic and cathodic parts of snorkel increased and was decreasing when nitrate was being consumed. MES C showed the highest current increase after nitrate addition on ZRA. This increase was also clear for experiment with MES A, but less

clear for the one with MES B. It is also consistent with the reaction for nitrate reduction in preliminary experiment.

A clear difference in the shape of CV was observed in presence and absence of nitrate. The biggest reduction signals in presence of nitrate were observed on CV of cathodes from experiment with MES C, which is consistent with the higher current increase observed with ZRA for this experiment. The shape of CV with nitrate is generally similar to the corresponding result from preliminary experiment (Fig.5.2 B). One can find a similar cathodic shape (with two cathodic signals) for biocathode reducing nitrate and nitrite in the work of Pous et al., where first signal was associated with nitrate reduction and another one with nitrite reduction [128]. Nitrite is an intermediate product in the process of denitrification and in this study, we observed a temporary increase of its concentration after nitrate additions, with one exception of experiment with MES B after second addition.

No significant differences were noticed in terms of nitrate reduction after the first addition, however, the fastest removal was observed after second nitrate addition for MES C, followed by MES A. There is a correlation between these results of nitrate reduction and electrochemical response: the higher currents and the fastest removal were observed for MES C. It therefore seems that it is the most electrochemically active snorkel, which reached nitrate reduction rate of 10.5 g NO_3^- m^{-3} day^{-1}. This result can be compared with other stationary BES for nitrate reduction of similar starting nitrate concentrations. Zhang and Angelidaki built a sediment MFC with a starting concentration of 10 mg N-NO_3^- L^{-1}. They reached the removal of 62% after 37 hours, which gives 3.9 g N m^{-3} d^{-1} [95]. Cucu et al. in MFC reached 96% of removal in 14 days, starting from 18.7 mg N-NO_3^- L^{-1}, therefore on average 1.28 g N m^{-3} d^{-1} [147]. The bioreactors inoculated with *Thiobacillus denitrificans*, studied by Yu et al. had a starting concentration of 2mM NO_3^-, therefore 28 mg N-NO_3^- L^{-1}. In the reactor with electrode poised at -0.5 V vs SHE, which gave the best results, 75.62% of nitrate was reduced during 15 days, which on average gives 1.4 g N m^{-3} d^{-1}, although the nitrate reduction was faster on the beginning of the experiment [136]. Huang et al. were also testing Ce-doped birnessite modified cathodes, also inoculated with *Thiobacillus denitrificans.* From starting concentration of 2 mM NO_3^- (28 mg N-NO_3^- L^{-1}), they reached 0.4 mM NO_3^- which corresponds to nitrate reduction of 1.49 g N m^{-3} d^{-1} [145]. This results show that nitrate reduction rate reached by MES C could be competitive to certain MFCs. Of course, in other studies the performances of MFCs were reaching much higher values, up to 410-500 g N m^{-3} d^{-1} [66,67]. However, these experiments were performed in flow and with much higher starting concentrations of nitrate. Therefore,

additional tests of MES with varying starting nitrate concentrations and in flow could allow to maximize the performance and compare it with the MFCs and other BES.

The slowest nitrate reduction (after second addition) was corresponding to poorer electrochemical response of MES B. This result could be the indication that the biofilm was not developed in the same way as for two other MES and this is why the response is not the same. This hypothesis was then verified by the study of this biofilm.

Study of microbial ecology

On the day 62, the experiment was stopped and the biofilms were detached from electrodes by placing the electrodes in ultrapure water and subjected to ultrasounds (two treatments at 25 W for 1 min) from a probe positioned one centimeter above the coupon surface. The detached sessile cells (cells from biofilm), as well as planktonic cell in water and cells from sediment, were then analyzed with 16S rRNA gene sequencing.

Fig. 5.11. shows the volcano plots comparing different sets samples in order to see differences in the relative abundance in orders in these samples. One should keep in mind that these plots illustrate abundance of different species and not population size. Fig. 5.11. A, B, C and D compare respectively the samples of sediment with samples of water, samples of cathodic biofilm with samples of water, samples of cathodic biofilm with samples of sediment, and samples of biofilm of cathodes1 and from cathodes2. Here, black dots represent the orders that were found in both compared sets of samples and red and green dots represent the orders specific for one of the sets of samples. On Fig. 5.11. A, B and C we therefore see the differences in compared sets of samples. It means that dissimilar communities of bacteria grew in the sediment, in water and on the biocathodes. However, Fig. 5.11. D shows only black dots, therefore all cathodic biofilms consisted the same orders of bacteria.

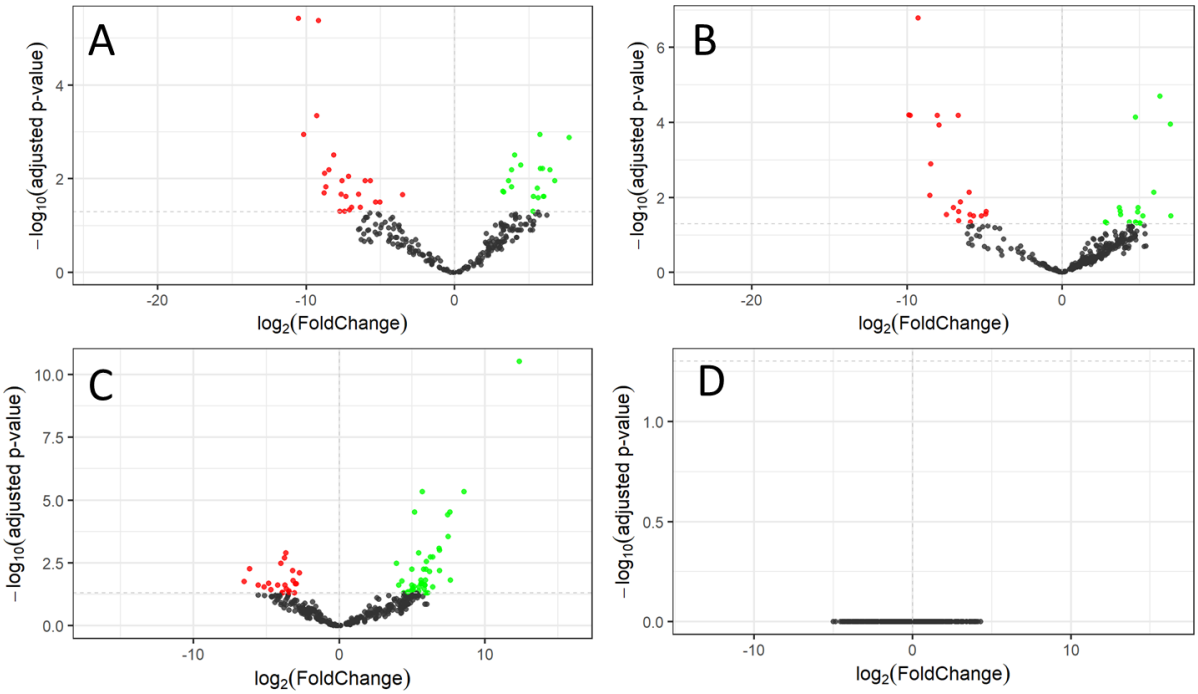

Figure 5.11. *Volcano plots of order-level taxonomic bins in the 16S rRNA gene data sets. The x axes display the fold changes in relative abundance (log2) between different data sets: A: between all sediment and all water samples; B: between all cathodes and all water samples; C: between all cathodes and all sediment samples; D: between all cathodes1 and all cathodes2. The black dots represent the orders common for compared sets of samples, the red and green dots represent orders specific only for one set from the compared pair. The y axes display the -log of the adjusted P values of the test statistic.*

To further understand the differences among these samples, the microbial compositions were compared using a Heatmap (Fig. 5.12.). Each row represents an OTU and each column represent a sample. This comparison confirms the differences between the sets of samples, but also gives an idea about the differences within the set. Looking from the top of the scheme, one can distinguish the clearly darker parts first for samples of water, then for samples of sediment and finally for cathodes. It can be also concluded that there are more elements in common for cathodes and sediment as well as for cathodes and water, than for sediment and water.

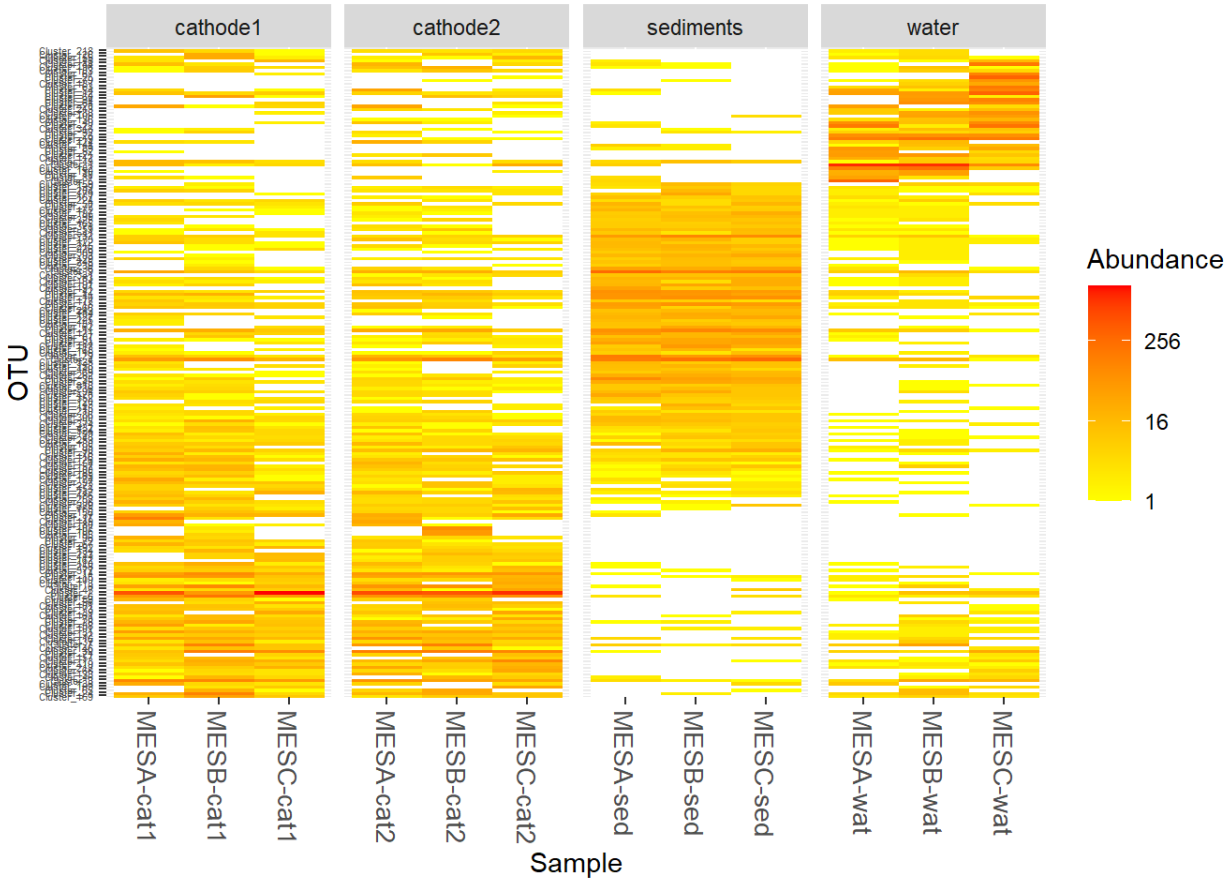

Fig. 5.12. *A heat map showing the abundance of operational taxonomic units (OTU) for each sample. The darker the color, the more abundant OTU present within the sample type.*

Fig. 5.13. presents more detailed information about composition of microbial samples on the order level. Again, clear differences are directly visible. In water, the dominating orders are *Burkholderiales* (13.7, 7.1 and 22.1% of abundance for MES A, B and C, respectively) and *Chitinophagales* (42.7, 46.3 and 5% for MES A, B and C, respectively), as well as *Cytophagales* experiment with MES A (10%) and *Rhizobiales* for experiment with MES C (12.3%). The order *Chitinophagales* belongs to phylum *Bacteroidetes*, the bacteria are usually aerobic or facultative anaerobic [239,240]. They are Gram-negative staining rods, often filamentous, and can be found in soils [241,242]. The amount of research linking this order with nitrate reduction is limited, however it was found in biodeposits in clams, which also showed high denitrification rates [243]. Gram-negative *Cytophagales* (phylum: *Bacteroidetes)* are short or long rods, or sometimes filaments, wildly distributed in nature [240]. Some bacteria from this order could use nitrate for the anaerobic respiration [244]. The other studies show that they can participate in partial nitrification [245].

In sediment, the dominating orders are *Anaerolineales* (4.2, 6.2 and 11.5% for MES A, B and C, respectively), again *Burkholderiales* (6.4, 5.9 and 7.4% for MES A, B and C, respectively), *Chloroplast* (5.3, 7.4 and 10% for MES A, B and C, respectively), *Competibacterales* (20, 10 and 11% for MES A, B and C, respectively) and *Methylococcales* (6.4, 10.6 and 8.7% for MES A, B and C, respectively). *Anaerolineales* is a strictly anaerobic, Gram-negative bacterium which belongs to phylum *Chloroflexi* [246]. This order was reported to appear in anammox reactors [247,248]. *Chloroplasts* which were also found in sediment (and in the smaller quantity on biocathodes), are organelles in plant and algal cells, which conduct photosynthesis. Although being a part of a cell, they possess their own DNA which is a heritage from their ancestors which were *Cyanobacteria* [249]. Therefore, this result is probably the sign of the presence of algae in the sediment. Some genera belonging to order *Competibacterales* were found to have abilities to reduce both nitrate and nitrite [250] and they were found in wastewater treatment plant [251]. *Methylococcales* are Gram-negative *Gammaproteobacteria* bacteria, which form rods or cocci and use C_1 compounds like methane to their metabolism [252]. Although some sources characterize them as strictly anaerobic [252], some studies suggest that they can also adapt to the environment poor in oxygen and they were found in the oxic-anoxic interface between sediment and water [253]. Some bacteria from this order can potentially use alternative to oxygen electron donors, such as nitrate [254].

In the biofilm of cathodes, the dominating order was *Beggiatoales* (notice that in some sources this order is known as *Thiotrichales* [252]) which was 17.1% and 18.7% for Cathodes 1 and 2 on MES A, 53 and 34% on Cathodes 1 and 2 on MES C, 16% on Cathode 2 of MES B, but only 1.6% on its Cathode1. One may notice here a correlation between the denitrification and electrochemical results and the abundance of this bacteria order. The highest current observed with ZRA and CVs were those from MES C, which here has the biggest percentage of *Beggiatoales.* MES B was showing the poorest results in terms of denitrification and in fact, Cathode1 which was giving unusual CV shape, is lacking *Beggiatoales.* Here, the main family for all samples was *Beggiatoaceae*. There is a wide range of bacteria from this family; they can be aerobic or nitrate-dependent and they oxidize sulfide in sulfur-based chemolithoautotrophy or in heterotrophic growth supplemented by sulfur oxidation. As these bacteria require both oxidized sulphur species and oxygen or nitrate, they are often found in the interface between water and sediment where they have access to both electron donors and acceptors [255]. For example, the large bacteria of genus *Beggiatoa* are able to transport nitrate from the surface of sediment and use to oxidize sulfides, which results in the formation of suboxic zones in sediment. Some nitrate can also accumulate inside of these bacteria [256,257]. For the moment,

there is not much information about the ability of bacteria from order *Beggiatoales* to exchange electrons with solid electrode via EET. In the study of Ridge et al., it was found *Beggiatoaceae*-associated sequences on the electrodes poised at -0.2 V vs SHE [258]. However, to our knowledge there was no study dedicated to test EET abilities of *Beggiatoales.* Our results here suggest the bacteria from this order could participate in bioelectrochemical denitrification, however further studies are demanded to confirm this hypothesis.

Bacteria from the order *Burkholderiales* were found in all the samples. *Burkholderiales* is the order of Gram-negative (like all *Proteobacteria*) *Betaproteobacteria*, known to dominate in denitrification process in wastewater treatment systems [259]. In the work of Gregoire et al., *Burkholderiales* was found in the biocathodic biofilm, therefore it is possible that bacteria from this order can be potential microbial cathode catalysts [123]. Zhang et al. in their denitrifying bioreactor found this order together with *Rhizobiales* [260], which is also present in this study, in particular on the cathodes (and in water from experiment with MES C). Both these orders were also a part of denitrifying community found in the study of Feng et al. [261]. *Rhizobiales* is an order belonging to *Alphaproteobacteria* [262], and bacteria from this order were dominant on denitrifying biocathode in the study of Vilar-Sanz et al. [263].

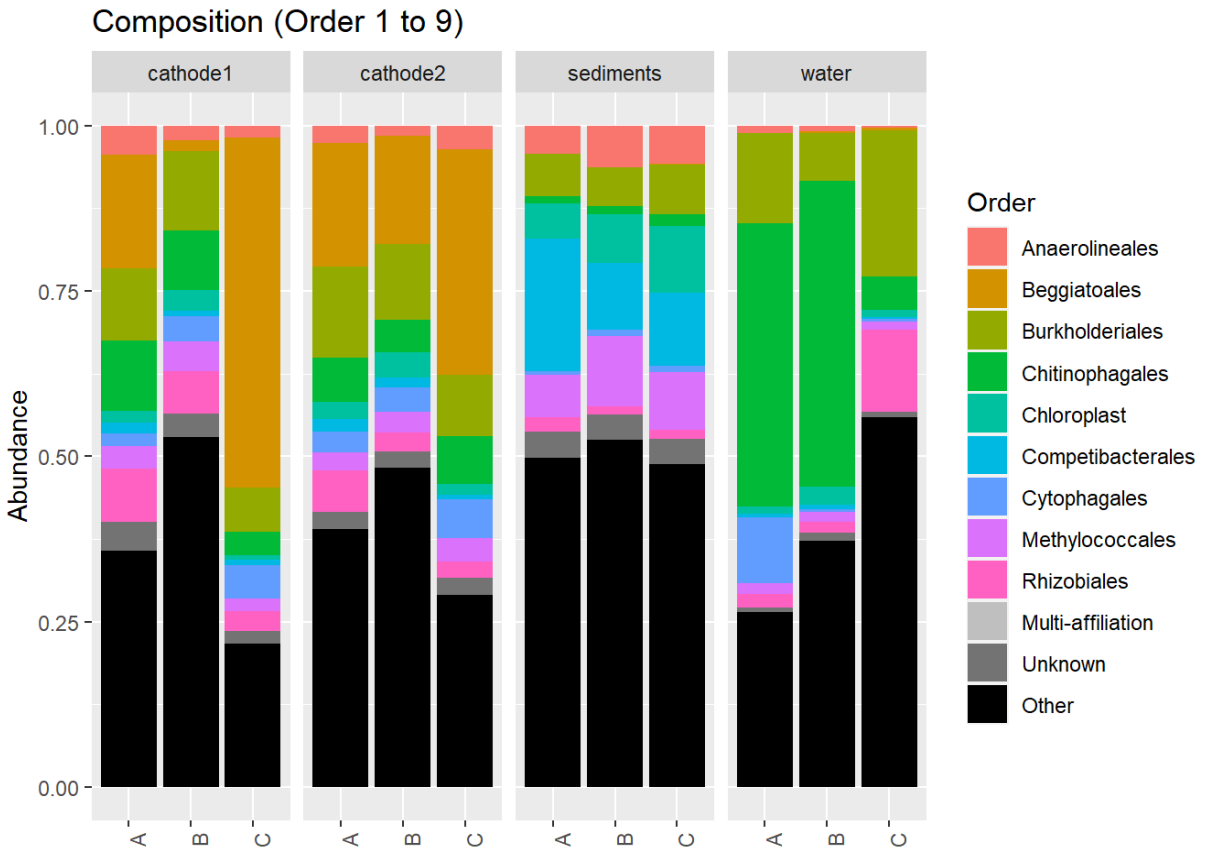

Figure 5.13. *Relative abundance of phylogenetic groups of bacteria in samples from cathodes of the MES and from water and sediments (from 16 S rRNA genes sequencing).*

5.3. Conclusions

This experiment shows the evidence that MES can be used to accelerate nitrate reduction. As it was already mentioned in part 1.2.4. of the introduction ("Microbial Electrochemical Snorkel"), some research was already dedicated to the application of MES to treat nitrate-polluted water, however they were using very low nitrate concentrations, which are usually not considered as a hazard. Here, we showed that MES can be used to treat nitrate from wastewater. The higher denitrification performances were corresponding to higher currents observed with ZRA and CV. Microbial analysis of the biofilms, sediments and water showed that the well-performing biocathodes had a big percentage of *Beggiatoales.* Although this order is not yet known for having electrochemical properties, these results show an indication that bacteria from this order could be studied in this direction.

6. Exploring the possibilities of nitrate reduction in sediment

6.1. Introduction

As it was proven in the General Introduction, oxygen is a competitive to nitrate electron acceptor and its increased concentration can inhibit denitrification. In Chapters 4&5, this inhibition was very limited due to the fact that the relatively tall and narrow reactors as well as lack of water movement created confined environment, in which oxygen's diffusion was limited. The molecules which reached the bottom of reactor were rapidly reduced by biocathodes, therefore the concentration of oxygen was low and nitrate was used as an electron acceptor.

However, thinking about application of MES in the constructed wetland, one should keep in mind that conditions are different than those in the laboratory. With more water movement, aquatic plants and sun, the concentration of oxygen will be higher, which can decrease the efficiency of denitrification. As it was already mentioned in Chapter 4, it has been shown in several papers that oxygen diffuses into sediment only on very limited depth of about 2-3 mm, but nitrate diffusion and reduction in sediment is possible and was observed even on 20 cm of sediment depth. Therefore, motivation of this chapter was to add the electrode to experiment with tubes and determine if it could influence the denitrification rate in stationary state and in flow. Sediment tubes were chosen to fasten the process.

6.2. The indirect effect of electrode on rapid nitrate reduction

6.2.1. Preliminary studies

Three different materials were used to prepare the tubes. The Graphite Tube and Steel Tube were both 35 cm high and had a diameter of 6 cm (Schematic 2.7). They were prepared from graphite felt and stainless steel grid, respectively. These materials were used to create the shape of the tube but also in order to increase their contact with sediment, two additional pieces of electrode (35 x 6 cm) were also put inside. Then, the tubes were filled with sediment. Isolated from water stainless steel wire was used to connect the electrodes with potentiostat. Finally, a third tube made of polypropylene tissue, was used as a control in order to distinguish the influence of the specific arrangement of the sediment from the influence of electrode material.

This preliminary experiment lasted for 45 days. Nitrate was present in synthetic water medium from the first day and was later added four times. It was noticed that in the experiments with electrodes, the nitrate removal was more rapid comparing to the control, and it was especially fast for graphite felt. In most of cases, on the next day after its addition it was not detected anymore in the solution (Fig. 6.1A, points "c') while for the steel and control experiment around 2-3 and 7-10 days were needed respectively (Fig. 6.1A, points "b" and "a" for stainless steel and control, respectively). In order to determine quantitatively the nitrate reduction rate, the first order kinetics ($C = C_0 e^{-kt}$) was used. Fig. 6.1 B shows the results from third nitrate addition (started on day 17) with the calculated rate. We found that the k = 0.27 day^{-1} for control experiment, 0.58 day^{-1} for experiment with steel electrode and 1.3 day^{-1} for the one with graphite electrode. From these data one can concluded that the stainless steel electrode increased the nitrate removal 2 times and graphite electrode almost 5 times.

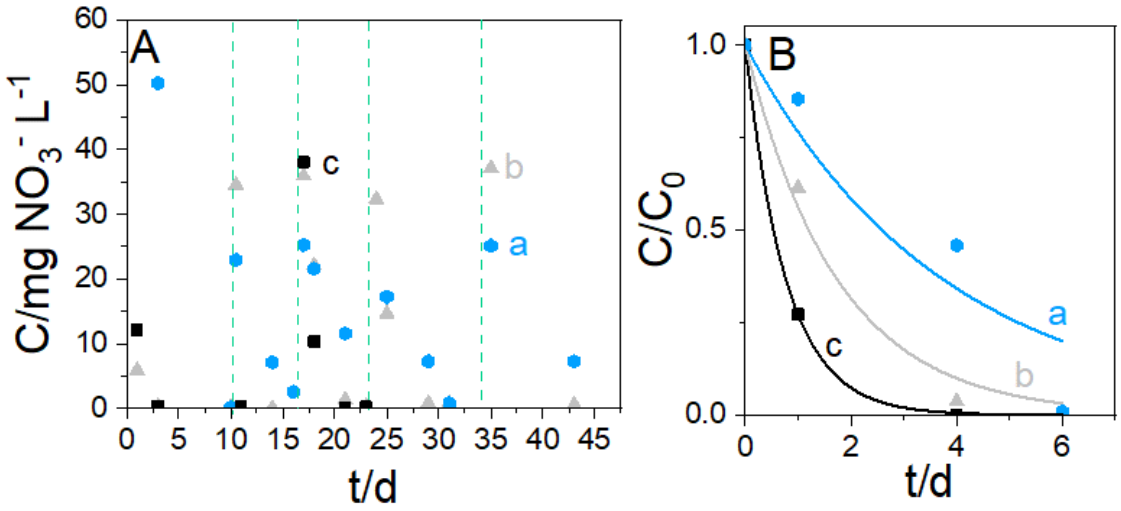

Figure 6.1 *Results of nitrate removal from preliminary experiments A. nitrate concentration during the whole duration of the experiment, B. Results from third nitrate addition (started on day 17) with the calculated rate (first order reaction). In both graphs a - experiment without electrodes, b - experiment with stainless steel electrode, c - experiment with graphite felt electrode.*

6.2.2. Repetition of the experiment in triplicate

In order to better understand the influence of the presence of electrode material on the faster nitrate reduction, the experiment was repeated with both stainless steel and graphite felt electrodes in triplicates. The experiment with steel was conducted in 10 - 12.2019 and the one with graphite on the 1-3.2020, with the use of the same sediment from Ville-sur-Illon.

Experiments with stainless steel

Three different experiments were prepared, each in triplicate. One was consisting of stainless steel grid in a form of the tube, filled with sediment, additionally with stainless steel inside of the tube. This tube and its dimensions were the same as in the previous experiment. The second series of tubes were made of polypropylene tissue, but had pieces of stainless steel inside. These pieces were in contact with sediment but their contact with water was more limited. The last series was consisting only of polypropylene tubes with sediment inside, but without any stainless steel electrode.

Nitrate was added three times to these experiments and the denitrification was taking around 8-10 days. Fig. 6.3A represents the results from first addition. The best fitting for experimental data was again obtained with first order kinetics and the results of constant for three additions are shown in Table 6.2. In this series of experiments, the presence of steel brought no clear improvement in terms of denitrification. However, no additional peaks were observed while performing chromatography analysis.

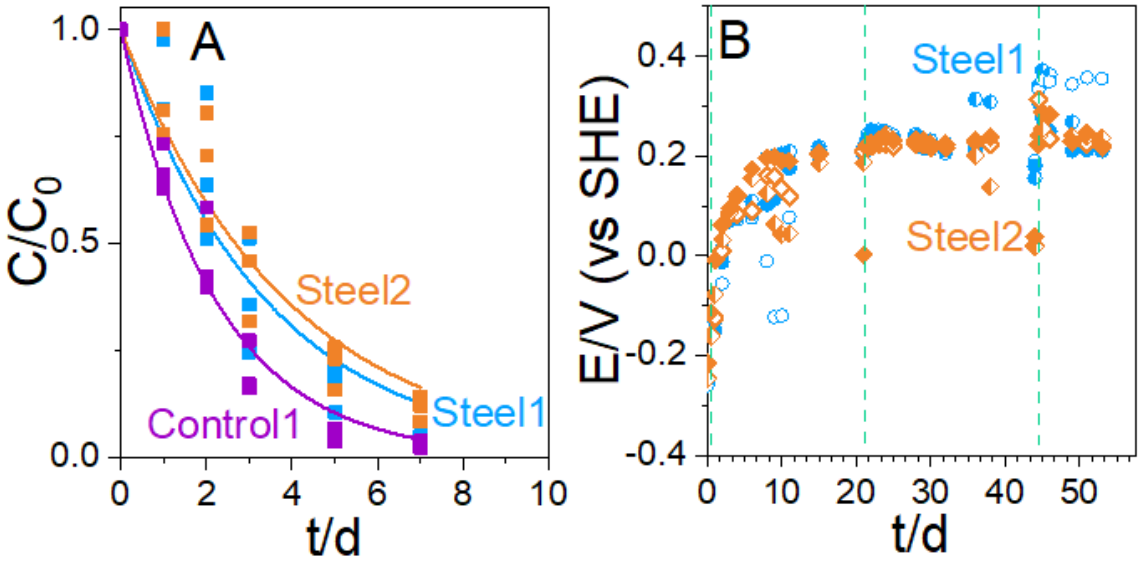

Figure 6.2. *Results for the experiments with stainless steel electrode. A. Results from nitrate reduction. B. Results from potential measurement. Green lines indicate the addition of nitrate*

Table 6.2 *Results of k calculated for nitrate reduction for experiments with steel electrode (first order reaction rate)*

Average k / $days^{-1}$	Steel1	Steel2	Control1
First addition	0.29	0.26	0.45
Second addition	0.23	0.27	0.4
Third addition	0.25	0.22	0.29

The potential of the electrodes was measured daily during this study (Fig. 6.2 B). All experiments were showing similar behavior, regardless the presence of stainless steel around the tube. The initial values of potential were around -0.25 V vs SHE, but they were gradually increasing after nitrate was added for the first time, up to the range of 0.2 V vs SHE. After the first addition of nitrate, the potential stayed on this high value for all experiments except for Steel2, for which it dropped to 0 V vs SHE. When nitrate was added for the second time, on day 21, the potential for this experiment went back to previous value and it was stable for several days. On the day 36, the potential of one of the Steel1 replicates increased and the potential of two Steel2 replicates decreased. After the third addition of nitrate, the potential of Steel1 experiments increased again to the range of 0.22 - 0.3 V vs SHE. These high values could be associated with reduction of oxygen on the external electrode. For the Steel2, the potential increased again to the values around 0.2 V vs SHE after third nitrate addition. In this case, it can be explained by the fact that oxygen has limited access to the external electrodes, it is consumed by bacteria on the interface between water and sediment. Nitrate, however, can penetrate deeper into the sediment. The decrease of potential is associated with the decrease of concentration of nitrate in the sediment and its increase was caused by addition of nitrate. However, this effect was not very strong in this experiment, therefore we decided to perform the tests with graphite felt electrodes.

<u>Experiments with graphite felt</u>

The similar set of experiments was also prepared with graphite felt. First tube consisted of both steel and felt - stainless steel was around the tubes and graphite felt was inside. In the second triplicate, graphite felt was only in the sediment, and the tube was made of

polypropylene tissue. As before, the control consisted only of filled with sediment tubes made with non-conductive material. All three setups were also prepared in triplicate.

The electrode's potential was monitored (Fig. 6.3). Without nitrate, potential for all experiments was reaching low values, in a range of -0.3 V vs SHE. The addition of water did not change the value of potential (Fig. 6.3 B). After nitrate addition, the potential increased and later decreased to initial value after nitrate's concentration dropped.

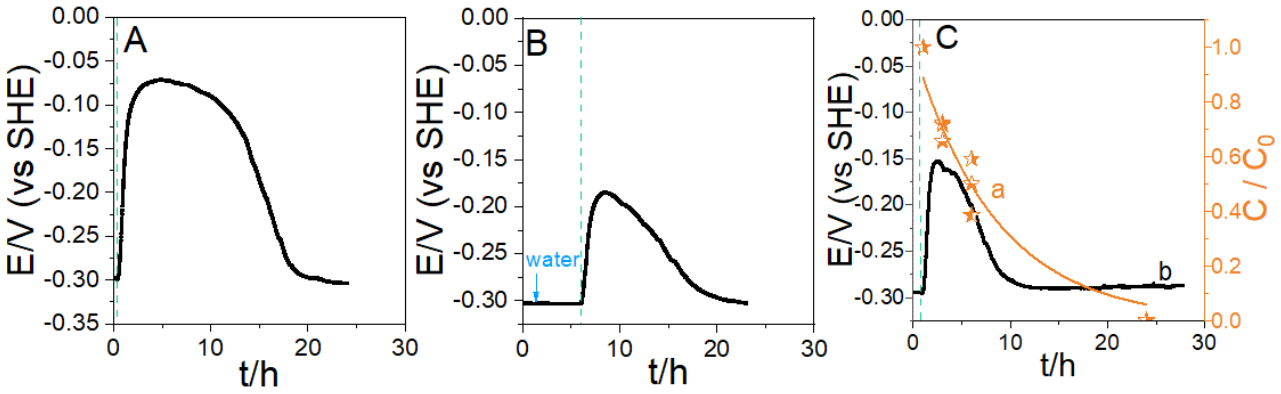

Fig. 6.3. *Potential measurements of MES with graphite felt. Addition of nitrate was indicated with green dotted line. A - Tube with graphite felt only inside (Graphite2), measurement on the 13.02. B - Tube with graphite felt inside and stainless steel around (Graphite1), measurement on the 07.02. The blue arrow indicates the addition of water. C - Tube with graphite felt inside and stainless steel around (Graphite3), measurement on the 19.02. The changes of potential (line b) were coupled with decreasing nitrate concentration (orange points and line a).*

In this experiment, rapid nitrate removal was observed again. Nitrate was no longer present on the next day after addition. During third addition, samples were taken three times during the same day in order to characterize the removal rate with first order kinetics. Fig. 6.4 presents the results of nitrate reduction of these experiments. It was found that in this experiment the constant was equal to 0.52, 1.6 and 2.56 day $^{-1}$ for control, experiment with only graphite felt and experiment with graphite felt and steel, respectively.

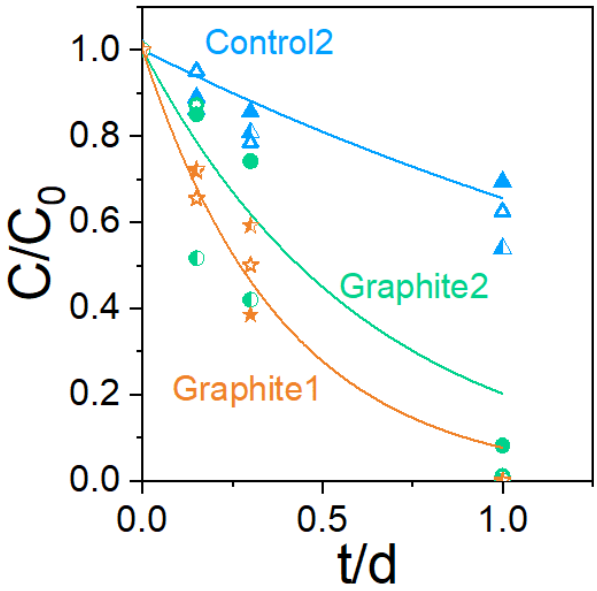

Figure 6.4. *Results graphite experiments nitrate removal*

Looking at the results of potential measurement and nitrate reduction, one can link the changes in potential with changes in nitrate concentration. Potential increases when nitrate is in the reactor and decreases when it is consumed. Experiment Graphite2 (graphite electrode inside of tube, without the stainless steel around it) was showing a little slower denitrification than Graphite1 (steel around the tube and graphite felt inside it). Similarly, the potential of the electrode in this experiment increased up to -0.075 V vs SHE, which is higher than for Graphite2 (up to -0.15 V vs SHE). The potential is increasing gradually when nitrate is in the environment until the certain low concentration of nitrate is reached, and after that it is decreasing. Therefore, the electrochemical response of bioelectrode can potentially give information about presence of nitrate in the environment.

However, in this series of experiments, some undefined peaks were observed during chromatography analysis, from minute 4.5 to minute 8, which were superposing the nitrate signals (Fig. 6.5). These peaks are probably corresponding to compound present in water, but they were not present, neither in the experiment with stainless steel nor in control. The presence of the graphite electrode caused the release of this compound to water.

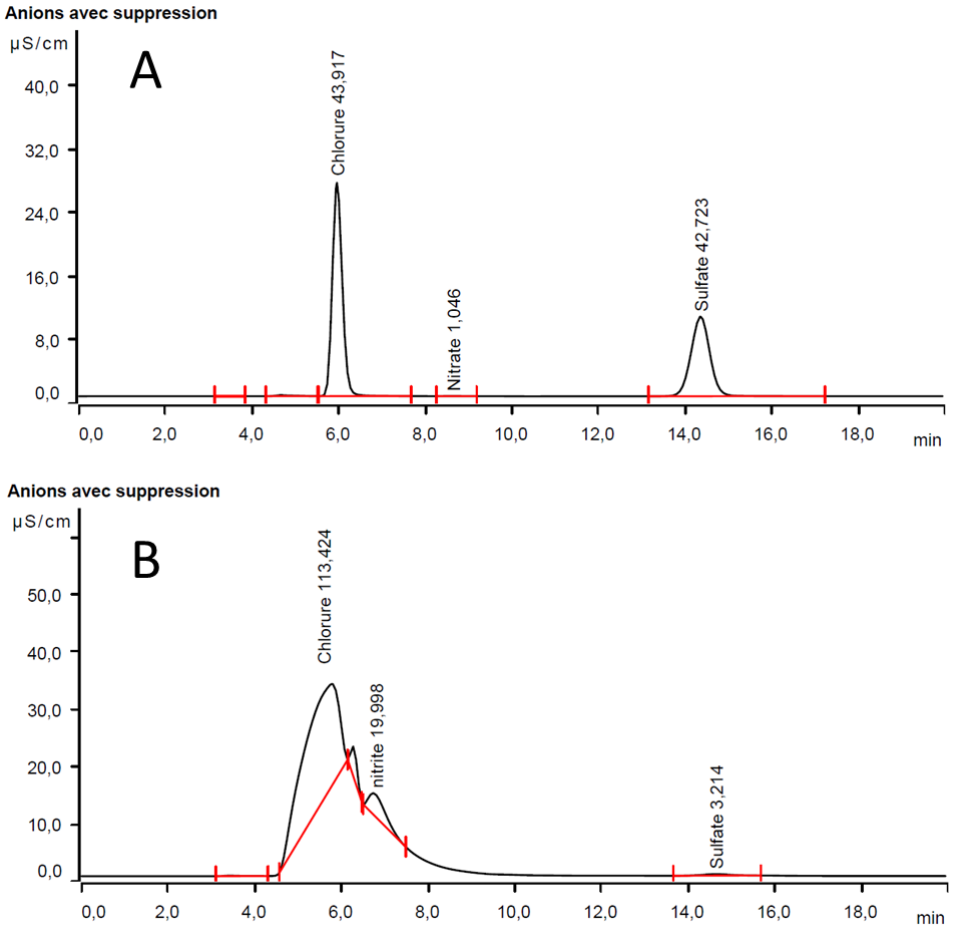

Figure 6.5 *Examples of the chromatograms of A. Control experiment without electrodes B. Experiment with graphite felt electrodes. In presence of graphite felt, the undefined peaks were observed.*

Denitrification in water

Similar experiments with the stainless steel or graphite felt electrodes inside of tubes filled with sediment were repeated. The change of the appearance of water was observed after few days from starting of the experiment. The water was still clear and transparent for the experiment with steel electrodes, however, for the one with graphite, it became cloudy.

100 ml of water from these two experiment were collected and placed in separated beakers. Additionally, 100 ml of deionized water was put in another beaker as comparison. Nitrate was added to all three beakers and samples were taken regularly. The results of this test are shown on Fig. 6.6. In distilled water and water from experiment with steel, no change in nitrate concentration was observed. However, it decreased to zero after 18 days in the experiment with graphite felt inside of the tube. From this observation it can be concluded that the presence of electrode in the sediment has an indirect effect on nitrate. It causes the release

of certain species to water, which react with nitrate in the solution. Peaks similar to previously observed appeared again on chromatograms. The reaction therefore does not occur directly on the bioelectrode, but the electrodes are causing changes occurring in the reactor.

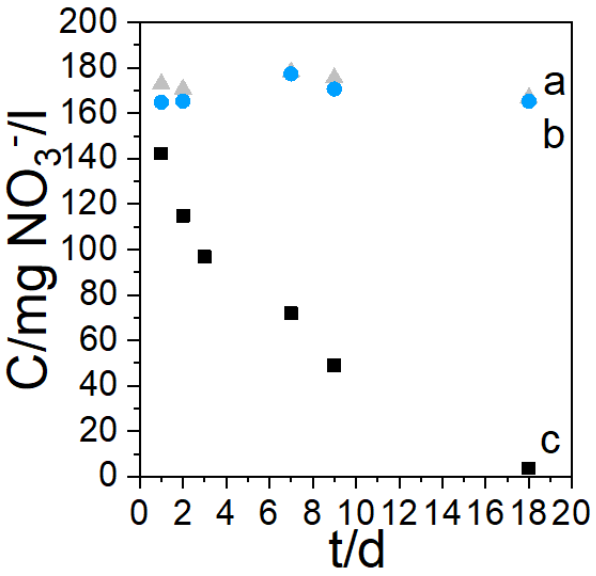

Figure 6.6. *Denitrification in water from experiments (without sediment and electrodes). a - deionized water, b - water from the experiment with steel, c - water from the experiment with graphite*

6.3. Experiment in flow

The released species which accelerated nitrate removal were a very interesting phenomenon, but they handicapped answering the question whether the electrode in the sediment has also a direct influence on faster denitrification. In other words, if nitrate can diffuse into the Tube, where it can be reduced.

In order to remove the effect of released species on nitrate removal, flow was introduced to the reactors of the same size, containing tubes with or without electrodes. Two experiments were compared, the control one without electrodes had the same design as previously described controls. The experiment with electrode in this case consisted of one piece of graphite felt (20x6 cm) inside, in contact with sediment but not with water. The inlet was on the bottom of the reactor and the outlet was higher, around 5 cm below the top of the reactor and around 4 cm above the top of the tube. The water from outlet was then transported to additional reactor of the same size, so it was circulating between them two in the loop, with the use of peristaltic

pomp. In the beginning, the water was changed a few times every one or two days in order to make sure that all initially released species will not play a role in denitrification process.

The results of two nitrate additions are presented on Fig. 6.7 A&B. After the first addition, the nitrate reduction was slightly faster in the experiment with the electrode, after the second one - in the control experiment without electrode. Therefore, the presence of the electrode did not bring any clear improvement of nitrate reduction rate.

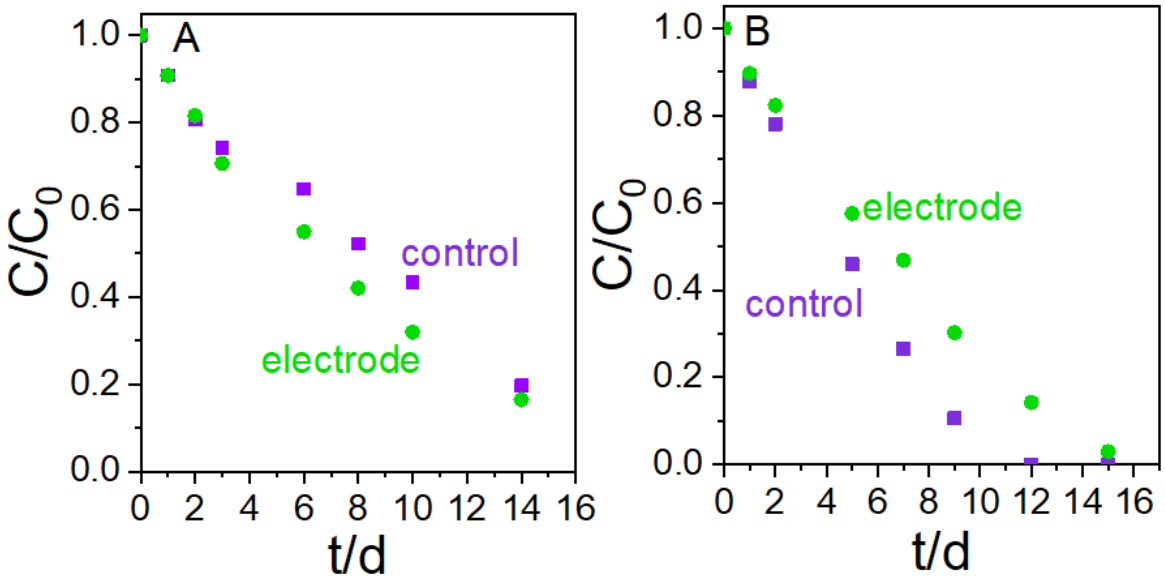

Figure 6.7. *Results of the nitrate reduction in experiments in flow: tube with electrode in the sediment (green) and control, which was tube with sediment without electrode (violet).*

The experiment was then repeated but with the potential of -0.303 V vs SHE (-0.5 vs 1M Ag/AgCl) applied on the working electrode in the tube with the purpose of ensuring the sufficiently low potential and the best conditions for denitrification. Stainless steel grid was additionally placed around the tube and it was connected as counter electrode. Reference electrode was in the same place as for the previous experiments, in the upper part of the reactor.

Figure 6.8 illustrates the chronoamperometry results of this second experiment in flow. Before the first nitrate addition, the current initially had increasing negative values (up to day 5), similarly to the previous results. From day 5 to 10, there was a plateau of about -0.25 mA and after that the current values started increasing until it reached the positive value on the day 16. Although we applied negative, cathodic potential, the electrode was inserted in the sediment with the big concentration of the reduced organic species. Therefore, we interpret that initially the bioelectrode was reducing all the possible species, which were however in limited quantity in the sediment. Once they were no longer available, the behavior of bioelectrode changed and

it started to oxidize the available compounds. Switching the properties of bioelectrode from anodic to cathodic and vice-versa were already described in the introduction to this thesis (Chapter 1.A.B.)

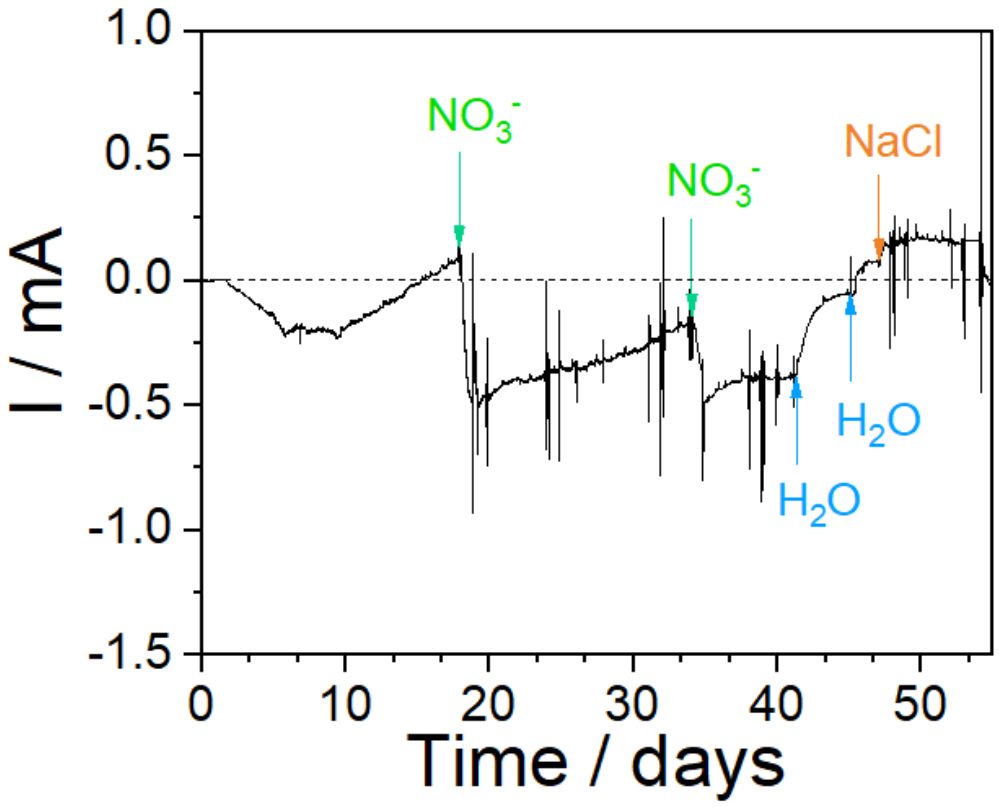

Figure 6.8. *Results of chronoamperometry analysis of bioelectrode in sediment in flow conditions. Applied potential was -0.303 V vs SHE (-0.5 vs 1M Ag/AgCl)*

To verify this, nitrate was added on day 18 and very fast, the change of current towards negative values was observed. This could be the consequence of the fact that nitrate diffused into the sediment and was reduced on the electrode. Sediment here is positioned vertically and the flow is introduced from the bottom of the tube, therefore, the negative current comes from reduction of nitrate diffused into sediment, with help of water movement.

After the sharp increase, the negative current was gradually decreasing until the second nitrate addition on day 33. This time, we also observed the rapid negative current increase. On the days 42 and 46, the water in additional tank was changed into new synthetic wastewater (without nitrate), which resulted in both cases in faster change of nitrate towards positive values. The NaCl solution added on the day 48 was a control experiment, in order to see if the current will change after addition of other than nitrate ions. However, no significant reaction was observed and the current was still positive.

Nitrate concentration was monitored during two additions; the results are shown on Fig. 6.9. After fitting the results to first order reaction rate, the obtained constant k was 0.12 and 0.05 day^{-1}, respectively. This is less than for the first control experiment introduced in this study (without flow), for which the k was 0.27 day^{-1}. It seems that the flow conditions are inhibiting the denitrification performance, which is probably caused by bigger concentration of oxygen caused by the water movement. In the stationary conditions, tall and narrow reactors were promoting anaerobic environment, which is beneficial for faster nitrate removal, and this benefit was lost while introducing flow. The presence of electrode, despite its clear response to nitrate in terms of current change, did not compensate the loss of performance caused by flow.

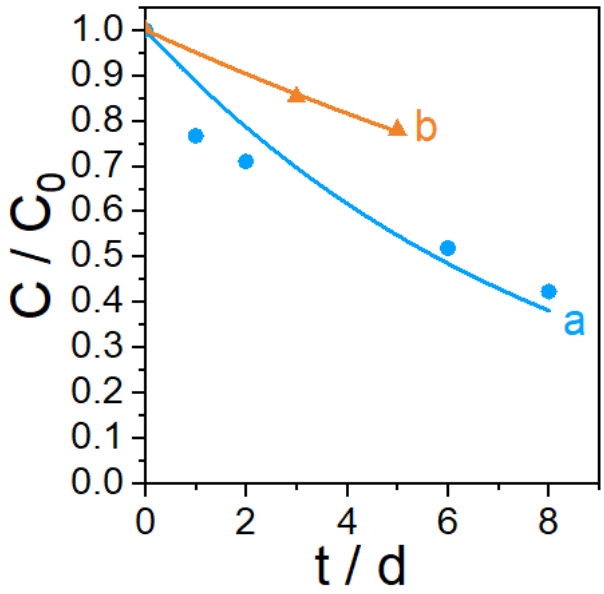

Figure 6.9 *Results of denitrification in flow. a - first addition (C_0 = 110 mg NO_3^- L^{-1}), b - second addition (C_0 = 90 mg NO_3^- L^{-1})*

6.4. Possibility of using electrodes in sediment as nitrate sensor

Another application of electrode in the sediment could be possible. Since the system was reacting rapidly and clearly for nitrate addition, it could be used as a sensor of nitrate in constructed wetlands. In order to verify this idea, small amounts of nitrate (20 mg L^{-1} each time) were added every two - three days, starting from day 54 of the experiment. Fig. 6.10 A shows the response of current after every addition (marked with green arrows). Fig. 6.10 B, shows changes of current in function of changing nitrate concentration. As it is shown in the top right corner of Fig. 6.10 B, until 60 mg L^{-1} this function in linear and only after that the current response started to decrease.

Several studies were already exploring the possibility using BES as sensors of different compounds [264], including nitrate. Wang et al. built a double chamber MFC, which was operating in constant flow and in open or closed circuit (400Ω in case of closed circuit) [265]. The nitrate was introduced to anodic chamber which had a consequence in voltage drop and the open circuit voltage drops were measured. The changes in voltage were corresponding to added nitrate concentrations in range from 10 to 40 mg L^{-1} and the sensor was more sensitive in case of open circuit (between 4.4 and 6.6 mV (mg L^{-1})$^{-1}$). Similar idea was proposed by Su et al., who prepared one chamber bioelectrochemical indicator, with carbon working electrode of applied potential -0.2 V Ag/AgCl (-0.023 V vs SHE) and platinum counter, inoculated with bacteria [266]. Nitrate was added to the reactor of constant electron donor concentration. The working electrode was bioanode and it was oxidizing the electron donors so the addition of nitrate was causing anodic current decrease. This is because of the competition between microbial nitrate reduction and electrogenesis. Yi et al. proposed a method of simultaneous detection of BOD and nitrate using electrochemically active bacteria [161]. They used *Shewanella loihica*, which has capability of bidirectional extracellular electron transfer. The bacteria were used in BES and they were fed with medium containing either organic compounds (outward BES, electrode poised at 0 V vs Ag/AgCl) or nitrate (inward BES, electrode poised at -0.5 V vs Ag/AgCl). The outward BES was reacting with increased positive current for BOD additions and in the outward BES, reversely, the negative current was increasing after nitrate reduction. Yu et al. created another nitrate-sensing MFC [267]. They found that it was giving better response for nitrate when it was powered by another, coupled MFC. Nitrate was introduced to biocathodic chamber and the increase of current was corresponding to its concentration.

These studies show that the MFCs can be used as nitrate sensors, however, the research in this direction is still limited. For example, for the moment the possibility of sensing nitrate with the use of SMFC or CW-MFC was not yet explored. This experiment is the first evidence that it could be possible to sense nitrate with the use of electrode immersed in the sediment. However, further continuation of this study in required in order to optimize the system for application.

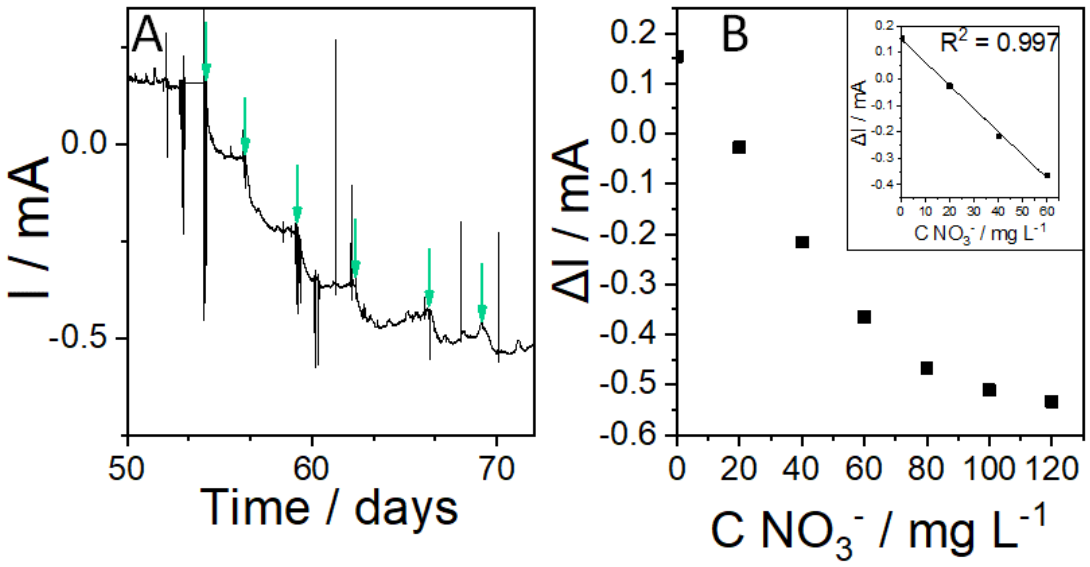

Figure 6.10 *A. The changes of current after nitrate additions to experiment in flow. Each green arrow represents addition of nitrate equivalent to 20 mg* L^{-1}*. B. "Plateau" current after each nitrate addition in function of nitrate concentration. The scheme in top right corner represents the linear fit for concentrations between 0 and 60 mg* NO_3^- L^{-1}.

6.5. Conclusions

This chapter was focusing on studying the consequences of inserting electrode in the sediment. The first part was exploring the experiments in stationary state. The stainless steel electrode did not seem to have any influence on the nitrate reduction rate. However, very fast reduction was observed in presence of graphite felt electrode in the sediment. Moreover, this reduction was corresponding to changes in potential of the electrode. The potential was initially low after electrode was placed in the sediment, but after nitrate addition it was increasing and decreasing again after nitrate was removed. Further studies indicated that the rapid nitrate reduction had different mechanism then we were initially expected. The reduction was not occurring on the surface of electrode, after nitrate's diffusion into the sediment, but in water. The presence of electrode in the sediment was inducing reaction which was resulting in release of undefined species from sediment to water, and these species were influencing the removal of nitrate.

To verify the initial theory of nitrate reduction on bioelectrode in the sediment, the experiment in flow was performed, aiming to exclude the influence of these released compounds. However, no improvement in denitrification was observed. Nevertheless, placing the electrode in the sediment can have another application which is nitrate sensing. The current was increasing proportionally to added nitrate concentration. The initial experiment is shown

in this chapter and the results are very promising, however more research in this direction should be performed for defining limits of detection and further optimization.

General Conclusions

This thesis was investigating methods of improving nitrate reduction rate in constructed wetlands. We identified that the limitation of this process is the fact that the electron donors such as organic carbon compounds appear in the sediment, while nitrate is present in water. The denitrification therefore will occur on the water/sediment interface. In this thesis, we were studying methods to make the electron donors in the sediments more accessible for denitrification.

Firstly, we increased the interface between sediment and water in order to study the influence of the area of this interface on nitrate reduction rate. This experiment was first performed in stationary state, where it was observed that increasing the interface 10 times can bring up to 6.5 times faster nitrate reduction. Similar improvement in reduction rate was observed for two sediments of different origin and composition, and no improvement was observed by simply increasing the volume of sediment. The experiment in flow gave stable NRR increase of 3.55 for at least 54 days. Increasing NRR 3.55 times in the constructed wetland on Rampillon should allow to achieve outlet concentration below 11.3 mg $N\text{-}NO_3^-$ L^{-1} during 94% of the calendar period, while currently it is 63%.

Secondly, we explored the possibility of employing electrochemistry to link the electron donor-rich sediment with water rich in electron acceptors. To study the bioelectrochemically-induced nitrate reduction, an MES was employed. This BES was not yet effectively used for nitrate reduction, therefore the first step of these studies was to deeply understand its behavior and electrochemical properties. We started by testing different electrode materials and we found stainless steel to best for this application. It was the only material out of tested ones which allowed to reach a proper potential for developing a nitrate-reduction biocathode without applying it externally. However, we found that one more parameter is influencing a mixed potential of the MES, which is a ratio between anodic part in the sediment and cathodic part in water. When disconnected, anodic part is going towards more negative potentials and cathodic part towards more positive, the mixed potential of MES is a compromise between them. The ratio 4:1 was chosen to be studied and it allowed to confirm the MES by measuring the current between parts in sediment and in water. The CV shape, as well as microbial community, were also clearly different for anode and cathode. However, this system allowed only to reach a modest improvement in nitrate reduction rate and one reason could be the increase of potential observed after the nitrate addition. Therefore, in the next chapter the MES was rebuilt, using

ratio 6:1 between anodes and cathodes as well as bigger electrodes. The clear electrochemical reaction was observed after nitrate addition: the current increased sharply on all replicates except for one when it was studied with use of ZRA. The cathodic peaks on the CV increased in the presence of nitrate and decreased again after it was consumed. The nitrate reduction was 40% faster than for the control without any electrodes and two times faster than in the MES experiment which did not clearly react on the nitrate addition. The microbial analysis showed the correlation between experiments which gave the clearest electrochemical response and the abundance of bacteria from order *Beggiatoales*. These bacteria are known to oxidize sulfur compounds and reduce oxygen or nitrate, however it was not yet proved that they can exchange the electrons with solid electrode in EET.

Finally, the last chapter is exploring the possibility of combining these two approaches by placing the electrode in the tube or around it. Another motivation for placing the electrodes in the sediment was testing the possibility of reduction of nitrate in this medium, because oxygen, which is an interfering agent, cannot diffuse into sediment. Stainless steel and graphite felt were tested for this purpose. No changes were observed in the experiments with stainless steel however, very fast denitrification rate was observed for experiments with graphite felt. Additional experiments showed that the reason of this phenomenon was not reduction on the electrode, but the reaction in water with species which were released because of the presence of electrode in the sediment. Moreover, an increase of potential was observed after nitrate was added and it was decreasing again as soon as nitrate was consumed. The experiment in flow was introduced in order to eliminate the effect of reaction in water and see if the reaction on the electrode brings any clear improvement in nitrate reduction. In this experiment, constant potential was applied to ensure the proper conditions for development of NRR. Although the nitrate reduction was not faster comparing to the control without electrode, the current was increasing proportionally to added nitrate concentration, which gives a new direction of application of NRB - as a nitrate sensor. Interestingly, without nitrate the positive current was observed which went towards negative values as soon as nitrate was added to the reactor. It means that without nitrate, the electrode in the sediment, devoid any electron acceptors, behaves like an anode and uses the organic matter as electron donors. As soon as nitrate was available, the bioelectrode was behaving like a cathode, which was favorable with this applied potential, and positive current was observed.

Overall, this thesis explores deeply the simple and cheap methods of improving NRR in constructed wetlands. It proposes two approaches, one employing bioelectrochemistry and another one basing on increasing the water/sediment interface. Deep electrochemical analysis

and microbial community studies are provided for the first method; scenario for application is proposed for the second one after long-time monitoring. This thesis opens several new directions for the studies, and some of them are listed below.

Perspectives

Based on conducted study, future perspectives can be proposed:

- Continuing the application of improvement sediment interface

Chapter 3 described the tests of increasing water/sediment contact surface in the laboratory wetlands in stationary and flow state, and it considered its application in the wetland. However, to reach the stage of application, the technique of increasing the interface should be optimized and adjusted for bigger-scale application, for example to prevent clogging, which possibly could be one problem. Moreover, the performance in real-life environment should be verified and compared to laboratory results. The influence of the modified sediment surface on the aquatic fauna and flora should be also considered.

- Optimization of MES

In Chapter 4, it was showed that introduction of MES can significantly improve NRR. However, the setup should be further explored to see if bigger improvement can be achieved (for example, by increasing even more the size of cathodes). The flow should be introduced in order to better mimic the conditions of constructed wetland. Finally, more simple and easier to apply setup should be proposed and tested in the wetland to see the results in the real-life environment.

- Studying bioelectrochemical properties of *Beggiatoales*

In this study, the large quantity of bacteria from order *Beggiatoales* was found in the biofilm from bioelectrodes and not in the other samples from sediment or water. Moreover, the abundance was correlating with the electrochemical response. However, there is no clear study proving the ability of *Beggiatoales* to exchange electrons with a solid electrode material. Therefore, it would be interesting to study these bacteria in that direction.

- Understanding the mechanism of fast denitrification

In Chapter 6, we observed a very fast nitrate reduction which was happening in water. The presence of the electrode in the sediment probably caused a release of some species to water which created this phenomenon. However, the exact mechanism was not studied in this work. It is unsure whether the fast denitrification is a part of some bacteria's metabolism, or if it is an abiotic chemical reaction. Understanding this mechanism could be the first step of proposing another method of denitrification.

- Optimization of sensor

The final part of Chapter 6 is exploring the possibility of using the electrode buried in the sediment as a nitrate sensor. Up to 80 mg L^{-1}, there was a linear correlation between the added nitrate concentration and registered current. This sensor should be further developed in other to simplify its setup and more exactly describe its precision and limits of detection.

Bibliography:

[1] V. Mateju, S. Cizinska, J. Krejci, T. Janoch, Biological water denitrification-- A review, Enzyme Microb. Technol. 14 (1992).

[2] R. Knowles, Denitrification, Microbiol. Rev. 46 (1982) 43–70.

[3] M.M.M. Kuypers, A.O. Sliekers, G. Lavik, M. Schmid, Anaerobic ammonium oxidation by anammox bacteria in the Black Sea, Nature. 422 (2003) 2–5. https://doi.org/10.1038/nature01526.1.

[4] J.N. Galloway, F.J. Dentener, D.G. Capone, E.W. Boyer, R.W. Howarth, S.P. Seitzinger, G.P. Asner, C.C. Cleveland, P.A. Green, E.A. Holland, D.M. Karl, A.F. Michaels, J.H. Porter, A.R. Townsend, C.J. Vo, Nitrogen cycles: past, present, and future, Biogeochemistry. 70 (2004) 153–226.

[5] D.E. Canfield, A.N. Glazer, P.G. Falkowski, The Evolution and Future of Earth's Nitrogen Cycle, Science (80-.). 330 (2010) 192–196.

[6] D. Fowler, M. Coyle, U. Skiba, M.A. Sutton, J.N. Cape, S. Reis, L.J. Sheppard, A. Jenkins, B. Grizzetti, N. Galloway, P. Vitousek, A. Leach, A.F. Bouwman, K. Butterbach-bahl, F. Dentener, D. Stevenson, M. Amann, M. Voss, D. Fowler, The global nitrogen cycle in the twenty- first century, (2013).

[7] P.M. Vitousek, H.A. Mooney, J. Lubchenco, J.M. Melillo, Human Domination of Earth ' s Ecosystems, 277 (1997).

[8] S. Benefits, How a century of ammonia synthesis changed the world, 1 (2008).

[9] N. Gruber, J.N. Galloway, An Earth-system perspective of the global nitrogen cycle, Nature. 451 (2008) 10–13. https://doi.org/10.1038/nature06592.

[10] J.A. Camargo, A. Alonso, A. Salamanca, Nitrate toxicity to aquatic animals : a review with new data for freshwater invertebrates, Chemosphere. 58 (2005) 1255–1267. https://doi.org/10.1016/j.chemosphere.2004.10.044.

[11] World Health Organization, Nitrate and nitrite in drinking-water, Backgr. Doc. Dev. WHO Guidel. Drink. Qual. 37 (2011) 227–231. https://doi.org/10.1159/000225441.

[12] DIRECTIVE (EU) 2020/2184 OF THE EUROPEAN PARLIAMENT AND OF THE COUNCIL of 16 December 2020 on the quality of water intended for human consumption (recast) (Text with EEA relevance), OJ L 435, 23.12.2020, p. 1–62. (n.d.).

[13] United States Environmental Protection Agency, National Primary Drinking Water Regulations, EPA 816-F-09-004 | MAY 2009. (n.d.).

[14] Consolidated text: Council Directive of 12 December 1991 concerning the protection of waters against pollution caused by nitrates from agricultural sources (91/676/EEC), (2008) 1–13.

[15] J. Tzilivakis, A. Green, D.J. Warner, K.A. Lewis, Identification of approaches and measures in action programmes under Directive 91 / 676 / EEC Final report, Rep. Prep. Dir. Environ. Eur. Comm. Proj. ENV.D.1/SER/2018/0017 by Agric. Environ. Res. Unit (AERU), Univ. Hertfordshire, United Kingdom. (2020).

[16] H. O'Neal Tugaoen, S. Garcia-segura, K. Hristovski, P. Westerhoff, Challenges in photocatalytic reduction of nitrate as a water treatment technology, Sci. Total Environ.

599–600 (2017) 1524–1551. https://doi.org/10.1016/j.scitotenv.2017.04.238.

[17] J. Schoeman, Nitrate-nitrogen removal with small-scale reverse osmosis , electrodialysis and ion-exchange units in rural areas, Water SA. 35 (2009) 721–728.

[18] Y. Kim, E. Hwang, W.S. Shin, J. Choi, Treatments of stainless steel wastewater containing a high concentration of nitrate using reverse osmosis and nanomembranes, 202 (2007) 286–292. https://doi.org/10.1016/j.desal.2005.12.066.

[19] J.J. Schoeman, A. Steyn, Nitrate removal with reverse osmosis in a rural area in South Africa, 5 (2003) 15–26.

[20] H. Demiral, G. Gündüzog, Removal of nitrate from aqueous solutions by activated carbon prepared from sugar beet bagasse, 101 (2010) 1675–1680. https://doi.org/10.1016/j.biortech.2009.09.087.

[21] G. V Nunell, M.E. Fernandez, P.R. Bonelli, A.L. Cukierman, Nitrate uptake improvement by modified activated carbons developed from two species of pine cones, J. Colloid Interface Sci. 440 (2015) 102–108. https://doi.org/10.1016/j.jcis.2014.10.058.

[22] M. Mazarji, B. Aminzadeh, M. Baghdadi, A. Bhatnagar, Removal of nitrate from aqueous solution using modified granular activated carbon, J. Mol. Liq. 233 (2017) 139–148. https://doi.org/10.1016/j.molliq.2017.03.004.

[23] C. V Lazaratou, D. V Vayenas, D. Papoulis, The role of clays, clay minerals and clay-based materials for nitrate removal from water systems: A review, Appl. Clay Sci. 185 (2020) 105377. https://doi.org/10.1016/j.clay.2019.105377.

[24] S. Samatya, N. Kabay, M. Yu, Removal of nitrate from aqueous solution by nitrate selective ion exchange resins, 66 (2006) 1206–1214. https://doi.org/10.1016/j.reactfunctpolym.2006.03.009.

[25] J. Kim, M.M. Benjamin, Modeling a novel ion exchange process for arsenic and nitrate removal, 38 (2004) 2053–2062. https://doi.org/10.1016/j.watres.2004.01.012.

[26] F. Rezvani, M. Sarrafzadeh, S. Ebrahimi, Nitrate removal from drinking water with a focus on biological methods : a review, (2017). https://doi.org/10.1007/s11356-017-9185-0.

[27] M. Li, C. Feng, Z. Zhang, Z. Shen, N. Sugiura, Electrochemical reduction of nitrate using various anodes and a Cu / Zn cathode, Electrochem. Commun. 11 (2009) 1853–1856. https://doi.org/10.1016/j.elecom.2009.08.001.

[28] I. Katsounaros, D. Ipsakis, C. Polatides, G. Kyriacou, Efficient electrochemical reduction of nitrate to nitrogen on tin cathode at very high cathodic potentials, 52 (2006) 1329–1338. https://doi.org/10.1016/j.electacta.2006.07.034.

[29] C. Su, R.W. Puls, Nitrate Reduction by Zerovalent Iron : Effects of Formate , Oxalate , Citrate , Chloride , Sulfate , Borate , and Phosphate, 38 (2004) 2715–2720. https://doi.org/10.1021/es034650p.

[30] M. Kumar, S. Chakraborty, Chemical denitrification of water by zero-valent magnesium powder, 135 (2006) 112–121. https://doi.org/10.1016/j.jhazmat.2005.11.031.

[31] T. Yang, K. Doudrick, P. Westerhoff, Photocatalytic reduction of nitrate using titanium

dioxide for regeneration of ion exchange brine, Water Res. 47 (2012) 1299–1307. https://doi.org/10.1016/j.watres.2012.11.047.

[32] E. Lacasa, P. Ca, C. Sáez, F.J. Fernández, M.A. Rodrigo, Removal of nitrates from groundwater by electrocoagulation, Chem. Eng. J. 171 (2011) 1012–1017. https://doi.org/10.1016/j.cej.2011.04.053.

[33] A. El, F. Elhannouni, M. Taky, L. Chay, M. Amine, M. Sahli, L. Echihabi, M. Hafsi, Optimization of nitrate removal operation from ground water by electrodialysis, 29 (2002) 235–244.

[34] K. Kesore, F. Janowski, V.A. Shaposhnik, Highly effective electrodialysis for selective elimination of nitrates from drinking water, 127 (1997) 17–24.

[35] L.J. Banasiak, A.I. Schäfer, Removal of boron , fluoride and nitrate by electrodialysis in the presence of organic matter, 334 (2009) 101–109. https://doi.org/10.1016/j.memsci.2009.02.020.

[36] H. Strathmann, Electrodialysis , a mature technology with a multitude of new applications, DES. 264 (2010) 268–288. https://doi.org/10.1016/j.desal.2010.04.069.

[37] P. Clauwaert, K. Rabaey, P. Aelterman, L. De Schamphelaire, T.H. Pham, P. Boeckx, N. Boon, W. Verstraete, Biological denitrification in microbial fuel cells, Environ. Sci. Technol. 41 (2007) 3354–3360. https://doi.org/10.1021/es062580r.

[38] S. Ghafari, M. Hasan, M.K. Aroua, Bio-electrochemical removal of nitrate from water and wastewater-A review, Bioresour. Technol. 99 (2008) 3965–3974. https://doi.org/10.1016/j.biortech.2007.05.026.

[39] L.U. Songliu, H.U. Hongying, S.U.N. Yingxue, Y. Jia, Effect of carbon source on the denitrification in constructed wetlands, J. Environ. Sci. 21 (2009) 1036–1043. https://doi.org/10.1016/S1001-0742(08)62379-7.

[40] B. Hu, J. Quan, K. Huang, J. Zhao, G. Xing, Effects of C/N ratio and dissolved oxygen on aerobic denitrification process : A mathematical modeling study, Chemosphere. 272 (2021). https://doi.org/10.1016/j.chemosphere.2020.129521.

[41] D. Patureau, N. Bernet, J.P. Delgenès, R. Moletta, Effect of dissolved oxygen and carbon-nitrogen loads on denitrification by an aerobic consortium, Appl. Microbiol. Biotechnol. 54 (2000) 535–542.

[42] M.O. Rivett, S.R. Buss, P. Morgan, J.W.N. Smith, C.D. Bemment, Nitrate attenuation in groundwater: A review of biogeochemical controlling processes, Water Res. 42 (2008) 4215–4232. https://doi.org/10.1016/j.watres.2008.07.020.

[43] T. Sirivedhin, K.A. Gray, Factors affecting denitrification rates in experimental wetlands : Field and laboratory studies, Ecol. Eng. 26 (2006) 167–181. https://doi.org/10.1016/j.ecoleng.2005.09.001.

[44] J. Van Rijn, Y. Tal, H.J. Schreier, Denitrification in recirculating systems: Theory and applications, Aquac. Eng. 34 (2006) 364–376. https://doi.org/10.1016/j.aquaeng.2005.04.004.

[45] S. Seitzngern, J.A. Harrison, J. Bohkle, A. Bouwman, R. Lowrance, B. Peterson, C. Tobias, G. Van Drecht, Denitrification across landscapes and waterscapes: a synthesis, Ecol. Appl. 16 (2006) 2064–2090.

[46] S. Rahimi, O. Modin, I. Mijakovic, Technologies for biological removal and recovery of nitrogen from wastewater, Biotechnol. Adv. 43 (2020) 107570. https://doi.org/10.1016/j.biotechadv.2020.107570.

[47] K.A. Karanasios, I.A. Vasiliadou, S. Pavlou, D. V. Vayenas, Hydrogenotrophic denitrification of potable water: A review, J. Hazard. Mater. 180 (2010) 20–37. https://doi.org/10.1016/j.jhazmat.2010.04.090.

[48] M. Gerardi, Nitrification and Denitrification in the Activated Sludge Process, John Wiley and Sons, New York, 2002.

[49] N. Bernet, N. Delgenes, R. Moletta, Denitrification by Anaerobic Sludge in Piggery Wastewater, Environ. Technol. 3330 (2010). https://doi.org/10.1080/09593331708616387.

[50] L.A. Schipper, W.D. Robertson, A.J. Gold, D.B. Jaynes, S.C. Cameron, Denitrifying bioreactors — An approach for reducing nitrate loads to receiving waters, Ecol. Eng. 36 (2010) 1532–1543. https://doi.org/10.1016/j.ecoleng.2010.04.008.

[51] J. Vymazal, Horizontal sub-surface flow and hybrid constructed wetlands systems for wastewater treatment, Ecol. Eng. 25 (2005) 478–490. https://doi.org/10.1016/j.ecoleng.2005.07.010.

[52] J.P. Van der Hoek, P. Van der Ven, A. Klapwlik, Combined Ion Exchange/Biological Denitrification for Nitrate Removal From Ground Water Under Different Process Conditions, Water Res. 22 (1988) 679–684.

[53] A. Matei, G. Racoviteanu, Review of the technologies for nitrates removal from water intended for human consumption, IOP Conf. Ser. Earth Environ. Sci. Pap. 664 (2021) 012–024. https://doi.org/10.1088/1755-1315/664/1/012024.

[54] O. Choi, B.I. Sang, Extracellular electron transfer from cathode to microbes: application for biofuel production, Biotechnol. Biofuels. (2016) 1–14. https://doi.org/10.1186/s13068-016-0426-0.

[55] S. Farah, N. Rusli, M. Hani, A. Bakar, K. Shyuan, M. Shahbudin, Review of high-performance biocathode using stainless steel and carbon-based materials in Microbial Fuel Cell for electricity and water treatment, Int. J. Hydrogen Energy. 44 (2018) 30772–30787. https://doi.org/10.1016/j.ijhydene.2018.11.145.

[56] S. Cosnier, Bioelectrochemistry. Design and Applications of Biomaterials, de Gruyter, Berlin/Boston, 2019.

[57] Y. Xiao, E. Zhang, J. Zhang, Y. Dai, Z. Yang, H.E.M. Christensen, J. Ulstrup, F. Zhao, Extracellular polymeric substances are transient media for microbial extracellular electron transfer, Sci. Adv. (2017) 1–9.

[58] B.E. Logan, Microbial Fuel Cells, 2011. https://doi.org/DOI: 10.1016/B978-0-444-53199-5.00098-1.

[59] H. Liu, B.E. Logan, Electricity generation using an air-cathode single chamber microbial fuel cell in the presence and absence of a proton exchange membrane, Environ. Sci. Technol. 38 (2004) 4040–4046. https://doi.org/10.1021/es0499344.

[60] P. Clauwaert, K. Rabaey, P. Aelterman, L. De Schamphelaire, T.H. Pham, P. Boeckx, N. Boon, W. Verstraete, Biological Denitrification in Microbial Fuel Cells, Environ.

Sci. Technol. 41 (2007) 3354–3360.

[61] D.D. Kozub, S.K. Liehr, Assessing denitrification rate limiting factors in a constructed wetland receiving landfill leachate, Water Sci. Technol. 40 (1999) 75–82. https://doi.org/10.1016/S0273-1223(99)00459-X.

[62] C. Zhang, Q. Yin, Y. Wen, W. Guo, C. Liu, Q. Zhou, Enhanced nitrate removal in self-supplying carbon source constructed wetlands treating secondary effluent : The roles of plants and plant fermentation broth, Ecol. Eng. 91 (2016) 310–316. https://doi.org/10.1016/j.ecoleng.2016.02.039.

[63] C.A. Schmidt, M.W. Clark, Efficacy of a denitrification wall to treat continuously high nitrate loads, Ecol. Eng. 42 (2012) 203–211. https://doi.org/10.1016/j.ecoleng.2012.02.006.

[64] L. Schipper, M. Vojvodic-Vukovic, Nitrate Removal from Groundwater Using a Denitrification Wall Amended with Sawdust: Field Trial, J. Environ. Qual. 27 (1998) 664–668.

[65] L.A. Schipper, D.A. Bruesewitz, W.T. Baisden, A comparison of different approaches for measuring denitrification rates in a nitrate removing bioreactor, 5 (2011). https://doi.org/10.1016/j.watres.2011.05.027.

[66] B. Virdis, K. Rabaey, Z. Yuan, J. Keller, Microbial fuel cells for simultaneous carbon and nitrogen removal, Water Res. 42 (2008) 3013–3024. https://doi.org/10.1016/j.watres.2008.03.017.

[67] P. Clauwaert, J. Desloover, C. Shea, R. Nerenberg, N. Boon, W. Verstraete, Enhanced nitrogen removal in bio-electrochemical systems by pH control, Biotechnol. Lett. 31 (2009) 1537–1543. https://doi.org/10.1007/s10529-009-0048-8.

[68] Y. Zhang, W. Xu, Y. Xiang, Kinetics and gene diversity of denitrifying biocathode in biological electrochemical systems †, RSC Adv. 7 (2017) 24981–24987. https://doi.org/10.1039/c7ra04070a.

[69] A. Al-mamun, T. Jafary, M. Said, S. Rahman, Energy recovery and carbon / nitrogen removal from sewage and contaminated groundwater in a coupled hydrolytic-acidogenic sequencing batch reactor and denitrifying biocathode microbial fuel cell, Environ. Res. 183 (2020) 109273. https://doi.org/10.1016/j.envres.2020.109273.

[70] A. Vijay, M. Vaishnava, M. Chhabra, Microbial fuel cell assisted nitrate nitrogen removal using cow manure and soil, Environ. Sci. Pollut. Res. 23 (2016) 7744–7756. https://doi.org/10.1007/s11356-015-5934-0.

[71] P. Srivastava, A. Kumar, R. Abbassi, V. Garaniya, T. Lewis, Denitrification in a low carbon environment of a constructed wetland incorporating a microbial electrolysis cell, J. Environ. Chem. Eng. 6 (2018) 5602–5607. https://doi.org/10.1016/j.jece.2018.08.053.

[72] M. Sun, G. Sheng, Z. Mu, X. Liu, Y. Chen, H. Wang, H. Yu, Manipulating the hydrogen production from acetate in a microbial electrolysis cell – microbial fuel cell-coupled system, 191 (2009) 338–343. https://doi.org/10.1016/j.jpowsour.2009.01.087.

[73] C. Wang, Y. Wu, W. Hu, Y. Li, Autotrophic Denitrification for Nitrate Removal from Groundwater with an Integrated Microbial Fuel Cells (MFCs) - Microbial Electrolysis Cell (MEC) System, Int. J. Electrochem. Sci. 16 (2021) 1–11.

https://doi.org/10.20964/2021.01.10.

[74] B. Erable, L. Etcheverry, A. Bergel, From microbial fuel cell (MFC) to microbial electrochemical snorkel (MES): maximizing chemical oxygen demand (COD) removal from wastewater., Biofouling. 27 (2011) 319–326. https://doi.org/10.1080/08927014.2011.564615.

[75] C. Cruz Viggi, E. Presta, M. Bellagamba, S. Kaciulis, S.K. Balijepalli, G. Zanaroli, M. Petrangeli Papini, S. Rossetti, F. Aulenta, The "Oil-Spill Snorkel": an innovative bioelectrochemical approach to accelerate hydrocarbons biodegradation in marine sediments, Front. Microbiol. 6 (2015). https://doi.org/10.3389/fmicb.2015.00881.

[76] C. Cruz, B. Matturro, E. Frascadore, S. Insogna, A. Mezzi, S. Kaciulis, A. Sherry, O.K. Mejeha, I.M. Head, E. Vaiopoulou, K. Rabaey, S. Rossetti, F. Aulenta, Bridging spatially segregated redox zones with a microbial electrochemical snorkel triggers biogeochemical cycles in oil-contaminated River Tyne (UK) sediments, Water Res. 127 (2017) 11–21. https://doi.org/10.1016/j.watres.2017.10.002.

[77] C.A. Ramírez-vargas, C.A. Arias, P. Carvalho, L. Zhang, A. Esteve-núñez, H. Brix, Electroactive biofilm-based constructed wetland (EABB-CW): A mesocosm-scale test of an innovative setup for wastewater treatment, Sci. Total Environ. 659 (2019) 796–806. https://doi.org/10.1016/j.scitotenv.2018.12.432.

[78] M. Mitov, I. Bardarov, E. Chorbadzhiyska, K.L. Kostov, First evidence for applicability of the microbial electrochemical snorkel for metal recovery, Electrochem. Commun. 122 (2021) 106889. https://doi.org/10.1016/j.elecom.2020.106889.

[79] Y. Yang, J. Guo, G. Sun, M. Xu, Characterizing the snorkeling respiration and growth of Shewanella decolorationis S12, Bioresour. Technol. 128 (2013) 472–478. https://doi.org/10.1016/j.biortech.2012.10.103.

[80] Q. Yang, H. Zhao, H.H. Liang, Denitrification of overlying water by microbial electrochemical snorkel, Bioresour. Technol. 197 (2015) 512–514. https://doi.org/10.1016/j.biortech.2015.08.127.

[81] M. Hoareau, B. Erable, A. Bergel, Microbial electrochemical snorkels (MESs): A budding technology for multiple applications . A mini review, Electrochem. Commun. 104 (2019) 106473. https://doi.org/10.1016/j.elecom.2019.05.022.

[82] C.-P. Huang, H.-W. Wang, P.-C. Chiu, Nitrate reduction by metallic iron, Water Res. 32 (1998) 2257–2264. https://doi.org/10.1016/S0043-1354(97)00464-8.

[83] M. Etique, F.P.A. Jorand, A. Zegeye, B. Grégoire, C. Despas, C. Ruby, Abiotic Process for Fe(II) Oxidation and Green Rust Mineralization Driven by a Heterotrophic Nitrate Reducing Bacteria (Klebsiella mobilis), Environ. Sci. Technol. 48 (2014) 3742–3751. https://doi.org/10.1021/es403358v.

[84] Y. Wang, J. Hu, L. Wang, D. Shan, X. Wang, Y. Zhang, X. Mao, L. Xing, D. Wang, Acclimated sediment microbial fuel cells from a eutrophic lake for the in situ denitrification process, RSC Adv. 6 (2016) 80079–80085. https://doi.org/10.1039/C6RA16510A.

[85] M.C. Potter, Electrical Effects Accompanying the Decomposition of Organic Compounds, Proc. R. Soc. B Biol. Sci. 84 (1911) 260–276. https://doi.org/10.1098/rspb.1911.0073.

[86] B.E. Logan, Exoelectrogenic bacteria that power microbial fuel cells, (n.d.).

[87] B.H. Kim, D.H. Park, P.K. Shin, I.S. Chang, H.J. Kim, Mediator-less Biofuel Cell, United States Pat. 5976719. (1999).

[88] J.M. Morris, P.H. Fallgren, S. Jin, Enhanced denitrification through microbial and steel fuel-cell generated electron transport, Chem. Eng. J. 153 (2009) 37–42. https://doi.org/10.1016/j.cej.2009.05.041.

[89] H. Rismani-yazdi, S.M. Carver, A.D. Christy, O.H. Tuovinen, Cathodic limitations in microbial fuel cells : An overview, 180 (2008) 683–694. https://doi.org/10.1016/j.jpowsour.2008.02.074.

[90] K.B. Gregory, D.R. Bond, D.R. Lovley, Graphite electrodes as electron donors for anaerobic respiration, 6 (2004) 596–604. https://doi.org/10.1111/j.1462-2920.2004.00593.x.

[91] H. Il, Y. Choi, D. Pak, Nitrate reduction using an electrode as direct electron donor in a biofilm-electrode reactor, 40 (2005) 3383–3388. https://doi.org/10.1016/j.procbio.2005.03.017.

[92] G. Chen, S. Choi, J. Cha, T. Lee, C. Kim, Microbial community dynamics and electron transfer of a biocathode in microbial fuel cells, Korean J. Chem. Eng. 27 (2010) 1513–1520. https://doi.org/10.1007/s11814-010-0231-6.

[93] J. Guo, J. Cheng, B. Li, J. Wang, P. Chu, Performance and microbial community in the biocathode of microbial fuel cells under different dissolved oxygen concentrations, J. Electroanal. Chem. 833 (2019) 433–440. https://doi.org/10.1016/j.jelechem.2018.12.015.

[94] W. Sima, R. Ma, F. Yin, H. Zou, H. Li, H. Ai, T. Ai, Prompt nitrogen removal by controlling the oxygen concentration in sediment microbial fuel cell systems : the electrons allocation and its microbial mechanism, Water Sci. Technol. 81 (2020) 1209–1220. https://doi.org/10.2166/wst.2020.222.

[95] Y. Zhang, I. Angelidaki, Bioelectrode-based approach for enhancing nitrate and nitrite removal and electricity generation from eutrophic lakes, Water Res. 46 (2012) 6445–6453. https://doi.org/10.1016/j.watres.2012.09.022.

[96] B. Virdis, K. Rabaey, R. Rozendal, Z. Yuan, J. Keller, Simultaneous nitrification, denitrification and carbon removal in microbial fuel cells, Water Res. 44 (2010) 2970–2980. https://doi.org/10.1016/j.watres.2010.02.022.

[97] B. Virdis, S.T. Read, K. Rabaey, R.A. Rozendal, Z. Yuan, J. Keller, Biofilm stratification during simultaneous nitrification and denitrification (SND) at a biocathode, Bioresour. Technol. 102 (2011) 334–341. https://doi.org/10.1016/j.biortech.2010.06.155.

[98] G. Zhu, G. Chen, R. Yu, H. Li, C. Wang, Enhanced simultaneous nitrification/denitrification in the biocathode of a microbial fuel cell fed with cyanobacteria solution, Process Biochem. 51 (2016) 80–88. https://doi.org/10.1016/j.procbio.2015.11.004.

[99] M. Kuroda, T. Watanabe, Y. Umedu, Simultaneous oxidation and reduction treatments of polluted water by a bio-electro reactor, Water Sci. Technol. 34 (1996) 101–108. https://doi.org/10.1016/S0273-1223(96)00792-5.

[100] L.A. Robertson, J.G. Kuenen, Hicrebinlegy Aerobic denitrification : a controversy revived *, Arch. Microbiol. 139 (1984) 351–354.

[101] J. Yang, L. Feng, S. Pi, D. Cui, F. Ma, H. Zhao, A. Li, A critical review of aerobic denitrification : Insights into the intracellular electron transfer, Sci. Total Environ. 731 (2020) 139080. https://doi.org/10.1016/j.scitotenv.2020.139080.

[102] F. Chen, Q. Xia, L. Ju, Competition Between Oxygen and Nitrate Respirations in Continuous Culture of Pseudomonas aeruginosa Performing Aerobic Denitrification, (2006). https://doi.org/10.1002/bit.

[103] J. Zhao, J. Wu, X. Li, S. Wang, B. Hu, X. Ding, The Denitrification Characteristics and Microbial Community in the Cathode of an MFC with Aerobic Denitrification at High Temperatures, 8 (2017) 1–11. https://doi.org/10.3389/fmicb.2017.00009.

[104] N. Yang, H. Liu, X. Jin, D. Li, G. Zhan, One-pot degradation of urine wastewater by combining simultaneous halophilic nitri fi cation and aerobic denitri fi cation in air-exposed biocathode microbial fuel cells (AEB-MFCs), Sci. Total Environ. 748 (2020) 141379. https://doi.org/10.1016/j.scitotenv.2020.141379.

[105] C. Feng, L. Huang, H. Yu, X. Yi, C. Wei, Simultaneous phenol removal , nitrification and denitrification using microbial fuel cell technology, Water Res. 76 (2015) 160–170. https://doi.org/10.1016/j.watres.2015.03.001.

[106] J. Sun, W. Xu, B. Cai, G. Huang, H. Zhang, Y. Zhang, High-concentration nitrogen removal coupling with bioelectric power generation by a self-sustaining algal-bacterial biocathode photo- bioelectrochemical system under daily light / dark cycle, Chemosphere. 222 (2019) 797–809. https://doi.org/10.1016/j.chemosphere.2019.01.191.

[107] M. Oliot, S. Galier, H. Roux de Balmann, A. Bergel, Ion transport in microbial fuel cells: Key roles, theory and critical review, Appl. Energy. 183 (2016) 1682–1704. https://doi.org/10.1016/j.apenergy.2016.09.043.

[108] N. Pous, S. Puig, M. Dolors Balaguer, J. Colprim, Cathode potential and anode electron donor evaluation for a suitable treatment of nitrate-contaminated groundwater in bioelectrochemical systems, Chem. Eng. J. 263 (2015) 151–159. https://doi.org/10.1016/j.cej.2014.11.002.

[109] O. Lefebvre, A. Al-Mamun, H.Y. Ng, A microbial fuel cell equipped with a biocathode for organic removal and denitrification, Water Sci. Technol. 58 (2008) 881–885. https://doi.org/10.2166/wst.2008.343.

[110] V.K. Nguyen, Y. Park, J. Yu, T. Lee, Bioelectrochemical denitrification on biocathode buried in simulated aquifer saturated with nitrate-contaminated groundwater, Environ. Sci. Pollut. Res. (2016) 15443–15451. https://doi.org/10.1007/s11356-016-6709-y.

[111] J. Sun, W. Xu, Y. Yuan, X. Lu, B. V Kjellerup, Z. Xu, H. Zhang, Y. Zhang, Bioelectrical power generation coupled with high-strength nitrogen removal using a photo-bioelectrochemical fuel cell under oxytetracycline stress, Electrochim. Acta. 299 (2019) 500–508. https://doi.org/10.1016/j.electacta.2019.01.036.

[112] S. Huang, Y. Lu, G. Zhu, Y. Kong, Effect of Organic Concentration in the Anode and Cathode on Bioelectricity Generation and Denitrification in a Single-Cathode Three-Anode Microbial Fuel Cell, J. Environ. Eng. 146 (2020) 1–8.

https://doi.org/10.1061/(ASCE)EE.1943-7870.0001769.

[113] P. Liang, L. Yuan, W. Wu, X. Yang, X. Huang, Enhanced performance of bio-cathode microbial fuel cells with the applying of transient-state operation modes, Bioresour. Technol. 147 (2013) 228–233. https://doi.org/10.1016/j.biortech.2013.08.007.

[114] Y.S. Oon, S.A. Ong, L.N. Ho, Y.S. Wong, Y.L. Oon, H.K. Lehl, W.E. Thung, Long-term operation of double chambered microbial fuel cell for bio-electro denitrification, Bioprocess Biosyst. Eng. 39 (2016) 893–900. https://doi.org/10.1007/s00449-016-1568-y.

[115] A. Al-Mamun, O. Lefebvre, M.S. Baawain, H.Y. Ng, A sandwiched denitrifying biocathode in a microbial fuel cell for electricity generation and waste minimization, Int. J. Environ. Sci. Technol. 13 (2016) 1055–1064. https://doi.org/10.1007/s13762-016-0943-1.

[116] Y. Mo, M. Du, S. Cui, H. Wang, X. Zhao, M. Zhang, Simultaneously enhancing degradation of refractory organics and achieving nitrogen removal by coupling denitrifying biocathode with MnO x / Ti anode, J. Hazard. Mater. 402 (2021) 123467. https://doi.org/10.1016/j.jhazmat.2020.123467.

[117] N. Pous, A.A. Carmona-Martínez, A. Vilajeliu-Pons, E. Fiset, L. Bañeras, E. Trably, M.D. Balaguer, J. Colprim, N. Bernet, S. Puig, Bidirectional microbial electron transfer: Switching an acetate oxidizing biofilm to nitrate reducing conditions, Biosens. Bioelectron. 75 (2016) 352–358. https://doi.org/10.1016/j.bios.2015.08.035.

[118] D. Cecconet, S. Bolognesi, A. Callegari, A.G. Capodaglio, Simulation tests of in situ groundwater denitrification with aquifer-buried biocathodes, Heliyon. 5 (2019) e02117. https://doi.org/10.1016/j.heliyon.2019.e02117.

[119] D. Cecconet, S. Bolognesi, A. Callegari, A.G. Capodaglio, Controlled sequential biocathodic denitri fi cation for contaminated groundwater bioremediation, Sci. Total Environ. 651 (2019) 3107–3116. https://doi.org/10.1016/j.scitotenv.2018.10.196.

[120] D. Liang, W. He, C. Li, Y. Yu, Z. Zhang, N. Ren, Y. Feng, Bidirectional electron transfer biofilm assisted complete bioelectrochemical denitrification process, Chem. Eng. J. 375 (2019) 121960. https://doi.org/10.1016/j.cej.2019.121960.

[121] N. Pous, C. Koch, A. Vilà-Rovira, M.D. Balaguer, J. Colprim, J. Muhlenberg, S. Muller, F. Harnisch, S. Puig, Monitoring and engineering reactor microbiomes of denitrifying bioelectrochemical systems †, RSC Adv. 5 (2015) 68326–68333. https://doi.org/10.1039/c5ra12113b.

[122] V.K. Nguyen, Y. Park, H. Yang, J. Yu, T. Lee, Effect of the cathode potential and sulfate ions on nitrate reduction in a microbial electrochemical denitrification system, J. Ind. Microbiol. Biotechnol. 43 (2016) 783–793. https://doi.org/10.1007/s10295-016-1762-6.

[123] K.P. Gregoire, S.M. Glaven, J. Hervey, B. Lin, L.M. Tender, Enrichment of a High-Current Density Denitrifying Microbial Biocathode, J. Electrochem. Soc. 161 (2014). https://doi.org/10.1149/2.0101413jes.

[124] S. Kondaveeti, B. Min, Nitrate reduction with biotic and abiotic cathodes at various cell voltages in bioelectrochemical denitrification system, Bioprocess Biosyst. Eng. (2013) 231–238. https://doi.org/10.1007/s00449-012-0779-0.

[125] A. Rezaee, M. Safari, H. Hossini, Bioelectrochemical denitrification using carbon felt / multiwall carbon nanotube, Environ. Technol. 36 (2015) 1057–1062. https://doi.org/10.1080/09593330.2014.974680.

[126] K.Y. Cheng, M.P. Ginige, A.H. Kaksonen, Ano-cathodophilic biofilm catalyzes both anodic carbon oxidation and cathodic denitrification, Environ. Sci. Technol. 46 (2012) 10372–10378. https://doi.org/10.1021/es3025066.

[127] R. Tang, D. Wu, W. Chen, C. Feng, C. Wei, Biocathode denitrification of coke wastewater effluent from an industrial aeration tank : Effect of long-term adaptation, Biochem. Eng. J. 125 (2017) 151–160. https://doi.org/10.1016/j.bej.2017.05.022.

[128] N. Pous, C. Koch, J. Colprim, S. Puig, F. Harnisch, Extracellular electron transfer of biocathodes : Revealing the potentials for nitrate and nitrite reduction of denitrifying microbiomes dominated by Thiobacillus sp ., Electrochem. Commun. 49 (2014) 93–97. https://doi.org/10.1016/j.elecom.2014.10.011.

[129] D. Cecconet, S. Bolognesi, A. Callegari, A.G. Capodaglio, Controlled sequential biocathodic denitrification for contaminated groundwater bioremediation, Sci. Total Environ. 651 (2018) 3107–3116. https://doi.org/10.1016/j.scitotenv.2018.10.196.

[130] S. Su, Y. Zhang, W. Hu, X. Zhang, D. Ju, C. Jia, J. Liu, Efficient and synergistic decolourization and nitrate removal using a single-chamber with a coupled biocathode-photoanode system, Bioelectrochemistry. 132 (2020) 107439. https://doi.org/10.1016/j.bioelechem.2019.107439.

[131] T. Philippon, J. Tian, C. Bureau, C. Chaumont, C. Midoux, Denitrifying bio-cathodes developed from constructed wetland sediments exhibit electroactive nitrate reducing biofilms dominated by the genera Azoarcus and Pontibacter, Bioelectrochemistry. 140 (2021). https://doi.org/10.1016/j.bioelechem.2021.107819.

[132] A. Ceballos-escalera, N. Pous, P. Chiluiza-ramos, B. Korth, F. Harnisch, L. Bañeras, M.D. Balaguer, S. Puig, Electro-bioremediation of nitrate and arsenite polluted groundwater, Water Res. 190 (2021) 116748. https://doi.org/10.1016/j.watres.2020.116748.

[133] V.K. Nguyen, Y. Park, J. Yu, T. Lee, Bioelectrochemical denitrification on biocathode buried in simulated aquifer saturated with nitrate-contaminated groundwater, Environ. Sci. Pollut. Res. (2016). https://doi.org/10.1007/s11356-016-6709-y.

[134] B. Virdis, K. Rabaey, Z. Yuan, R.A. Rozendal, J. Keller, Electron Fluxes in a Microbial Fuel Cells Performing Carbon and Nitrogen Removal, Environ. Sci. Technol. 43 (2009) 5144–5149.

[135] N. Pous, S. Puig, M. Dolors Balaguer, J. Colprim, Cathode potential and anode electron donor evaluation for a suitable treatment of nitrate-contaminated groundwater in bioelectrochemical systems, Chem. Eng. J. 263 (2015) 151–159. https://doi.org/10.1016/j.cej.2014.11.002.

[136] L. Yu, Y. Yuan, S. Chen, L. Zhuang, S. Zhou, Direct uptake of electrode electrons for autotrophic denitrification by Thiobacillus denitrificans, Electrochem. Commun. 60 (2015) 126–130. https://doi.org/10.1016/j.elecom.2015.08.025.

[137] V.K. Nguyen, S. Hong, Y. Park, K. Jo, T. Lee, Autotrophic denitrification performance and bacterial community at biocathodes of bioelectrochemical systems with either

abiotic or biotic anodes, J. Biosci. Bioeng. 119 (2015) 180–187. https://doi.org/10.1016/j.jbiosc.2014.06.016.

[138] Y.H. Jia, H.T. Tran, D.H. Kim, S.J. Oh, D.H. Park, R.H. Zhang, D.H. Ahn, Simultaneous organics removal and bio-electrochemical denitrification in microbial fuel cells, Bioprocess Biosyst. Eng. 31 (2008) 315–321. https://doi.org/10.1007/s00449-007-0164-6.

[139] J. Wei, P. Liang, X. Huang, Recent progress in electrodes for microbial fuel cells, Bioresour. Technol. 102 (2011) 9335–9344. https://doi.org/10.1016/j.biortech.2011.07.019.

[140] Y. Zhang, J. Sun, Y. Hu, S. Li, Q. Xu, Bio-cathode materials evaluation in microbial fuel cells : A comparison of graphite felt , carbon paper and stainless steel mesh materials, Int. J. Hydrogen Energy. 37 (2012) 16935–16942. https://doi.org/10.1016/j.ijhydene.2012.08.064.

[141] G. Zhu, T. Onodera, M. Tandukar, S.G. Pavlostathis, Simultaneous carbon removal, denitrification and power generation in a membrane-less microbial fuel cell, Bioresour. Technol. 146 (2013) 1–6. https://doi.org/10.1016/j.biortech.2013.07.032.

[142] Y. Wang, J. Hu, L. Wang, D. Shan, X. Wang, Y. Zhang, X. Mao, L. Xing, D. Wang, Acclimated sediment microbial fuel cells from a eutrophic lake for the in situ denitrification process, RSC Adv. 6 (2016) 80079–80085. https://doi.org/10.1039/C6RA16510A.

[143] A. Vijay, A. Khandelwal, M. Chhabra, T. Vincent, Microbial fuel cell for simultaneous removal of uranium (VI) and nitrate, Chem. Eng. J. 388 (2020) 124157. https://doi.org/10.1016/j.cej.2020.124157.

[144] J. Kim, B. Kim, H. Kim, Z. Yun, Effects of ammonium ions from the anolyte within bio-cathode microbial fuel cells on nitrate reduction and current density, Int. Biodeterior. Biodegradation. 95 (2014) 122–126. https://doi.org/10.1016/j.ibiod.2014.04.015.

[145] G. Huang, Y. Zhang, L. Qu, L. Zhang, Denitrification performance of ce-doped birnessite modified cathode in bioelectrochemical system, J. Electroanal. Chem. 871 (2020). https://doi.org/10.1016/j.jelechem.2020.114313.

[146] Y. Xiao, Y. Zheng, S. Wu, Z.H. Yang, F. Zhao, Bacterial Community Structure of Autotrophic Denitrification Biocathode by 454 Pyrosequencing of the 16S rRNA Gene, Microb. Ecol. 69 (2015) 492–499. https://doi.org/10.1007/s00248-014-0492-4.

[147] A. Cucu, A. Tiliakos, I. Tanase, C. Elena, I. Stamatin, A. Ciocanea, C. Nichita, Microbial Fuel Cell for Nitrate Reduction, Sustain. Solut. Energy Environ. 85 (2016) 156–161. https://doi.org/10.1016/j.egypro.2015.12.286.

[148] C. Jiang, Q. Yang, D. Wang, Y. Zhong, F. Chen, X. Li, G. Zeng, X. Li, M. Shang, Simultaneous perchlorate and nitrate removal coupled with electricity generation in autotrophic denitrifying biocathode microbial fuel cell, Chem. Eng. J. 308 (2017) 783–790. https://doi.org/10.1016/j.cej.2016.09.121.

[149] N. Samrat, K.R. K, B. Ruggeri, T. Tommasi, Denitrification of water in a microbial fuel cell (MFC) using seawater bacteria, J. Clean. Prod. 178 (2017) 449–456. https://doi.org/10.1016/j.jclepro.2017.12.221.

[150] N. Afsham, R. Roshandel, S. Yaghmaei, V. Vajihinejad, M. Sherafatmand, R. Roshandel, S. Yaghmaei, V. Vajihinejad, M. Sherafatmand, Bioelectricity Generation in a Soil Microbial Fuel Cell with Biocathode Denitrification, Energy Sources, Part A Recover. Util. Environ. Eff. 7036 (2015) 2092–2098. https://doi.org/10.1080/15567036.2012.671900.

[151] A. Vilar-Sanz, S. Puig, A. García-Lledó, R. Trias, M.D. Balaguer, J. Colprim, L. Bañeras, Denitrifying Bacterial Communities Affect Current Production and Nitrous Oxide Accumulation in a Microbial Fuel Cell, PLoS One. 8 (2013). https://doi.org/10.1371/journal.pone.0063460.

[152] F. Tetteh, J. Ding, Q. Zhao, P. Antwi, F. Koblah, Pollutant removal and bioelectricity generation from urban river sediment using a macrophyte cathode sediment microbial fuel cell (mSMFC), Bioelectrochemistry. 128 (2019) 241–251. https://doi.org/10.1016/j.bioelechem.2019.01.007.

[153] S. Kondaveeti, E. Kang, H. Liu, B. Min, Continuous autotrophic denitrification process for treating ammonium-rich leachate wastewater in bioelectrochemical denitrification system (BEDS), Bioelectrochemistry. 130 (2019) 107340. https://doi.org/10.1016/j.bioelechem.2019.107340.

[154] N. Pous, S. Puig, M. Coma, M.D. Balaguer, J. Colprim, Bioremediation of nitrate-polluted groundwater in a microbial fuel cell, J. Chem. Technol. Biotechnol. 88 (2013) 1690–1696. https://doi.org/10.1002/jctb.4020.

[155] S. Puig, M. Coma, J. Desloover, N. Boon, J. Colprim, M.D. Balaguer, Autotrophic denitrification in microbial fuel cells treating low ionic strength waters, Environ. Sci. Technol. 46 (2012) 2309–2315. https://doi.org/10.1021/es2030609.

[156] W. Chen, D. Wu, H. Wan, R. Tang, C. Li, G. Wang, C. Feng, Carbon-based cathode as an electron donor driving direct bioelectrochemical denitrification in biofilm-electrode reactors: Role of oxygen functional groups, Carbon N. Y. 118 (2017) 310–318. https://doi.org/10.1016/j.carbon.2017.03.062.

[157] Y. Sun, J. Wei, P. Liang, X. Huang, Microbial community analysis in biocathode microbial fuel cells packed with different materials, AMB Express. 2 (2012) 21. https://doi.org/10.1186/2191-0855-2-21.

[158] S. Puig, M.D. Balaguer, J. Colprim, Long-term assessment of six-stacked scaled-up MFCs treating swine manure with different electrode materials, Environ. Sci. Water Res. Technol. 3 (2017) 947–959. https://doi.org/10.1039/c7ew00079k.

[159] B. Erable, N. Byrne, L. Etcheverry, W. Achouak, A. Bergel, Single medium microbial fuel cell: Stainless steel and graphite electrode materials select bacterial communities resulting in opposite electrocatalytic activities, Int. J. Hydrogen Energy. 42 (2017) 26059–26067. https://doi.org/10.1016/j.ijhydene.2017.08.178.

[160] H. Cheng, X. Tian, C. Li, S. Wang, S. Su, H. Wang, B. Zhang, A. Wang, Microbial Photoelectrotrophic Denitrification as a Sustainable and Efficient Way for Reducing Nitrate to Nitrogen, Environ. Sci. Technol. (2017) 12948–12955. https://doi.org/10.1021/acs.est.7b02557.

[161] Y. Yi, T. Zhao, B. Xie, Y. Zang, H. Liu, Dual detection of biochemical oxygen demand and nitrate in water based on bidirectional Shewanella loihica electron transfer, Bioresour. Technol. 309 (2020) 123402.

https://doi.org/10.1016/j.biortech.2020.123402.

[162] W. Zhi, Z. Ge, Z. He, H. Zhang, Methods for understanding microbial community structures and functions in microbial fuel cells : A review, Bioresour. Technol. 171 (2014) 461–468. https://doi.org/10.1016/j.biortech.2014.08.096.

[163] S. Wang, J. Zhao, S. Liu, Effect of Temperature on Nitrogen Removal and Electricity Generation of a Dual-Chamber Microbial Fuel Cell, (2018). https://doi.org/10.1007/s11270-018-3840-z.

[164] C. Zhu, H. Wang, Q. Yan, R. He, G. Zhang, Enhanced denitrification at biocathode facilitated with biohydrogen production in a three-chambered bioelectrochemical system (BES) reactor, Chem. Eng. J. 312 (2017) 360–366. https://doi.org/10.1016/j.cej.2016.11.152.

[165] Y. Cong, Q. Xu, H. Feng, D. Shen, Efficient electrochemically active biofilm denitrification and bacteria consortium analysis, Bioresour. Technol. 132 (2013) 24–27. https://doi.org/10.1016/j.biortech.2013.01.004.

[166] G. Chen, S. Choi, T. Lee, G. Lee, J. Cha, C. Kim, Application of biocathode in microbial fuel cells : cell performance and microbial community, Biotechnol. Prod. Process Eng. (2008) 379–388. https://doi.org/10.1007/s00253-008-1451-0.

[167] S. Philips, H.J. Laanbroek, W. Verstraete, Origin , causes and effects of increased nitrite concentrations in aquatic environments, Re/Views Environ. Sci. Bio/Technology. (2002) 115–141.

[168] H. Kroupova, J. Machova, Z. Svobodova, Nitrite influence on fish : a review, Vet. Med. - Czech. 2005 (2005) 461–471.

[169] M.J. Kampschreur, H. Temmink, R. Kleerebezem, M.S.M. Jetten, M.C.M. Van Loosdrecht, Nitrous oxide emission during wastewater treatment, Water Res. 43 (2009) 4093–4103. https://doi.org/10.1016/j.watres.2009.03.001.

[170] T. Van Doan, T. Kwon, S. Kumar, J.M. Tiedje, J. Park, Increased nitrous oxide accumulation by bioelectrochemical denitrification under autotrophic conditions : Kinetics and expression of denitrification pathway genes, Water Res. 47 (2013) 7087–7097. https://doi.org/10.1016/j.watres.2013.08.041.

[171] V. Srinivasan, J. Weinrich, C. Butler, Nitrite accumulation in a denitrifying biocathode microbial fuel cell, Environ. Sci. Water Res. Technol. 2 (2016) 344–352. https://doi.org/10.1039/c5ew00260e.

[172] E. Blanchet, S. Pécastaings, B. Erable, C. Roques, A. Bergel, Protons accumulation during anodic phase turned to advantage for oxygen reduction during cathodic phase in reversible bioelectrodes, Bioresour. Technol. 173 (2014) 224–230. https://doi.org/10.1016/j.biortech.2014.09.076.

[173] H. Yun, B. Liang, D. Kong, A. Wang, Improving biocathode community multifunctionality by polarity inversion for simultaneous bioelectroreduction processes in domestic wastewater, Chemosphere. 194 (2018) 553–561. https://doi.org/10.1016/j.chemosphere.2017.12.030.

[174] Z. Lin, S. Cheng, Z. Yu, J. Yang, H. Huang, Y. Sun, Enhancing bio-cathodic nitrate removal through anode-cathode polarity inversion together with regulating the anode electroactivity, Sci. Total Environ. 764 (2021) 142809.

https://doi.org/10.1016/j.scitotenv.2020.142809.

[175] S. Xie, P. Liang, Y. Chen, X. Xia, X. Huang, Simultaneous carbon and nitrogen removal using an oxic/anoxic-biocathode microbial fuel cells coupled system, Bioresour. Technol. 102 (2011) 348–354. https://doi.org/10.1016/j.biortech.2010.07.046.

[176] F. Zhang, Z. He, Integrated organic and nitrogen removal with electricity generation in a tubular dual-cathode microbial fuel cell, Process Biochem. 47 (2012) 2146–2151. https://doi.org/10.1016/j.procbio.2012.08.002.

[177] L. Xu, Y. Zhao, X. Wang, W. Yu, Applying multiple bio-cathodes in constructed wetland-microbial fuel cell for promoting energy production and bioelectrical derived nitrification-denitrification process, Chem. Eng. J. 344 (2018) 105–113. https://doi.org/10.1016/j.cej.2018.03.065.

[178] Y. Qiu, Y. Yu, H. Li, Z. Yan, Z. Li, G. Liu, Z. Zhang, Enhancing carbon and nitrogen removals by a novel tubular bio- electrochemical system with functional biocathode coupling with oxygen- producing submerged plants, Chem. Eng. J. 402 (2020) 125400. https://doi.org/10.1016/j.cej.2020.125400.

[179] M.I. San-martín, R. Mateos, B. Carracedo, A. Escapa, A. Morán, Pilot-scale bioelectrochemical system for simultaneous nitrogen and carbon removal in urban wastewater treatment plants, J. Biosci. Bioeng. 126 (2018) 758–763. https://doi.org/10.1016/j.jbiosc.2018.06.008.

[180] P. Liang, J. Wei, M. Li, X. Huang, Scaling up a novel denitrifying microbial fuel cell with an oxic-anoxic two stage biocathode, Front. Environ. Sci. Eng. 7 (2013) 913–919. https://doi.org/10.1007/s11783-013-0583-3.

[181] Y. Li, I. Williams, Z. Xu, B. Li, B. Li, Energy-positive nitrogen removal using the integrated short-cut nitrification and autotrophic denitrification microbial fuel cells (MFCs), Appl. Energy. 163 (2016) 352–360. https://doi.org/10.1016/j.apenergy.2015.11.021.

[182] M.S.M.J. Y, M. Strous, K.T. Van De Pas-schoonen, J. Schalk, U.G.J.M. Van Dongen, A.A. Van De Graaf, S. Logemann, G.M.I. Y, M.C.M. Van Loosdrecht, J.G. Kuenen, The anaerobic oxidation of ammonium, FEMS Microbiol. Rev. 22 (1999) 421–437.

[183] C. Li, H. Ren, M. Xu, J. Cao, Study on anaerobic ammonium oxidation process coupled with denitrification microbial fuel cells (MFCs) and its microbial community analysis, Bioresour. Technol. 175 (2015) 545–552. https://doi.org/10.1016/j.biortech.2014.10.156.

[184] S. Qiao, X. Yin, J. Zhou, L. Wei, J. Zhong, Integrating anammox with the autotrophic denitrification process via electrochemistry technology, Chemosphere. 195 (2018) 817–824. https://doi.org/10.1016/j.chemosphere.2017.12.058.

[185] S. Susarla, T.W. Collette, S.C. Mccutcheon, Perchlorate Identification in Fertilizers, 33 (1999) 3469–3472.

[186] COMMISSION RECOMMENDATION (EU) 2015/682 of 29 April 2015 on the monitoring of the presence of perchlorate in food, 12 (2015) 2014–2015. https://doi.org/10.2903/j.efsa.2014.3869.

[187] C. Shea, P. Clauwaert, W. Verstraete, R. Nerenberg, Adapting a denitrifying

biocathode for perchlorate reduction, Water Sci. Technol. 58 (2008) 1941–1946. https://doi.org/10.2166/wst.2008.551.

[188] D. Xie, H. Yu, C. Li, Y. Ren, C. Wei, C. Feng, Competitive microbial reduction of perchlorate and nitrate with a cathode directly serving as the electron donor, Electrochim. Acta. 133 (2014) 217–223. https://doi.org/10.1016/j.electacta.2014.04.016.

[189] J. Lian, X. Tian, Z. Li, J. Guo, Y. Guo, The effects of different electron donors and electron acceptors on perchlorate reduction and bioelectricity generation in a microbial fuel cell, Int. J. Hydrogen Energy. 42 (2016) 544–552. https://doi.org/10.1016/j.ijhydene.2016.11.027.

[190] C. Wang, J. Dong, W. Hu, Y. Li, Enhanced simultaneous removal of nitrate and perchlorate from groundwater by bioelectrochemical systems (BESs) with cathodic potential regulation, Biochem. Eng. J. 173 (2021) 108068. https://doi.org/10.1016/j.bej.2021.108068.

[191] Q. Mahmood, P. Zheng, J. Cai, Y. Hayat, Sources of sulfide in waste streams and current biotechnologies for its removal, (2007). https://doi.org/10.1631/jzus.2007.A1126.

[192] T. Ai, H. Zhan, L. Zou, J. Fu, Q. Fu, Q. He, H. Ai, Potential applications of endogenous sulfide for enhanced denitrification of low C / N domestic wastewater in anodic mixotrophic denitrification microbial fuel cell : The mechanism of electrons transfer and microbial community, Sci. Total Environ. 722 (2020) 137830. https://doi.org/10.1016/j.scitotenv.2020.137830.

[193] K. Rabaey, K. Van de Sompel, L. Maignien, N. Boon, P. Aelterman, P. Clauwaert, Microbial Fuel Cells for Sulfide, 40 (2006) 5218–5224.

[194] J. Cai, P. Zheng, Simultaneous anaerobic sulfide and nitrate removal in microbial fuel cell, Bioresour. Technol. 128 (2013) 760–764. https://doi.org/10.1016/j.biortech.2012.08.046.

[195] L. Zhong, S. Zhang, Y. Wei, R. Bao, Power recovery coupled with sulfide and nitrate removal in separate chambers using a microbial fuel cell, Biochem. Eng. J. 124 (2017) 6–12. https://doi.org/10.1016/j.bej.2017.04.005.

[196] J. Cai, M. Qaisar, Y. Sun, K. Wang, J. Lou, R. Wang, Coupled substrate removal and electricity generation in microbial fuel cells simultaneously treating sulfide and nitrate at various influent sulfide to nitrate ratios, Bioresour. Technol. 306 (2020) 123174. https://doi.org/10.1016/j.biortech.2020.123174.

[197] X. Ge, X. Cao, X. Song, Y. Wang, Z. Si, Y. Zhao, W. Wang, Bioenergy generation and simultaneous nitrate and phosphorus removal in a pyrite-based constructed wetland-microbial fuel cell, Bioresour. Technol. 296 (2020) 122350. https://doi.org/10.1016/j.biortech.2019.122350.

[198] J. Tournebize, C. Gramaglia, F. Birmant, S. Bouarfa, C. Chaumont, B. Vincent, Co-design of constructed wetlands to mitigate pesticide pollution in a drained catch-Basin: A solution to improve groundwater quality, Irrig. Drain. 61 (2012) 75–86. https://doi.org/10.1002/ird.1655.

[199] J.D. Lebrun, S. Ayrault, A. Drouet, L. Bordier, L.C. Fechner, Ecodynamics and

bioavailability of metal contaminants in a constructed wetland within an agricultural drained catchment, Ecol. Eng. 136 (2019) 108–117. https://doi.org/10.1016/j.ecoleng.2019.06.012.

[200] C. Gaullier, S. Dousset, N. Baran, G. Kitzinger, C. Coureau, Influence of hydrodynamics on the water pathway and spatial distribution of pesticide and metabolite concentrations in constructed wetlands, J. Environ. Manage. 270 (2020). https://doi.org/10.1016/j.jenvman.2020.110690.

[201] F. Escudié, L. Auer, M. Bernard, M. Mariadassou, L. Cauquil, K. Vidal, S. Maman, G. Hernandez-Raquet, S. Combes, G. Pascal, FROGS: Find, Rapidly, OTUs with Galaxy Solution, Bioinformatics. 34 (2018) 1287–1294. https://doi.org/10.1093/bioinformatics/btx791.

[202] L. Foglar, High nitrate removal from synthetic wastewater with the mixed bacterial culture, Bioresour. Technol. 96 (2005) 879–888. https://doi.org/10.1016/j.biortech.2004.09.001.

[203] G.Z.J. Winter, Removal of organic pollutants and of nitrate from wastewater from the dairy industry by denitrification, Appl. Microbiol. Biotechnol. 49 (1998) 469–474.

[204] T. Kuba, M.C.M. Van Loosdrecht, J.J. Heijnen, Phosphorus and nitrogen removal with minimal COD requirement by intergration of denitrifying dephosphatation and nitrification in a two-sludge system, Water Res. 1354 (1996) 1702–1710.

[205] G. Carvalho, P.C. Lemos, A. Oehmen, M.A.M. Reis, Denitrifying phosphorus removal : Linking the process performance with the microbial community structure, Water Res. 41 (2007) 4383–4396. https://doi.org/10.1016/j.watres.2007.06.065.

[206] W. Zeng, L. Li, Y. Yang, X. Wang, Y. Peng, Denitrifying phosphorus removal and impact of nitrite accumulation on phosphorus removal in a continuous anaerobic – anoxic – aerobic (A 2 O) process treating domestic wastewater, Enzyme Microb. Technol. 48 (2011) 134–142. https://doi.org/10.1016/j.enzmictec.2010.10.010.

[207] N. Fonder, T. Headley, The taxonomy of treatment wetlands : A proposed classification and nomenclature system, Ecol. Eng. 51 (2013) 203–211. https://doi.org/10.1016/j.ecoleng.2012.12.011.

[208] M. Kalcic, I. Chaubey, J. Frankenberger, A Geospatial Approach to Targeting Constructed Wetlands for Nitrate Removal in Agricultural Watersheds, Appl. Eng. Agric. 28 (2013) 347–357. https://doi.org/10.13031/2013.41497.

[209] J. Tournebize, C. Chaumont, Ü. Mander, Implications for constructed wetlands to mitigate nitrate and pesticide pollution in agricultural drained watersheds, Ecol. Eng. 103 (2017) 415–425. https://doi.org/10.1016/j.ecoleng.2016.02.014.

[210] C. Christian, D. Zak, B. Kronvang, C. Kjaergaard, M. Vodder, J. Audet, An overview of nutrient transport mitigation measures for improvement of water quality in Denmark, Ecol. Eng. 155 (2020) 105863. https://doi.org/10.1016/j.ecoleng.2020.105863.

[211] C.C. Tanner, R.H. Kadlec, Influence of hydrological regime on wetland attenuation of diffuse agricultural nitrate losses, Ecol. Eng. 56 (2013) 79–88. https://doi.org/10.1016/j.ecoleng.2012.08.043.

[212] J. Koskiaho, M. Puustinen, Suspended solids and nutrient retention in two constructed

wetlands as determined from continuous data recorded with sensors, Ecol. Eng. 137 (2019) 65–75. https://doi.org/10.1016/j.ecoleng.2019.04.006.

[213] R.H. Kadlec, Comparison of free water and horizontal subsurface treatment wetlands, Ecol. Eng. 5 (2008) 159–174. https://doi.org/10.1016/j.ecoleng.2008.04.008.

[214] Y. Lin, S. Jing, D. Lee, Y. Chang, Nitrate removal from groundwater using constructed wetlands under various hydraulic loading rates, Bioresour. Technol. 99 (2008) 7504–7513. https://doi.org/10.1016/j.biortech.2008.02.017.

[215] M.E. Karpuzcu, W.T. Stringfellow, Kinetics of nitrate removal in wetlands receiving agricultural drainage, Ecol. Eng. 42 (2012) 295–303. https://doi.org/10.1016/j.ecoleng.2012.02.015.

[216] USEPA Regulated Drinking Water Contaminants: Inorganic Chemicals., (n.d.). https://www.epa.gov/ground-water-and-drinking-water/table-regulateddrinking-water-contaminants., (n.d.).

[217] Ü. Mander, J. Tournebize, M. Espenberg, C. Chaumont, R. Torga, J. Garnier, M. Muhel, M. Maddison, J.D. Lebrun, E. Uher, K. Remm, J. Pärn, K. Soosaar, High denitrification potential but low nitrous oxide emission in a constructed wetland treating nitrate-polluted agricultural run-off, Sci. Total Environ. 779 (2021).

[218] P. Taylor, R.H. Kadlec, Constructed Marshes for Nitrate Removal, Crit. Rev. Environ. Sci. Technol. 42 (2012) 934–1005. https://doi.org/10.1080/10643389.2010.534711.

[219] P. Xu, E.R. Xiao, D. Xu, Y. Zhou, F. He, B.Y. Liu, L. Zeng, Z. Bin Wu, Internal nitrogen removal from sediments by the hybrid system of microbial fuel cells and submerged aquatic plants, PLoS One. 12 (2017) 1–20. https://doi.org/10.1371/journal.pone.0172757.

[220] A.D. McNaught, A. Wilkinson, IUPAC. Compendium of Chemical Terminology, 2nd ed. (the “Gold Book”), 2014. https://doi.org/10.1351/goldbook.M03944.

[221] Y. Wang, J. Hu, L. Wang, D. Shan, X. Wang, Y. Zhang, X. Mao, L. Xing, D. Wang, Acclimated sediment microbial fuel cells from a eutrophic lake for the in situ denitrification process, RSC Adv. 6 (2016) 80079–80085. https://doi.org/10.1039/c6ra16510a.

[222] V. Scotto, R. Di Cintio, G. Marcenaro, The Infuence of Marine Aerobic Microbial Film on Stainless Steel Corrosion Behaviour, Corros. Sci. 25 (1985) 185–194.

[223] D. Thierry, N. Larche, C. Leballeur, S.L. Wijesinghe, T. Zixi, Corrosion potential and cathodic reduction efficiency of stainless steel in natural seawater, Mater. Corros. (2015) 453–458. https://doi.org/10.1002/maco.201307497.

[224] L. Soussan, B. Erable, M. Delia, A. Bergel, The open circuit potential of Geobacter sulfurreducens bioanodes depends on the electrochemical adaptation of the strain, Electrochem. Commun. 33 (2013) 35–38. https://doi.org/10.1016/j.elecom.2013.04.013.

[225] B.E. Logan, J.M. Regan, Electricity-producing bacterial communities in microbial fuel cells, Trends Microbiol. 14 (2006) 512–518. https://doi.org/10.1016/j.tim.2006.10.003.

[226] D.A. Finkelstein, L.M. Tender, J.G. Zeikus, Effect of Electrode Potential on Electrode-Reducing Microbiota, Environ. Sci. Technol. 40 (2006) 6990–6995.

https://doi.org/10.1021/es061146m.

[227] J. Chi, S. Zhang, X. Lu, L. Dong, S. Yao, Chemical reduction of nitrate by metallic iron, J. Water Supply Res. Technol. (2018) 37–41.

[228] M. Rimboud, A. Bergel, B. Erable, Multiple electron transfer systems in oxygen reducing biocathodes revealed by different conditions of aeration/agitation, Bioelectrochemistry. 110 (2016) 46–51. https://doi.org/10.1016/j.bioelechem.2016.03.002.

[229] D.R. Bond, D.R. Lovley, Electricity Production by Geobacter sulfurreducens Attached to Electrodes, Appl. Environ. Microbiol. 69 (2003) 1548–1555. https://doi.org/10.1128/AEM.69.3.1548.

[230] D.R. Bond, D.E. Holmes, L.M. Tender, D.R. Lovley, Electrode-reducing microorganisms that harvest energy from marine sediments, Science (80-.). 295 (2002) 483–485. https://doi.org/10.1126/science.1066771.

[231] S. Debuy, S. Pecastaings, A. Bergel, B. Erable, Oxygen-reducing biocathodes designed with pure cultures ofmicrobial strains isolated from seawater biofilms, Int. Biodeterior. Biodegrad. 103 (2015) 16–22. https://doi.org/10.1016/j.ibiod.2015.03.028.

[232] M. Rothballer, M. Picot, T. Sieper, J.B.A. Arends, M. Schmid, A. Hartmann, N. Boon, C.J.N. Buisman, F. Barrière, D.P.B.T.B. Strik, Monophyletic group of unclassified γ-Proteobacteria dominates in mixed culture biofilm of high-performing oxygen reducing biocathode, Bioelectrochemistry. 106 (2015) 167–176. https://doi.org/10.1016/j.bioelechem.2015.04.004.

[233] K. Rabaey, S.T. Read, P. Clauwaert, S. Freguia, P.L. Bond, L.L. Blackall, J. Keller, Cathodic oxygen reduction catalyzed by bacteria in microbial fuel cells, ISME J. 2 (2008) 519–527. https://doi.org/10.1038/ismej.2008.1.

[234] J. Tournebize, C. Chaumont, C. Fesneau, A. Guenne, B. Vincent, J. Garnier, Ü. Mander, Long-term nitrate removal in a buffering pond-reservoir system receiving water from an agricultural drained catchment, Ecol. Eng. 80 (2015) 32–45. https://doi.org/10.1016/j.ecoleng.2014.11.051.

[235] P.A.G. Hofman, S.A. De Jong, E.J. Wagenvoort, A.J.J. Sandee, Apparent sediment diffusion coefficients for oxygen and oxygen consumption rates measured with microelectrodes and bell jars : applications to oxygen budgets in estuarine intertidal sediments, Mar. Ecol. Prog. Ser. 69 (1991) 261–272.

[236] L.P. Nielsen, N. Risgaard-petersen, H. Fossing, P.B. Christensen, M. Sayama, Electric currents couple spatially separated biogeochemical processes in marine sediment, Nature. 463 (2010) 1071–1074. https://doi.org/10.1038/nature08790.

[237] P. Ibanhez, C. Leote, C. Rocha, Porewater nitrate profiles in sandy sediments hosting submarine groundwater discharge described by an advection – dispersion-reaction model, Biogeochemistry. 103 (2011) 159–180. https://doi.org/10.1007/s10533-010-9454-1.

[238] H.H.P. Fang, M. Zhang, T. Zhang, J. Chen, Predictions of nitrate diffusion in sediment using horizontal attenuated total reflection (HATR) by Fourier transform infrared (FTIR) spectrometry, Water Res. 42 (2008) 903–908. https://doi.org/10.1016/j.watres.2007.08.038.

[239] R. Munoz, R. Rosselló-móra, R. Amann, Revised phylogeny of Bacteroidetes and proposal of sixteen new taxa and two new combinations including Rhodothermaeota phyl . nov ., Syst. Appl. Microbiol. 39 (2016) 281–296. https://doi.org/10.1016/j.syapm.2016.04.004.

[240] N.R. Krieg, J.T. Staley, D. Brown, B.P. Hedlund, B.J. Paster, N. Ward, W. Ludwig, W.B. Whitman, Bergey's Manual of Systematic Bacteriology, Volume 4, Second, Springer-Verlag, New York, NY, 2010.

[241] A. Zverev, A. Petrov, A. Kimeklis, A. Kichko, E. Andronov, A. Petrov, E. Abakumov, Microbiomes of the initial soils of mining areas of Yakutsk City (Eastern Siberia , Russia), 10 (2020) 69–82. https://doi.org/10.5817/CPR2020-1-7.

[242] S. Hyun, M. Myung, K. Kim, J. Hwee, J. Hana, Flavisolibacter galbus sp . nov ., isolated from soil in Jeju Island, Antonie Van Leeuwenhoek. 112 (2019) 1559–1565. https://doi.org/10.1007/s10482-019-01282-8.

[243] A.E. Murphy, R. Kolkmeyer, B. Song, I. Anderson, J. Bowen, Bioreactivity and Microbiome of Biodeposits from Filter-Feeding Bivalves, Microb. Ecol. 77 (2019) 343–357.

[244] P. Dabert, B. Sialve, Characterisation of the microbial 16S rDNA diversity of an aerobic phosphorus-removal ecosystem and monitoring of its transition to nitrate respiration, (2001) 500–509. https://doi.org/10.1007/s002530000529.

[245] Q. Kong, J. Zhang, M. Miao, L. Tian, N. Guo, S. Liang, Partial nitrification and nitrous oxide emission in an intermittently aerated sequencing batch biofilm reactor, Chem. Eng. J. 217 (2013) 435–441. https://doi.org/10.1016/j.cej.2012.10.093.

[246] T. Yamada, Y. Sekiguchi, S. Hanada, H. Imachi, A. Ohashi, H. Harada, Y. Kamagata, Anaerolinea thermolimosa sp . nov ., Levilinea saccharolytica gen . nov ., sp . nov . and Leptolinea tardivitalis gen . nov ., sp . nov ., novel filamentous anaerobes , and description of the new classes Anaerolineae classis nov . and Caldilineae classis nov . in the bacterial phylum Chloroflexi, (2006) 1331–1340. https://doi.org/10.1099/ijs.0.64169-0.

[247] L. De Almeida, A. Duarte, C. Dutra, R. Davenport, D. Werner, C. Rossas, M. Filho, T. Bressani-ribeiro, C. Augusto, D.L. Chernicharo, J. Calabria, D. Araújo, Effect of temperature on microbial diversity and nitrogen removal performance of an anammox reactor treating anaerobically pretreated municipal wastewater, Bioresour. Technol. 258 (2018) 208–219. https://doi.org/10.1016/j.biortech.2018.02.083.

[248] A.D. Pereira, A. Cabezas, C. Etchebehere, C. Augusto, D.L. Chernicharo, J.C. De Araújo, C.A. De, Microbial communities in anammox reactors : a review, 2515 (2017). https://doi.org/10.1080/21622515.2017.1304457.

[249] L. Falcon, S. Magallo, A. Castillo, Dating the cyanobacterial ancestor of the chloroplast, ISME J. 4 (2010) 777–783. https://doi.org/10.1038/ismej.2010.2.

[250] S.J. Mcilroy, M. Albertsen, E.K. Andresen, A.M. Saunders, ' Candidatus Competibacter ' -lineage genomes retrieved from metagenomes reveal functional metabolic diversity, ISME J. (2014) 613–624. https://doi.org/10.1038/ismej.2013.162.

[251] L. Morin, A. Goubet, C. Madigou, J.J. Pernelle, K. Palmier, K. Labadie, A. Lemainque, O. Michot, L. Astoul, P. Barbier, J.L. Almayrac, A. Sghir, Colonization kinetics and

implantation follow - up of the sewage microbiome in an urban wastewater treatment plant, Sci. Rep. 10 (2020). https://doi.org/10.1038/s41598-020-68496-z.

[252] D.J. Brenner, N.R. Krieg, J.T. Staley, G.M. Garrity, Bergey's Manual of Systematic Bacteriology, Volume 2, Part B, Williams & Wilkins, Baltimore., New York, NY, 2005.

[253] A.J. Rissanen, T. Saarela, J. Helena, M. Buck, S. Peura, S.L. Aalto, A. Ojala, J. Pumpanen, M. Tiirola, M. Elvert, H. Nyk, Vertical stratification patterns of methanotrophs and their genetic controllers in water columns of oxygen-stratified boreal lakes, (2021) 1–16. https://doi.org/10.1093/femsec/fiaa252.

[254] S. Van Grinsven, J.S.S. Damsté, A.A. Asbun, J.C. Engelmann, J. Harrison, L. Villanueva, Methane oxidation in anoxic lake water stimulated by nitrate and sulfate addition, Environ. Microbiol. 22 (2020) 766–782. https://doi.org/10.1111/1462-2920.14886.

[255] E. Rosenberg, E.F. Delong, S. Lory, E. Stackebrandt, F. Thompson, The Prokaryotes. Gammaproteobacteria, Springer-Verlag, Berlin Heidelberg, 2014.

[256] M. Sayama, N. Risgaard-petersen, L.P. Nielsen, H. Fossing, P.B. Christensen, Impact of Bacterial NO3- Transport on Sediment Biogeochemistry, Appl. Environ. Microbiol. 71 (2005) 7575–7577. https://doi.org/10.1128/AEM.71.11.7575.

[257] M. Mußmann, H.N. Schulz, B. Strotmann, T. Kjær, L.P. Nielsen, R.A. Rosselló-mora, R.I. Amann, B.B. Jørgensen, Phylogeny and distribution of nitrate-storing Beggiatoa spp . in coastal marine sediments, Environ. Microbiol. 5 (2003) 523–533.

[258] M. Ridge, R.M. Jones, T.D. Angelo, B.N. Orcutt, Using Cathodic Poised Potential Experiments to Investigate Extracellular Electron Transport in the Crustal Deep Biosphere of North, 8 (2020) 1–18. https://doi.org/10.3389/fenvs.2020.00011.

[259] K. Chon, Y. Kim, N. Ik, J. Cho, Evaluating wastewater stabilizing constructed wetland , through diversity and abundance of the nitrite reductase gene nirS , with regard to nitrogen control, Desalination. 264 (2010) 201–205. https://doi.org/10.1016/j.desal.2010.05.010.

[260] Y. Zhang, L. Wang, W. Han, X. Wang, Z. Guo, F. Peng, F. Yang, M. Kong, Y. Gao, J. Chao, D. Wu, B. Xu, Y. Zhu, Nitrate removal, spatiotemporal communities of denitrifiers and the importance of their genetic potential for denitrification in novel denitrifying bioreactors, Bioresour. Technol. 241 (2017) 552–562. https://doi.org/10.1016/j.biortech.2017.05.205.

[261] W. Feng, J. Liu, J. Gu, B. Mu, Nitrate-reducing community in production water of three oil reservoirs and their responses to different carbon sources revealed by nitrate-reductase encoding gene (napA), Int. Biodeterior. Biodegradation. 65 (2011) 1081–1086. https://doi.org/10.1016/j.ibiod.2011.05.009.

[262] D.J. Brenner, N.R. Krieg, J.T. Staley, G.M. Garrity, Bergey's Manual of Systematic Bacteriology, Volume 2, Part C, 2nd ed., Springer-Verlag, New York, NY, 2005.

[263] A. Vilar-sanz, N. Pous, S. Puig, M.D. Balaguer, J. Colprim, L. Bañeras, Denitrifying nirK -containing alphaproteobacteria exhibit different electrode driven nitrite reduction capacities, Bioelectrochemistry. 121 (2018) 74–83. https://doi.org/10.1016/j.bioelechem.2018.01.007.

[264] F.I. Id, A. Zuliani, M. Fallah, M. Mashkour, M. Rahimnejad, R. Luque, Novel Applications of Microbial Fuel Cells in Sensors and Biosensors, Appl. Sci. 8 (2018). https://doi.org/10.3390/app8071184.

[265] D. Wang, P. Liang, Y. Jiang, P. Liu, B. Miao, W. Hao, X. Huang, Open external circuit for microbial fuel cell sensor to monitor the nitrate in aquatic environment, Biosens. Bioelectron. 111 (2018) 97–101. https://doi.org/10.1016/j.bios.2018.04.018.

[266] S. Su, H. Cheng, T. Zhu, H. Wang, A. Wang, A novel bioelectrochemical method for real-time nitrate monitoring, Bioelectrochemistry. 125 (2019) 33–37. https://doi.org/10.1016/j.bioelechem.2018.09.002.

[267] Y. Yu, X. Ding, W. Quan, Q. Niu, Z. Fang, Dynamically controlling the electrode potential of a microbial fuel cell-powered biocathode for sensitive quantification of nitrate, Electrochim. Acta. 369 (2021) 137661. https://doi.org/10.1016/j.electacta.2020.137661.

[268] O. Lefebvre, A. Al-Mamun, H.Y. Ng, A microbial fuel cell equipped with a biocathode for organic removal and denitrification, Water Sci. Technol. 58 (2008) 881–885. https://doi.org/10.2166/wst.2008.343.

[269] Y. Wang, J. Hu, L. Wang, D. Shan, X. Wang, Y. Zhang, X. Mao, L. Xing, D. Wang, Acclimated sediment microbial fuel cells from a eutrophic lake for the in situ denitrification process, RSC Adv. 6 (2016) 80079–80085. https://doi.org/10.1039/C6RA16510A.

[270] P. Xu, E. Xiao, J. Wu, F. He, Y. Zhang, Z. Wu, Enhanced nitrate reduction in water by a combined bio-electrochemical system of microbial fuel cells and submerged aquatic plant Ceratophyllum demersum, J. Environ. Sci. 78 (2018) 338–351. https://doi.org/10.1016/j.jes.2018.11.013.

[271] M.V.V. Naga Samrat, K. Kesava Rao, B. Ruggeri, T. Tommasi, Denitrification of water in a microbial fuel cell (MFC) using seawater bacteria, J. Clean. Prod. 178 (2018) 449–456. https://doi.org/10.1016/j.jclepro.2017.12.221.

[272] Y. Mo, M. Du, S. Cui, H. Wang, X. Zhao, M. Zhang, Simultaneously enhancing degradation of refractory organics and achieving nitrogen removal by coupling denitrifying biocathode with MnO x / Ti anode, J. Hazard. Mater. 402 (2021) 123467. https://doi.org/10.1016/j.jhazmat.2020.123467.

[273] S. Perazzoli, J.P. de Santana Neto, H. Soares, Anoxic-biocathode microbial desalination cell as a new approach for wastewater remediation and clean water production, Water Sci. Technol. 81 (2020) 550–563. https://doi.org/10.2166/wst.2020.134.

Appendix 1. Nitrate-reducing biocathodes in the literature: conditions and results.

NI - no information

Table 1: experiments in batch

Type of BES	Cathodic medium	Cathode material	Bacteria source	Atmosphere	Applied cathode potential	Resistance	Starting nitrate concentration	Nitrate reduction rate	Energy production	Ref
MFC	Buffer synthetic wastewater	graphite–Fe(III) electrode	Anaerobic digester sludge	N_2	/	10 or 1000 Ω	65 mg N-NO_3^- L^{-1}	0.084 mg NO_3^-–N cm^{-2} (electrode surface area) day^{-1}	Max 1.7 mW m^{-2}	[138] (2008)
MFC	Buffer synthetic wastewater	non wet-proof carbon paper	A mixed culture of denitrifying bacteria	Anaerobic	/	1000Ω	117 - 134 mg N-NO_3^- L^{-1} 2g/l $NaHCO_3$	2.3 - 4%	9.4mWm^{-2} of anode surface 0.19Wm^{-3} of TAC	[268] (2008)
SMFC	Synthetic lake water	Carbon paper	Sediment	He	/	470 Ω	10 mg N-NO_3^- L^{-1}	62%	Max 38 mW m^{-2}	[95] (2012)
Bioelectrochemical denitrification system	Phosphate buffer with nitrate and bicarbonate	Carbon paper	Sludge cake	NI	-150 or -300 mV vs Ag/AgCl	Applied cell voltage: 0.5, 0.7, 1 V	50 mg N-NO_3^- L^{-1}	0.204 mg NO_3^--N cm^{-2} d^{-1} (for voltages 0.7 and 1V)	2.8 mA	[124] (2013)
Soil MFC	Groundwater	Graphite bars	Sediment and groundwater	Aerobic or anaerobic (N_2)	NI	3000Ω	Around 180 mg N-NO_3^- L^{-1}	55 mg NO_3^- L^{-1} d^{-1}	24 mW m^{-2} 129 mA m^{-2} (anaerobic conditions)	[150] (2015)

BES	Modified DSM medium 113	Carbon cloth	*Thiobacillus denitrificanans*	CO_2	-500, -300, -100, +250 mV vs SHE (poised)	Potential applied to biocathode	14 mg $N\text{-}NO_3^-$ L^{-1} (2 mM NO_3^-)	21.12 mmol NO_3^-–N L^{-1} d^{-1} m^{-2} (for potential -500 mV vs SHE)	160.83µA (for potential -500 mV vs SHE)	[136] (2015)
MES	Solution of nitrate	Iron rod	Sediment	NI	NI	0Ω (shortcut)	2 mg $N\text{-}NO_3^-$ L^{-1}	98% in 16 days	No power production (MES)	[80] (2015)
BES	Synthetic nitrate-contaminated water	Graphite felt	Sludge from wastewater treatment process (WWTP)	NI	From +0.5V to +0.05V vs Ag/AgCl	1000Ω	50 mg $N\text{-}NO_3^-$ L^{-1}	75.4% 2.39 mg N L^{-1} d^{-1}	NI	[137] (2015)
MFC	Wastewater	Carbon felt	Sediment and wastewater	NI	NI	50Ω	18.7 mg NO_3^--N L^{-1}	96% (14 days)	353 mA m^{-2} (shortcut current) 88m ·m^{-2}	[147] (2016)
MFC	Buffer medium	Graphite rod	Cow manure and soil	N_2	NI	100Ω	69 to 966 mg NO_3^--N L^{-1} (initially 345 mg)	Up to 8.2 kg m^{-3} d^{-1} (highest C/N ratio)	190 mA m^{-2} 31.92 mW m^{-2}	[70] (2016)
BES	Buffer media	Graphite rod	Switched anodic biofilm	N_2	-303 mV vs SHE	Potential applied to biocathode	30 mg $N\text{-}NO_3^-$ L^{-1} 1.398 g L^{-1} NaHCO3	Max 532 mgN m^{-2} d^{-1}	NI	[117] (2016)
SMFC	Lake water	Graphite felt	Lake sediment and water	DO, 2.3 mg L^{-1}	NI	1000, 510, 100, 51, 10 or 1Ω	2.5 mg $N\text{-}NO_3^-$ L^{-1} (lake conditions)	60% in 115h for 1Ω	From 1.6 mW m^{-2} (1000Ω) to	[269] (2016)

									0.85 mW m^{-2} (1Ω)	
Microbial Electrochemical Denitrification System	Synthetic buffer groundwater	Graphite felt	Sludge from WWTP	Ar	Applied potential -300; -500; -700 or -900 mV vs SHE	Potential applied to biocathode	50 mg N-NO_3^- L^{-1} 2 g L−1 of NaHCO3	3.5 mg N-NO_3^- L^{-1} d^{-1} (-700mV vs SHE)	NI	[122] (2016)
BES	Synthetic buffer groundwater	Graphite felt	Anaerobic sludge from WWTP	Ar	Applied potential: −0.7 V vs. SHE	Potential applied to biocathode	50 mg N-NO_3^- L^{-1} 2 g L^{-1} NaHCO3	831.5 mg m^{-2} d^{-1} of N- NO_3^- (biocathode in water)	NI	[110] (2016)
BES	Medium	Carbon felt	Activated sludge from WWTP	Ar	-0.2 V vs SCE	Potential applied to biocathode	440 mg N-NO_3^- L^{-1}	86.1% (5 days)	NI	[68] (2017)
Bioelectrochemical reactor	Medium	Graphite felt + graphite granules	Mixed culture from sludge-based reactions	NI	-0.5 V vs SCE	Potential applied to biocathode	40 mg N-NO_3^- L^{-1}	Up to 16.5 mg N-NO_3^- L^{-3} day^{-1}	Up to -2.25 mA	[127] (2017)
Biofilm-electrode reactor	Medium	Graphite granules with different surface oxygen content	Liquid from suspended sludge reactor	NI	-0.5 V vs SCE	Potential applied to biocathode	40.0 mg L^{-1} NO_3^--N 2.70 g L^{-1} NaHCO3	Up to 27.36 mg NO_3^--N L^{-1} d^{-1}	Up to 2mA	[156] (2017)
SMFC	River water	Graphite felt	Sediment from lake	NI	From 200 to 250 mV vs Ag/AgCl	1000Ω or open circuit	2.87 mg NO3 −-N / l	Up to 79.1% (no plant)	9.82 mW/m2 (R=400Ω)	[270] (2018)

BES	Synthetic buffer groundwater	Granular graphite	Effluent of parent BES	NI	-0.303 V vs SHE	Potential applied to biocathode	30 mg N-NO_3^- L^{-1} 0.551 g L^{-1} $NaHCO_3$	39.7 g N m^{-2} d^{-1}	NI	[118] (2019)
Microbial Electrochemical System	Buffer media	Graphite brush	Domestic wastewater	NI	-0.5 V vs SCE	Potential applied to biocathode	22.5 mg N-NO_3^- L^{-1} 1 g L^{-1} bicarbonate	98%	NI	[120] (2019)
MFC for nitrate and uranium removal	Phosphate-free medium	Graphite felt	Consortia from previously operating MFC	N_2	No information	1000Ω	680 mg N-NO_3^- L^{-1}	0.130 kg N-NO_3 m^{-3} d^{-1}	2.91 W m^{-3} & 29.7 A m^{-3}	[143] (2020)
biocathode photo-bioelectrochemical system	Phosphate buffer medium 0.48 g/L NaHCO3	Nickel foam	Aerobic sludge and *Chlorella vulgaris*	Aerobic	From -0.37 to ~-0.47 V vs SCE	50 or 500Ω	330 mg N-NO_3^- L^{-1}	86% (192h)	40mW m^{-2} (while reducing nitrate)	[106] (2019)
algal-bacterial biocathode photo-bioelectrochemical fuel cell	Phosphate buffer medium 0.4 g L^{-1} NaHCO3	Carbon felt	Aerobic sludge and *Chlorella vulgaris*	Anaerobic	From -0.3 to ~-0.5 V vs SCE (dark)	500Ω	500 mg N-NO_3^- L^{-1}	From 150 to 200 mg N-NO_3^- L^{-1} in effluent after 160h	8.5 mW m^{-2} (while reducing nitrate)	[111] (2019)
single-cathode three-anode microbial fuel cell	Buffer artificial wastewater	Graphite felt	Sewage treatment plant and sludge system	NI	From ~120 to 50 mV vs SCE	1000Ω	110 mgNO_3^--N · L^{-1}	Up to 75.52%	795.70 mW m^{-3}	[112] (2020)

Mediator less SMFC	River water	Carbon fiber brush	River sediment and water	Aerobic	No information	1000 Ω	125.59 mg N-NO_3^- L^{-1}	99% in ~60 days	Up to 86.06 mW m^{-3}	[152] (2019)
double-chamber bioelectrochemical system	DSM medium	Carbon felt	T.denitrificans	Anaerobic	-500mV vs SHE	Potential applied to biocathode	2 mM NO3 −-N	54.47 mmol NO3 -−N L−1 m−2 d−1	NI	[145] (2020)
MFC with different external circuits/ operation modes	Phosphate buffer	Graphite felt	Mixed bacterial cultures from previous MFC	NI	///	Alternative charging and discharging (ACD), intermittent charging (IC) and constant external resistance (R)	140 mg N-NO_3^- L^{-1} 1.92 g/L NaHCO3	15.5 mg NO_3^- L^{-1} d^{-1}	Up to 0.91 W m^{-3}	[113] (2013)
BES	Wetland water unriched with sodium bicarbonate	Graphite granules + stainless steel grid	Sediment from wetland	Aerobic	-0.5 vs SCE (applied)	Potential applied to biocathode	90 or 113 mg N-NO_3^- L^{-1}	Up to 2.04 g N-NO_3^- d^{-1} m^{-2}	Max -0.4 A	[131] (2021)

Table 2: Experiments in flow

Type	Cathodic medium and flow	Cathode material	Bacteria source	Atmosphere	Cathode potential	Resistance	Inflow nitrate concentration	Nitrate reduction rate	Energy production	Ref
MFC	Modified M9 medium 6 L^{-1}	Granular graphite	Mixed sludge and sediment	Ar	Varying depending on R and NO_3^- concentration	5-50Ω	Up to 0.160 kg N m^{-3} NCC d^{-1}	Max. 0.146 kg NO_3^--Nm^{-3} NCC d^{-1} or 0.080 kg NO_3^--Nm^{-3} TCC d^{-1}	Max 8 W m^{-3} NCC (R = 25Ω)	[37] (2007)
MFC	Adapted M9 medium 200mL min^{-1}	Granular graphite	Mixed denitrifying sludge	No information	From around -0.3 to -0.1 V vs SHE (after stabilization, day 16)	5-100 Ω	55-66 mg N-NO_3^- L^{-1}	Up to 0.41 kg NO_3^--N m^{-3} NCC d^{-1} (R = 5Ω)	Max 34.6 W m^{-3} NCC (R = 20Ω)	[66] (2008)
MFC	Modified M9 medium 0.700 L · d^{-1}	Granular graphite	Microbial consortium from previous MFC	He, (tests of produced gas product)	100, 0, -100, -200 mV vs SHE	5Ω	0.652 g $NaNO_3$ L^{-1} 1.119mM-N h^{-1}	-0.484 mM-N · h^{-1} (continuous feeding conditions)	12.4 mA ($E_{cath\ applied}$ = -100 mV vs SHE)	[134] (2009)
BES	Medium 0.79 L d^{-1}	Granular graphite	NI	N_2	NI for MFC	1.1 Ω	From 0.137 to 0.684 kg NO_3^- Nm^{-3} NCC d^{-1}	Up to 0.50 kg NO_3^- Nm^{-3} NCC d^{-1} (adjusted pH)	NI for MFC	[67] (2009)
MFC	Synthetic wastewater 1.3ml/min	Granular graphite	Sludge from WWTP	Air	−435 mV vs Ag/AgCl	30Ω	2.5 g NO_3^-/l	35.21%	1.92 W/m^2	[92] (2010)

MFC	Medium with varying ionic strength 1.44L/day	Granular graphite	Effluent from previous MFC	N_2	From -0.09 to -0.15 V vs SHE	25Ω	From 14.42 to 15.64 mg N-NO_3^-/L	From -0.076 to -0.105 mM N h^{-1} (increasing with ionic strength)	4,4 W/m^3 NCC	[155] (2012)
Membrane-less MFC	Growth medium 0.633 L d^{-1}	Carbon cloth	Denitrifying consortium	NI	NI	100Ω	32,4 mg/L	0.186 g N-$NO_3^-m^{-3}$ day^{-1}	Max 71,2 mW m^{-3}	[141] (2013)
MFC	Groundwater 1.21 L d^{-1}	Granular graphite	Effluent from previous MFC	N_2	From 53 to -122 mV vs SHE	25Ω	28.32 mg N-NO_3^-/L	Max 51.37 gN m^{-3} NCC d^{-1}	No information	[154] (2013)
MFC	Nitrate-enriched mineral medium or effluent from other MFC From 1.2 to 1.5 L day^{-1}	Rod graphite	Effluent from previous MFC	NI	NI	100Ω	26.6 mg N-NO_3^-/L (autotrophic denitrification)	17% (autotrophic conditions)	15 A m^{-3} NCC (autotrophic conditions)	[151] (2013)
MFC	Freshwater, bicarbonate buffered media HRT: 318–1250 min, initially no flow	Graphite rod	Freshwater sediment or denitrifying biomass, enriched with Fe oxidizing, NO_3^-reducing bacteria	N_2/CO_2	0 and -0.25 V vs Ag/AgCl	Potential applied to biocathode	64.8 mg N-NO_3^- L^{-1}	Up to 11.4 g NO_3^--N m^{-2} day^{-1}	Max −3200 mA m^{-2}	[123] (2014)
BES	Medium NI	Graphite rod	Inoculum from cathode from previous MFC	N_2	-0.32 V vs Ag/AgCl	Potential applied to biocathode	14.28 mmol $NO_3^-\cdot L^{-1}$ (200 mgN$\cdot L^{-1}$)	Up to 2.78 mmol $NO_3^-\cdot L^{-1}$	NI	[128] (2014)
MFC	Modified M9 medium (with ammonium)	Graphite felt	Sludge from WWTP	N_2	NI	100Ω	37.9 mg N-NO_3^- L^{-1}	7.89 g N-$NO_3^-m^{-3}$ day^{-1}	176.1 mA/m^2 of electrode surface area	[144] (2014)

BES	Synthetic wastewater HRT: 2-24h	Carbon felt/ multiwall carbon nanotube composite	Sludge from WWTP	N_2	-100 mV	Potential or current applied to biocathode	50 mg N-NO_3^- L^{-1} (0.303 g $NaNO_3$ L^{-1})	92.7%	NI	[125] (2015)
BES	Nitrate contaminated groundwater Or tap water From 1.26 to 2.76 L day^{-1}	Granular graphite	Inoculum from previous MFC	N_2	from +597 to -703 mV vs SHE	Potential applied to biocathode	33.11 mg N–NO_3^- L^{-1}	2.59 mg N-NO_3^- L NCC^{-1} h^{-1} (93.9%) (E = -123mV vs SHE, conversion to N_2)	Up to 24.6 (E = -123mV vs SHE)	[135] (2015)
MFC	Synthetic buffer medium 0.93 mL/min	Activated carbon flakes	Anaerobic mixed cultures sludge from WWTP	Anaerobic	NI	1000Ω	NH_4NO_3 (0.176 g/L) 141 ± 14 mg NO_3^- L^{-1}	88%	Max 669 mW/m^3 3487 mA/m^3	[114] (2016)
MFC	Buffer media 1.25 ml min-1	Granular graphite	Aerobic and anaerobic sludge and sediments	NI	NI	12.5Ω	From 12.5 to 45 mg N L-1 2 g $NaHCO_3$	88.93 g NO_3^--N m^{-3} NCC day^{-1}	6.6 W m-3 NCC (for 37 mg N/L)	[115] (2016)
MFC	Synthetic wastewater Lagging time: from 44 to 72h	Carbon felt	Sludge from WWTP	Anaerobic	NI	1000Ω	From 0.08 to 0.64 mmol L^{-1} (in presence of different concentrations of perchlorate)	Up to 87.05% (for $C_0 \leq 0.32$ mmol NO_3^- /L)	Up to 0.66 W/m^3 (only nitrate)	[148] (2017)
Controlled biocathodic denitrification	Synthetic buffer wastewater From 2 to 9 L d^{-1}	Granular graphite	Culture from parent CBD	NI	−0.303 V vs SHE	Potential applied to biocathode	40 mgNO3 −-N L−1	Close to 100% for lower loading rates	Up to 70 A m^{-3}_{NCC}	[129] (2018)
MFC	Buffer medium	Carbon felt	Enriched inoculum	N_2 and Ar	NI	1500Ω	100mg NO3/L	100% in 2 days	2.1W/m3 and 26.6 A/m3	[271] (2018)

	36 ml/min for cicular MFC									
BES	Buffer synthetic groundwater HRT from 1.6 to 7.5h	Graphite granules	Effluent from a denitrifying BES reactor	N_2	-0.123 V vs SHE	Potential applied to biocathode	33 mg N-NO 3− L −1 420.0 mg L −1 NaHCO 3	519 g N-NO_3^- − m^{-3} Net Cathodic Compartment d^{-1}	NI	[132] (2021)
Denitrifying biocathode-electrocatalytic reactor	Buffer cathodic medium 10 mL min^{-1}	Graphite felt	Active sludge and a previously enriched denitrifying biocathode consortium	N_2	No information	Applied voltage: 1.3 and 1.5 V	5.05 g/L KNO3 1.92 g/L NaHCO3	0.45 kg NO3 −-N/m3 NCC/d	NI	[272] (2021)
single chamber biocathode-TiO2/g-C3N4 nanosheet/graphene composite photoan - ode	Buffer nutrient medium 150 mL d^{-1}	Carbon paper	Effluent from a bioelectrochemical reactor and active sludge	No information	-0.5 V vs Ag/AgCl	100 Ω	From 6 to 18 $mgNL^{-1}$	Final concentration: less than 1 mg N/L in 21h	NI	[130] (2020)
Microbial desalination cell	Nutrient medium 0.6 L d^{-1} HRT=1.3 days	Granular activated carbon	Denitrifying sludge from the wastewater treatment system	Anoxic	NI	560, 100 and 22 Ω	0.05 g NO3-L?1 2.5 g NaHCO3	99.85%	0.425 W m^{-3}	[273] (2020)

MFC combined with anaerobic sequencing batch reactor	Phosphate buffer solution 1.7 ml min^{-1}	Carbon fiber brush	Dewatered sludge	NI	NI	10.5 Ω	From7 to 70 mg NO_3^--N per L 2 g $NaHCO_3$	125.7 g NO_3^--N/m3 NCC/d	40.69 ± 0.8 A/m3 NCC (C= 49.35 mg NO_3^--N per L)	[69] (2020)
MFC	Buffer medium 1 g $NaHCO_3$ L^{-1}	Carbon bush	Inoculated sludge	1.5, 3.4 or 4.4 mg DO L^{-1}	NI	1000 Ω	0.722 g/L KNO_3	Up to 1.565 mg NO_3^--N $(L \cdot h)^{-1}$	Max 1776 mW m^{-3}	[93] (2019)
bioelectrochemical denitrification system	Phosphate buffer solution $NaHCO_3$ (2 g) HRT from 41.6 to 8.3 h	Carbon brush	Sludge from WWTP	Ar	~-0.5 V vs Ag/AgCl	15 Ω (applied voltage 0.7 V)	From 0.031 to 0.132 kg NO_3^-\\N/m3 · D	Max 0.121 kg NO_3^-\\N/m3	Up to 4.38 kWh/kg NO_3^--N	[153] (2019)
MFC	Buffer catholyte HTR = 120h	Carbon felt	Activated sludge	0.2-0.5 mg of DO L^{-1}	Around 0.1V vs Ag/AgCl (200Ω)	200 or 500 Ω	1.5 mM $NaNO_3$	92.5 % (200Ω)	1.5 mA (200Ω)	[146] (2015)

Appendix 2. Supplementary results

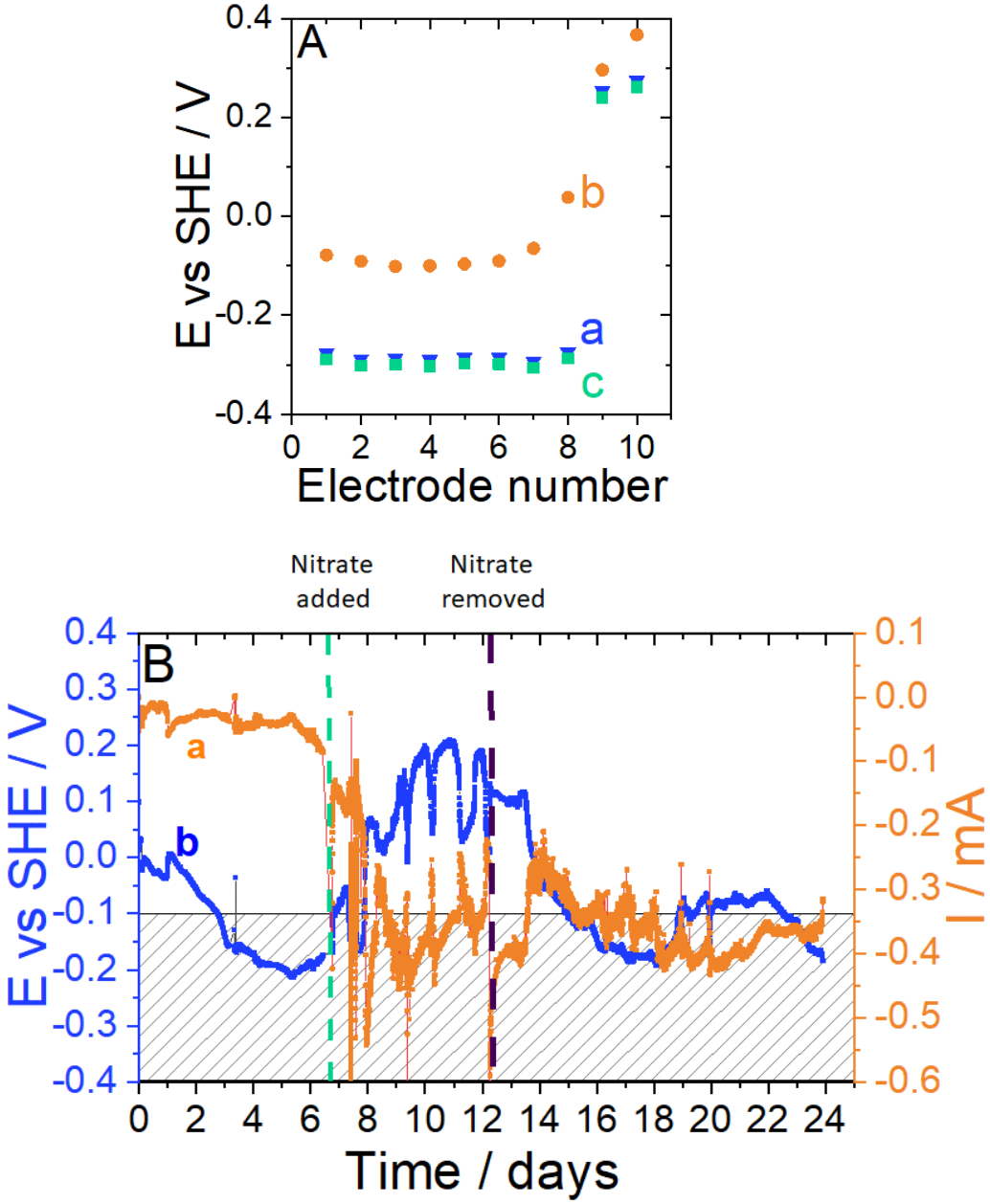

Figure A2.1. Results for the MES build of 10 stainless steel grid electrodes built in a parallel to MES described in the main text, but with Ville-sur-Illon sediments. A. Open Circuit Potential of each electrode individually in absence of nitrate (a, blue triangles), presence of nitrate (b, orange dots) and after changing water so there was again no nitrate in the reactor (c, green squares). B. Zero-Resistance Potentiometry. Blue line represents potential of MES (mixed potential of all electrodes connected in shortcut) and orange line represents the current between Electrodes 1-8 (anodes - in sediment) and Electrodes 9&10 (cathodes – in water).

In this experiment, the potential and current were measured constantly in order to observe the MES reaction for addition of nitrate (the same concentration). We observed a rapid change of the negative current after nitrate addition; it increased from around -0.05 mA to a value varying from -0.35 to -0.45 mA (Fig. S5). Also the potential increased gradually up to the value of +200

mV vs SHE. This values were stable for several days and indicate that the addition of nitrate increased the current of the biocathodic part of snorkel.

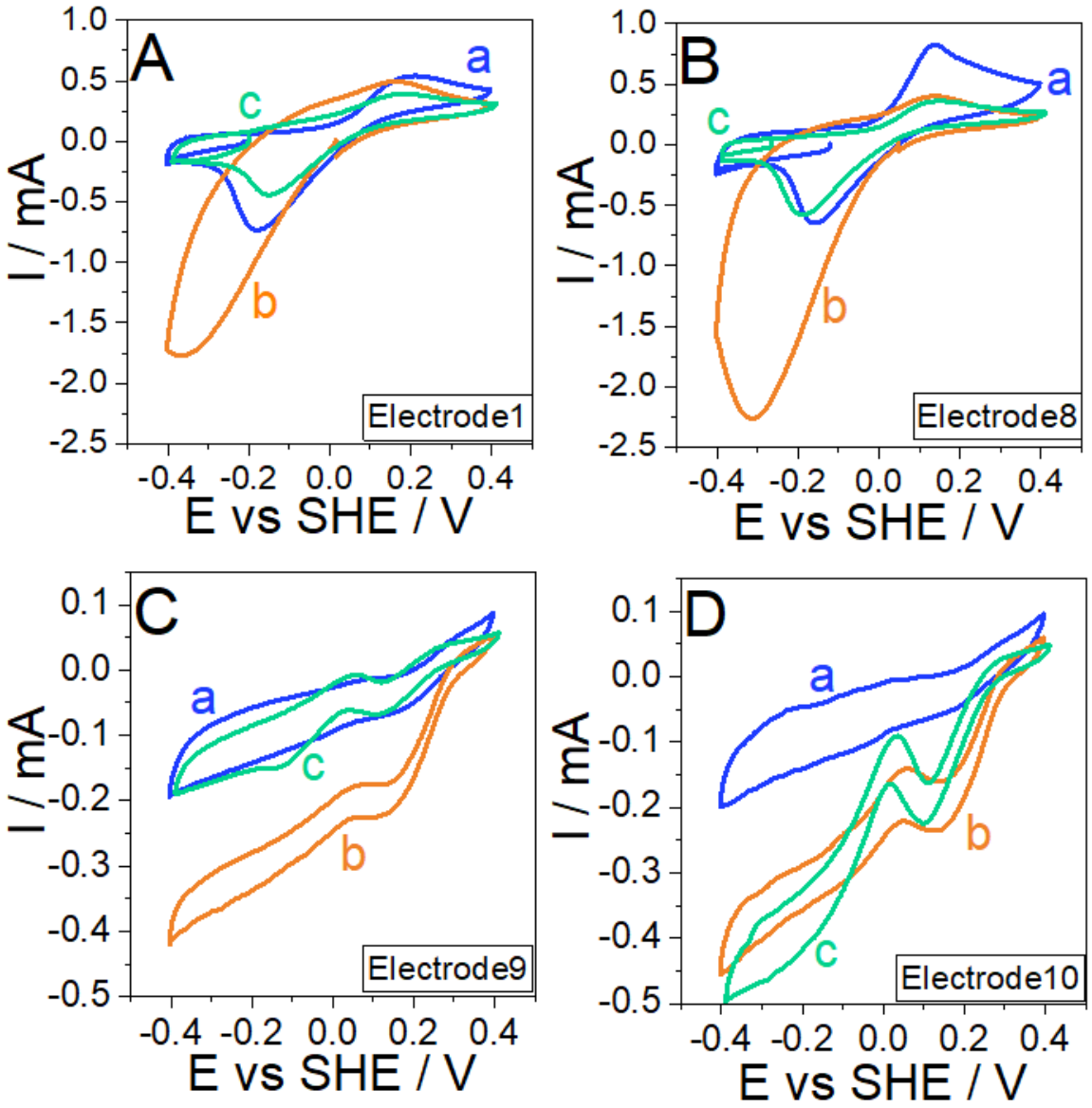

Figure A2.2. Cyclic voltammetry results for the MES built of 10 stainless steel grid electrodes, identical to MES described in the main text, prepared with Ville-sur-Illon sediments. Line a (blue) represents the initial scan without nitrate, line b (orange) - with nitrate addition and line c (green) - when the water was replaced with new synthetic wastewater without nitrate. A - Electrode1, B - Electrode8, C - Electrode9, D - Electrode10.

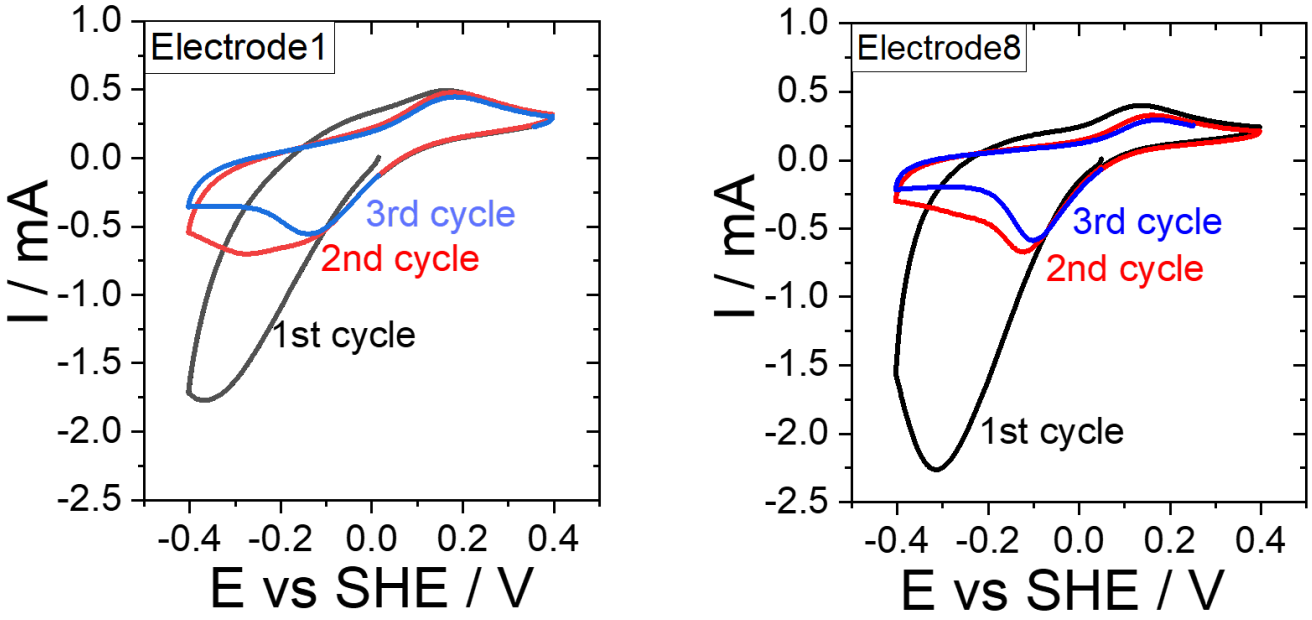

Figure A2.3. Cyclic voltammetry of Electrodes1 and 8 in presence of nitrate, 3 scans. Sediments from Ville sur Illon.

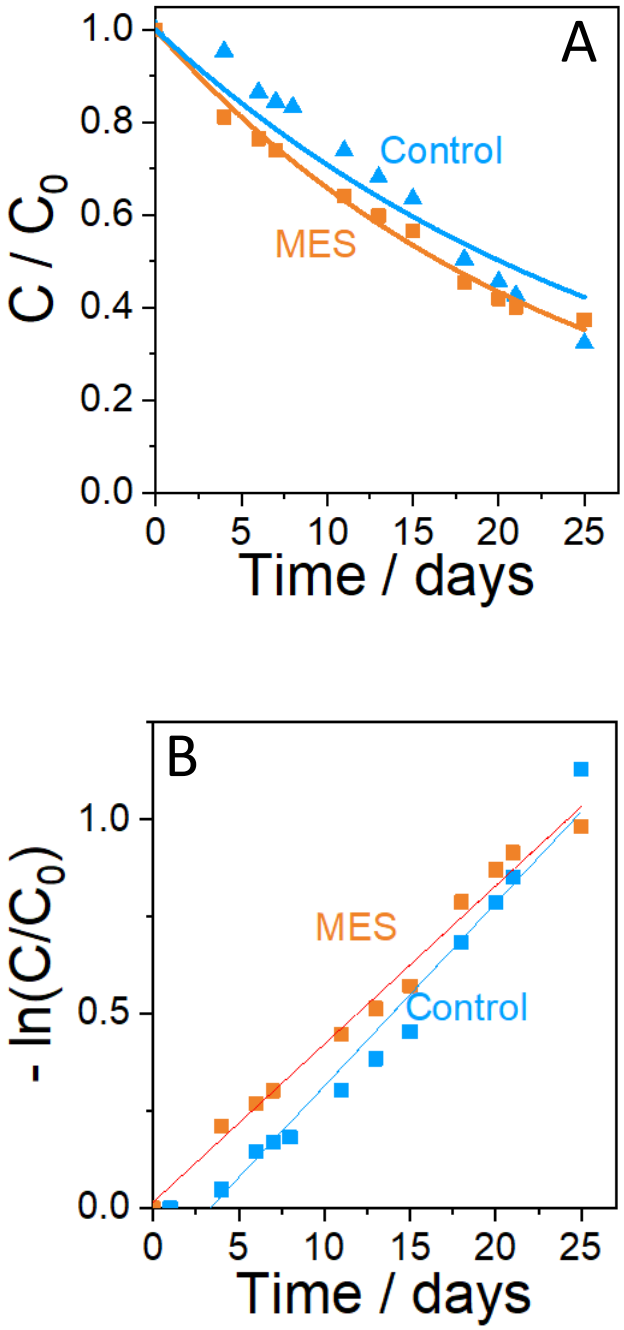

Figure A2.4. Nitrate removal in the presence of microbial electrochemical snorkel (MES), compared with control without MES, both prepared with sediments from Ville-sur-Illon. Results normalized to the same starting concentration C_0 in order to extract the kinetics. The best fit to adjust the model to experimental data was obtained by considering an apparent first order reaction with $C = C_0e^{-kt}$. Based on the values from day 0 to 25, we observed the reaction constant $k_{MES} = 0.0418 \pm 8.7*10^{-4}$ day^{-1} which is 20% higher than $k_{Control} = 0.0345 \pm 2.3*10^{-3}$ day^{-1}. A: Graphical representation of C/C_0 vs. t. B: Graphical representation of $-\ln(C/C_0)$ vs. t shows the linear dependence. R^2 (Control) = 0.969, R^2 (MES) = 0.987.

Appendix 3. The internship on University of Tartu

During this thesis, an internship in University of Tartu, Estonia, in group of prof. Ulo Mander was realized. It was funded with International Mobility Support for PhD Students DrEAM (University of Lorraine). The main aim was to measure the gas products of various experiments in order to see if the presence of Microbial Electrochemical Snorkel influences the nitrous oxide or methane emissions. Additionally, several experiments with MES made of carbon felt was prepared in order to study the influence of different size of cathodes (ratio 1:1, 1:2 and 1:4 plus control without cathode). During this study, the abundances of sediment bacteria and archaea and their potential to perform different nitrogen removal processes for treating nitrate-rich waters were measured and linked to N_2O emissions. The results were published in following article:

S. Gadegaonkar, T. Philippon, J. Roginska, Ü. Mander, M. Maddison, M. Etienne, F. Barrière, K. Kasak, R. Lust, M. Espenberg, Effect of Cathode Material and its Size on the Abundance of Nitrogen Removal Functional Genes in Microcosms of Integrated Bioelectrochemical-Wetland Systems, Soil Syst. 4 (2020) 1–15.

Résumé long de la thèse en français

En raison de la croissance démographique et du développement de l'homme, l'émission de différents polluants, telles que les espèces carbonées et azotées, augmente et contribue aux changements climatiques et à d'autres effets négatifs sur l'environnement. Parmi ces polluants, il y a le nitrate (NO_3^-), qui peut contaminer les eaux de surface et les eaux souterraines, s'échappant des champs agricoles alimentés en engrais azotés. Afin de diminuer sa concentration dans les eaux, de nombreuses approches ont déjà été étudiées, telles que des méthodes chimiques ou biologiques. L'une de ces dernières est la dénitrification - la réduction microbienne des nitrates en azote. La première partie du chapitre d'introduction présentera donc le cycle de l'azote, les défis actuels liés à l'augmentation de la concentration de nitrates et les méthodes courantes d'élimination des nitrates. Ces méthodes comprennent les zones humides artificielles - systèmes de traitement des eaux usées. Cependant, cette approche peut ne pas être assez rapide, surtout dans les périodes où la concentration de nitrates est élevée et dans les zones humides de taille insuffisante. Cette thèse explore alors des stratégies pour accélérer la réduction des nitrates.

Les systèmes bioélectrochimiques (BES), qui utilisent des microbes comme catalyseurs pour convertir l'énergie chimique en énergie électrique (ou inversement), ont émergé ces dernières années pour la purification de l'eau et la récupération d'énergie. Actuellement, la recherche utilisant la réduction bioélectrochimique des nitrates sur les biocathodes suscite de plus en plus d'intérêt. Les biocathodes de réduction des nitrates (NRB) se sont avérées efficaces pour traiter les eaux usées polluées par les nitrates. Cependant, elles nécessitent des conditions spécifiques et n'ont pas encore été appliquées à grande échelle. Dans la deuxième partie de l'introduction, les connaissances actuelles sur les NRBs sont résumées. Les principes fondamentaux des biocathodes sont discutés, ainsi que les progrès réalisés dans leur application pour la réduction des nitrates. Les NRBs sont comparées à d'autres techniques d'élimination des nitrates et les défis et opportunités de cette approche sont identifiés.

La dénitrification nécessite un donneur d'électrons, tel que le carbone organique. Ces composés apparaissent davantage dans les sédiments, alors que le nitrate est présent dans l'eau. Nous avons donc émis l'hypothèse que l'augmentation de l'interface sédiment/eau faciliterait l'accès aux donneurs d'électrons et accélérerait la dénitrification, ce que nous avons évalué dans la première partie de ce travail. Le Chapitre 3 explore l'effet de cette interface sur la réduction des nitrates. Le sédiment a été disposé verticalement dans les tubes faits de tissu perméable à l'eau. Cette expérience a d'abord été réalisée en état stationnaire et en augmentant de 10 fois la surface de l'interface, la réduction des nitrates a été augmentée jusqu'à 6,5 fois. Le volume du

sédiment, son origine et sa composition, n'ont pas eu d'influence significative sur la réduction des nitrates. Cette expérience a ensuite été répétée en flux, ce qui a permis une réduction des nitrates 3,5 fois plus rapide et stable pendant 53 jours. Nous avons calculé la surface de zone humide nécessaire pour atteindre une faible concentration de nitrates pour l'expérience témoin et le système avec interface augmentée, et nous avons constaté qu'elle est 3,5 fois plus petite (Fig. 1). L'application de cette méthode dans la zone humide construite a alors été envisagée.

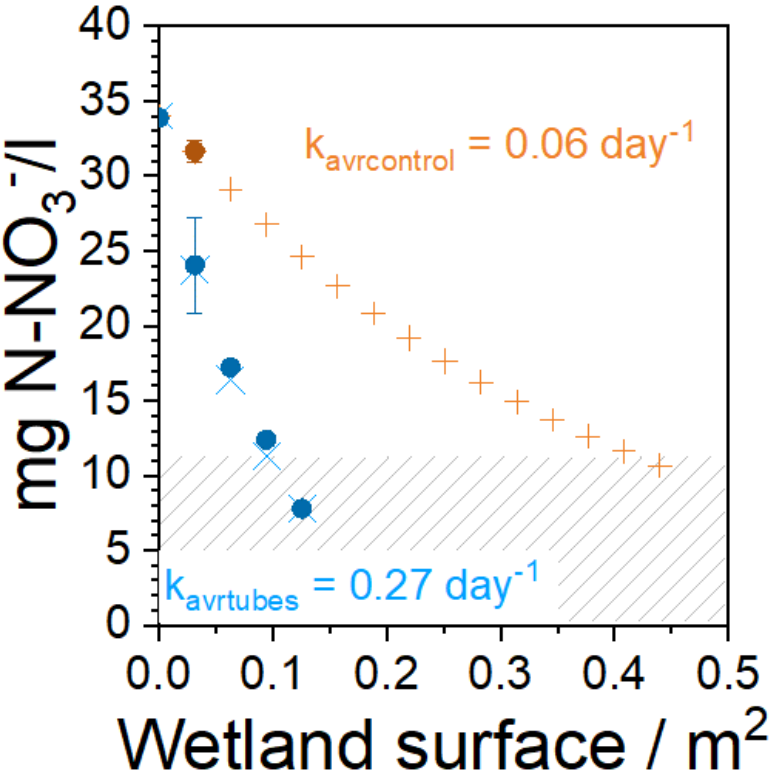

Figure 1. *La surface expérimentale et calculée de la zone humide nécessaire pour atteindre la faible concentration de nitrate. Points - valeurs expérimentales pour les expériences tubes (bleu) et contrôle (orange). X - valeur calculée pour l'expérience des tubes. + - valeur calculée pour l'expérience du contrôle.*

Une autre stratégie pour augmenter cette interface a été de mettre en place un système bioélectrochimique avec une biocathode réduisant les nitrates. Le système que nous avons étudié est un tuba électrochimique microbien (MES), qui consiste en une pièce d'électrode immergée dans deux milieux différents, ici dans le sédiment et l'eau (Fig. 2). Sur la partie dans le sédiment, un biofilm anodique se développe, qui oxyde la matière organique. Les électrons sont ensuite transportés vers la partie de l'électrode dans l'eau, où le biofilm cathodique se

développe et le processus de réduction de l'oxygène ou des nitrates se produit. La MES est une pile à combustible microbienne court-circuitée ; le potentiel de l'électrode est donc un potentiel mixte et aucune puissance ne peut être produite dans cette configuration, mais un courant élevé peut être atteint. Par conséquent, la décontamination de l'eau pourrait être plus efficace.

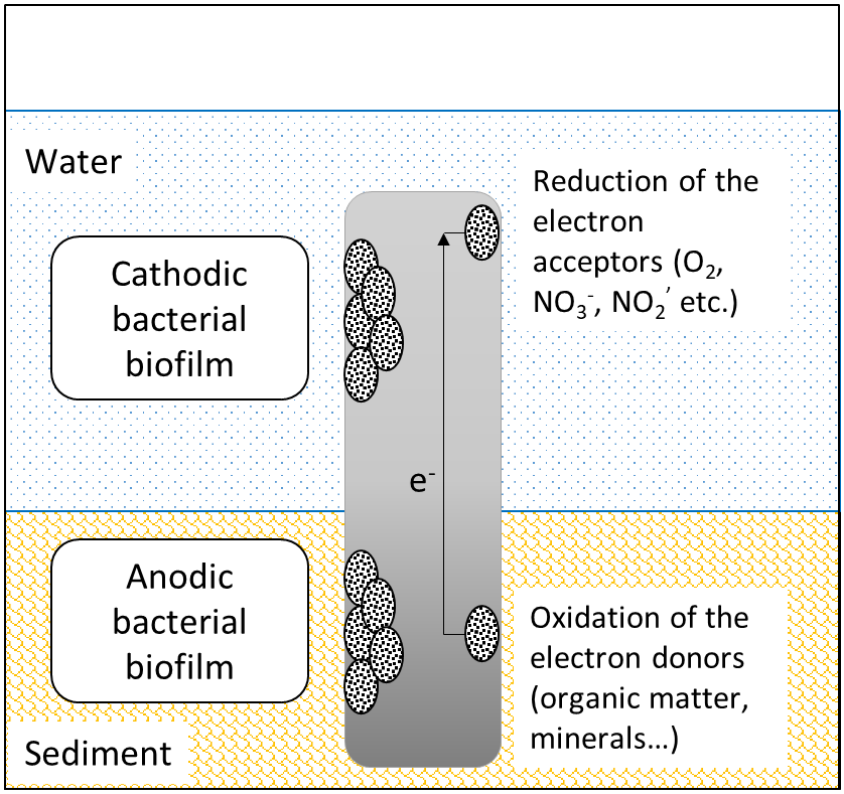

***Figure 2**. Schéma du tuba électrochimique microbien.*

Ce travail visait à créer les conditions pour développer une MES avec une partie biocathodique réduisant les nitrates et à caractériser ses propriétés électrochimiques, sa communauté microbienne et son efficacité de réduction des nitrates. Dans le Chapitre 4, le matériel d'électrode (fer, acier inoxydable et graphite poreux) et la configuration afin d'obtenir le potentiel mixte approprié pour l'élimination des nitrates, sans polarisation externe, ont été examinés. En particulier, le potentiel dans la gamme de -300 à -100 mV vs. ESH est ciblé car il devrait être le plus approprié pour le développement de la biocathode réduisant les nitrates, comme discuté dans l'introduction. Un modèle de MES est construit, dans lequel les parties cathodiques et anodiques pourraient être étudiées dans leurs environnements individuellement. L'ajout de nitrate a provoqué l'augmentation du courant cathodique et le déplacement du potentiel.

Deux situations du tuba ont été identifiées, sur la base des réponses électrochimiques enregistrées. En fonction de son activité, le côté biocathodique délivrait un courant cathodique faible (ligne unie) ou élevé (ligne pointillée). Le côté anodique est considéré comme plus stable dans le temps et seul un profil de courant typique avec le potentiel est représenté (l'unité de courant est ici arbitraire). Pour un faible courant cathodique, le potentiel du tuba électrochimique atteint la région des bas potentiels (-200 mV vs ESH pour ce scénario), avec les électrons provenant d'une première vague anodique initiée autour de -300 mV vs ESH. Lorsqu'un courant plus élevé doit être délivré à la cathode, en raison de l'activité plus importante du biofilm électroactif ou de la concentration plus élevée en nitrate, un potentiel mixte plus élevé doit être atteint (+135 mV vs ESH pour ce deuxième scénario). Cette expérience a également été placée dans une zone humide expérimentale construite en taille réelle et exposée au nitrate à une concentration pertinente pour une telle application. L'électrochimie et la microbiologie des systèmes en laboratoire et en zone humide ont ensuite été étudiées et comparées, et les défis de l'application de la MES pour la dénitrification ont été discutés.

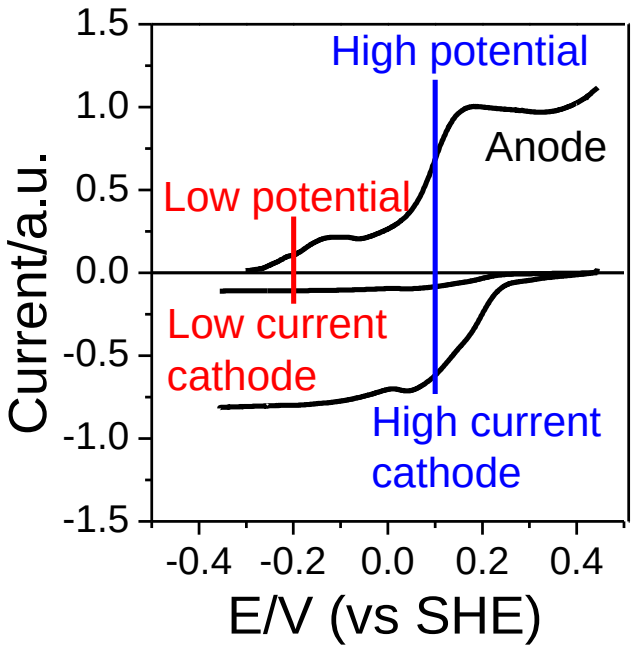

Figure 3. *Scénario illustratif menant à un tuba électrochimique microbien à bas ou à haut potentiel.*

Dans le chapitre suivant, une MES de plus grande taille et de distribution optimisée entre les sédiments et l'eau, avec des électrodes couvrant toute la surface du réacteur, a été construite. L'ambition ici était de confirmer que la MES peut augmenter le taux de dénitrification dans une

zone humide de laboratoire, que la biocathode réduisant les nitrates peut être cultivée de manière répétée, et de fournir plus d'informations sur l'écologie de la biocathode.

Une augmentation du courant cathodique a été observée après l'ajout de nitrate, et elle a diminué après la réduction du nitrate (Fig. 4). Cette augmentation du courant en présence de nitrate a également été observée lors de la voltampérométrie cyclique des biocathodes. Dans cette expérience, le nitrate a été réduit 43% plus rapidement par rapport au contrôle. La réduction du nitrate après la deuxième addition était très similaire à la première. Après la deuxième addition et après que le nitrate ait été complètement éliminé du milieu réactionnel, toutes les électrodes ont été déconnectées, ce qui a causé une perte d'efficacité. Les électrodes ont été reconnectées après un mois, mais ni la réponse électrochimique au nitrate, ni sa réduction plus rapide n'ont pu être récupérées. Ainsi, une biocathode efficace peut-être promue et elle est maintenue par l'apport constant d'électron provenant de la bioanode.

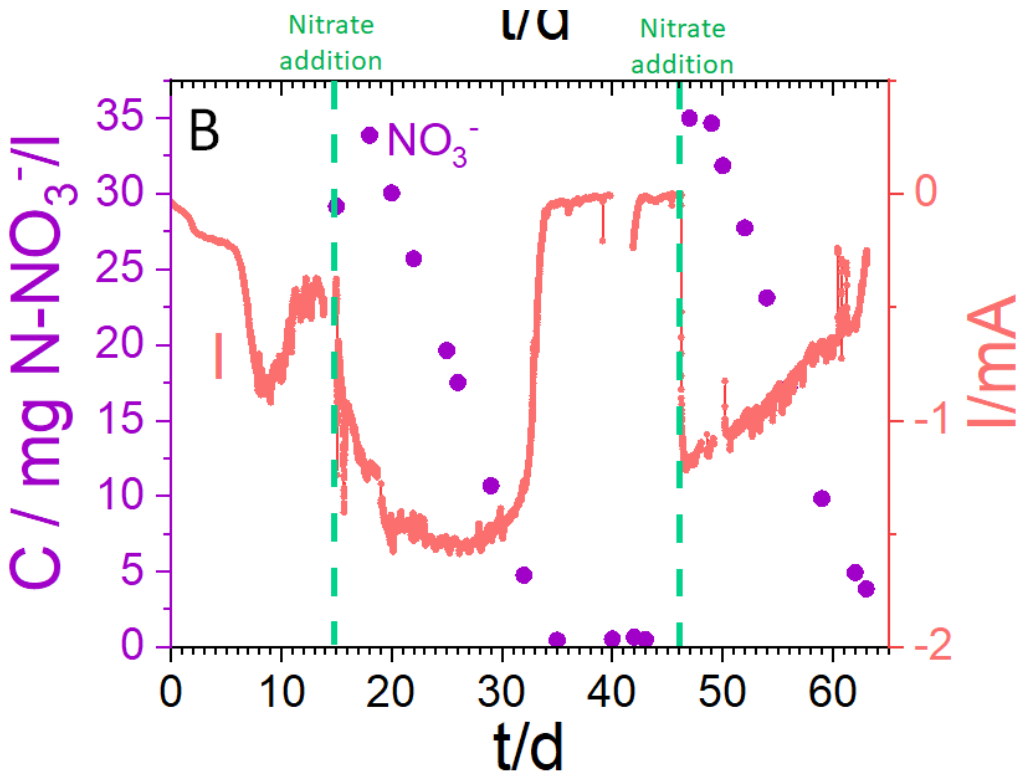

Figure 4. *Les variations du courant (ligne rouge) au cours de l'expérience, couplées aux concentrations en nitrate (points violets).*

L'expérience a ensuite été répétée en trois exemplaires. La réaction électrochimique claire a été observée à nouveau après l'ajout de nitrate : le courant a fortement augmenté dans deux exemplaires du triplicat. Le troisième montrait généralement des réactions moins visibles lors de l'ajout de nitrate. Les pics cathodiques sur la voltampérométrie cyclique ont augmenté

en présence de nitrate et ont diminué à nouveau après sa consommation. La réduction du nitrate était 40 % plus rapide que pour le contrôle sans aucune électrode et deux fois plus rapide que dans l'expérience MES qui n'a pas réagi clairement à l'ajout de nitrate. L'analyse écologique microbienne a montré une corrélation entre les expériences qui ont donné la réponse électrochimique la plus visible et l'abondance des bactéries de l'ordre des *Beggiatoales*. Sur la Figure 5, cette bactérie était observée en grande quantité sur toutes les cathodes des expériences A et C, et sur la Cathode 2 de l'expérience B, mais pas dans les sédiments et l'eau des autres expériences. Ces bactéries sont connues pour oxyder les composés sulfureux et réduire l'oxygène ou les nitrates, mais il n'a pas encore été prouvé qu'elles pouvaient échanger des électrons avec l'électrode solide par le transfert extracellulaire d'électrons.

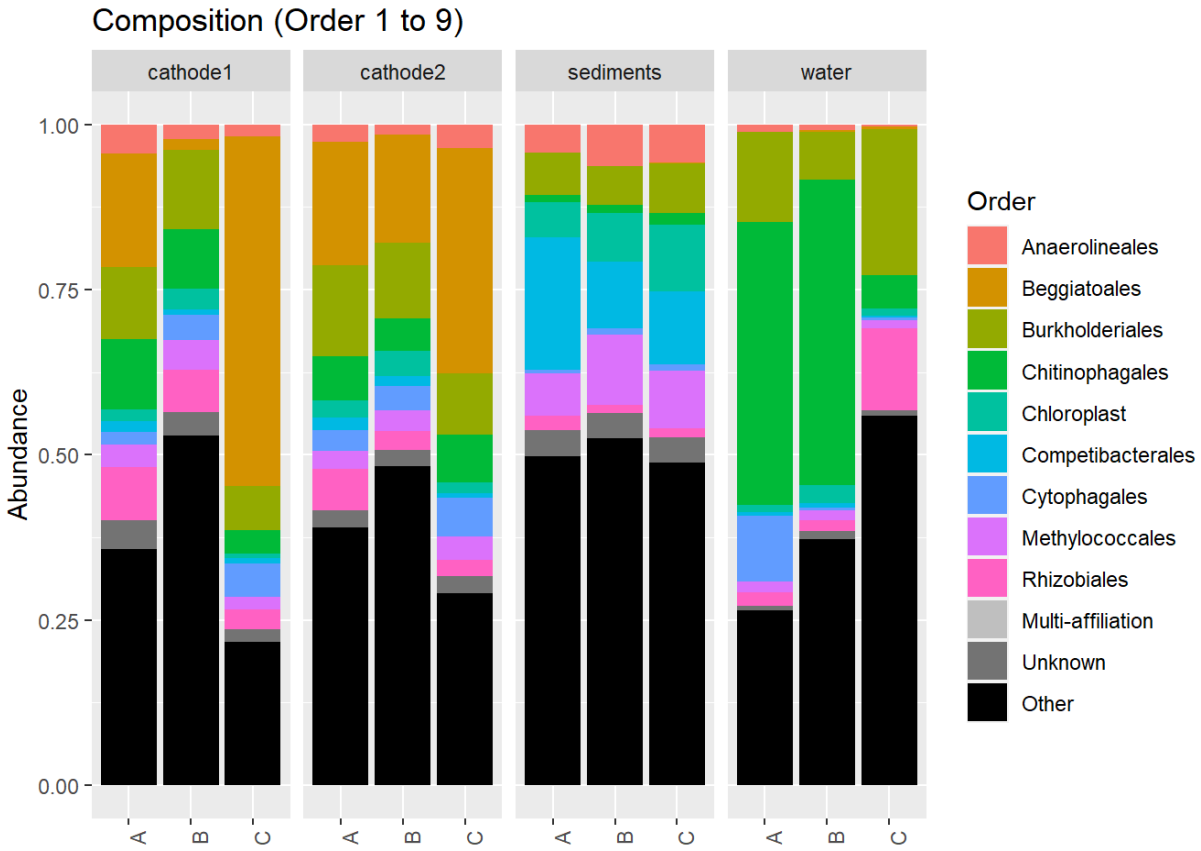

Figure 5. *Abondance relative des groupes phylogénétiques de bactéries dans les échantillons provenant des cathodes de la SEM et de l'eau et des sédiments (à partir du séquençage des gènes d'ARN 16 S).*

Enfin, le dernier chapitre explore la possibilité de combiner l'augmentation de surface des sédiments et un système bioélectrochimique en plaçant des électrodes dans ou autour des tubes sédimentaires. Une autre motivation pour placer les électrodes dans le sédiment était de tester la possibilité de réduction du nitrate dans ce milieu, car l'oxygène, qui est un agent

interférent, est rapidement consommé dans le sédiment. Des feutres en acier inoxydable et en graphite ont été testés à cette fin. Aucun changement n'a été observé dans les expériences avec l'acier inoxydable ; en revanche, un taux de dénitrification très rapide a été observé dans les expériences avec le feutre graphite. Des expériences supplémentaires ont montré que la raison de ce phénomène n'était pas la réduction sur l'électrode, mais la réaction dans l'eau avec des espèces qui ont été libérées en raison de la présence de l'électrode dans les sédiments. De plus, une augmentation du potentiel a été observée après l'ajout de nitrate et il diminuait à nouveau dès que le nitrate était consommé. L'expérience en flux a été introduite afin d'éliminer l'effet de la réaction dans l'eau et pour voir si la réaction sur l'électrode apporte une nette amélioration dans la réduction des nitrates. Dans cette expérience, un potentiel constant a été appliqué pour assurer les conditions appropriées pour le développement de la NRR. Bien que la réduction du nitrate n'ait pas été plus rapide par rapport au contrôle sans électrode, le courant a augmenté proportionnellement à la concentration de nitrate ajoutée, ce qui donne une nouvelle direction d'application du NRB - comme capteur de nitrate (Fig. 6). Il est intéressant de noter que, sans nitrate, un courant positif a été observé qui est passé à des valeurs négatives dès que le nitrate a été ajouté au réacteur. Cela signifie que sans nitrate, l'électrode dans les sédiments, dépourvue de tout accepteur d'électrons, se comportait comme une anode et utilisait la matière organique comme donneur d'électrons. Dès que le nitrate était disponible, la bioélectrode se comportait comme une cathode, ce qui était favorable avec ce potentiel appliqué, et un courant positif a été observé.

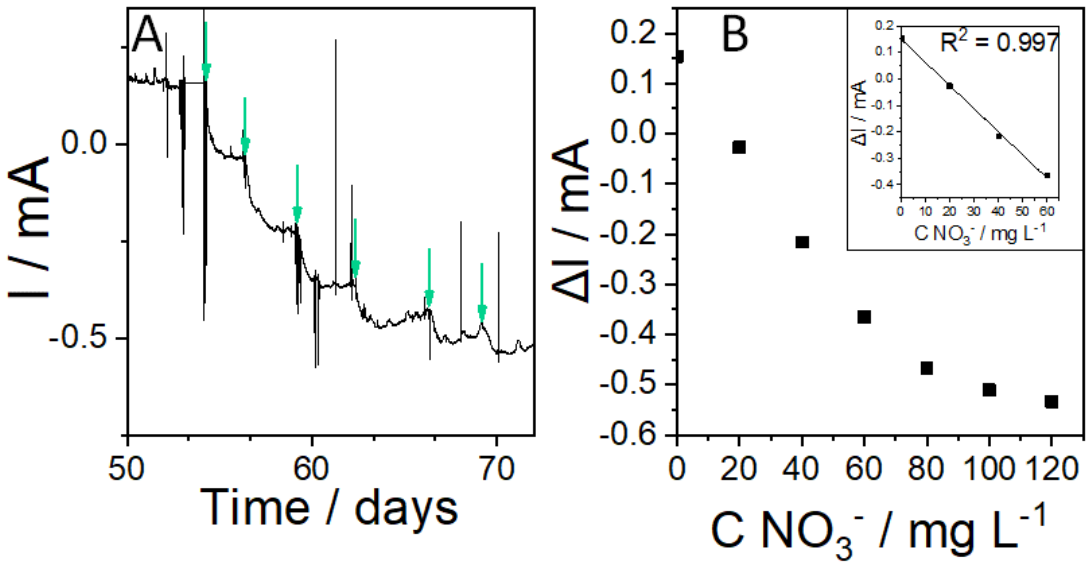

***Figure 6**. A. Les changements de courant après les additions de nitrate à l'expérience en flux. Chaque flèche verte représente un ajout de nitrate équivalent à 20 mg L^{-1}. B. Courant "plateau"*

après chaque ajout de nitrate en fonction de la concentration en nitrate. Le schéma dans le coin supérieur droit représente l'ajustement linéaire pour les concentrations entre 0 et 60 mg NO_3^- L^{-1}.

Globalement, cette thèse explore en profondeur les méthodes simples et peu coûteuses d'amélioration de la NRR dans les zones humides construites. Elle propose deux approches, l'une utilisant la bioélectrochimie et l'autre reposant sur l'augmentation de l'interface eau/sédiments. Des analyses électrochimiques approfondies et des études de la communauté microbienne sont fournies pour la première méthode ; un scénario d'application est proposé pour la seconde après un suivi à long terme. Cette thèse ouvre plusieurs nouvelles directions pour l'application des systèmes bioélectrochimiques dans l'environnement et la dénitrification à grande échelle des eaux polluées par les pratiques agricoles actuelles.